University of Liège
Department of life sciences
Laboratory of genetics and physiology of microalgae

Exploration of the use of chlorophyll fluorescence to identify complex I mutants in *Chlamydomonas reinhardtii*

Thesis submitted by Massoz Simon in fulfillment of the requirements for the degree in doctor in Sciences

Promoter : Remacle Claire
Co-promoter : Larosa Véronique

Academic year 2015-2016

Thanks

I would like to thank all the people I met in the Laboratory; Nico, Damien, Lorenzo, Van, Benjamin, Remi, Emilie, Barbara, Hector (for saving me from Poland), Michelle and Nadine (those who know), Judith, Vero, and more probably, for the great atmosphere that helped working in great conditions and for the numerous advice when times were needed.

Thanks to Claire, Pierre for their advice and great supervision, I never felt leftover!

Thanks to Marc for his precious advice and involvements during thesis committee and more!

Summary

English - During this work, we investigated the possibility to use fluorescence measurements, usually used to characterize photosynthesis, to screen complex I mutants in *C. reinhardtii*. Complex I mutations barely having any impact on photosynthesis, we added two photosynthetic mutations (*stt7* or *pgrl1*) to try and trigger specific phenotypes, tied to complex I deficiency, on photosynthesis. While the *stt7* mutation did not show any sign of photosynthetic deficiencies related to complex I deficiencies, the Use of *pgrl1* allowed us to produce a photosynthetic phenotype to identify complex I mutation in such background. We then started a random insertional mutagenesis searching for complex I mutants in *pgrl1* background using photosynthetic measurements (ϕPSII). This allowed us to identify a mutant affected in the *NUOAF3* gene, an assembly factor for complex I homologous to NDUFAF3 in Human. This mutant, in addition of 3 strains (RNAi-*NUO9* and RNAi-*NUO7* cell lines and *nuo9* insertional mutant) affected for core subunits of complex I, were studies for their complex I assembly. While these mutants showed depleted assembled complex I, some subcomplexes, such as the dehydrogenase module, were found to be still present, leading us to conclude that such subcomplex would assemble itself independently in *C. reinhardtii* as reported in other organisms.

Résumé

Français – Lors de ce travail, nous avons investigué la possibilité d'utiliser des mesures de fluorescence, généralement utilisées pour étudier la photosynthèse, pour identifier des mutants du complexe I chez *C. reinhardtii*. Les mutations du complexe I n'ayant quasi aucun impact sur la photosynthèse, celle-ci ont été couplées à des mutations photosynthétiques (*stt7* ou *pgrl1*) afin de faire apparaitre des défauts photosynthétiques spécifiques à l'addition des mutations complexe I. Si la mutation *stt7* ne nous a pas permis de faire ressortir une mutation du complexe I en observant l'efficacité photosynthétique, l'utilisation de *pgrl1* nous a permis de faire apparaitre un phénotype photosynthétique spécifique de l'ajout de la mutation complexe I. Nous avons donc réalisé une mutagenèse insertionnelle aléatoire afin de récupérer des mutants de complexe I dans un contexte *pgrl1* en criblant sur base de mesures de fluorescence (ϕPSII). Cela nous a permis d'identifier un mutant affecté dans *NUOAF3*, un facteur d'assemblage du complexe I homologue à NDUFAF3 chez l'homme. Ce mutant, ainsi que trois autres souches (mutants RNAi-*NUO9* et RNAi-*NUO7*, et un mutant insertionnel *nuo9*) affectées dans des sous unités cœur du complexe I, ont été étudiées en regard à leur assemblage du complexe I. Si tous ces mutants possédaient un default d'assemblage du complexe I, certains sous-complexes intermédiaires d'assemblage, tel que le module dehydrogénase, ont pu être retrouvés. Ceci démontre que ce sous-complexe s'assemble de façon indépendante par rapport aux autres, comme cela a été observé chez d'autres organismes.

List of abbreviations

Acetyl-CoA: acetyl coenzyme A
ADP: adenosine diphosphate
ATP: adenosine triphosphate
BNC: binuclear center
CEF: cyclic electron flow
FAD: flavin adenine dinucleotide
Fe-S: iron-sulfur
FMN: flavin mononucleotide
FNR: Ferredoxin NADP oxidoreductase
Hyg^R: Hygromycine resistant
IMS: intermembrane space
LEF: linear electron flow
N module: module dehydrogenase of complex I
NAD+: nicotinamide adenine dinucleotide
NADH: reduced form of nicotinamide adenine dinucleotide
NADP+: nicotinamide adenine dinucleotide phosphate
NADPH: reduced form of nicotinamide adenine dinucleotide phosphate
NDH: NAD(P)H dehydrogenase
OXPHOS: oxidative phosphorylation
Q: ubiquinone
QH_2: ubiquinol
Q module: module hydrogenase of complex I
P_d module: Proton pumping module distal region of complex I
Pi: inorganic phosphate
Pm^R: paromomycin resistant
PQ: plastoquinone
PQH_2: plastoquinol
P_P module: Proton pumping module, proximal region of complex I
PLS: proton loading site
PSI: photosystem I
PSII; photosystem II
ROS: reactive oxygen species

Index

INTRODUCTION

1. Introduction

1.1 *Chlamydomonas reinhardtii*

Chlamydomonas reinhardtii is a unicellular green alga from the class of Chlorophyceae. It is about 10 µm in diameter and swims in liquid medium thanks to its 2 flagella. It has been a model organism for photosynthetic and mitochondrial studies for a long time (Wiseman et al. 1977; Rochaix 2002). Indeed, *C. reinhardtii* is able to survive deficiencies in its photosynthesis apparatus when provided with an exogenous carbon source while it can also survive mitochondrial deficiencies if maintained in the light.

C. reinhardtii possesses one large chloroplast and numerous mitochondria (Fig *A*). Inside the chloroplast, the thylakoids, harboring the photosynthetic apparatus, are found. The pyrenoid, an area surrounded by starch plaques and important for the carbon concentration mechanisms (Giordano et al. 2005), is also located in the chloroplast. Mitochondria are divided between the intermembrane space and the matrix area. These areas are delimited by the mitochondrial inner membrane which forms invaginations called cristae. In addition to these organelles, *C. reinhardtii* also possesses peroxisomes (Lauersen et al. 2016)(Fig *A*).

Chloroplast and mitochondria are semi-autonomous, meaning that both possess their own functional DNA coding for part of their components. The chloroplastic genome is about 200 kb long (Maul et al. 2002). This genome possesses 99 genes coding notably for various components of the chloroplastic apparatus. It also possesses a complete set of tRNAs. A specific feature of the chloroplastic genome is a remarkable amount of repeated sequences (~20% of total) including two inverted repeated "dividing" the chloroplastic genome in two regions of ~80 kb. The small linear mitochondrial genome is about 15.8 kb long (Vahrenholz et al. 1993). It codes for some OXPHOS components (ND1, 2, 4, 5, 6, COB and COX1), only three tRNA (Q, W, M) and various fragments of the mitochondrial ribosomal RNAs. The nuclear haploid genome is composed of 120 Mbps divided in 17 chromosomes (Merchant et al. 2007; Blaby et al. 2014) with 17144 loci annotated.

C. reinhardtii grows using asexual and sexual divisions. Most of the time, mitosis is used for growth with a very short life cycle (average doubling time of about 8 h for WT strains).

Sexual reproduction can be triggered under nitrogen deprivation stress. Two types of opposite gametes (mt+ and mt-) can then fuse together, producing a diploid zygote. When better conditions are re-introduced, meiosis occurs and releases the four newly formed haploid cells. Under controlled conditions, the duration between production of the gametes and obtaining of meiotic products takes around two weeks.

Transformation of *Chlamydomonas* genome is possible and has been used in numerous studies. Random mutagenesis is the most performed type of genome transformation, mainly because targeted mutagenesis involves homologous recombination which is not efficient in *Chlamydomonas* (Jinkerson and Jonikas 2015). Recent protocols attempting to improve targeted mutagenesis have been developed including i) improvement of homologous recombination using engineered Zinc-finger nucleases as enhancer (Sizova et al. 2013), ii) development of functional CRISPR/CAS9 system in *C.reinhardtii*. Indeed, recent studies showed that *C. reinhardtii* cells transformed with transiently express *CAS9* gene and single guide RNA gene were able to cleave the desired targeted region (Jiang et al. 2014). It is to note that this method remains so far not very efficient.

Three type of random mutagenesis, UV, chemical and insertional (Dent et al. 2005; Barbieri et al. 2011; Godaux et al. 2013; Zhang et al. 2014; Massoz et al. 2015; Li et al. 2016) are regularly performed. Regarding insertional mutagenesis, many antibiotic resistance markers have been developed over the years. These include Hygromycine (Berthold et al. 2002), Paromomycin (Sizova et al. 2001) or Zeocin (Stevens et al. 1996) resistances. For an efficient expression, these resistance genes must be flanked by endogenous regulatory elements (promoter/terminator) and an intron can be added (Jinkerson and Jonikas 2015). Endogenous added elements usually come from the *PsaD, RBCS2* or *HSP70A* genes of *C. reinhardtii.*

The knowledge of all 3 genomes and the ability to induce mutations that are easily identified make *Chlamydomonas* particularly suited for the research of unknown elements involved in the energetic metabolism.

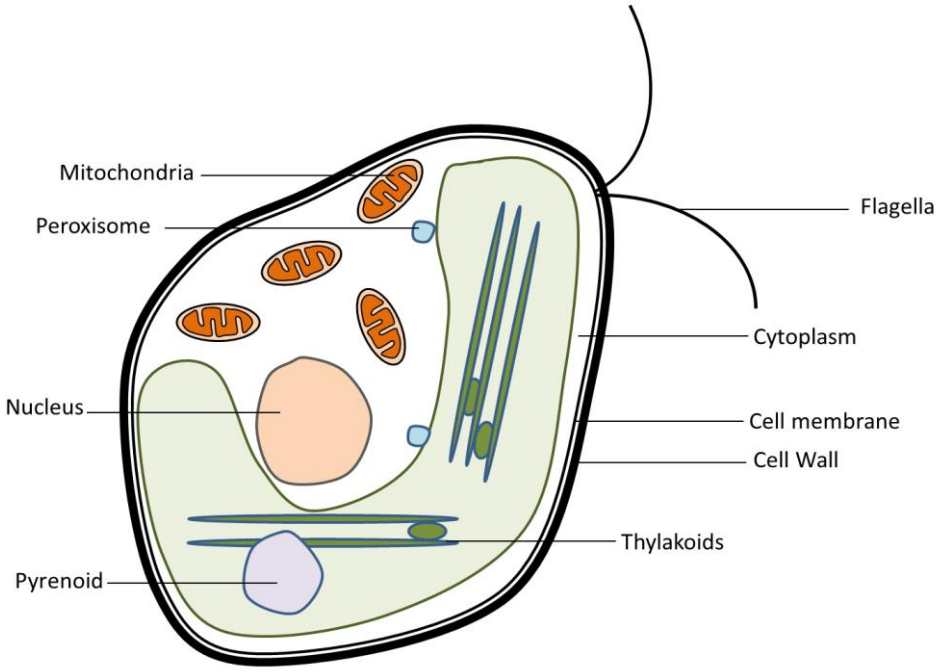

Fig *A*. Illustration of *C. reinhardtii* and its main components.

Mitochondrial bioenergetics pathways in *Chlamydomonas*

Simon Massoz, Pierre Cardol, Diego González-Halphen, Claire Remacle, Springer book series Microbiology Monographs, in '***Chlamydomonas* Biology, Biotechnology and Biomedicine**', chapter 6th, edited by M. Hippler.

The next part of the introduction is a review written for the 'Microbiology Monographs', in the book entitled '*Chlamydomonas* Biology, Biotechnology and Biomedicine',edited by Springer (Germany). The basis of this review was to upgrade the publication of Salinas et al. 2014. We decided to focus our review towards an informative and updated view on respiratory complexes structure, assembly and functioning as no general review had been made in recent years to our knowledge. The idea to give an overall view for new scientists deciding to work on *C. reinhardtii* energetic metabolism seemed an interesting one. Genomic data from Salinas et al. were updated, especially on complex I assembly where lot of progress has been mode in recent years. I wrote the complex I, II, III and IV paragraphs as my thesis subject brought me to learn about mitochondrial complexes, especially complex I. We asked the help of D. González-Halphen, an expert regarding ATP synthase, to provide us with his knowledge on complex V. For this review, we decided to include 3 figures i) a general scheme of mitochondria, giving context to what we were talking about ii) a theorical complex I assembly model for *C. reinhardtii*. As many progresses have been mode on the topic, we felt confident that such model, at the level of conserved core subunits, could be proposed for *C. reinhardtii*. iii) a precise ATP synthase subunits localization scheme provided by D. González-Halphen.

All the authors participated to the corrections asked by the reviewers when revision of the chapter was received. The version presented here is the revised version.

1.2 Mitochondrial bioenergetics pathways in *Chlamydomonas*

Simon Massoz[a], Pierre Cardol[a], Diego González-Halphen[b], Claire Remacle[a*]

[a] Liège University, Genetics and Physiology of Microalgae, Chemin de la Vallée 4, 4000 Liège 1, Belgium
[b] Universidad Nacional Autónoma de México, Instituto de Fisiología Celular, México D.F., Mexico
[*] Corresponding author

List of content

List of abbreviations
acetyl-CoA: acetyl coenzyme A
ADP: adenosine diphosphate
ATP: adenosine triphosphate
BNC: binuclear center
FAD: flavin adenine dinucleotide
Fe-S: iron-sulfur
FMN: flavin mononucleotide
IMS: intermembrane space
NAD+: nicotinamide adenine dinucleotide
NADH: reduced form of nicotinamide adenine dinucleotide
NADP+: nicotinamide adenine dinucleotide phosphate
NADPH: reduced form of nicotinamide adenine dinucleotide phosphate
OXPHOS: oxidative phosphorylation
Q: ubiquinone
QH_2: ubiquinol
Pi: inorganic phosphate
PLS: proton loading site
ROS: reactive oxygen species

Abstract

Mitochondrion is the site where the Krebs cycle and oxidative phosphorylation (OXPHOS) take place. After a brief overview of Krebs cycle and acetate metabolism in *Chlamydomonas*, this chapter focuses on OXPHOS components. OXPHOS is composed of five major multiprotein complexes: NADH:ubiquinone oxidoreductase (complex I), succinate dehydrogenase (complex II), ubiquinone:cytochrome *c* oxidoreductase (complex III), cytochrome *c* oxidase (complex IV) and ATP synthase. Three complexes (complexes I, III and IV) pump protons from the matrix to the intermembrane space (IMS) and build a gradient which is used by ATP synthase to produce ATP. In *Chlamydomonas* and other eukaryotes, proteins forming these complexes have a dual genetic origin. A few proteins, mostly hydrophobic polypeptides, are mitochondrion-encoded while the vast majority are nucleus-encoded and imported from the cytoplasm. Here we will review our current knowledge about these complexes.

1. Krebs cycle and acetate metabolism

The mitochondrion houses the Krebs cycle in the matrix and OXPHOS in the inner mitochondrial membrane (Fig. 1). Pyruvate, the end product of glycolysis, is imported inside the mitochondria by crossing both the outer and the inner mitochondrial membrane. Similar to most ions and metabolites, pyruvate is hypothesized to cross the outer membrane through the voltage-dependent anion channel (VDAC) based on the fact that humans deficient for VDAC1 show impaired pyruvate oxidation and ATP production (McCommis and Finck 2015). In *Chlamydomonas*, two VDAC proteins have been identified in the genome, ASC1 and ASC2, sharing 64% of sequence identity to each other (Salinas T, unpublished). In contrast, specific pyruvate carriers for the inner mitochondrial membrane have been identified in yeast, *Drosophila* and humans (Bricker et al. 2012). Accordingly, two genes described as encoding mitochondrial pyruvate carriers are present in version 5.5 of the *Chlamydomonas* genome (https://phytozome.jgi.doe.gov): Cre02.g113100.t1.1 and Cre10.g433400.t1.1. Once pyruvate enters the matrix, it is converted into acetyl-CoA by the mitochondrial pyruvate dehydrogenase complex (PDH, composed of three subunits encoded by *PDC1*, *PDC2* and *PDH1* genes, Fig. 1). Acetyl-CoA then enters the Krebs cycle, consisting of eight mitochondrial enzymes, whose presence have been confirmed in the mitochondria by proteomic analysis (Atteia et al. 2009). The

following genes encode the components of *Chlamydomonas* Krebs cycle (Atteia et al. 2009): (i) Fumarase (FUM, Fig. 1) is encoded by *FUM1*; (ii) malate dehydrogenase (MDH, Fig. 1) is represented by two isoforms encoded by the *MDH3* and *MDH4* genes; (iii) citrate synthase (CIS, Fig. 1) is represented by one isoform encoded by *CIS1*; (iv) aconitase (ACH, Fig. 1) is represented by the lone isoform encoded by *ACH1*; (v) isocitrate dehydrogenase (IDH, Fig. 1) is represented by three isoforms, two are NAD-dependent and encoded by *IDH1* and *IDH2*, while one isoform encoded by *IDH3* is NADP-dependent; (vi) the 2-oxoglutarate dehydrogenase complex (OGDH, Fig. 1) is composed of three subunits, encoded by *OGD1*, *OGD2* and *OGD3*; (vii) succinyl-CoA synthase (SCS, Fig. 1) is composed of two subunits encoded by *SCLA1* and *SCLB1* genes; (viii) succinate dehydrogenase (complex II/SDH, Fig. 1) will be described in the OXPHOS section.

Exchange of metabolites between cellular compartments involves different transporters (Fig. 1). Thirteen genes corresponding to mitochondrial substrate carrier proteins (MITC) are identified in the Phytozome 5.5 version of *Chlamydomonas* nuclear genome. In particular, MITC10, 11 and 14 have been found by proteomics analysis of mitochondria (Atteia et al. 2009). *MITC14* codes for a putative 2-oxoglutarate/malate carrier.

One particularity of *Chlamydomonas* is its ability to sustain heterotrophic growth (growth in the dark) through acetate assimilation. Five putative acetate transporters belonging to the GRP1/FUN34/Yaa family (GFY, Fig. 1) have been recently identified in *Chlamydomonas* (Goodenough et al. 2014) based on homology to fungal acetate permease A. These proteins bear six transmembrane segments, suggesting membrane localization. Once inside the cell, acetate is metabolized into acetyl-CoA by acetyl-CoA synthase. Three isoforms of acetyl-CoA synthase are present: ACS1 is cytosolic (Lauersen et al. 2016), ACS2 is chloroplastic (Terashima et al. 2010) while ACS3 would be colocalized in mitochondria (Atteia et al. 2009) and peroxisomes (Lauersen et al. 2016) (Fig. 1). Acetyl-CoA can be used in the glyoxylate cycle to fuel gluconeogenesis and other anabolic pathways or in the Krebs cycle to produce NADH for the respiratory chain and ATP production, both processes being necessary for effective growth in the dark (Salinas et al. 2014; Plancke et al. 2014). Indeed, respiratory deficient mutants and the recently characterized mutant deficient for isocitrate lyase (*icl1*), one of the two specific enzymes of the glyoxylate cycle (Fig. 1), are unable to grow under heterotrophic conditions. The localization of the enzymes of the glyoxylate cycle has been recently elucidated (Lauersen et al.

2016). Five of the six enzymes associated with the glyoxylate cycle are located within peroxisomal microbodies: one of the isoforms of malate dehydrogenase (MDH1), citrate synthase (CIS2) and acetyl-CoA synthase (ACS3), the lone form of malate synthase (MAS1) and of aconitase (ACH1), which defines for the first time a central role of peroxisomal microbodies in acetate assimilation. Only the single form of isocitrate lyase (ICL1) was found in the cytosol, which implies shuttling of metabolites such as isocitrate, succinate and glyoxylate between peroxisomal microbodies, cytosol and mitochondria (Fig. 1). Pore-like membrane structures and specific transporters would permit these exchanges but the molecular identify of such channel proteins remains undetermined (Kunze and Hartig 2013).

2. OXPHOS

2.1 Complex I

Complex I (EC 1.6.5.3), the first complex of OXPHOS, catalyzes the reaction

$[NADH + H^+] + Q + 4\ H^+_{matrix} \Rightarrow NAD^+ + QH_2 + 4\ H^+_{IMS}$ (Q= ubiquinone)

In all organisms investigated so far, complex I is an L-shaped multiprotein complex (Vinothkumar et al. 2014) with a molecular weight of ~1 MDa and 45 subunits (in humans), out of which 41 are conserved among eukaryotes (Cardol 2011). Fourteen of these subunits represent the core of the complex as they form the structure of the most simplistic bacterial complex I (type I NDH) (Efremov et al. 2010; Berrisford et al. 2016) and are conserved in all eukaryotic complex I. Amongst these 14 core subunits, the mitochondrially-encoded subunits ND1, ND2, ND4, ND5, ND6, ND3 (NUO3) and ND4L (NUO11) form the membrane arm of the complex. The nucleus-encoded 75 kDa (NUOS1), 51 kDa (NUO6), 24 kDa (NUO5), 49 kDa (NUO7), 30 kDa (NUO9), TYKY (NUO8) and PSST (NUO10) subunits form the matrix part of the complex (bovine and *Chlamydomonas* nomenclature). In addition to these core subunits, around 30 supernumerary subunits are present in the eukaryotic complex I. Though their role remains unclear, these subunits are thought to stabilize and protect complex I (Hirst et al. 2003).

In complex I, electrons are channeled from NADH to an ubiquinone molecule through a flavin mononucleotide (FMN) and seven iron-sulfur (Fe-S) clusters named N3, N1b, N4, N5, N6a, N6b, N2. An eigth Fe-S cluster is located near the FMN, named N1a and thought to serve as an electron store meant to avoid an excessive reactive oxygen species (ROS) production (Zickermann et al. 2015). These Fe-S clusters are mostly reduced under physiological conditions

(Kotlyar et al. 1990). The FMN with a midpoint redox potential at pH7 of ~ -340 mV serves as the first electron acceptor from NADH; the N3, N1b, N4, N5, N6a, N6b are equipotential at ~-250 mV and serve as a path for electron transport (Ohnishi 1998; Brandt 2011). The high potential N2 cluster (-120 mV) serves as final electron acceptor and catalyzes electron transfer to the ubiquinone molecule.

The prokaryotic core complex I is divided into modules based on function and position within the complex (Fig. 2). The N module, located at the most distal part of the matrix arm, is related to NAD+-reducing hydrogenases (Friedrich and Weiss, 1997). It is responsible for NADH oxidation and is composed of the 75 kDa, 51 kDa and 24 kDa subunits. The 51 kDa subunit bears the FMN and the N1b Fe-S cluster. The 24 kDa bears the N1a Fe-S cluster. The large 75 kDa bears the N3, N4 and N5 Fe-S clusters.

The Q module, or quinone reduction module, is composed of the 49 kDa, 30 kDa, TYKY and PSST subunits. This module allows electron transfer to the ubiquinone through the N6a and N6b Fe-S clusters located on the TYKY subunit and through N2 reaction center cluster. The 49 kDa, TYKY, PSST subunits are thought to be derived from a Ni-Fe type hydrogenase (Friedrich and Weiss 1997; Vignais and Billoud 2007) where the proximal Fe-S cluster from the Ni-Fe reaction center became the current N2 cluster (Kerscher et al. 2001). It is interesting to note that the N2 cluster, long thought to be harbored by the 49 kDa and PSST subunits, has been shown to be only linked to the PSST subunit (Sazanov and Hinchliffe 2006) with the 49 kDa subunit being at the interface of this cluster. Despite the fact that the 49 kDa and 30 kDa proteins are the only core subunits of the matrix arm that do not provide ligands for cofactors, *Chlamydomonas* cells inactivated for their expression fail to assemble whole complex I as also observed in all species (*Neurospora* and *E. coli*) investigated so far (Schulte and Weiss 1995; Duarte et al. 1998; Massoz et al. 2014).

The P module, often divided into the proximal (P_p) and distal region (P_d), is composed of the remaining membrane subunits. The ND1, ND2, ND3, ND4L and ND6 subunits compose the P_p module (Fig. 1). The P_d module is composed of the ND4 and ND5 subunits. ND2, ND4 and ND5 are homologous to the *E. coli* cation/H^+ antiporter MrpA/MrpD (Mathiesen and Hägerhäll 2002). These three subunits are responsible for three out of four proton pumping sites in complex I. The fourth site is thought to be a channel located in the small ND subunits (ND3, ND4L and ND6) with maybe part of the ND1 subunit (Zickermann et al. 2015; Berrisford et al. 2016).

The current proton-pumping mechanism model for complex I is supported by crystal structures in the bacterium *Thermus thermophilus* [reviewed in (Sazanov 2015)], the fungus *Yarrowia lipolytica* (Zickermann et al. 2015) and mammals (Vinothkumar et al. 2014). The proton pumping channels through the membrane domain are distant from the redox-active groups mediating electron transfer through the hydrophilic domain (Efremov and Sazanov 2011). As a consequence, the proton-coupled electron transfer in complex I is expected to differ mechanistically from that in other respiratory complexes. The current model for proton- pumping is based on a two stage stabilization-change mechanism. This model proposes that the stabilization of a negatively charged ubiquinone drives a conformational change causing energy transmission to the membrane arm and resulting in proton pumping (Brandt 2011). This model combines computational simulations with biochemical experiments based on bacterial complex I (Sharma et al. 2015; Hummer and Wikström 2016). The bacterial complex I structure revealed an unusual ubiquinone-binding cavity (Baradaran et al. 2013). The reduction of bound ubiquinone would create a significant charge imbalance in the catalytic cavity. The charge imbalance would be transmitted to the antiporter-like subunits by long-range conformational transmission. The antiporter-like subunits define a central flexible axis containing charged and polar residues which extend from the ubiquinone-binding site at the junction between the two main domains to the tip of the hydrophobic arm and thus represent a hydrophilic central axis along the hydrophobic domain by which these concerted conformational changes are transmitted. This would lead to changes in exposure to solvent and in the pKa of key residues in the antiporters subunits, allowing proton translocation (Berrisford et al. 2016; Hummer and Wikström 2016). Displaced ubiquinone would then be protonated. Once protonated, the charge imbalanced would be compensated and the newly formed ubiquinol would exit the cavity.

Complex I is the biggest complex of OXPHOS, with a large number of proteins encoded in both the mitochondrial and the nuclear genomes. The assembly of complex I is expected to involve of lot of chaperones and is not yet fully understood. Because most data on complex I assembly were obtained in mammals, assembly description will here be explained based on knowledge gained in humans. Thus human nomenclature will be used for the assembly description. As many other OXPHOS complexes, complex I seems to be orderly assembled into subcomplexes before these subcomplexes are assembled together to form the holoenzyme (Fig. 2). The process starts with the assembly of the Q module containing NDUFS2, NDUFS3,

NDUFS8, and NDUFS7. This requires the intervention of at least four factors named NDUFAF7, NDUFAF3 NDUFAF4 and NDUFAF6. NDUFAF7 is a methyltransferase which methylates NDUFS2 (Rhein et al. 2013). NDUFAF6 has been shown to stabilize NDUFS3 and ND1. NDUFAF3 and NDUFAF4 are interdependent factors that recruit the subunits of the Q module to assemble them with the ND1 membrane subunit (Saada et al. 2009), ND1 being itself stabilized by the NDUFAF5/NDUFAF6 assembly factors. The Q module + ND1 represent an early 400 kDa subcomplex. The second subcomplex (460 kDa) is composed of the small ND subunits (ND3, ND4L, and ND6) and ND2 and assembles independently from the 400 kDa. The four assembly factors NDUFAF1, ACAD9, TMEM126B and ECSIT (also called MCIA complex) are known to allow the assembly of this 460 kDa subcomplex [reviewed in (Sánchez-Caballero et al. 2016a)]. The two subcomplexes merge together with the help of TIMMDC1 (Guarani et al. 2014) into a 650 kDa subcomplex. Following these events, the assembled P_d module merges with the rest of the subunits into a 830 kDa subcomplex stabilized by the Foxred1 assembly factor. The assembled N module also proceeds to merge with the now complete complex I with the help of the NDUFAF2 assembly factors (not present in *C. reinhardtii*), though the role of the NDUFAF2 in N module assembly has been contested in recent years (Kmita et al. 2015) where it was speculated to potentially maintain the Q module into a proper conformation until later stage of assembly . The completion of the assembly triggers the release of all remaining assembly factors. Recombinant assembly factor Ind1 from humans (huInd1) expressed in *E. coli* has been shown to bind Fe-S clusters *in vitro* and depletion of huInd1 was shown to be responsible for decreased complex I assembly (Sheftel et al. 2009). These results point toward a role of huInd1 in Fe-S cluster insertions. The apoptosis inducing factor (AIF) also plays a role in complex I assembly since cells depleted for this factor display decreased complex I activity (Mimaki et al. 2012), though the exact role of this assembly factor remains unknown.

Whether plant complex I assembly follows the same pathway as in humans or not is difficult to say. On the one hand, on the 14 assembly factors described in humans, 11 have putative homologs in *Arabidopsis* (Table 1), suggesting that similar patterns of assembly could be found. On the other hand, as plant complex I contains an additional gamma carbonic anhydrase module attached to the Pp module (Sunderhaus et al. 2006; Klodmann et al. 2010; Fromm et al. 2016), this suggests that the assembly should follow a different assembly pattern than that found in humans at least for the attachment of these subunits to complex I. Indeed, the carbonic

anhydrase subunits of the module seem to be crucial for the beginning of assembly of complex I in *A. thaliana* (Fromm et al. 2016). At that stage, our knowledge is extremely limited since only two assembly factors have been demonstrated to participate in complex I assembly in plants: INDL (homolog of huInd1) and L-galactono-1,4-lactone dehydrogenase (GLDH). The role of INDL in complex I assembly of *A. thaliana* is more complex than in humans as the factor has been suggested to participate to both complex I assembly and mitochondrial translation (Wydro et al. 2013). GLDH catalyzing the last step of ascorbate biosynthesis is found in 400 kDa to 850 kDa subcomplexes in *A. thaliana* and has been shown to be necessary for the assembly of membrane arm of the complex (Schimmeyer et al. 2016). GLDH thus represents the first plant-specific assembly factor since GLDH is not conserved in humans (Schimmeyer et al. 2016).

In *C. reinhardtii*, gamma carbonic anhydrase subunits are found by proteomic analysis of complex I (Cardol et al. 2004). These subunits should also form a domain like in *Arabidopsis*, as a gamma carbonic domain similar to that of *Arabidopsis* has been found in *Polytomella* (Sunderhaus et al. 2006), a very close relative of *Chlamydomonas*. This suggests that insertion of these subunits in the complex should follow similar pattern to that proposed in plants. Ten out of the 14 assembly factors found in humans have putative homologs (Table 1), and the plant specific factor (GLDH) has also an homolog in *C. reinhardtii* (Table 1) but no functional analysis has never been undertaken on these putative factors. Nevertheless, subcomplexes observed in mutants obtained in the core subunits allow us to suggest a pattern for complex I assembly. Indeed, in *nd5* or *nd4* mutants and in a mutant affected in the nucleus-encoded NUOB10 subunit (PDSW), a 700 kDa subcomplex assembles and contains all modules except the P_d module, as proteomic analysis suggested (Cardol et al. 2002; Cardol et al. 2008; Barbieri et al. 2011). A 200 kDa soluble subcomplex, bearing NADH dehydrogenase activity, is observed in wild type, *nd4* and *nd5* mutants, and is the only module detected in *nd1*, *nd6, nd3* and *nd4L* mutants (Cardol et al. 2002; Cardol et al. 2006). It has been shown to contain at least the NUOS1 (75 kDa) subunit (N module), and the NUO7 (ND7) subunit (Q module) (Cardol et al. 2002) and was postulated to be an early assembly intermediate (Subrahmanian et al. 2016). Interestingly, recent studies showed that a *NUO7*-RNAi cell line still possesses the 200 kDa module (Massoz et al. 2014) despite the strong-down regulation of the *NUO7* transcript and the absence of whole complex I. In addition, the NUOS1 subunit (75 kDa subunit) was detected in the *NUO7*-RNAi cell line by immunoblotting on membrane extracts while the NUO8 (TYKY) and NUO10 (PSST) subunits of

the Q module were absent (Massoz et al. 2014). Thus the question of the nature of the 200 kDa module arises. Considering that both the N module and an early Q module would have similar size (Fig. 2), they would co-migrate in BN-PAGE. We thus propose that the subunits identification made in 2002 when we isolated the subcomplex at 200 kDa was performed on both modules, which explains the presence of NUO7 (Q module) and NUOS1 (75 kDa subunit) (N module) in this previous analysis. This co-migration also explains that the *NUO7*-RNAi cell line would still present the 200 kDa module (N module) while the Q module would be absent. Together these results suggest that the Q and N module assembles independently.

In conclusion, if the 200 kDa indeed contains two modules, three subcomplexes could be detected in *Chlamydomonas* complex I mutants isolated so far: (i) a 700 kDa subcomplex still possessing NADH dehydrogenase activity and barely attached to the membrane. A subcomplex similar to the 700 kDa subcomplex has been identified in maize deficient for ND4 (Karpova and Newton 1999) while in human cell lines ND4-deficient cell lines do not assemble the membrane components of complex I (Hofhaus and Attardi 1993). (ii) A 200 kDa module maintaining a NADH dehydrogenase activity would correspond to the N module alone; such module containing NDUFS1, NDUFV2 and NDUFV1 was reported to accumulate in TIMMDC1 deficient knock down cell lines in humans (Guarani et al. 2014) ; and (iii) a putative ± 200 kDa early intermediate corresponding to the Q module, and containing at least NUO7/NUO8/NUO9/NUO10. It could be similar to the 'subcomplex 3' observed in various organisms including humans during complex I assembly (Vogel et al. 2007a; Guarani et al. 2014). These elements are summarized in Fig. 2.

In *Chlamydomonas*, complex I is a 950 kDa complex composed of up to 47 subunits (Subrahmanian et al. 2016). All core subunits are conserved but the NUO3 (ND3) and NUO11 (ND4L) subunits are nucleus-encoded, as opposed to their mammalian counterparts (Cardol et al. 2006). In addition to the 14 core subunits, *C. reinhardtii* complex I is also composed of up to 33 supernumerary subunits (see Table 1). Two subunits, NUOP4 and NUOP5 are specific to *C. reinhardtii* and *Volvox sp* (see https://phytozome.jgi.doe.gov/). The CAG1, CAG2 and CAG3 subunits are homologous to the gamma carbonic anhydrase (CA) subunits of *A. thaliana* where two additional subunits (CAL1, CAL2) are also present (see above).

C. reinhardtii is attractive for studying complex I because algae deficient for that complex survive due to the support of alternative NADH dehydrogenases (Lecler et al. 2012) and photosynthesis. Many mutants have been identified, mostly impaired in core mitochondria- or

nucleus-encoded subunits, and some of them in supernumerary ones [reviewed in (Salinas et al. 2014; Subrahmanian et al. 2016)] including the NUOP4 subunit specific to *C. reinhardtii* (Massoz et al. 2015). Complex I mutants are generally screened based on their slow growth in the dark phenotype. Indeed, their growth is significantly slower than wild type in these conditions because they only retain two of the three phosphorylation sites that are operational when electron transfer proceeds through the whole respiratory chain. In contrast complex III and complex IV mutants do not grow in the dark (see further) because they lack the cytochrome pathway and thus only retain one of the proton pumping enzymes of the respiratory chain. The less stringent phenotype of complex I mutants compared to complex III and complex IV mutants is also observed in the light under mixotrophic conditions (light + acetate) for the same reason (Remacle et al. 2001; Cardol et al. 2002; Massoz et al. 2014). As a consequence, very little changes of their proteome is observed while a decreased ROS production of about 30% is found (Massoz et al. 2014). Overall, this phenotype is much less severe than that observed in vascular plants like maize, tobacco and *Arabidopsis thaliana*, which are male sterile and/or display abnormal leaf development (reviewed in Subramanian et al. 2016).

2.2 Complex II

Complex II (1.3.5.1) catalyzes the reversible conversion of succinate into fumarate and as such is also part of the Krebs cycle (Fig. 1):

succinate + Q <==> fumarate + QH_2

It is a small multiprotein complex of about 110 kDa composed of four subunits in most eukaryotes, including *Chlamydomonas*. The two matrix subunits, Sdh1 and Sdh2, are anchored to the membrane by the Sdh3 and Sdh4 membrane subunits. The Sdh1 subunit contains a flavin adenine dinucleotide (FAD) cofactor. The Sdh2 subunit is an iron sulfur containing protein bearing three Fe-S centers (2Fe-2S, 4Fe-4S and 3Fe-4S). Sdh3 and Sdh4 harbor two ubiquinone reduction sites and a *b*-type heme at the interface of both subunits. Only the high affinity ubiquinone reduction site (Q_p) is used during electron transport and the crystal structure of complex II has shown that the Q_p is formed by Sdh3, Sdh4 but also part of the Sdh2 domain. The role of both the *b*-type heme and low affinity ubiquinone reduction (Q_d) sites remain unclear. Yeasts deprived of their *b*-type heme are still able to assemble a functional complex II (Oyedotun et al. 2007).

Unlike complex I, III or IV, complex II does not contribute to the formation of the proton gradient. The succinate oxidation into fumarate has been described to function as a two state 'free – occupied mechanism' (Cheng et al. 2015) where the reaction would go as follows: binding of succinate to complex II induces conformational changes of the enzyme from free to occupied. During occupied conformation, the FAD cofactor is reduced. The occupied conformation becomes unstable once the FAD is reduced into $FADH^-$ and the conformational equilibrium is shifted toward free again, where fumarate binding is unfavorable and thus released. The electron can then be transferred to the nearest Fe-S cluster (2Fe-2S) and then to the 4Fe-4S and 3Fe-4S centers and the cycle is repeated.

In OXPHOS complexes, the most hydrophobic subunits are encoded in the mitochondrial genome, while most hydrophilic subunits are encoded in the nuclear genome. In contrast, all four subunits, including the membrane anchored Sdh3 and Sdh4, are usually encoded in the nuclear genome except in primitive mitochondrial genomes such as the one of *Reclinomonas americana* where Sdh3 is found (Lang et al. 1997). The exact mechanism for the assembly of complex II has yet to be fully comprehended but clues have been given by studies on yeast. We currently know six assembly factors involved in complex II biogenesis [reviewed in (Rutter et al. 2010; Van Vranken et al. 2015)]. It is accepted that Sdh1 and Sdh2 matrix proteins dimerize prior to the assembly with Sdh4 and Sdh3 membrane proteins. The first step of the assembly process is the maturation of the Sdh1 and Sdh2 subunits. The insertion of the FAD cofactor to Sdh1 requires Flx1, a protein involved in maintaining the mitochondrial matrix balance in flavin nucleotide (Tzagoloff et al. 1996).The flavinylation of FAD requires Sdh5, a mitochondrial assembly factor (Hao et al. 2009), which is only found associated with Sdh1, when the latter is not dimerized with Sdh2. Sdh5 is likely to interact with Sdh1 but not directly with the FAD group. Interestingly, loss of Sdh5 does not lead to complete impairment of complex II (Van Vranken et al. 2015;Eletsky et al. 2012). During this stage, the Sdh8 assembly factor has been shown to be associated with Sdh1 until dimerization occurs. Its role has been speculated to protect FAD and to maintain Sdh1 in an assembly competent state (Van Vranken et al. 2015).

Regarding Sdh2 maturation, incorporation of the Fe-S clusters is needed prior to dimerization. This step involves at least two assembly factors named Sdh6 and Sdh7. Despite the fact that both proteins possess a LYR motif, recently identified as interacting with Fe-S centers in mammals (Rouault 2015), no direct evidence currently points at those proteins as actually playing

a role in Fe-S clusters transfer into the Sdh2 subunits. These two assembly factors are thought to protect the Sdh2 subunits and the Sdh1/Sdh2 dimers before assembly with Sdh3 and Sdh4 (Un et al. 2014). Little is known about the Sdh3 and Sdh4 subunits assembly process, beside the fact that Sdh1 and Sdh2 seem to be needed for Sdh3 and Sdh4 to assemble. At last, a protein named Tcm62 has been shown to play a role in complex II assembly. A mutant isolated in yeast was shown to be depleted in complex II activity (Dibrov et al. 1999). The exact role of Tcm62 is still under discussion but it has been suggested to support protein folding, most likely primarily Sdh2 (Rutter et al. 2010;Dibrov et al. 1999).

In *C. reinhardtii* three out of these six assembly factors have been predicted based on genome analysis (Table 1), but little is known about eventual similarities or differences in the assembly steps. To our knowledge, no complex II mutants have been characterized so far but a mutant potentially affected for Sdh3 has been identified in the indexed mutant library recently produced (Li et al. 2016). It is interesting to note that even though *C. reinhardtii* is part of the green lineage, its complex II doesn't share the complexity of complex II in land plants which is composed of eight subunits (Salinas et al. 2014).

2.3 Complex III

Complex III (EC 1.10.2.2), the third complex of the OXPHOS chain and the second proton pumping complex, catalyzes the following reaction

$2QH_2$ + 2 ferricytochrome *c* + $2H^+_{Matrix}$ => QH2 + 2 ferrocytochrome *c* + $4H^+_{IMS}$

It functions as a multiprotein homodimeric structure of approximately 490 kDa, each monomer containing ten to eleven subunits in yeast and mammals. Among these, the three core subunits are homologs to the three subunits of prokaryotic complex III (Trumpower 1990b): cytochrome *b* (COB), cytochrome c_1 (CYC1) and Rieske iron-sulfur protein (ISP) while eight subunits are supernumerary subunits. Cytochrome *b* contains the ubiquinone oxidation site (Q_o) and ubiquinone reduction site (Q_i) separated by two *b*-type hemes. One heme (b_L) is close to the Q_o site and has a low redox potential, and the other heme (b_H) has a high potential heme (Wenz et al. 2009). The Rieske protein contains a 2Fe-2S center allowing transfer from cytochrome *b* to cytochrome c_1. Cytochrome c_1 contains a *c*-type heme.

Complex III participates to proton gradient formation through the Q cycle (Trumpower 1990a). In short, upon oxidation of ubiquinol at the Q_o site (on the IMS side), two protons are

released into the IMS while two electrons are transferred through complex III. The first electron will be transferred successively to iron sulfur Rieske protein, to cytochrome c_1 and then to soluble cytochrome *c*. The second electron will be transferred on the b_L heme and then on the b_H heme. This electron will then reduce a ubiquinone into a semiquinone at the Q_i site on the matrix side. The newly oxidized ubiquinone will then leave the Q_o site and the cycle is repeated when a second ubiquinol enters and gets oxidized, leading to a second electron being transferred to cytochrome *c*, and the semiquinone to be fully reduced into ubiquinol on the Q_i site by the second electron. In terms of protons, the result of this four electrons transfer is four protons being ejected into the IMS and two protons from the matrix being used to produce a ubiquinone on the Q_i site. The key to the Q cycle is the correct routing of both electrons to either the Rieske protein or the b_L heme. The flexibility of the Rieske protein and its dual conformation in oxidizing and reducing competent positions (Zhang et al. 1998) seem to be one of the main elements for the Q cycle. Recently, the so called "surface-affinity modulated ISP-ED (extrinsic domain of iron sulfur protein) motion switch hypothesis" (Xia et al. 2013), proposes that the binding of an ubiquinol into the Qo site will trigger conformational changes, maybe due to the widening of Qo to accept the substrate. This would transmit a signal to an alpha helix around Qo to switch into "on" position, increasing the affinity of the Rieske protein for cytochrome *b*. This will lock the Rieske protein in a position where it can receive an electron from cytochrome *b* but cannot give it to cytochrome c_1, now too far away. The Rieske protein is locked in docking position with cytochrome *b* until ubiquinone has been released. This will force the second electron to go through b_L. Once both electrons are transferred and the ubiquinone released, the Rieske protein is freed from its interactions with cytochrome *b*, allowing it to move to a closer position to cytochrome c_1 and transfer its electron. It has been proposed that the reduction events in both Rieske and b_L happens simultaneously (Zhu et al. 2007).

In complex III, only the COB subunit is synthesized inside the mitochondrion, all other proteins are imported from the cytosol. Currently, our knowledge about complex III assembly is scarce. Indeed, only a limited number of assembly factors have been described from investigation in yeast. Accordingly, the yeast nomenclature will be used for the following description.

COB is known to be the first protein in the assembly process. Cpb6 and Cpb3 assembly factors are known to be part of the COB assembly process. These proteins have been proposed to interact early in the assembly process directly with the ribosome and to be needed for efficient

translation (Gruschke et al. 2011); these two assembly factors are also important for complex III maturation since they are found on early subcomplex intermediates (Gruschke et al. 2012). The Cpb4p assembly factor has also been shown to be part of an early COB subcomplex, though it does not interact with the Cpb3 and Cbp6 assembly factors (Brand et al. 2014). During this first stage of assembly, Qcr7 and Qcr8 supernumerary subunits are added to the newly synthetized COB subunit. Qcr7 and Qcr8 seem important for the progress of assembly, since the deletion of the corresponding genes prevent further subcomplexes to be produced (Zara et al. 2007). The next step is the assembly of the core protein 1 (encoded by COR1) and core protein 2 (encoded by QCR2) subunits and cytochrome c_1. There is currently no data on how these subunits are assembled, but because their absence prevents the assembly of later subcomplexes, they might be incorporated simultaneously (Zara et al. 2007). It has also been shown that these subunits are able to interact together and form small complexes if the initial COB subcomplex is not present. The incorporation of core proteins 1 and 2 triggers the release of the Cpb4 assembly factor (Gruschke et al. 2012). This stage of assembly is referred to as the late core assembly stage. In addition to the core proteins 1 and 2 and cytochrome c_1 subunits, this intermediary subcomplex also contains the Qcr6 and Qcr9 supernumerary subunits and an additional assembly factor called Bcs1. Bcs1 is an AAA ATPase needed for the latter insertion of ISP (Rieske) protein (Conte et al. 2015). The Bca1 assembly factor has also been shown to play a role in the formation of the late core assembly stage though its exact role is still unknown (Mathieu et al. 2011). At this stage, complex III has been shown to already be in its dimeric conformation (Conte et al. 2015). The last stage of assembly consists in the addition of the ISP (Rieske) protein and the Qcr10 subunits and requires the Bcs1p and Mmz1p assembly factors. Qcr9, along with Mzm1, has been shown to be able to interact specifically with ISP in yeast, in strains where early assembly intermediates are stalled (Phillips et al. 1993; Smith et al. 2012). The Mzm1p possesses a LYR motif that might interact with the Fe-S center of ISP (Smith et al. 2012). The Coq8 protein has been predicted to be a chaperone for complex III (Brasseur et al. 1997), and was also linked to coenzyme Q synthesis pathways (Do et al. 2001). Its role in complex III assembly has thus been proposed to be related to quinone availability. Though only known to be present in metazoans, TTC19, an inner membrane protein possessing a tetratricopeptide motif, has been shown to be involved in complex III assembly (Ghezzi et al. 2011), possibly as a chaperone. In *C. reinhardtii*, only four assembly factors have been identified so far in the genomic sequence (Table 1).

Cytochromes *c* are redox active proteins containing a *c*-type heme covalently bound by two cysteine residues. In mitochondria, cytochromes *c* are represented by cytochrome c_1 in complex III and soluble cytochrome *c*. Various assembly mechanisms have been identified and described for cytochromes *c* (Mavridou et al. 2013;Allen et al. 2008). In mitochondria, system III is used to import and mature cytochrome *c* while cytochrome *c1* is imported differently through the TIM/TOM machineries (Mavridou et al. 2013). System III requires the intervention of a unique enzyme for cytochrome *c* maturation, the cytochrome *c* heme lyase or the cytochrome *c1* heme lyase.-In yeast, Cyt2 has been shown to be a cytochrome c_1 heme lyase (Zollner et al. 1992) and Cyc3 have been shown to be a cytochrome *c* heme lyase (Dumont et al. 1987), though the later was shown to also be active on cytochrome c_1 (Bernard et al. 2003). In *C. reinhardtii*, cytochrome *c* and cytochrome c_1 lyases are also present (Bernard et al. 2003). Humans only possess one gene with both functions (Prakash et al. 2002). In yeast, Cyc2 is also involved in cytochrome c/c_1 maturation. Cyc2 was proposed to regulate Cyc3 activity and participate in heme attachment. It seems to be essential when Cyt2 is inactive (Bernard et al. 2003;Smith et al. 2012). No Cyc2 homolog was found in *C. reinhardtii* (Salinas et al. 2014).

Complex III in *C. reinhardtii* possesses eleven subunits (Table 1). Among them, ten are conserved between *C. reinhardtii*, humans and *A. thaliana*, MPPA1 being the only protein specific to *C. reinhardtii*. Core protein 1 and core protein 2 from higher plants possess a proteolytic activity (Mitochondrial Processing Peptidase or MPP) that cleaves the transit peptide of preproteins when they are imported into mitochondria (Glaser and Dessi 1999). In *Chlamydomonas*, QCR1 (homolog of core 1 protein) exhibits consensus sequences typical of β-MPP protein while MPPA2 (homolog of core 2 protein) does not share consensus sequences for α-MPP activity (van Lis et al. 2003). Nevertheless, a third component, with the characteristics of an MPP α subunit (MPPA1) is also encoded in *Chlamydomonas* (Cardol et al. 2009a). The question of the *in vivo* mitochondrial processing activity of complex III in *C. reinhardtii* remains thus open.

In *C. reinhardtii*, only *cob* mutants have ever been produced (listed in Salinas et al. 2014), resulting in a lack of complex III activity and assembly due to the central position of cytochrome *b* subunit. *Chlamydomonas* complex III mutants lack the whole cytochrome pathway of respiration due to the colinearity of both complexes III and IV. The resulting lack of ATP caused by the loss of the two proton-pumping enzymes leads to the inability of such mutants to

grow under heterotrophic condition (acetate + dark) (Salinas et al. 2014). This inability to grow in the dark is the main screening method currently used to obtain complex III mutants. Mutants can also be identified using a TTC (triphenyltetrazolium chloride) reducing test (Dorthu et al. 1992). In *C. reinhardtii*, complex III deficiencies have been shown to be impactful enough to disturb photosynthesis (Cardol et al. 2003). When coupled with a *stt7* mutation, leading to the lack of flexibility in energy redistribution between photosystems, complex III mutants display a drop in photosynthetic efficiency when measured both in the dark and the light. This phenotype allows easy identification of complex III mutants using fluorescence measurements (Cardol et al. 2009b; Massoz et al. 2015).

2.4 Complex IV

Complex IV (1.9.3.1) is the last proton pumping complex of the OXPHOS chain with a size of approximately 200 kDa. It catalyzes the reaction

4 ferrocytochrome *c* + O_2 + $8H^+_{matrix}$ -> 4 ferricytochrome *c* + $2H_2O$ + $4H^+_{IMS}$

The Cox1, Cox2 and Cox3 subunits are the core subunits of complex IV. The Cox1 subunit bears heme *a*, heme a_3 and the Cu_B center. The Cox2 subunit carries the Cu_A center while the Cox3 subunit does not bear any prosthetic groups. In most organisms, Cox1, Cox2 and Cox3 are encoded in the mitochondrial genome as they are membrane embedded subunits. In addition, around seven to eleven supernumerary subunits have been identified in mammals, yeasts or plants (reviewed in Salinas et al. 2014).

In complex IV, four electrons are transported onto molecular oxygen to produce two water molecules, while four protons are transferred into the IMS. Two proton-transfer channels have been identified in the Cox1 protein. They are called D and K channels, based on the presence of conserved Asp (D) and Lys (K) residues at the beginning of each channel respectively. The D channel is filled with a series of ordered water molecules forming a proton conductive pathway and helping to reach a conserved Glu residue at its end. Electrons are transferred from soluble cytochrome *c* through Cu_A and heme *a* towards the binuclear center (Cu_B and heme a_3; BNC). The proton transfer mechanisms contain several steps involving the BNC and are reviewed in (Kaila et al. 2010). In short, the ligation of the molecular oxygen to the BNC leads to a split of the molecule. Following that event, four cycles of one electron reduction step occur, accompanied by the pumping of two protons each time; one into the proton-loading site (PLS) and one into the

BNC for chemistry. Though the four cycles have identical chemical balance, they all possess different kinetics. The proton pumped into the PLS is transferred into the IMS by a still unknown mechanism. It has been shown that the K channel only participates in one (maybe two) proton transfer(s) (Wikström et al. 2000; Svensson-Ek et al. 2002). Notably, during the reductive phase when the heme a_3 might be already bound to a water molecule, (the) proton(s) would be pumped through the K channel which is the closest to the Cu_B center. This would lead the D channel to effectively pump the four protons leading to the PLS and at least two of the protons leading to the BNC. From this perspective, one can ask how protons from the same channel can be routed toward PLS or BNC. Water wire pathways would form leading preferentially toward one site or another (Wikström et al. 2000). This water gate phenomenon has been shown to be dependent on the redox state of the two hemes of the enzyme and helps redirect proton toward the right site. The Cox3 subunit is a major subunit of complex III but it does not carry any redox component. It has been shown that a mutant in COIII (Cox3 homologue) of *Paracoccus denitrificans* might assemble a COI and COII (Cox1 and Cox2 homologue) subcomplex, though not properly functional (Haltia et al. 1989). Studies showed that Cox3 was important for maintaining the correct function of the D channel (Hosler 2004). The Cox3 area surrounding the conserved Asp in the D channel has been proposed to raise the proton affinity for this conserved amino acid to trap protons. In addition, COXIII has been shown to stabilize a hydrocarbon chain in close proximity to the water chain inside the D channel, potentially helping them to maintain a correct arrangement inside the channel. COXIII also plays a key role in maintaining the exit proton pathway.

Complex IV biogenesis is by far the most understood assembly process among OXPHOS complexes in yeast with more than thirty assembly factors identified so far, with various functions from RNA stabilizing to heme maturation. Unfortunately, most of these identified proteins have no equivalents in *Chlamydomonas* (Table 1). It is accepted that the three Cox subunits assemble and mature independently of each other before being assembled together. This process is reviewed in (Soto et al. 2012). The Cox1 subunit is the first to be inserted in the membrane, a process which requires at least the conserved Oxa1 protein. Cox2 is then inserted and processes in the membrane thanks to at least Oxa1 in addition to the Cox20 and Cox18 assembly factors. The two proteins will then be attached to each other. The Cox3 subunit will then be assembled and attached to the Cox1 and Cox2 subcomplex. Unlike the Cox assembly

process, the heme insertion and maturation assembly seem much more conserved between yeast and *Chlamydomonas*. The current knowledge is reviewed in (Barrientos et al. 2009; Soto et al. 2012). The copper cofactor maturation pathway involved the Cox17, Cox19 and Cox23 assembly factors; these three soluble proteins possess copper binding motifs and are thought to be part of a copper distribution pathway. The Cox17 assembly factor would also transfer copper to Sco1 and Cox11, two membrane chaperones proposed to facilitate copper insertion into the Cox1 and Cox2 subunits. *Cox17* mutants have been produced in *Chlamydomonas* (Remacle et al. 2010). In *cox17* mutants, total amount of complex IV was found unchanged, but complex IV activity was decreased, an observation that was explained by a diminished copper availability. Inside complex IV, hemes *a* are present. These hemes are derived from heme *b* transformed into heme *O* and then finally into heme *a.* The conversion from heme *b* to heme *O* is processed by at least Cox10 while the conversion from heme *O* to heme *a* is processed through two discrete monooxygenase steps. The first step is catalyzed by at least Cox15, Mfdx (Yah1 in yeast) (Barros et al. 2001) and Arh1 (Soto et al. 2012). No enzyme has been yet identified as candidate for the subsequent oxidation step (Soto et al. 2012). Interestingly, a *C. reinhardtii* mutant (called w17) was recently identified in a hydroxylase/monooxygenase with a partial dark growth defect phenotype (Massoz et al. 2015). It was later shown that this mutant possessed a 30% reduced complex IV activity (Massoz, unpublished data), though a clear relationship between the depleted gene and the actual phenotype remains to be demonstrated.

In *C. reinhardtii*, ten subunits have been confirmed to compose complex IV and eight potential subunits homologous to those found in other eukaryotes were found in the genome (Cardol et al. 2005;van Lis et al. 2003) including the subunit COX90 specific to *Chlamydomonas* (Lown et al. 2001). COX2 and COX3 are encoded in the nucleus in *C. reinhardtii* (Perez-Martinez et al. 2001; Perez-Martinez et al. 2002). In addition, the *COX2* gene is split into *COX2a* and *COX2b* genes, a characteristic shared by all chlorophycean algae (Rodriguez-Salinas et al. 2012). Both *COX3* and *COX2a/b* have gained attributes from nuclear genomes, proper codon usage and introns, and an overall decreased hydrophobicity in the corresponding gene products compared to their mitochondria-encoded counterparts (Perez-Martinez et al. 2001).

Complex IV nuclear mutant (*cox3* mutant) or mitochondrial mutant (*cox1* mutant) in *C. reinhardtii*, show no complex IV activity or assembly altogether (Colin et al. 1995; Remacle et al. 2010) and, like complex III mutants, lack the whole cytochrome pathway of respiration.

2.5 ATP synthase

Mitochondrial F_1Fo-ATP synthase (EC 3.6.1.3) has a pivotal role in OXPHOS by catalyzing the reaction ADP + Pi + nH^+_{IMS} <=> ATP + nH^+_{Matrix}. The complex is present in the inner mitochondrial membrane and forms oligomers that are believed to determine the morphology of the yeast mitochondrial cristae (Paumard et al. 2002). Although exhibiting some differences, the well-characterized yeast and the beef heart enzymes share a similar subunit composition. The enzyme works as a molecular motor (Oster and Wang 2003) with a central rotary axis [formed by subunits γ/δ/ε/*c*-ring] and several fixed elements that include the catalytic core (subunits α_3/β_3), a peripheral stalk (OSCP/*b*/*d*/F6), a dimerization module (A6L/*e*/*f*/*g*) and other fixed elements (subunit *a*) (Arselin et al. 2004; Walker and Dickson 2006). Proton passage through both subunit *a* and the *c*-ring induces the rotation of the γ/δ/ε central-stalk (Wächter et al. 2011). The rotation of subunit γ impels the three catalytic β subunits to form ATP from ADP + Pi (Yasuda et al. 1998). The peripheral stalk impedes rotation of the α_3/β_3 moiety while counteracting the torque generated by the rotation of the γ subunit (Dickson et al. 2006). Regulatory polypeptides such as the inhibitory protein IF_1, prevents the enzyme from hydrolyzing ATP (Gledhill and Walker 2005).

The mitochondrial ATP synthase of chlorophycean algae has diverged substantially from the yeast and bovine enzymes and exhibits salient differences in terms of subunit composition and structural features. For example, both the *C. reinhardtii* β- and α-subunits exhibit atypical sequences extensions of 70 residues in the C-terminus and of 18 residues in the N-terminus respectively (Franzén and Falk 1992;Nurani and Franzén 1996). Much has been learned on the structure and function of the mitochondrial ATP synthase from algae by studying the enzyme from *Polytomella* sp., a colorless, close relative of *Chlamydomonas* that lacks chloroplasts and a cell wall (Figueroa-Martinez et al. 2015). Lauryl maltoside-solubilized mitochondrial F_1Fo-ATP synthases of *C. reinhardtii* and *Polytomella* sp. migrate in blue-native electrophoresis as a 1,600 kDa dimer (van Lis et al. 2003; Villavicencio-Queijeiro et al. 2009). When the *C. reinhardtii* genome became known (Merchant et al. 2007), the components of the enzyme whose N-terminal sequences had been previously obtained by Edman degradation (Funes et al. 2002) were identified Thus, the enzyme was found to be constituted by the classical subunits α, β, γ, δ, *a* (ATP6), *c* (ATP9), and OSCP, while no homologs of the ε, *b*, *d*, *e*, *f*, *g*, IF_1, A6L, and F6 subunits could be found encoded in the algal genome . In addition, the enzyme contained polypeptides with no known counterparts in the

databases and these were named Asa1 to Asa9, for "ATP synthase associated components" (Fig. 3). The polypeptide composition of the mitochondrial ATP synthase of *Polytomella* sp. was found to be similar to the one of *C. reinhardtii* enzyme (Vazquez-Acevedo et al. 2006;van Lis et al. 2007). Although the biochemical characterization of the mitochondrial ATP synthase has been carried out mainly with *C. reinhardtii* and *Polytomella* sp., genes encoding homologs of Asa subunits are found in other chlorophycean algae including members of the genera *Chlamydomonas, Chloroccocum, Dunaliella*, *Polytomella, Scenedesmus* and *Volvox* (Lapaille et al. 2010;Colina-Tenorio et al. 2015). The idea that these unique proteins could be the main constituents of the peripheral stalk of the complex and the elements responsible of the enzyme dimeric nature was formulated (Lapaille et al. 2010;Colina-Tenorio et al. 2015). All the subunits that form the mitochondrial ATP synthase of chlorophycean algae seem to be nucleus-encoded; to date, no genes encoding a subunit of the enzyme has been identified in the corresponding algal mitochondrial genomes (Vahrenholz et al. 1993;Smith and Lee 2009;Smith et al. 2010; Hamaji et al. 2013), not even the three mitochondrial genes frequently present in mtDNA: *atp6*, *atp8* and *atp9*.

.The isolated mitochondrial ATPases from the green alga *C. reinhardtii* exhibited a specific activity of 2.9 U/mg with only 40% sensitivity to oligomycin (Nurani and Franzén 1996), an antibiotic that usually fully inhibits the enzyme. The *Polytomella* sp. enzyme showed a very low ATPase activity that markedly increased up to 3.8 U/mg when non-ionic detergents are present in the activity assay. The hydrolytic activity is sensitive to the classical inhibitors oligomycin and DCCD (Villavicencio-Queijeiro et al. 2015), although oligomycin seems to bind loosely. Indeed, while oligomycin readily inhibits algal growth, respiration, and ATP levels in several classes of Chlorophytes, chlorophycean algae seem not to be affected (Lapaille et al. 2010).

Neighboring interactions of Asa subunits in the ATP synthase of *Polytomella* sp. have been studied by silencing the expression of Asa subunits; generating sub-complexes by partial dissociation of complex V; reconstituting sub-complexes using recombinant subunits *in vitro*; cross-linking the purified enzyme and modelling the complex by EM image reconstruction. Knock-down experiments using RNA interference abolished expression of the Asa7 subunit in *C. reinhardtii*. Although neither growth nor OXPHOS of the alga were affected, the intact enzyme could not be isolated, since it dissociated upon lauryl maltoside solubilization (Lapaille et al. 2010). Therefore, Asa7 was proposed to play a pivotal role in maintaining the stability of the

peripheral stalk. Asa1 is thought to be the main support of the peripheral stalk, playing a structural role analogous to subunit *b* in orthodox enzymes (Colina-Tenorio et al. 2015), probably making a bridge between the OSCP subunit and other polypeptides that may be embedded in or closer to the membrane (Asa3, Asa5, Asa8, *a* and c_{10}-ring). Subunits Asa2, Asa4 and Asa7 interact to form an Asa2/Asa4/Asa7 subcomplex that establishes contacts with Asa1 and with OSCP (Miranda-Astudillo et al. 2014), thus, the peripheral stalk seems to be formed by the intertwining of several polypeptides, including Asa1, Asa2, Asa4 and Asa7. In contrast, the smaller subunits Asa6, Asa8 and Asa9 are predicted to have transmembrane stretches and to form the dimerization domain of the algal mitochondrial ATP synthase. An updated model for the topological disposition of the 17 polypeptides that constitute the algal enzyme has been proposed recently (Vázquez-Acevedo et al. 2016) and is shown in Fig. 3.

The dimeric algal ATP synthase has been observed in several electron-microscopy studies including 3D tomography (Dudkina et al. 2005;Cano-Estrada et al. 2010; Dudkina et al. 2010). The ATP synthase oligomers seem to make helical arrangements along the cristae membranes, confirming the role of complex V in determining the shape of the inner mitochondrial membrane (Dudkina et al. 2006). An electron cryo-microscopy map of the *Polytomella* sp. dimeric ATP synthase at 6.2 Å resolution (Allegretti et al. 2015) has revealed some finer architectural details (Fig. 3). A salient feature is that the peripheral stalks are very robust and constituted by alpha-helices that seem to form coil-coiled structures that contact the F_1 sector more than once. The overall dimeric structure is further reinforced by protein-protein contacts that unite the two peripheral stalks in their middle region. Subunit *a* was found to contain four alpha-helices that are embedded in the bilayer almost horizontally, partially surrounding the *c*-ring. A high resolution structure of the algal mitochondrial ATP synthase is still needed in order to learn about the detailed topology of all its components.

Although some studies have addressed the biogenesis of the CF_1-CFo chloroplast ATP synthase of *Chlamydomonas* (Drapier et al. 2007), almost nothing is known about the assembly of its mitochondrial counterpart. Nevertheless, the mitochondrial enzyme is expected to follow the almost universal three-module process that has been described for the F_1Fo-ATPases of bacteria, chloroplasts and mitochondria (Rühle and Leister 2015). The biogenesis of the mitochondrial system has been studied in depth in yeast, where complex V assembles in distinct independent modules (Rak et al. 2011): *i*) the soluble F_1 module comprising subunits $\alpha_3/\beta_3/\gamma/\delta/\varepsilon$,

ii) the c_{10}-ring of the Fo sector, and *iii*) a stator module comprising subunits *a*/*b*/*d*/*h*/8. In consecutive steps, the F_1 module associates to the membrane-bound c_{10}-ring forming a $\alpha_3/\beta_3/\gamma/\delta/\varepsilon/c_{10}$ subcomplex and subsequently to subunit *a* of the stator module, giving rise to a $\alpha_3/\beta_3/\gamma/\delta/\varepsilon/c_{10}$ /*a*/*b*/*d*/*h*/8 subcomplex. The possibility of futile proton efflux in early stages of the assembly of such a complex enzyme driven by the chemiosmotic potential is avoided by the late addition of the c_{10}-ring to the proton-translocating subunit *a*. The whole complex is then completely stabilized by the further incorporation of the membrane-bound subunit *f* and of the OSCP subunit, the latter one binding to the peripheral stalk and to the α_3/β_3 catalytic core, therefore fixing together all the stator components of the ATP synthase. Dimerization of the enzyme must occur upon the incorporation of the membrane-bound subunits *e* and *g*. One can only speculate that the *C. reinhardtii* complex V will follow a similar biogenesis pathway with a three-module assembly process, nevertheless, it is clear it will exhibit some distinct features, since the highly robust peripheral arm and the dimerization sector must be assembled through sequential incorporation of all the atypical Asa subunits found only in chlorophycean algae.

The complex assembly of the mitochondrial F_1Fo-ATP synthase is assisted at all stages by several chaperones and assembly factors. The biogenesis of the soluble F_1 module (subunits $\alpha_3/\beta_3/\gamma/\delta/\varepsilon$) is facilitated by the matrix-localized chaperones Fmc1p, Hsp90, Atp11p and Atp12p (Lefebvre-Legendre et al. 2001); (Wang et al. 2001); (Francis and Thorsness 2011). Homologs of all these four proteins are present in *C. reinhardtii* (see Table 1). In addition, other players in the formation of the Fo sector have also been identified in the green alga: Atp25, that participates in the expression and oligomerization of subunit *c* (Zeng et al. 2008) and Oxa1, that plays a role in the association of the *c*-ring with subunit *a* (Jia et al. 2007). In contrast, other assembly factors previously characterized in the yeast system including Atp22 (that promotes synthesis of subunit *a*), Atp23 (that is involved in the maturation of subunit *a*), and Atp10 (that promotes the association of subunit *a* with subunit 8) seem not to be present in the green alga.

3. Alternative pathways

In addition to the four main complexes, alternative type-II NAD(P)H dehydrogenases can transfer electrons from NADH to ubiquinone and alternative oxidase (AOX) from ubiquinone to molecular oxygen (Fig. 1). These alternative enzymes do not participate in the formation of a proton gradient. Mitochondrial type-II NAD(P)H dehydrogenases located on the surface of the

mitochondrial inner membrane face either the intermembrane space or the matrix. They are monomeric enzymes of 40 to 60 kDa contrary to the multimeric type-I NADH dehydrogenases (complex I) and usually contain one non-covalently bound FAD as prosthetic group (Møller et al. 1993). Alternative oxidases are homodimeric and the monomeric unit has a size of about 40 kDa. They contain a covalently bound diiron center that catalyzes the four-electron reduction of dioxygen to water by ubiquinol (Siedow et al. 1995; Shiba et al. 2013). The presence of these two types of enzymes allows for better survival of *C. reinhardtii* mutants affected in complex I, III or IV and partly explains why isolating mutants deficient for OXPHOS complexes in *C. reinhardtii* is possible.

In *C. reinhardtii*, alternative oxidase is encoded by two genes: *AOX1* and *AOX2* (Dinant et al. 2001), with *AOX1* being the most abundant transcript. Multiple roles are assigned to alternative oxidase. First it serves as security valve preventing over-reduction of the ubiquinone pool, and thus acting as against ROS accumulation (Milani et al. 2001) and allowing a better functioning for complex III, since ubiquinone is required in the Q cycle. Second, the AOX pathway, serving as a modular exit point for electrons, would allow a more constant reoxidation of NADH, which is used as electron acceptor upstream of the OXPHOS. Such functions are reflected in *Chlamydomonas* AOX-RNAi cell lines (Mathy et al. 2010), where ROS production is increased up to 5 fold and the ROS scavenging enzymes are overexpressed. The mutant cell lines also exhibit heavy metabolic changes (Mathy et al. 2010) with an overall decrease in the catabolic pathways such as glycolysis, Krebs cycle, glyoxylate cycle and a shift toward anabolic pathways. These metabolic changes lead to increased cell size and biomass without any impact on growth rate. In complex III mutants or WT strain exposed to H_2O_2, *AOX1* transcripts exhibit increased expression (Dinant et al. 2001) correlated to an increased amount of proteins (Molen et al. 2006).

AOX has also been shown to be induced in *Chlamydomonas* by a variety of stresses including cold, ROS exposure, change in the source of nitrogen source (Molen et al. 2006) or heat (Zalutskaya et al. 2015). All these external conditions are likely to activate several specific transcription factors, since a reporter gene built with a 1073 bp fragment of the *AOX1* promoter would not respond to all stresses (Molen et al. 2006). Post-transcriptional regulations are also involved since the complex III inhibitor antimycin A leads to an increase at the transcript level but not at the protein level (Molen et al. 2006).

Alternative NADH dehydrogenase transfers electrons from NADH to the ubiquinone pool. Among the six type II NADH dehydrogenases identified in *Chlamydomonas* (Cardol et al. 2005), the 53 kDa NDA1 has been shown to be localized at the inner side of the mitochondrial membrane (Lecler et al. 2012) (Fig. 1) while NDA2 and NDA3 were found to be located in the chloroplast (Jans et al. 2008;Terashima et al. 2010). The loss of NDA1 was correlated to a slight decrease of NADH dehydrogenase activity but no impact on heterotrophic growth was observed. However, when coupled to a complex I mutation, severe respiratory and growth defects could be observed, underlining the importance of the enzyme in NADH oxidation in the absence of complex I (Lecler et al. 2012).

Acknowledgements

Simon Massoz is a recipient of PhD FRIA fellowship (Fond pour la formation à la Recherche dans l'Industrie et dans l'Agriculture). Pierre Cardol is a research associate from F.R.S.-FNRS (Fond de la Recherche Scientifique). Technical support from Q.B.P. Miriam Vázquez-Acevedo and financial support from grants 245486 from CONACyT-F.R.S.-FNRS (Mexico-Belgium) and from grants 239219 (CONACyT, Mexico), IN203311-3 (DGAPA-UNAM, Mexico) and MIS F.4520, FRFC 2.4597, and CDR J.0032 (Belgian F.R.S.-FNRS) are also gratefully acknowledged.

References

Allegretti M, Klusch N, Mills DJ, et al (2015) Horizontal membrane-intrinsic α-helices in the stator a-subunit of an F-type ATP synthase. Nature 521:237–40. doi: 10.1038/nature14185

Allen JWA, Jackson AP, Rigden DJ, et al (2008) Order within a mosaic distribution of mitochondrial c-type cytochrome biogenesis systems? FEBS J 275:2385–2402. doi: 10.1111/j.1742-4658.2008.06380.x

Arselin G, Vaillier J, Salin B, et al (2004) The modulation in subunits e and g amounts of yeast ATP synthase modifies mitochondrial cristae morphology. J Biol Chem 279:40392–40399. doi: 10.1074/jbc.M404316200

Atteia A, Adrait A, Brugire S, et al (2009) A proteomic survey of Chlamydomonas reinhardtii mitochondria sheds new light on the metabolic plasticity of the organelle and on the nature of the α-proteobacterial mitochondrial ancestor. Mol Biol Evol 26:1533–1548. doi: 10.1093/molbev/msp068

Baradaran R, Berrisford JM, Minhas GS, Sazanov LA (2013) Crystal structure of the entire respiratory complex I. Nature 494:443–8. doi: 10.1038/nature11871

Barbieri MR, Larosa V, Nouet C, Subrahmanian N, Remacle C, Hamel PP (2011) A forward genetic screen identifies mutants deficient for mitochondrial complex I assembly in Chlamydomonas reinhardtii. Genetics. 188:349-58. doi: 10.1534/genetics.

Barrientos A, Gouget K, Horn D, et al (2009) Suppression mechanisms of COX assembly defects in yeast and human: Insights into the COX assembly process. Biochim Biophys Acta - Mol Cell Res 1793:97–107. doi: 10.1016/j.bbamcr.2008.05.003
Barros MH, Carlson CG, Glerum DM, Tzagoloff A (2001) Involvement of mitochondrial ferredoxin and Cox15p in hydroxylation of heme O. FEBS Lett 492:133–138. doi: 10.1016/S0014-5793(01)02249-9
Bernard DG, Gabilly ST, Dujardin G, et al (2003) Overlapping Specificities of the Mitochondrial Cytochrome c and c 1 Heme Lyases. J Biol Chem 278:49732–49742. doi: 10.1074/jbc.M308881200
Berrisford JM, Baradaran R, Sazanov LA (2016) Structure of bacterial respiratory complex I. BBA - Bioenerg. doi: 10.1016/j.bbabio.2016.01.012
Brand AM Van Den, Jonckheere A, Wanschers BFJ, et al (2014) A mutation in the human CBP4 ortholog UQCC3 impairs complex III assembly , activity and cytochrome b stability. 23:6356–6365. doi: 10.1093/hmg/ddu357
Brandt U (2011) A two-state stabilization-change mechanism for proton-pumping complex i. Biochim Biophys Acta - Bioenerg 1807:1364–1369. doi: 10.1016/j.bbabio.2011.04.006
Brasseur G, Tron P, Dujardin G, Slonimski P (1997) The nuclear ABCl gene is essential for the correct conformation and functioning of the cytochrome bc, complex and the neighbouring complexes I1 and IV in the mitochondrial respiratory chain. Eur J Biochem 246:103–111.
Bricker DK, Taylor EB, Schell JC, et al (2012) A mitochondrial pyruvate carrier required for pyruvate uptake in yeast, Drosophila, and humans. Science 337:96–100. doi: 10.1126/science.1218099
Cano-Estrada A, Vazquez-Acevedo M, Villavicencio-Queijeiro A, et al (2010) Subunit-subunit interactions and overall topology of the dimeric mitochondrial ATP synthase of Polytomella sp. Biochim Biophys Acta - Bioenerg 1797:1439–1448. doi: 10.1016/j.bbabio.2010.02.024
Cardol P (2011) Mitochondrial NADH:Ubiquinone oxidoreductase (complex I) in eukaryotes: A highly conserved subunit composition highlighted by mining of protein databases. Biochim Biophys Acta - Bioenerg 1807:1390–1397. doi: 10.1016/j.bbabio.2011.06.015
Cardol P, Alric J, Girard-bascou J, Franck F, et al (2009b) Impaired respiration discloses the physiological significance of state transitions in Chlamydomonas. Proc Natl Acad Sci U S A 106:15979–15984.
Cardol P, Boutaffala L, Memmi S, et al (2008) In Chlamydomonas, the loss of ND5 subunit prevents the assembly of whole mitochondrial complex I and leads to the formation of a low abundant 700 kDa subcomplex. Biochim Biophys Acta - Bioenerg 1777:388–396. doi: 10.1016/j.bbabio.2008.01.001
Cardol P, Gloire G, Havaux M, et al (2003) Photosynthesis and State Transitions in Mitochondrial Mutants of Chlamydomonas reinhardtii Affected in Respiration. Plant Physiol 133:2010–2020. doi: 10.1104/pp.103.028076.transition
Cardol P, González-Halphen D, Reyes-Prieto A, et al (2005) The mitochondrial oxidative phosphorylation proteome of Chlamydomonas reinhardtii deduced from the Genome Sequencing Project. Plant Physiol 137:447–459. doi: 10.1104/pp.104.054148
Cardol P, Lapaille M, Minet P, et al (2006) ND3 and ND4L subunits of mitochondrial complex I, both nucleus encoded in Chlamydomonas reinhardtii, are required for activity and assembly of the enzyme. Eukaryot Cell 5:1460–1467. doi: 10.1128/EC.00118-06
Cardol P, Matagne RF, Remacle C (2002) Impact of mutations affecting ND mitochondria-encoded subunits on the activity and assembly of complex I in chlamydomonas. Implication for the structural organization of the enzyme. J Mol Biol 319:1211–1221. doi:

10.1016/S0022-2836(02)00407-2
Cardol P, Figueroa F, Remacle C, et al (2009a). Oxidative phosphorylation: Building blocks and related component. The *Chlamydomonas* sourcebook, second edition, Vol 2, pp 469-503
Cardol P, Vanrobaeys F, Devreese B, et al (2004) Higher plant-like subunit composition of mitochondrial complex I from Chlamydomonas reinhardtii: 31 Conserved components among eukaryotes. Biochim Biophys Acta - Bioenerg 1658:212–224. doi: 10.1016/j.bbabio.2004.06.001
Cheng VWT, Piragasam RS, Rothery RA, et al (2015) Redox State of Flavin Adenine Dinucleotide Drives Substrate Binding and Product Release in Escherichia coli Succinate Dehydrogenase. Biochemistry 54:1043–1052. doi: 10.1021/bi501350j.Redox
Colin M, Dorthu MP, Duby F, et al (1995) Mutations affecting the mitochondrial genes encoding the cytochrome oxidase subunit I and apocytochrome b of Chlamydomonas reinhardtii. Mol Gen Genet 249:179–184. doi: 10.1007/bf00290364
Colina-Tenorio L, Miranda-Astudillo H, Cano-Estrada A, et al (2015) Subunit Asa1 spans all the peripheral stalk of the mitochondrial ATP synthase of the chlorophycean alga polytomella sp. Biochim Biophys Acta - Bioenerg 1857:359–369. doi: 10.1016/j.bbabio.2015.11.012
Conte A, Papa B, Ferramosca A, Zara V (2015) The dimerization of the yeast cytochrome bc 1 complex is an early event and is independent of Rip1. Biochim Biophys Acta - Mol Cell Res 1853:987–995. doi: 10.1016/j.bbamcr.2015.02.006
Dibrov E, Fu S, Lemire BD (1999) The Saccharomyces cerevisiae TCM62 gene encodes a chaperone necessary for the assembly of the mitochondrial succinate dehydrogenase (complex II). J Biol Chem 273:32042–32048. doi: 10.1074/jbc.273.48.32042
Dickson VK, Silvester J a, Fearnley IM, et al (2006) On the structure of the stator of the mitochondrial ATP synthase. EMBO J 25:2911–8. doi: 10.1038/sj.emboj.7601177
Dinant M, Baurain D, Coosemans N, et al (2001) Characterization of two genes encoding the mitochondrial alternative oxidase in Chlamydomonas reinhardtii. Curr Genet 39:101–108. doi: 10.1007/s002940000183
Do TQ, Hsu AY, Jonassen T, et al (2001) A Defect in Coenzyme Q Biosynthesis is Responsible for the Respiratory Deficiency in Saccharomyces cerevisiae abc1 Mutants. J Biol Chem 276:18161–18168. doi: 10.1074/jbc.M100952200
Dorthu MP, Remy S, Michel-Wolwertz MR, et al (1992) Biochemical, genetic and molecular characterization of new respiratory-deficient mutants in Chlamydomonas reinhardtii. Plant Mol Biol 18:759–772.
Drapier D, Rimbault B, Vallon O, et al (2007) Intertwined translational regulations set uneven stoichiometry of chloroplast ATP synthase subunits. Embo J 26:3581–3591. doi: 7601802 [pii]\r10.1038/sj.emboj.7601802
Duarte M, Mota N, Pinto L, Videira A (1998) Inactivation of the gene coding for the 30.4-kDa subunit of respiratory chain NADH dehydrogenase: Is the enzyme essential for Neurospora? Mol Gen Genet 257:368–375. doi: 10.1007/s004380050659
Dudkina N V., Heinemeyer J, Keegstra W, et al (2005) Structure of dimeric ATP synthase from mitochondria: An angular association of monomers induces the strong curvature of the inner membrane. FEBS Lett 579:5769–5772. doi: 10.1016/j.febslet.2005.09.065
Dudkina N V, Oostergetel GT, Lewejohann D, et al (2010) Row-like organization of ATP synthase in intact mitochondria determined by cryo-electron tomography. Biochim Biophys Acta - Bioenerg 1797:272–277. doi: 10.1016/j.bbabio.2009.11.004
Dudkina N V, Sunderhaus S, Braun HP, Boekema EJ (2006) Characterization of dimeric ATP synthase and cristae membrane ultrastructure from Saccharomyces and Polytomella

mitochondria. FEBS Lett 580:3427–3432. doi: 10.1016/j.febslet.2006.04.097
Dumont ME, Ernst JF, Hampsey DM, Sherman F (1987) Identification and sequence of the gene encoding cytochrome c heme lyase in the yeast Saccharomyces cerevisiae. EMBO J 6:235–241.
Efremov RG, Baradaran R, Sazanov L a (2010) The architecture of respiratory complex I. Nature 465:441–445. doi: 10.1038/nature09066
Efremov RG, Sazanov LA (2011) Structure of the membrane domain of respiratory complex I. supplementary information. Nature 476:414–20. doi: 10.1038/nature10330
Eletsky A, Jeong M, Kim H, et al (2012) Solution NMR Structure of Yeast Succinate Dehydrogenase Flavinylation Factor Sdh5 Reveals a Putative Sdh1 Binding Site. Biochemistry 51:8475–8477. doi: 10.1038/nature13314.A
Figueroa-Martinez F, Nedelcu AM, Smith DR, Reyes-Prieto A (2015) When the lights go out: The evolutionary fate of free-living colorless green algae. New Phytol 206:972–982. doi: 10.1111/nph.13279
Francis BR, Thorsness PE (2011) Hsp90 and mitochondrial proteases Yme1 and Yta10/12 participate in ATP synthase assembly in Saccharomyces cerevisiae. Mitochondrion 11:587–600. doi: 10.1016/j.mito.2011.03.008
Franzén LG, Falk G (1992) Nucleotide sequence of cDNA clones encoding the β subunit of mitochondrial ATP synthase from the green alga Chlamydomonas reinhardtii: The precursor protein encoded by the cDNA contains both an N-terminal presequence and a C-terminal extension. Plant Mol Biol 19:771–780. doi: 10.1007/BF00027073
Friedrich T, Weiss H (1997) Modular evolution of the respiratory NADH:ubiquinone oxidoreductase and the origin of its modules. J Theor Biol 187:529–40. doi: 10.1006/jtbi.1996.0387
Fromm S, Braun H, Peterhansel C (2016) Mitochondrial gamma carbonic anhydrases are required for complex I assembly and plant reproductive development. New Phytol 211:194–207. doi: 10.1111/nph.13886
Funes S, Davidson E, Gonzalo Claros M, et al (2002) The typically mitochondrial DNA-encoded ATP6 subunit of the F1F0-ATPase is encoded by a nuclear gene in Chlamydomonas reinhardtii. J Biol Chem 277:6051–6058. doi: 10.1074/jbc.M109993200
Ghezzi D, Arzuffi P, Zordan M, et al (2011) Mutations in TTC19 cause mitochondrial complex III deficiency and neurological impairment in humans and flies. Nat Genet 43:259–63. doi: 10.1038/ng.761
Glaser E, Dessi P (1999) Integration of the mitochondrial-processing peptidase into the cytochrome bc1 complex in plants. J Bioenerg Biomembr 31:259–274. doi: 10.1023/A:1005475930477
Gledhill JR, Walker JE (2005) Inhibition sites in F1-ATPase from bovine heart mitochondria. Biochem J 386:591–598. doi: 10.1042/BJ20041513
Goodenough U, Blaby I, Casero D, et al (2014) The path to triacylglyceride obesity in the sta6 strain of Chlamydomonas reinhardtii. Eukaryot Cell 13:591–613. doi: 10.1128/EC.00013-14
Gruschke S, Kehrein K, Römpler K, et al (2011) Cbp3-Cbp6 interacts with the yeast mitochondrial ribosomal tunnel exit and promotes cytochrome b synthesis and assembly. J Cell Biol 193:1101–1114. doi: 10.1083/jcb.201103132
Gruschke S, Römpler K, Hildenbeutel M, et al (2012) The Cbp3–Cbp6 complex coordinates cytochrome. J Cell Biol 199:137–150. doi: 10.1083/jcb.201206040
Guarani V, Paulo J, Zhai B, et al (2014) TIMMDC1/C3orf1 Functions as a Membrane-Embedded Mitochondrial Complex I Assembly Factor through Association with the MCIA Complex.

Mol Cell Biol 34:847–861. doi: 10.1128/MCB.01551-13
Haltia T, Finel M, Harms N, et al (1989) Deletion of the gene for subunit III leads to defective assembly of bacterial cytochrome oxidase. EMBO J 8:594–596.
Hamaji T, Smith DR, Noguchi H, et al (2013) Mitochondrial and Plastid Genomes of the Colonial Green Alga Gonium pectorale Give Insights into the Origins of Organelle DNA Architecture within the Volvocales. PLoS One. doi: 10.1371/journal.pone.0057177
Hao H, Khalimonchuk O, Schraders M, et al (2009) SDH5, a Gene Required for Flavination of Succinate Dehydrogenase Is Mutated in Paraganglioma. Science (80-) 325:1139–1142.
Helfenbein KG, Ellis TP, Dieckmann CL, Tzagoloff A (2003) ATP22, a nuclear gene required for expression of the F0 sector of mitochondrial ATPase in Saccharomyces cerevisiae. J Biol Chem 278:19751–19756. doi: 10.1074/jbc.M301679200
Hirst J, Carroll J, Fearnley IM, et al (2003) The nuclear encoded subunits of complex I from bovine heart mitochondria. Biochim Biophys Acta - Bioenerg 1604:135–150. doi: 10.1016/S0005-2728(03)00059-8
Hofhaus G, Attardi G (1993) Lack of assembly of mitochondrial DNA-encoded subunits of respiratory NADH dehydrogenase and loss of enzyme activity in a human cell mutant lacking the mitochondrial ND4 gene product. EMBO J 12:3043–3048.
Hosler JP (2004) The influence of subunit III of cytochrome c oxidase on the D pathway, the proton exit pathway and mechanism-based inactivation in subunit I. Biochim Biophys Acta - Bioenerg 1655:332–339. doi: 10.1016/j.bbabio.2003.06.009
Hummer G, Wikström M (2016) Molecular simulation and modeling of complex I. Biochim et Biophysica Acta - Bioenerg 1–7. doi: 10.1016/j.bbabio.2016.01.005
Jans F, Mignolet E, Houyoux P-A, et al (2008) A type II NAD(P)H dehydrogenase mediates light-independent plastoquinone reduction in the chloroplast of Chlamydomonas. Proc Natl Acad Sci U S A 105:20546–51. doi: 10.1073/pnas.0806896105
Jia L, Dienhart MK, Stuart RA (2007) Oxa1 Directly Interacts with Atp9 and Mediates Its Assembly into the Mitochondrial F1Fo-ATP Synthase Complex. Mol Biol Cell 18:986–994. doi: 10.1091/mbc.E06
Kaila VR, Verkhovsky MI, Wikström M (2010) Proton-coupled electron transfer in cytochrome oxidase. Chem Rev 110:7062–7081. doi: 10.1021/cr1002003
Karpova O V, Newton KJ (1999) A partially assembled complex I in NAD4-deficient mitochondria of maize. Plant J 17:511–521. doi: 10.1046/j.1365-313X.1999.00401.x
Kerscher S, Kashani-poor N, Zwicker K, et al (2001) Exploring the Catalytic Core of Complex I by Yarrowia lipolytica Yeast Genetics 1.
Klodmann J, Braun H-P (2011) Proteomic approach to characterize mitochondrial complex I from plants. Phytochemistry 72:1071–1080. doi: 10.1016/j.phytochem.2010.11.012
Klodmann J, Sunderhaus S, Nimtz M, et al (2010) Internal architecture of mitochondrial complex I from Arabidopsis thaliana. Plant Cell 22:797–810. doi: 10.1105/tpc.109.073726
Kmita K, Wirth C, Warnau J, et al (2015) Accessory NUMM (NDUFS6) subunit harbors a Zn-binding site and is essential for biogenesis of mitochondrial complex I. Proc Natl Acad Sci 112:201424353. doi: 10.1073/pnas.1424353112
Kotlyar AB, Sled VD, Burbaev DS, et al (1990) Coupling site I and the rotenone-sensitive ubisemiquinone in tightly coupled submitochondrial particles. FEBS Lett 264:17–20. doi: 10.1016/0014-5793(90)80753-6
Kunze M, Hartig A (2013) Permeability of the peroxisomal membrane: Lessons from the glyoxylate cycle. Front Physiol 4 AUG:1–12. doi: 10.3389/fphys.2013.00204
Lang FB, Burger G, O' Kelly CJ, Cedergren R, et al (1997) An ancestral mitochondrial genome

resembling a eubacterial genome in miniature. Nature 387: 493-497
Lapaille M, Escobar-Ram??rez A, Degand H, et al (2010) Atypical subunit composition of the chlorophycean mitochondrial F 1FO-ATP synthase and role of asa7 protein in stability and oligomycin resistance of the enzyme. Mol Biol Evol 27:1630–1644. doi: 10.1093/molbev/msq049
Lauersen K, Willamme R, Coosemans N, et al (2016) Peroxisomal microbodies are at the crossroads of acetate assimilation in the green microalga Chlamydomonas reinhardtii. Algal Res 16:266–274.
Lecler R, Cardol P, Remacle C, Barbare E (2012) Characterization of an internal type-II NADH dehydrogenase from Chlamydomonas reinhardtii mitochondria. Curr Genet 58:205–216. doi: 10.1007/s00294-012-0378-2
Lefebvre-Legendre L, Vaillier J, Benabdelhak H, et al (2001) Identification of a nuclear gene (FMC1) required for the assembly/stability of yeast mitochondrial F(1)-ATPase in heat stress conditions. J Biol Chem 276:6789–6796. doi: 10.1074/jbc.M009557200
Li X, Zhang R, Patena W, et al (2016) An Indexed , Mapped Mutant Library Enables Reverse Genetics Studies of Biological Processes in Chlamydomonas reinhardtii. Plant Cell. doi: 10.1105/tpc.16.00465
Lown FJ, Watson AT, Purton S (2001) Chlamydomonas nuclear mutants that fail to assemble respiratory or photosynthetic electron transfer complexes. Biochem Soc Trans 29:452–5. doi: 10.1042/BST0290452
Massoz S, Larosa V, Horrion B, et al (2015) Isolation of Chlamydomonas reinhardtii mutants with altered mitochondrial respiration by chlorophyll fluorescence measurement. J Biotechnol 1–8. doi: 10.1016/j.jbiotec.2015.05.009
Massoz S, Larosa V, Plancke C, et al (2014) Inactivation of genes coding for mitochondrial Nd7 and Nd9 complex I subunits in Chlamydomonas reinhardtii. Impact of complex I loss on respiration and energetic metabolism. Mitochondrion 19:365–374. doi: 10.1016/j.mito.2013.11.004
Mathiesen C, Hägerhäll C (2002) Transmembrane topology of the NuoL, M and N subunits of NADH:quinone oxidoreductase and their homologues among membrane-bound hydrogenases and bona fide antiporters. Biochim Biophys Acta - Bioenerg 1556:121–132. doi: 10.1016/S0005-2728(02)00343-2
Mathieu L, Marsy S, Saint-Georges Y, et al (2011) A transcriptome screen in yeast identifies a novel assembly factor for the mitochondrial complex III. Mitochondrion 11:391–396. doi: 10.1016/j.mito.2010.12.002
Mathy G, Cardol P, Dinant M, et al (2010) Proteomic and functional characterization of a chlamydomonas reinhardtii mutant lacking the mitochondrial alternative oxidase. J Proteome Res 9:2825–2838. doi: 10.1021/pr900866e
Mavridou DAI, Ferguson SJ, Stevens JM (2013) Cytochrome c assembly. IUBMB Life 65:209–216. doi: 10.1002/iub.1123
McCommis KS, Finck BN (2015) Mitochondrial pyruvate transport: a historical perspective and future research directions. Biochem J 466:229–262. doi: 10.1007/978-1-4614-5915-6
Merchant SS, Prochnik SE, Vallon O, et al (2007) The Chlamydomonas Genome Reveals the Evolution of Key Animal and Plant Functions. Science (80-) 318:245–252.
Milani G, Jarmurszkiewicz W, Sluse-Goffart CM, et al (2001) Respiratory chain network in mitochondria of Candida parapsilosis: ADP / O appraisal of the multiple electron pathways. FEBS Lett 508:231–235.
Mimaki M, Wang X, McKenzie M, et al (2012) Understanding mitochondrial complex I

assembly in health and disease. Biochim Biophys Acta - Bioenerg 1817:851–862. doi: 10.1016/j.bbabio.2011.08.010
Miranda-Astudillo H, Cano-Estrada A, Vazquez-Acevedo M, et al (2014) Interactions of subunits Asa2, Asa4 and Asa7 in the peripheral stalk of the mitochondrial ATP synthase of the chlorophycean alga Polytomella sp. Biochim Biophys Acta - Bioenerg 1837:1–13. doi: 10.1016/j.bbabio.2013.08.001
Molen TA, Rosso D, Piercy S, Maxwell DP (2006) Characterization of the alternative oxidase of Chlamydomonas reinhardtii in response to oxidative stress and a shift in nitrogen source. Physiol Plant 127:74–86. doi: 10.1111/j.1399-3054.2006.00643.x
Møller IM, Rasmusson AG, Fredlund KM (1993) NAD(P)H-ubiquinone oxidoreductases in plant mitochondria. J Bioenerg Biomembr 25:377–384. doi: 10.1007/BF00762463
Nurani G, Franzén LG (1996) Isolation and characterization of the mitochondrial ATP synthase from *Chlamydomonas reinhardtii*. cDNA sequence and deduced protein sequence of the alpha subunit. Plant Mol Biol 31:1105–16.
Ohnishi T (1998) Iron-sulfur clusters/semiquinones in Complex I. Biochim Biophys Acta - Bioenerg 1364:186–206. doi: 10.1016/S0005-2728(98)00027-9
Oster G, Wang H (2003) Rotary protein motors. Trends Cell Biol 13:114–121. doi: 10.1016/S0962-8924(03)00004-7
Oyedotun KS, Sit CS, Lemire BD (2007) The Saccharomyces cerevisiae succinate dehydrogenase does not require heme for ubiquinone reduction. Biochim Biophys Acta - Bioenerg 1767:1436–1445. doi: 10.1016/j.bbabio.2007.09.008
Paumard P, Vaillier J, Coulary B, et al (2002) The ATP synthase is involved in generating mitochondrial cristae morphology. EMBO J 21:221–230. doi: 10.1093/emboj/21.3.221
Paupe V, Prudent J, Dassa EP, et al (2015) CCDC90A (MCUR1) is a cytochrome c oxidase assembly factor and not a regulator of the mitochondrial calcium uniporter. Cell Metab 21:109–116. doi: 10.1016/j.cmet.2014.12.004
Perez-Martinez X, Antaramian A, Vazquez-Acevedo M, et al (2001) Subunit II of Cytochrome c Oxidase in Chlamydomonad Algae Is a Heterodimer Encoded by Two Independent Nuclear Genes. J Biol Chem 276:11302–11309. doi: 10.1074/jbc.M010244200
Perez-Martinez X, Funes S, Tolkunova E, et al (2002) Structure of nuclear-localized cox3 genes in Chlamydomonas reinhardtii and in its colorless close relative Polytomella sp. Curr Genet 40:399–404. doi: 10.1007/s00294-002-0270-6
Phillips JD, Graham LA, Trumpower BL (1993) Subunit 9 of the Saccharomyces cerevisiae cytochrome bc1 complex is required for insertion of EPR-detectable iron-sulfur cluster into the Rieske iron-sulfur protein. J Biol Chem 268:11727–11736.
Plancke C, Vigeolas H, Höhner R, et al (2014) Lack of isocitrate lyase in Chlamydomonas leads to changes in carbon metabolism and in the response to oxidative stress under mixotrophic growth. Plant J 77:404–417. doi: 10.1111/tpj.12392
Prakash SK, Cormier TA, Mccall AE, et al (2002) Loss of holocytochrome c -type synthetase causes the male lethality of X-linked dominant micro- phthalmia with linear skin defects (MLS) syndrome. Hum Mol Genet 11:3237–3248.
Rak M, Gokova S, Tzagoloff A (2011) Modular assembly of yeast mitochondrial ATP synthase. EMBO J 30:920–930. doi: 10.1038/emboj.2010.364
Remacle C, Baurain D, Cardol P, Matagne F (2001) Mutants of Chlamydomonas reinhardtii Deficient in Mitochondrial Complex I: Characterization of Two Mutations Affecting the nd1 Coding Sequence. Genetics 158:1051–1060.
Remacle C, Coosemans N, Jans F, et al (2010) Knock-down of the COX3 and COX17 gene

expression of cytochrome c oxidase in the unicellular green alga Chlamydomonas reinhardtii. Plant Mol Biol 74:223–233. doi: 10.1007/s11103-010-9668-6
Rhein VF, Carroll J, Ding S, et al (2013) NDUFAF7 methylates arginine 85 in the NDUFS2 subunit of human complex i. J Biol Chem 288:33016–33026. doi: 10.1074/jbc.M113.518803
Rodriguez-Salinas E, Riveros-Rosas H, Li Z, et al (2012) Lineage-specific fragmentation and nuclear relocation of the mitochondrial cox2 gene in chlorophycean green algae (Chlorophyta). Mol Phylogenet Evol 64:166–176. doi: 10.1016/j.ympev.2012.03.014
Rouault TA (2015) Mammalian iron-sulphur proteins: novel insights into biogenesis and function. Nat Rev Mol Cell Biol 16:45–55. doi: 10.1038/nrm3909
Rühle T, Leister D (2015) Assembly of F1F0-ATP synthases. Biochim Biophys Acta 1847:849–860. doi: 10.1016/j.bbabio.2015.02.005
Rutter J, Winge DR, Schiffman JD (2010) Succinate dehydrogenase - Assembly, regulation and role in human disease. Mitochondrion 10:393–401. doi: 10.1016/j.mito.2010.03.001
Saada A, Vogel RO, Hoefs SJ, et al (2009) Mutations in NDUFAF3 (C3ORF60), Encoding an NDUFAF4 (C6ORF66)-Interacting Complex I Assembly Protein, Cause Fatal Neonatal Mitochondrial Disease. Am J Hum Genet 84:718–727. doi: 10.1016/j.ajhg.2009.04.020
Salinas T, Larosa V, Cardol P, et al (2014) Biochimie Respiratory-de fi cient mutants of the unicellular green alga Chlamydomonas: A review. Biochimie 100:207–218. doi: 10.1016/j.biochi.2013.10.006
Sánchez-Caballero L, Guerrero-Castillo S, Nijtmans L (2016) Unraveling the complexity of mitochondrial complex I assembly; a dynamic process. Biochim Biophys Acta - Bioenerg. doi: 10.1016/j.bbabio.2016.03.031
Sazanov LA (2015) A giant molecular proton pump: structure and mechanism of respiratory complex I. Nat rev Mol Cell Biol 16:375–388. doi: 10.1038/nrm3997
Sazanov LA, Hinchliffe P (2006) Structure of the Hydrophilic Domain. Science 311:1430–1437.
Schimmeyer J, Bock R, Meyer EH (2016) l-Galactono-1,4-lactone dehydrogenase is an assembly factor of the membrane arm of mitochondrial complex I in Arabidopsis. Plant Mol Biol 90:117–126. doi: 10.1007/s11103-015-0400-4
Schulte U, Weiss H (1995) Generation and characterization of NADH: ubiquinone oxidoreductase mutants in Neurospora crassa. Method Enzymol 260:3–13.
Sharma V, Belevich G, Gamiz-Hernandez AP, et al (2015) Redox-induced activation of the proton pump in the respiratory complex I. Proc Natl Acad Sci U S A 112:11571–6. doi: 10.1073/pnas.1503761112
Sheftel AD, Stehling O, Pierik AJ, et al (2009) Human ind1, an iron-sulfur cluster assembly factor for respiratory complex I. Mol Cell Biol 29:6059–6073. doi: 10.1128/MCB.00817-09
Shiba T, Kido Y, Sakamoto K, et al (2013) Structure of the trypanosome cyanide-insensitive alternative oxidase. Proc Natl Acad Sci 110:4580–4585. doi: 10.1073/pnas.1218386110
Siedow JN, Umbach AL, Moore AL (1995) The active site of the cyanide-resistant oxidase from plant mitochondria contains a binuclear iron center. FEBS Lett 362:10–14. doi: 10.1016/0014-5793(95)00196-G
Smith DR, Hua J, Lee RW (2010) Evolution of linear mitochondrial DNA in three known lineages of Polytomella. Curr Genet 56:427–438. doi: 10.1007/s00294-010-0311-5
Smith DR, Lee RW (2009) The mitochondrial and plastid genomes of Volvox carteri: bloated molecules rich in repetitive DNA. BMC Genomics 10:132. doi: 10.1186/1471-2164-10-132
Smith PM, Fox JL, Winge DR (2012) Biogenesis of the cytochrome bc 1 complex and role of assembly factors. Biochim Biophys Acta - Bioenerg 1817:276–286. doi: 10.1016/j.bbabio.2011.11.009

Soto IC, Fontanesi F, Liu J, Barrientos A (2012) Biogenesis and assembly of eukaryotic cytochrome c oxidase catalytic core .Biochim Biophys Acta - Bioenerg 1817:883–897. doi: 10.1016/j.bbabio.2011.09.005
Subrahmanian N, Remacle C, Hamel PP (2016) Plant mitochondrial Complex I composition and assembly: a review. BBA - Bioenerg. doi: 10.1016/j.bbabio.2016.01.009
Sun F, Huo X, Zhai Y, et al (2005) Crystal structure of mitochondrial respiratory membrane protein Complex II. Cell 121:1043–1057. doi: 10.1016/j.cell.2005.05.025
Sunderhaus S, Dudkina N V., Jansch L, et al (2006) Carbonic anhydrase subunits form a matrix-exposed domain attached to the membrane arm of mitochondrial complex I in plants. J Biol Chem 281:6482–6488. doi: 10.1074/jbc.M511542200
Svensson-Ek M, Abramson J, Larsson G, et al (2002) The X-ray crystal structures of wild-type and EQ(I-286) mutant cytochrome c oxidases from Rhodobacter sphaeroides. J Mol Biol 321:329–339. doi: 10.1016/S0022-2836(02)00619-8
Terashima M, Specht M, Naumann B, Hippler M (2010) Characterizing the anaerobic response of Chlamydomonas reinhardtii by quantitative proteomics. Mol Cell Proteomics 9:1514–1532. doi: 10.1074/mcp.M900421-MCP200
Trumpower B (1990a) The protonmotive Q cycle. J Biol Chem 265:11409–11412. doi: 10.3109/10409239409086800
Trumpower BL (1990b) Cytochrome bc1 complexes of microorganisms. Microbiol Rev 54:101–129.
Tucker EJ, Wanschers BFJ, Szklarczyk R, et al (2013) Mutations in the UQCC1-Interacting Protein , UQCC2 , Cause Human Complex III Deficiency Associated with Perturbed Cytochrome b Protein Expression. Genetics. doi: 10.1371/journal.pgen.1004034
Tzagoloff A, Jang J, Glerum M, Wu M (1996) FLX1 Codes for a Carrier Protein Involved in Maintaining a Proper Balance of Flavin Nucleotides in Yeast Mitochondria. J Biol Chem 271:7392–7397.
Un N, Yu, Ywe D, Cox J, et al (2014) The LYR factors SDHAF1 and SDHAF3 mediate maturation of the iron-sulfur subunit of succinate dehydrogenase. Cell Metab 253–266. doi: 10.1021/jf104742n.Biological
Vahrenholz C, Riemen G, Pratje E, et al (1993) Mitochondrial DNA of Chlamydomonas reinhardtii: the structure of the ends of the linear 15.8-kb genome suggests mechanisms for DNA replication. Curr Genet 24:241–247. doi: 10.1007/BF00351798
van Lis R, Atteia A, Mendoza-hernández G, González-halphen D (2003) Identification of Novel Mitochondrial Protein Components of Chlamydomonas reinhardtii . A Proteomic Approach. Plant Physiol 132:318–330. doi: 10.1104/pp.102.018325.proteins
van Lis R, Mendoza-Hernández G, Groth G, Atteia A (2007) New insights into the unique structure of the F0F1-ATP synthase from the chlamydomonad algae Polytomella sp. and Chlamydomonas reinhardtii. Plant Physiol 144:1190–9. doi: 10.1104/pp.106.094060
Van Vranken J, Na U, R.Wing D, Rutter J (2015) Protein-mediated assembly of succinate dehydrogenase and its cofactors. Crit Rev Biochem Mol Biol 50:168–180. doi: 10.1530/ERC-14-0411.Persistent
Vazquez-Acevedo M, Cardol P, Cano-Estrada A, et al (2006) The mitochondrial ATP synthase of chlorophycean algae contains eight subunits of unknown origin involved in the formation of an atypical stator-stalk and in the dimerization of the complex. J Bioenerg Biomembr 38:271–282. doi: 10.1007/s10863-006-9046-x
Vázquez-Acevedo M, Vega-deLuna F, Sánchez-Vásquez L, et al (2016) Dissecting the peripheral stalk of the mitochondrial ATP synthase of chlorophycean algae. Biochim Biophys Acta -

Bioenerg. doi: 10.1016/j.bbabio.2016.02.003
Vignais PM, Billoud B (2007) Occurrence, classification, and biological function of hydrogenases: An overview. Chem Rev 107:4206–4272.
Villavicencio-Queijeiro A, Pardo JP, Gonzalez-Halphen D (2015) Kinetic and hysteretic behavior of ATP hydrolysis of the highly stable dimeric ATP synthase of Polytomella sp. Arch Biochem Biophys 575:30–37. doi: 10.1016/j.abb.2015.03.018
Vinothkumar KR, Zhu J, Hirst J (2014) Architecture of mammalian respiratory complex I. Nature 515:80–84. doi: 10.1038/nature13686.Architecture
Vogel RO, Dieteren CEJ, Van Den Heuvel LP, et al (2007) Identification of mitochondrial complex I assembly intermediates by tracing tagged NDUFS3 demonstrates the entry point of mitochondrial subunits. J Biol Chem 282:7582–7590. doi: 10.1074/jbc.M609410200
Wächter A, Bi Y, Dunn SD, et al (2011) Two rotary motors in F-ATP synthase are elastically coupled by a flexible rotor and a stiff stator stalk. Proc Natl Acad Sci U S A 108:3924–3929. doi: 10.1073/pnas.1011581108
Walker JE, Dickson VK (2006) The peripheral stalk of the mitochondrial ATP synthase. Biochim Biophys Acta - Bioenerg 1757:286–296. doi: 10.1016/j.bbabio.2006.01.001
Wang ZG, White PS, Ackerman SH (2001) Atp11p and Atp12p are Assembly Factors for the F1-ATPase in Human Mitochondria. J Biol Chem 276:30773–30778. doi: 10.1074/jbc.M104133200
Wenz T, Hielscher R, Hellwig P, et al (2009) Role of phospholipids in respiratory cytochrome bc1 complex catalysis and supercomplex formation. Biochim Biophys Acta - Bioenerg 1787:609–616. doi: 10.1016/j.bbabio.2009.02.012
Wikström M, Jasaitis A, Backgren C, et al (2000) The role of the D- and K-pathways of proton transfer in the function of the haem-copper oxidases. Biochim Biophys Acta - Bioenerg 1459:514–520. doi: 10.1016/S0005-2728(00)00191-2
Wydro MM, Sharma P, Foster JM, et al (2013) The evolutionarily conserved iron-sulfur protein INDH is required for complex I assembly and mitochondrial translation in Arabidopsis. Plant Cell 25:4014–27. doi: 10.1105/tpc.113.117283
Xia D, Esser L, Tang WK, et al (2013) Structural analysis of cytochrome bc1 complexes: Implications to the mechanism of function. Biochim Biophys Acta - Bioenerg 1827:1278–1294. doi: 10.1016/j.bbabio.2012.11.008
Yasuda R, Noji H, Kinosita K, Yoshida M (1998) F1-ATPase is a highly efficient molecular motor that rotates with discrete 120 degree steps. Cell 93:1117–1124. doi: 10.1016/S0092-8674(00)81456-7
Zalutskaya Z, Lapina T, Ermilova E (2015) The Chlamydomonas reinhardtii alternative oxidase 1 is regulated by heat stress. Plant Physiol Biochem 97:229–234. doi: 10.1016/j.plaphy.2015.10.014
Zara V, Conte L, Trumpower BL (2007) Identification and characterization of cytochrome bc1 subcomplexes in mitochondria from yeast with single and double deletions of genes encoding cytochrome bc1 subunits. FEBS J 274:4526–4539. doi: 10.1111/j.1742-4658.2007.05982.x
Zeng X, H. Barros M, SHulman T, Tzagoloff A (2008) ATP25, a New Nuclear Gene of Saccharomyces cerevisiae Required for Expression and Assembly of the Atp9p Subunit of Mitochondrial ATPase. Mol Biol Cell 19:308–317. doi: 10.1091/mbc.E07
Zhang Z, Huang L, Shulmeister VM, et al (1998) Electron transfer by domain movement in cytochrome bc1. Nature 392:677–684. doi: 10.1038/33612
Zhu J, Egawa T, Yeh S-R, et al (2007) Simultaneous reduction of iron-sulfur protein and

cytochrome b(L) during ubiquinol oxidation in cytochrome bc(1) complex. Proc Natl Acad Sci U S A 104:4864–9. doi: 10.1073/pnas.0607812104
Zickermann V, Wirth C, Nasiri H, et al (2015) Mechanistic insight from the crystal structure of mitochondrial complex I. 5:4–10.
Zollner A, Rödel G, Haid A (1992) Molecular cloning and characterization of the Saccharomyces cerevisiae CYT2 gene encoding cytochrome-c1-heme lyase. Eur J Biochem 207:1093–1100.

Figures

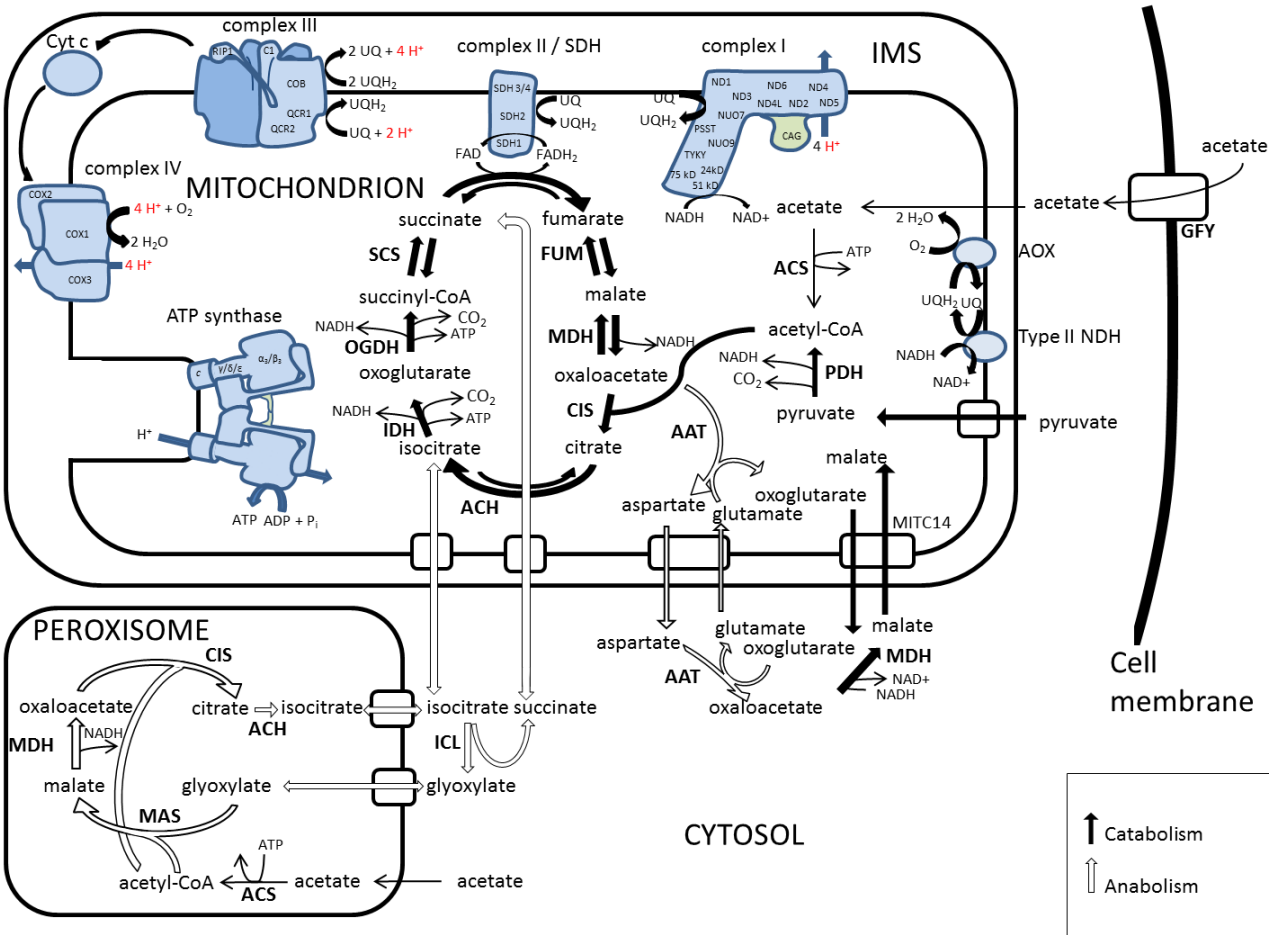

Figure 1. General scheme of mitochondrial carbon metabolism in *C. reinhardtii*. OXPHOS: Only bacterial core subunits and *Chlamydomonas* specific modules (green) are represented. Only H^+ involved in ΔpH (red) are depicted in complexes I, III and IV. AAT: aspartate aminotransferase, ACH: aconitase, ACS: acetyl CoA synthase, CIS citrate synthase, FUM: fumarase, GFY: putative acetate transporters, ICL: isocitrate lyase, IDH: isocitrate dehydrogenase, MAS: malate synthase MDH: malate dehydrogenase, MITC14: oxoglutarate/malate carrier, OGDH: 2-oxoglutarate dehydrogenase, PDH: pyruvate dehydrogenase complex, SCS: succinyl coenzyme A synthetase.

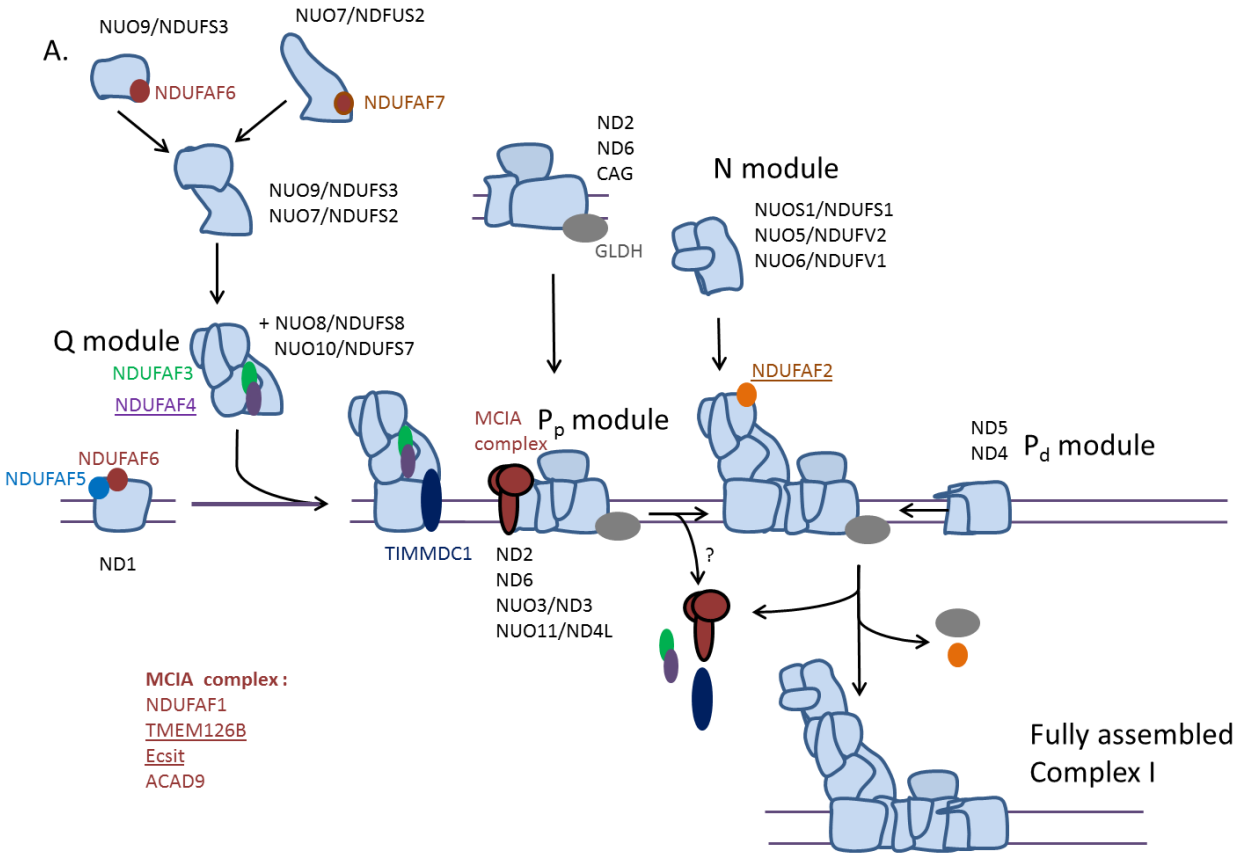

Figure 2. Hypothetical assembly model for complex I in *Chlamydomonas*. Nomenclature for *Chlamydomonas*/humans is used for core subunits, and human nomenclature is used for assembly factors. One name indicated means similar nomenclature. The plant specific assembly factor (GLDH) is also shown. Underlined assembly factors have been identified in humans but no homologs have been found in *C. reinhardtii*.

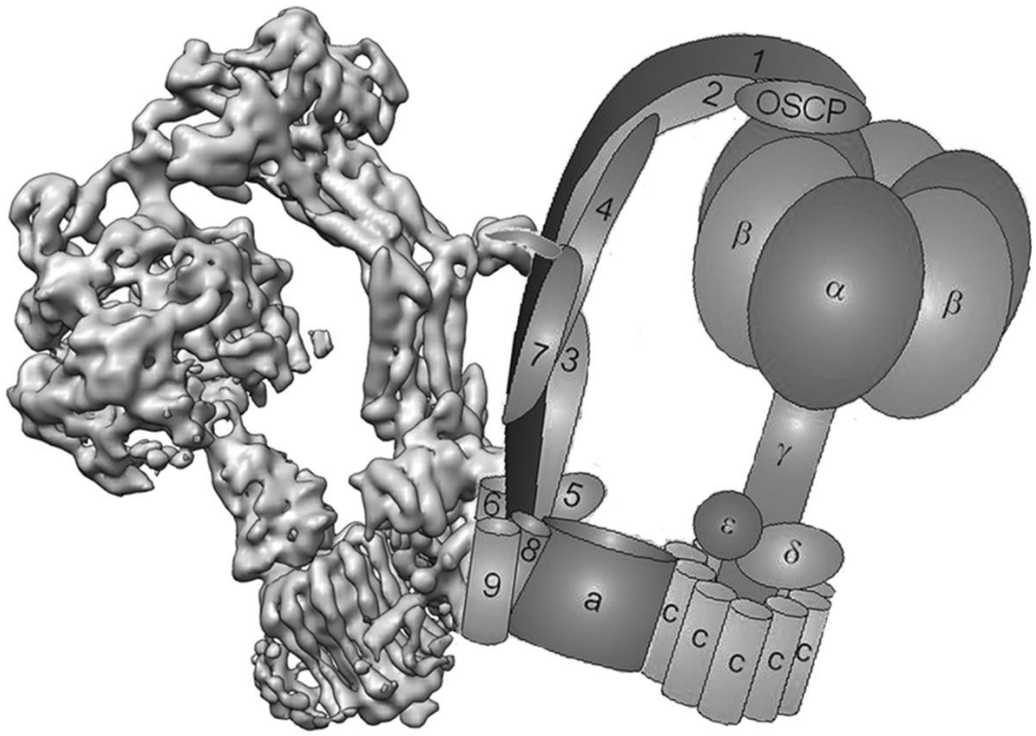

Figure 3. Subunits composition and localization of *Chlamydomonas* mitochondrial ATP synthase.

Homo sapiens	*Saccharomyces cerevisiae*	*Arabidopsis thaliana*	*Chlamydomonas reinhardtii*	Reference
Complex I				
Core subunits				
NDUFS7	nuo19.3 [m]	PSST	*NUO10* (PSST)	a,f
NDUFS8	nuo21.3c [m]	TYKY	*NUO8* (TYKY)	a,f
NDUFV2	nuo24 [m]	24 kDa	*NUO5* (24 kDa)	a,f
NDUFS1	nuo78 [m]	75 kDa	*NUOS1* (75 kDa)	a,f
NDUFV1	Nuo51 [m]	51 kDa	*NUO6* (51 kDa)	a,f
NDUFS2	nuo49 [m]	Nad7	*NUO7* (ND7)	a,f
NDUFS3	nuo30.4 [m]	Nad9	*NUO9* (ND9)	a,f
ND1	ndh-1 [m]	Nad1	nd1	a,f
ND2	ndh-2 [m]	Nad2	nd2	a,f

ND3	ndh-3 [m]	Nad3	*NUO3* (ND3)	a,f
ND4	ndh-4 [m]	Nad4	nd4	a,f
ND4L	Mt-nd4l [m]	Nad4L	*NUO11* (ND4L)	a,f
ND5	ndh-5 [m]	Nad5	nd5	a,f
ND6	ndh-6 [m]	Nad6	nd6	a,f
Supernumerary subunits				
NDUFA1	nuo9.8 [m]	MWFE	*NUOA1*	a,f
NDUFA2	nuo10.5 [m]	B8	*NUOB8*	a,f
NDUFB3	nuo10.6 [m]	B12	*NUOB12*	a,f
NDUFA5	nuo29.9 [m]	B13	*NUOB13*	a,f
NDUFS6	nuo18.4 [m]	13 kDa	*NUOS6*	a,f
NDUFA6	nuo14.8 [m]	B14	*NUOB14*	a,f
NDUFA11	nuo21.3b [m]	B14.7	*TIM17*	a,f
NDUFB11	nuo11.7 [m]	NDU12	*NUO17*	a,f
NDUFS5	nuo11.5 [m]	15 kDa	*NUOS5*	a,f
NDUFB4	nuo6.6 [m]	NDU8	*NUOB4*	a,f
NDUFA12	nuo13.4 [m]	DAP13 / B17.2	*NUO13*	a,f
NDUFA13	nuo14 [m]	b16.6	*NUOB16*	a,f
NDUFB7	NB8M [m]	B18	NUOB18	a,f
NDUFS4	NUO21 [m]	18 kDa	NUOS4	a,f
NDUFB7	NCU11348 [m]	B18	*NUOB18*	a,f
NDUFS4	nuo21 [m]	18 kDa	*NUOS4*	a,f
NDUFA8	nuo20.8 [m]	PGIV	*NUOA8*	a,f
NDUFB9	NCU11258 [m]	B22	*NUOB22*	a,f
NDUFB10	Nuo12.3 [m]	PDSW	*NUOB10*	a,f
NDUFA9	Nuo40 [m]	39 kDa	*NUOA9*	a,f
NDUFB8	Nuo20.1 [m]	ASHI	*TEF29*	a,f
NDUFB2	NCU01436 [m]	AGGG	_	a,f
NDUFB1	Nuo20.9 [m]	20.9 kDa	*NUO21*	a,f
NDUFC2	Nuo10.4 [m]	NDU9	*NUOP1*	a,f
NDUFC1	NCU08300 [m]	NDU10	Cre17.g725400	a,f
NDUFA3	nuo9.5 [m]	B9	Cre12.g537050	a,f

NDUFAB1	SDAP [m]	_	*ACP1*	a,f
NDUFA7	NCU08930 [m]	B14.5a	Cre12.g484700	a,f
NDUFA4	NCU02016 [m]	At3g29970	_	a,f
NDUFB5	nuo17.8 [m]	SGDH	_	a,f
NDUFA10		ATDNK	*DNK1*	a,f
_	_	CA1	*CAG1,CAG2, CAG3*	a,f
_	_	CA2		
_	_	CA3		
_	_	CAL1		
_	_	CAL2		
_	_	P1	_	a,f
_	_	P2	_	a,f
_	_	_	*NUOP4*	a,f
_	_	_	*NUOP5*	a,f
_	_	At3g07480	*NUOP3*	a,f
Candidate plant-specific subunits			_	
_	_	At1g68680	_	a,f
_	_	P3	_	a,f
_	_	TIM23-2	TIM23	a,f
_	_	At2g28430	_	a,f
_	_	DUF543	_	a,f
Assembly factors				
NDUFAF1	CIA30 [m]	At1g17350	*NUOAF1*	a,f
_	CIA84 [m]	_	_	a
NUBPL	IND1 [n]	INDL	*MNP1*	a,f
Foxred1	_	At2g24580	Cre16.g671450	a,f
NDUFA2	NCU00278 [m]	At4g26965	_	a,f
NDUFAF3	_	At3g60150	Cre12.g496800	a,f
NDUFAF4	_	_	_	f
NDUFAF5	_	At1g22800	Cre13.g584750	f
NDUFAF6	NCU09517 [m]	At1g62730	Cre03.g194300	f
NDUFAF7	_	At3g28700	Cre02.g096400	f

TIMMDC1	_	At1g20350	Cre10.g452650	f
TMEM126B	_	_	_	f
Ecsit	_	_	_	f
_	_	GLDH	GLDH	f,g
ACAD9	NCU06543 [m]	IVD	Cre06.g296400	f
AIF	_	MDAR4	*MDAR1*	f

Complex II

SDHA	SDH1	SDH1-1, SDH1-2	*SDH1*	a
SDHB	SDH2	SDH2-1, SDH2-2	*SDH2*	a
SDHC	SDH3	SDH3-1	*SDH3*	a
SDHD	SDH4	SDH4	*SDH4*	a
_	_	SDH5	_	a
_	_	SDH6	_	a
Assembly factors				
SDHAF1	SDH6	At2g39725	*LYR1*	a,b
SDHAF2	SDH5	SDHAF2	Cre12.g550750	a,b
SDHAF3	SDH7	_	_	b
SDHAF4	SDH8	_	_	b
_	FLX1	_	Cre04.g217913	a
_	TCM62	_	_	a

Complex III

UQCRC1	COR1	COR1	*QCR1*	a
UQCRC2	QCR2	At3g16480, At1g51980	*MPPA2*	a
_	_	_	*MPPA1*	a
MT-CYB	COB	AtMg00220	*cob*	a
CYC1	CYT1	At3g27240, At5g40810	*CYC1*	a
UQCRCFS1	ISP	At5g13440, At5g13430	*RIP1*	a
UQCRQ	QCR7	At4g32470, At5g25450	*QCR7*	a
UQCRB	QCR8	At3g10860, At5g05370	*QCR8*	a
UQCRH	QCR6	At2g01090, At1g15120	*QCR6*	a

UQCR10	QCR9	At3g52730	*QCR9*	a
UQCR10	QCR10	At2g40765	*QCR10*	a
UQCRFS1	_	_	_	a
Assembly factors				
BCS1	BCS1	At5g17760	*BCS1*	a
ABC1	COQ8	At4g01660	*COQ8*	a
_	BCA1	_	_	a
UQCC1	CBP3	At5g51220	Cre01.g052050	a
UQCC3	CBP4	_	_	a,d
UQCC2	CBP6	_	_	a,c
TTC19	_	_	_	a
_	CYC2	_	_	a
LYRM7	MZM1	_	Cre07.g332150	a
Cytochrome c				
CYC	CYC1	At1g22840, At4g10040	*CYC*	a
Assembly factors				
System III	System III	System I	System III	a
CCHL	CYT2	_	*HCS1*	a
_	CYC2	_		a
_	CYC3	_	*HCS2*	a
_	_	_	*HCS3*	a
_	_	AtMg00830	_	a
_	_	AtMg00900	_	a
_	_	AtMg00960	_	a
_	_	AtMg00110	_	a
_	_	AtMg00180	_	a
_	_	At1g15220, At3g51790	_	a
Complex IV				
MT-CO1	COX1	COX1	cox1	a
MT-CO2	COX2	COX2	*COX2a*	a

–	–	–	*COX2b*	a
MT-CO3	COX3	COX3	*COX3*	a
COX5b	COX4	–	*COX4/5b*	a
COX4I-1	COX5a	–	–	a
COX4I-2	COX5b	COX5B-1, COX5B-2	–	a
–	–	At3g62400, At2g47380, COX5C	*COX5C*	a
COX5a	COX6	–	–	a
COX7a	COX7	–	–	a
COX7c	COX8	–	–	a
COX6c	COX9	–	–	a
COXVIIb	–	–	–	a
COX8	–	–	–	a
COX6b	COX12	COX6B-1, COX6B-3	*COX12*	a
COX6a	COX13	COX6A	*COX13*	a
–	–	–	*COX90*	a
Assembly factors				
Membrane insertion and processing of complex IV subunits				
OXA1L	OXA1	OXA1	*OXA1*	a
COX20	COX20	–	–	a
COX18	COX18	–	*COX18*	a
–	MSS2	–	–	a
–	MSS51	–	–	a
–	PNT1	–	–	a
–	IMP1	–	*IMP1*	a
IMMP2L	IMP2	At3g08980	*IMP2*	a
–	SOM1	–	–	a
Copper metabolism and insertion into complex IV				a
COX17	COX17	COX17-2	*COX17*	a
SCO1, SCO2	SCO1, SCO2	HCC1, HCC2	*SCO1*	a
COX11	COX11	COX11	*COX11*	a
COX19	COX19	COX19-1	*COX19*	a

COX23	COX23	At1g02160	*COX23*	a
PET191	PET191	At1g10865	*PET191*	a
CMC1/CMC2	CMC1/CMC2	At2g07681, ccmC	_	a
Heme A biosynthesis				a
COX10	COX10	COX10	*COX10*	a
COX15	COX15	COX15	*COX15*	a
FDX2	YAH1	MFDX1, MFDX2	*MFDX*	a
ADR	ARH1	_	*ARH1*	a
Assembly				a
_	PET100	At4g14615, At1g52821	_	a
SURF1	SHY1	SURF1	*SUR1*	a
_	COX14	_	_	a
_	COA1/2/3	_	_	a
_	COX25	_	_	a
_	CMC3	_	_	a
_	COA4	_	_	a
CCDC90A	FMP32	_	_	e
Unknown function				a
COX16	COX16	At4g14145	*COX16*	a
CSRP2BP	PET117	_	_	a

ATP synthase

Fo subcomplex

ATP6	ATPA	ATP-1	*ATP6*	a
_	_	ATP6-2	_	a
ATP5F1	ATPB	AtMg00640	_	a
ATP5G3	ATPC	AtMg01080, At2g07671	*ATP9A*	a
_	_	_	*ATP9B*	a
ATP5H	ATPD	At3g52300	_	a
ATP5I	ATPE	At5g15320	_	a
ATP5J2	ATPF	At4g30010	_	a
ATP5L	ATPG	At2g19680	_	a

ATP5J	ATPH	_	_	a
ATP8	ATP8	AtMg00480		a
ATP5O	ATP5	At5g13450	*ATP5*	a
ATPI	INH1, STF1	At5g04750	_	a
_	STF2	_	_	a
_	ATPJ/I	_	_	a
F1 subcomplex				
ATP5A1	α	AtMg01190,At2g07698	*ATP1(α)*	a
ATP5B	β	At5g08670, At5g08680	*ATP2 (β)*	a
		At5g08690		a
ATP5C1	γ	At2g33040	*ATP3 (γ)*	a
ATP5D	δ	At5g47030	*ATP16 (δ)*	a
ATP5E	ε	At1g51650	*ATP15 (ε)*	a
_	ATPK	_	_	a
_	_	At2g21870	_	a
_	_	_	*ASA1*	a
_	_	_	*ASA2*	a
_	_	_	*ASA3*	a
_	_	_	*ASA4*	a
_	_	_	*ASA5*	a
_	_	_	*ASA6*	a
_	_	_	*ASA7*	a
_	_	_	*ASA8*	a
_	_	_	*ASA9*	a
Assembly factors				
Fo subcomplex				
_	ATP10	AAF18252	_	a
ATP23	ATP23	_	_	a
_	ATP25	At3g03420.1	Cre17.g697934	a
OXA1L	OXA1	OXA1	*OXA1*	a
_	ATP22	_	_	i
F1 subcomplex				

ATPAF1	ATP11	At2g34050	*ATP11*	a
ATPAF2	ATP12	At5g40660	*ATP12*	a
_	FMC1	_	*FMC1*	a
_	HSP90	_	*HSP90*	h
Alternative oxidase				
_	AOX-AAC37481 [m]	AOX1a,AOX1b, AOX1c,AOX1d,	*AOX1*	a
_		AOX2	*AOX2*	
Type-II NAD(P)H dehydrogenase family				
_	NDAe1,NDAe2, NDAi1	NDA1, NDA2	*NDA1, NDA5*	a
		NDB, NDB2	*NDA6, NDA7*	
		NDB3, NDB4		
		NDC		

Table 1. Gene name of subunits and assembly factors of the mitochondrial OXPHOS chain. Adapted from (a) Salinas et al. 2014, (b) Van Vranken et al. 2015, (c) Tucker et al. 2013, (d) Brand et al. 2014, (e) Paupe et al. 2015, (f) Subrahmanian et al. 2016, (g) Klodmann & Braun 2011, (h) Francis and Thorsness 2011, (i) Helfenbein et al. 2003. [m] : data retrieved from *N. crassa*, [n] : data retrieved from *Y. lipolytica*. Gene names are from UNIPROT (http://www.uniprot.org) and Phytozome (https://phytozome.jgi.doe.gov).

1.3 Complex I assembly factors

Complex I assembly is a complicated process requiring several steps involving the assembly of different modules (see above, reviewed in Sánchez-Caballero et al. 2016), some of them containing proteins from both nuclear and mitochondrial origins. The first assembly factors were identified in 1998 in *N. crassa*. Scientist studying a mutant accumulating the membrane arm of complex I decided to purify and analyze the protein composition of this subcomplex (Kuffner et al. 1998). In addition to some known structural proteins, they discovered two unknown peptides of 30 kDa and 84 kDa attached to the membrane subcomplex. Subsequent analyses demonstrated a specific presence of these proteins in membrane intermediates, while they were not present in the fully assembled complex I. These proteins were named CIA30 and CIA84 (for complex I assembly) and were the first complex I assembly factors discovered. Thought *N. crassa* was used to identify the first assembly factors, the following assembly factors were discovered in other organisms, mainly in humans. As of today, 15 assembly factors have been identified. Here we will review each of them in more details. The presence or absence of homolog proteins in *C. reinhardtii* was determined based on Subrahmanian et al. 2016.

1.3.1. NDUFAF1; NUOAF1; CIA30 (Human; *C. reinhardtii; N. crassa*)

CIA30 is the first assembly factor that was discovered in the fungus *N. crassa* (Kuffner et al. 1998), along with another potential assembly factor named CIA84. The human homolog of CIA30, NDUFAF1, was functionally characterized by Vogel et al. in 2005 using knock-down studies. NDUFAF1 belongs to the non-catalytic carbohydrate binding modules family (Elurbe and Huynen 2016), where such domain is used on catalytic variant to recruit appropriate ligand. NDUFAF1 is found on healthy cells on subcomplexes from ~460 kDa to 830 kDa (Sánchez-Caballero et al. 2016a). The smallest 460 kDa represents the P_P module of complex I, while the biggest 830 kDa subcomplex represents the whole complex I without the N module. In a patient deficient for NDUFAF1, complex I assembly is stopped at a 460 kDa subcomplex that can only barely be detected (Dunning et al. 2007). Recently, NDUFAF1 was found to be part of a multiprotein assembly complex, called MCIA (Heide et al. 2012) including at least four assembly factors including NDUFAF1, TMEM126B, ACAD9 and ECSIT in humans. Altogether, these results point toward a role of NDUFAF1 into stabilizing the P_P module and assembling it to

(ND1+Q module) subcomplex. A homolog named NUOAF1 has been identified in *C. reinhardtii* but no functional analysis has been done.

1.3.2. NDUFAF2; B17.2L (Human; *Bos Taurus*)

NDUFAF2 is a paralogue of a structural subunit of complex I: NDUFA12 (B17.2). It was first identified in a patient showing progressive encephalopathy who was demonstrated to possess a null mutation in NDUFAF2 (Ogilvie et al. 2005). NDUFAF2 was found to be present in a 830 kDa subcomplex in cells depleted of NDUFV1 (NUO6 *Chlamydomonas* homolog), a protein of the N module. Mammal cells depleted for NDUFAF2 could still assemble some complex I entirely, although less efficiently (Schlehe et al. 2013). The current model regarding NDUFAF2 and its paralog NDUFAF12 is that the assembly factor would hold the place of NDUFA12 until the latter is finally inserted into complex I, at a later stage of assembly (Pereira et al. 2013), since the release of NDUFAF2 depends on NDUFS4, NDUFS6 and NDUFA12 that are thought to be tardily assembled (Rak and Rustin 2014). The exact role of NDUFAF2 is still debated. In the literature, its presence into the 830 kDa subcomplex when the N module cannot be assembled led to the conclusion that NDUFAF2 would help for the assembly of this module, in the late stage of the process. But recently, new model for this assembly factor was proposed. Study of the NDUFS6 structural subunit showed that this supernumerary subunit would interact with a cluster of the TYKY subunits (Kmita et al. 2015) in the late stage of assembly. It was shown that NDUFS6, a protein interacting with its iron sulfur cluster at the late stage of assembly, is required to be in integrated for NDUFAF2 to be released (Kmita et al. 2015), leading to the proposition that NDUFAF2 might help stabilizing complex I in a configuration where the iron sulfur centers could be accessible for the late stage assembled proteins such NDUFS6. This assembly factor would then contribute to maintain complex I in adequate configuration instead of allowing the assembly of the N module. No homolog of NDUFAF2 has been identified so far in *C. reinhardtii*.

1.3.3. ECSIT (Human)

ECSIT is a protein first described as cytosolic signaling protein, that was later found to co-migrate in the same subcomplex as NDUFAF1 (Vogel et al. 2007b) and finally found to be part of

the MCIA complex (Heide et al. 2012). It is interesting to note that if ECSIT was found to interact with NDUFAF1, the knock-down of both proteins does not lead to the exact same phenotype, suggesting that their respective role may differ (Vogel et al. 2007b). No homolog of ECSIT has been identified so far in *C. reinhardtii*.

1.3.4. ACAD9 (Human)

Acyl-CoA dehydrogenase 9 (ACAD9) is an enzyme possessing both Acyl-CoA dehydrogenase activity and a role in complex I assembly. Both roles were found to be important for healthy human cells (Schiff et al. 2014). This enzyme was found to be linked to several complex I deficiencies in humans such as encephalomyopathy (Garone et al. 2013) and is the last protein part of the MCIA complex so far identified (Heide et al. 2012). The exact role of this protein remains unknown. Homolog of this protein (Cre06.g296400) has been found in *C. reinhardtii*.

1.3.5. NDUFAF3; NUOAF3, NUAF3 (Human; *C. reinhardtii; C. elegans*)

NDUFAF3 is an assembly factor functionally characterized in humans (Saada et al. 2009), *C. elegans* (van den Ecker et al. 2012) and *C. reinhardtii* (this work). The loss of this protein in the organisms characterized so far leads to an important reduction of complex I assembly. This assembly factor was shown to interact with proteins from the Q module (NDUFS3, NDUFS2, NDUFS8) and another assembly factor named NDUFAF4 in humans (Saada et al. 2009). NDUFAF3 is thought to stabilize/help associate the Q module, and most likely anchoring it to the membrane domain. Indeed, a significant fraction of NDUFAF3 can be found membrane-bound despite the absence of transmembrane domain in the protein (Zurita Rendón and Shoubridge 2012). In addition, NDUFAF3 possesses ortholog in bacterial operons involved in the interaction/insertion of proteins into the membrane (Saada et al. 2009). The interaction between NDUFAF3 and the membrane part of the domain seems to be of strong nature since a portion of NDUFAF3 can still be traced to heavier subcomplexes such as the 830 kDa membrane bound intermediate (Zurita Rendón and Shoubridge 2012) composed of both Q Module and the P_P

module. It was speculated that such strong interaction might be the consequence of NDUFAF3 serving to prevent proteolysis of early subcomplexes and potential protection of the redox cofactors of the Q module.

1.3.6. NDUFAF4 (Human)

NDUFAF4 was identified in humans as an assembly factor interacting with NDUFAF3. It is present in the same subcomplexes and seems to be co-regulated with NDUFAF3, since knock-down of one of them results in a absence of protein for the second (Saada et al. 2009). Though their roles seem to be tied together, it is interesting to note that not all organisms possess both proteins. Indeed, no homolog to human NDUFAF4 was found in *C. reinhardtii*.

1.3.7. NDUFAF5 (Human)

NDUFAF5 is methyltransferase whose role has remained so far relatively elusive. A patient mutated in this gene showed complex I assembly deficiency and no detectable ND1 (Sugiana et al. 2008). Many researchers speculated a role of this assembly factor in ND1 biogenesis, though no direction interaction could be demonstrated so far. Homolog of this protein (Cre13.g584750) was found in *C. reinhardtii.*

1.3.8. NDUFAF6 (Human)

NDUFAF6 is an assembly factor that was discovered in a patient bearing complex I deficiency and suffering from Leigh syndrome disease (McKenzie et al. 2011). The deficiency was linked to the loss of the ND1 biogenesis, linking this assembly factor to ND1 biogenesis. NDUFAF6 contains a squalene/phytoene synthase domain but it is unknown if this domain is still active. Like NDUFAF3, NDUFAF6 possesses orthologs inside bacterial operons that are involved in the interaction/insertion of proteins into the membrane (Elurbe and Huynen 2016;Saada et al. 2009). Together, this indicates that NDUFAF6 might serve to help anchoring ND1 in the mitochondrial inner membrane. In addition to its role in ND1 biogenesis, NDUFAF6 homolog in *Drosophila melanogaster* was found to interact in the cytosol with NDUFS3 and NDUFA10 to chaperone

them until they enter mitochondria. NDUFAF6 is part of the assembly factors not found associated with any subcomplexes during complex I biogenesis. Homolog of this protein (Cre03.g194300) was found in *C. reinhardtii*.

1.3.9. NDUFAF7 (Human)

NDUFAF7, like NDUFAF5, is a methyltransferase. The protein was shown to interact with NDUFS2 first in yeast (Carilla-Latorre et al. 2010), then in vertebrates (Zurita Rendon et al. 2014) and in humans (Rhein et al. 2013). NDUFAF7 was shown to methylate arg85 of NDUFS2. The transient suppression of NDUFAF7 in Human was shown to be correlated to a suppression of small sized subcomplexes assembly such as the ~400 kDa including the Q module, whose NDUFS2 is part of, and ND1, whose turnover is known to be increased when the Q module isn't assembled (Zurita Rendón and Shoubridge 2012). This led to the conclusion that NDUFAF7 methylates NDUFS2 and is essential for the early stages assembly processes. Homolog of NDUFAF7 (Cre02.g096400) was found in C. *reinhardtii* genome.

1.3.10. IND1; INDH; NUBPL; MNP1 (*Y. lipolytica*; *Arabidopsis thaliana*; Human; *Chlamydomonas*)

IND1 is a conserved assembly factor for complex I identified in various organisms such as yeast, humans and plants (Sheftel et al. 2009;Wydro et al. 2013;Bych et al. 2008). IND1 was shown to bind 4Fe-4S cluster, thanks to a conserved (CXXC) cysteine motif, largely present in the matrix arm in complex I. Knockout of IND1 leads to the accumulation of a membrane arm of complex I, of 450 kDa in humans (Sheftel et al. 2009) and 650 kDa in plants (Wydro et al. 2013). The difference in size might be due to the extra anhydrase carbonic domain found in plant but not in mammals around the P_P module . As a result, it was speculated to play a role in iron-sulfur centers assembly in complex I in the N and Q module (Sheftel et al. 2009). In addition, plant INDH was shown to play an extra role in mitochondrial translation. Indeed, isolated mitochondria exposed to radiolabeled ^{35}S-M failed for the most part to incorporate the radiolabeled ^{35}S-M in INDH mutant (Wydro et al. 2013) compared to wild type. This experiment was performed with added ATP in order to insure the lack of complex I activity wasn't the cause of translation defect.

1.3.11. FOXRED1 (Human)

FOXRED1, a FAD-dependent oxidoreductase, was identified in a patient bearing complex I deficiency and suffering from encephalopathy (Fassone et al. 2010). Recent studies in humans showed that FOXRED1 was important for complex I assembly since only 10% of complex I were found assembled in human cells lacking the assembly factor (Formosa et al. 2015). Complex I assembly in deficient cells were stucked with a ~475 kDa subcomplex, that was shown to be a breakdown of a bigger 815 kDa subcomplex produced "successfully". The 475 kDa subcomplex contained most mitochondria-encoded subunits but not anymore membrane assembly factors such as NDUFAF1. Though the exact reason of the breakdown was not clear, similar phenotype is seen in a mutant deficient for NDUFA9, a protein at the junction of the Q and P module. The breakdown might then be linked to the matrix and membrane arm splitting apart. Homolog of this assembly factor (Cre16.g671450) is found in *C. reinhardtii*

1.3.12. GLDH (*A. thaliana*, *C. reinhardtii*)

L-Galactono-1,4-lactone dehydrogenase (GLDH) was thought for some time to be part of the structural complex I (Salinas et al. 2014;Cardol 2011) in photosynthetic organisms. But recent studies pointed towards a role in complex I assembly since the protein was not detected in completely assembled complex I but only into intermediate subcomplexes from 400 to 850 kDa, especially visible in *ndufs4* mutant of *A. thaliana* (Schimmeyer et al. 2016). In *gldh* mutant, a 200 kDa subcomplex would accumulate containing the carbonic anhydrase (CA) subunits. This led the authors to postulate that GLDH was an assembly factor incorporated to help the assembly of the 200 kDa carbonic anhydrase containing subcomplex into a 400 kDa membrane subcomplex (most likely P_P module). This is the only assembly factor specific to plants as GLDH is not conserved in humans (Schimmeyer et al. 2016).

1.3.13. TMEM126B (Human)

TMEM126B was recently identified using complexome profiling (Heide et al. 2012) where it was

found to associate with known assembly factors such as ACAD9, EXCIT and NDUFAF1, these 4 assembly factors were termed MCIA. Knockdown of TMEM126B was shown to lead to a severe complex I assembly decrease. Interestingly, TMEM126B knockdown has no effect of the stability of the other MCIA assembly factors which can still assemble themselves, though not as efficiently. It was thus speculated that TMEM126B serves to help recruiting the different proteins of the MCIA complex for a proper assembly around the P_P module. No homolog has been found in *C. reinhardtii*.

1.3.14. TIMMDC1 (Human)

TIMMDC1 is the latest complex I assembly factor found. It was identified by proteomic analysis by Guarani et al. 2014 in rat.TIMMDC1 is homologous to NDUFA11 and the Tim17-23 inner mitochondria transporter family (Elurbe and Huynen 2016). TIMMDC1 depleted human cell lines showed several subcomplexes including a ND4/ND5 containing subcomplex, a ± 300 kDa subcomplex containing the Q module, and the ± 200 kDa N module. These results taken together suggested that TIMMDC1 would play a critical role to merge the ND1 embedded subcomplex to the Q module. This step seems to be critical for the later insertion of the rest of the membrane arm. Homolog of this protein (Cre10.g452650) has been found in *C. reinhardtii* genome.

1.3.15. AIF (Human)

Apoptosis-inducing factor (AIF) is a protein which was first described as inducing apoptosis in healthy mammal cells (Susin et al. 1999). Later is was shown that mice lacking AIF showed a decreased level of complex I activity in heart and muscle (Joza et al. 2005), which led to the conclusion that AIF was involved in the maintenance of complex I, most likely as assembly factor. The exact way in which this assembly factor impact complex I remains to be discovered. Homolog of this protein (Cre17.g712100) has been found in *C. reinhardtii*.

1.4. Photosynthesis

Photosynthesis is the process by which photosynthetic organisms use light to fix CO_2 into organic compounds. This pathway takes place inside the chloroplast. *Chlamydomonas* possesses a single large chloroplast bounded by two membranes (Sager and Palade 1957). These two membranes delimit an aqueous phase called stroma where thylakoids which are membrane-bound compartments are found. The inside of the thylakoids is called the lumen. *Chlamydomonas* thylakoids are divided into the "classical" thylakoid structure with partially stacked regions called grana and unstacked region called lamellae, though the grana proportion is highly reduced compared to plants (Sager and Palade 1957).

Photosynthesis is divided into two phases. The light phase, allowing for conversion of light into energy (ATP) and reductive power (NADPH), takes place in the thylakoid membranes. The dark phase, allowing for CO_2 fixation, takes place in the stroma region. In addition to photosynthesis, the chloroplast provides the early steps for glycolysis in *Chlamydomonas* (Klein 1986). We will here mainly talk about the photosynthetic electron transport chain (light phase) and its main components.

1.4.1. Photosystem II

Photosystem two (PSII) is the first complex of the photosynthetic electron transport chain. This complex uses light energy to split water molecule into molecular oxygen (and protons) while extracting electrons. These electrons (4 electrons retrieved per molecular oxygen produced) are in fine transferred onto plastoquinones (PQH_2) that will diffuse in the thylakoid membranes.

PSII is composed of about 30 subunits (reviewed in Hankamer et al. 1997;Minagawa and Tokutsu 2015). Among those, four major central subunits are called D1, D2, CP47 and CP43. The D1 and D2 proteins harbor the elements involved in electron transfer: the manganese center, the P680 reaction center, the pheophytin, the mobile plastoquinone acceptor Q_B on D1, and the fixed plastoquinone acceptor Q_A on D2. The chlorophyll *a* binding proteins CP47 and CP43 serve mainly to transfer the energy from light excitation to the reaction center, though CP43 has also been shown to participate in the ligation of the manganese center (Umena et al. 2011). PSII possesses light harvesting antennas named LHCII (for Light Harvesting complex of PSII) which

are mainly made of the LHCB proteins (Jansson 1999). These proteins bind both chlorophyll *a* and *b*. LHCB1, 2 and 3 constitute the major antenna system and are organized as trimmers (Tokutsu et al. 2012). The LHCB4 and LHCB5 proteins, also called P26 and P29, are only present in monomers and thought to serve as anchor the major LHCII antennas. Unlike land plants, *Chlamydomonas* does not possess the lhcb6 (P24) minor antenna. These LHCB antennas are part of an outer antenna system that can be phosphorylated and disconnected from the PSII (see state transition below). PSII usually form supercomplexes with antenna (LHCII, P26, P29) situated on both sides of the supercomplex (Tokutsu et al. 2012).

Light energy is captured by antenna and transmitted to the PSII P680 center (primary electron donor), where a single excited electron is transferred from P680 to a chlorophyll *a* molecule then to a pheophytin intermediate, then to a tightly bound plastoquinone Q_A and finally on the mobile Q_B plastoquinone. The initial chlorophyll electron donor will be reduced with electron from a manganese center situated on the lumen side of the PSII and connected to the P680 via a tyrosine. This manganese center has been characterized and involves manganese and calcium atoms in a 4:1 ratio (Umena et al. 2011), in addition to water and oxygen atoms. The four manganese atoms will undergo four successive oxidation steps. Once all four manganese atoms are oxidized, a concerted split of two water molecules will occur, leading to the formation of molecular oxygen (Kok et al. 1970;Yano et al. 2015). The manganese reaction center is hold by the OEC (oxygen evolving complex) situated on the surface of the thylakoids in PSII, oriented towards the lumen side. This OEC is composed of three proteins called PsbO, PsbP and PsbQ. PsbO is the main protein stabilizing the manganese center. PsbP and psbQ are thought to play a role in optimizing the level of Ca_2^+ and Cl^- , which are required for the water splitting reaction (Nield et al. 2000).

1.4.2. Cytochrome b6f

Cytochrome b6f is the second electron-transferring complex in the photosynthetic electron transport chain. It transfers electron from the plastoquinone pool to the soluble plastocyanine and serves as an intermediate between PSII and PSI. Cytochrome b6f is very similar to the mitochondrial complex III described above. It is composed of eight subunits, compared to the 11 of complex III (reviewed in Baniulis et al. 2008). The cytochrome b6,

cytochrome f and ISP (Iron sulfur protein) contain the cofactors needed for electron transport and are homologous to the cytochrome b, cytochrome c1 and ISP in complex III, with the exception of the presence of an heme f replacing the heme c1. In addition to those, cytochrome b6f contains 3 extra prosthetic elements all binding cytochrome b6: a β carotene, a heme c_i and a chlorophyll *a* molecule. The later has been shown to interact with the Qo site of cytochrome b6f (Hasan et al. 2014) and might be part of the sensing system for state transitions activation (see below)(De Lavalette et al. 2008). The five other subunits of cytochrome b6f have no homolog in complex III. Electron transfer through cytochrome b6f is coupled to proton pumping through the thylakoid membrane. Mechanisms involving electron transfer and protons pumping are thought to be similar to the one involved in complex III (see above; Q cycle). Cytochrome b6f is thought to be a key element in photosynthesis regulation since it is involved in both linear and cyclic electron flow. The PQH_2 to ISP electron transfer reaction is the limiting step in photosynthetic electron transport chain and is regulated by proton gradient (Tikhonov 2014).

1.4.3. Photosystem I

Photosystem one (PSI) is the third complex of the photosynthetic electron transport chain. It is composed of 12 core subunits including the electrons transferring PsaA and PsaB subunits (Suga et al. 2016) and nine LHCI (light harvesting complex of PSI) in *C. reinhardtii* (Stauber et al. 2003). This high number of LHCI differs from the 4 LHCI proteins in higher plants. These LHCI antennas forms a belt on one side of PSI (Dekker and Boekema 2005). The 'free' side of the PSI allows for the docking of LHCII during state transition (see below). Unlike cyanobacteria, plant PSI are only present in monomeric form (Amunts et al. 2010). This is thought to be due to the addition of one protein in plant PSI (PsaH) compared to cyanobacteria PSI at the interface where PSI would link together to form (di)trimers in the cyanobacteria.

PSI uses light energy to initiate a charge separation at the P700 center, the P700 being then reduced by an electron from the plastocyanine pool. The PSI possesses two symmetrical electron transfer pathways on PsaA and PsaB branching themselves from the P700 and joining together at the first Fe-S center of PSI at the interface of both PsaA and PsaB, bound by cysteine residues from the 2 proteins. Each of these branches (called branch A and B) is composed of two chlorophyll molecules and one phylloquinone. Electron split from P700 will be transferred to one

of these branches and then to the first Fe-S center named F_x. The frequency of use for the 2 branches of PSI is still debated but seems to vary among organisms. Indeed, while some organism seems to mainly use the branch A for electron transport (Cohen et al. 2004) , branch B in *C. reinhardtii* has been showed to be crucial for photoautotrophic growth (Fairclough et al. 2003). Once on F_x, electrons will be transferred through two additional Fe-S centers (F_A and F_B) to a ferredoxin, the final electron acceptor for PSI. Thanks to a FNR (Ferredoxin NADP oxidoreductase), electron from ferredoxin will be transferred to NADP to form NADPH.

In addition to transferring electrons from plastocyanine to ferredoxin, PSI can also participate in ROS-generating reactions, directly reducing molecular oxygen into anion superoxide (O_2^-). This reaction is called "Melher" reaction. The produced ROS (reactive oxygen species) are then taken over by by the SOD (superoxide dismutase) and APX (ascorbate peroxidase) system (see review in Asada 2000). The Melher reaction has been shown to be most active when linear electron transport isn't restricted in *C. reinhardtii* (Roach et al. 2015) and is thought to play several roles during photosynthesis. Oxygen might serve as an electron sink when the carbon fixation pathway (Calvin cycle) is insufficient and NADP acceptor starts being limited. In such case, Melher reaction would work in conjunction with cyclic electron transfer to protect PSI (Chaux et al. 2015). The interplay between the two pathways is reinforced by the fact that H_2O_2 reactive species has been shown to activate the NDH cyclic pathways in plants (Strand et al. 2015). In addition to PSI photoprotection, Melher in algae is also thought to potentially have additional regulatory role, since several genes expression are changed upon H_2O_2 addition (Shao et al. 2008). Notably, state transition has been shown to be decreased in the presence of H_2O_2 (Roach et al. 2015), preventing excessive state transition while linear electron flow is available.

1.4.4. Chloroplastic ATP synthase

The last element of the photosynthetic main apparatus is the chloroplastic ATP synthase. Just like its mitochondrial counterpart, this enzyme consumes the protons gradient (generated by the PSII/cytochrome b6f) to produce ATP. The photosynthetic ATP synthase is a 9 subunits multiprotein complex (Mccarty et al. 2000). It is a monomer with a F_1 matrix domain catalyzing the ATP producing reaction with the help of a F_0 membrane domain allowing for the processing

of the proton motive force. Contrary to the Chlamydomonas mitochondrial ATP synthase, both the F_1 and F_0 modules of the chloroplastic ATP synthase have a dual origin, being encoded in the nuclear and chloroplastic genome (reviewed in Strotmann et al. 1998). The ATP synthase reaction of the chloroplastic enzyme is similar to its mitochondrial counterpart (see mitochondrial ATP synthase). In *C. reinhardtii*, the subunit III (constituting the c ring for proton translocation) was shown to be made of a constant number of 13 monomers in a wide range of conditions (Meyer Zu Tittingdorf et al. 2004), this is different from the 14 monomers found in land plants and impact the ATP/NADH ratio produced during photosynthesis.

1.4.5. Cyclic electron flow

Cyclic electron flow consists of the rerouting of electrons from PSI acceptor through PQ, b6f, and PSI again. Linear electron flow (LEF) from PSII to NADH produces ATP and reductive power (ferredoxin/NADPH) that can be used notably for carbon fixation. The linear electron flow allows for the oxidation of two water molecules with eight photons and the pumping of 13 protons across the thylakoid membranes into the lumen. Due to the likely 13 subunits of the c-ring of the chloroplastic ATP synthase (Meyer Zu Tittingdorf et al. 2004), the linear electron flow pathway isn't able to produce by itself the 3/2 ATP/NADH ratio needed for a proper functioning of the Calvin cycle with only a 2.8/2 ratio being produced (Allen et al. 2002). This means that production of extra ATP is required in order to maintain an adequate redox balance for photosynthesis. Cyclic electron flow (CEF) around PSI allows the production of ATP at the detriment of NADPH, therefore allowing for a proper ratio of ATP/NADPH (Figure 4). CEF is thought to be regulated by the redox state of the stroma (Takahashi et al. 2013;Johnson et al. 2014) and to adapt to conditions requiring increased ATP/NAPDH ratio such as limited inorganic carbon availability under phototrophic conditions (Lucker and Kramer 2013). CEF is also important in condition where PSI acceptors are limited (such as photosynthesis activation (Godaux et al. 2015)). This allows a better oxidation of electron acceptors and an increase of their availability to prevent PSI photoinhibition. It is interesting to note that LEF and CEF are in direct competition for oxidized PQ. In land plant, compartmentalization has been shown to help reduce competition since part of the PQ has no access to the PSII positioned inside the grana structure (Alric 2015). In C. *reinhardtii*, supercomplexes containing PSI-LHCI-LHCII-FNR-Cyt b6f-

PGRL1 were identified as CEF favoring supercomplexes (Iwai et al. 2010).

Two main pathways for CEF have been identified (reviewed in Peltier et al. 2010): an antimycin A insensitive pathway, involving type I NDH (NADH dehydrogenase) in plants (Suorsa et al. 2009) and type II NDH in *C. reinhardtii* (Jans et al. 2008;Desplats et al. 2009), and an antimycin A sensitive pathway. The later involves the PGRL1 and PGR5 proteins. PGR5 is a small thylakoid protein of about 14 kDa first characterized in plants (Munekage et al. 2002). The mutant in *A. thaliana* showed reduced NPQ (non-photochemical quenching of PSII fluorescence) that was linked to a decrease ΔpH production in reduced Calvin activity conditions, hence the name PGR5 (proton gradient regulation 5). Low light growth under phototrophic conditions wasn't affected. PGR5 was postulated to be part of a cyclic electron transport pathway around PSI occuring prior the ferredoxin-NADPH electron transfer. Later, the PGRL1 protein (proton gradient regulation like 1) was identified in plants (Dalcorso et al. 2008) and in *C. reinhardtii* (Tolleter et al. 2011) as leading to the same phenotype as PGR5 deficient mutant: at high light, decreased electrons transfer rate and reduced NPQ also attributed to a lower ΔpH. PGRL1 is a thylakoid protein anchored in the membrane by 2 transmembrane domains. It was shown to interact with PSI, PGR5 and cytochrome b6f though PGR5 was not found in the CEF promoting supercomplexes (Iwai et al. 2010). PGRL1 was later shown to be able to reduce PQ analogues in vitro (Hertle et al. 2013), though it could only receive electrons from ferredoxin with the help of PGR5. The exact way in which PGR5 allows electron transfer is still under discussion, since the PGR5 isn't part of the CEF supercomplex and is present in a several fold lower amount than PGRL1. PGRL1 has been shown to fold into homo- or heterodimer. The homodimerization allows for a control of PGRL1 activity thanks to the reduction/oxidation of 2 of the 6 conserved cysteine residues (Hertle et al. 2013) in *A. Thalinana*. This monomer/homodimer conformation change is controlled by the thioredoxin system. The heterodimerization involved a PGR5-PGRL1 dimer and is essential for PQ reductase activity. PGRL1 has also been show to bind an iron cofactor (Petroutsos et al. 2009) and to be involved in the iron acclimation response in *C. reinhardtii*. PGRL1 has been shown to interact with CAS (calcium sensor) and ANR1 (anaerobic response 1), 2 proteins that could help tuning the activity of CEF under anaerobic conditions (Terashima et al. 2012). PGRL1 growth phenotype is detected during ATP requiring conditions, such as fluctuating light or low CO_2 concentration. Indeed, *pgrl1* mutant was shown to be more impacted by alternating light intensities in *C. reinhardtii* (high light/low light) (Dang et al. 2014)

rather than by continuous high light. This suggested that alternative mechanisms could occur overtime to compensate for the lack of ATP for photosynthesis. One of these mechanisms was proposed to be the import/export of ATP/NAD(P)H from/to the mitochondria. Indeed, photosynthetic efficiency measurement by fluorescence showed a decrease photosynthetic efficiency in *pgrl1* mutant when mitochondrial inhibitors of the AOX and cytochrome respiration pathways (SHAM+myxothiazol) are added (Dang et al. 2014).

1.4.6. Plastoquinone terminal oxidase

An alternate electron transport pathway during photosynthesis consists of electron transfer from the plastoquinone pool through the plastoquinone terminal oxidase (PTOX) to reduce molecular oxygen (Peltier et al. 2010). This enzyme is encoded by 2 genes in *C. reinhardtii* and plays a role in chlororespiration (NADH to O_2 electron transfer) and water-water cycle (PSII to PTOX electron transfer). PTOX has been proposed to serve as a security valve preventing over-reduction of the plastoquinone pool.

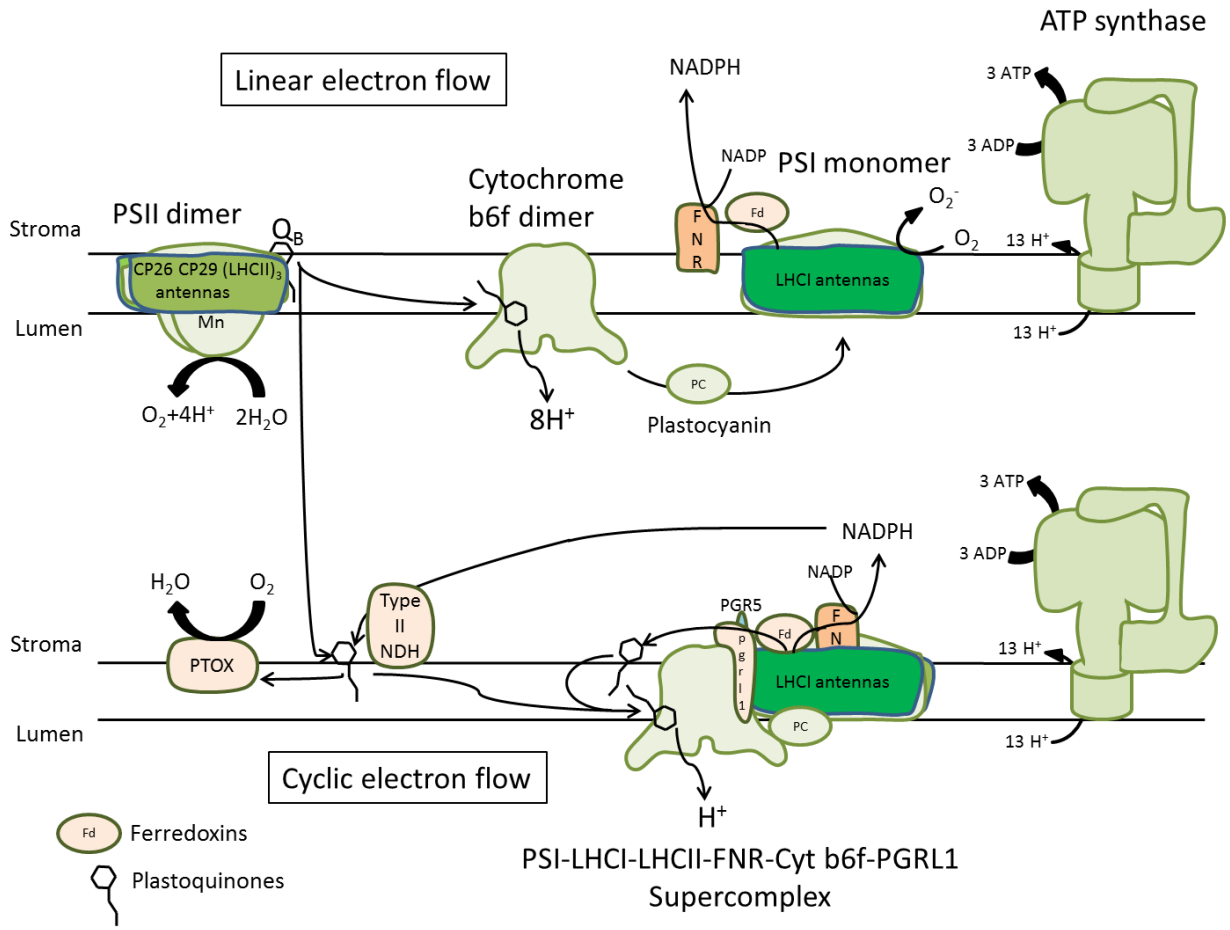

Figure 4: General scheme of photosynthetic electron transport chain for linear electron flow (top) or cyclic electron flow (bottom). Produced NADPH and ATP can serve for carbon fixation in the Calvin cycle (not shown).

1.4.7. State transition

State transition represents a short-term adaptation mechanism involving the remodeling of photosystems apparatus (Figure 5). This includes reversible phosphorylation migration of part of the PSII antenna LHCII to the PSI (reviewed in (Minagawa 2011)). The state in which LHCII are still attached to PSII is called state 1 while the state where LHCII are found attached to PSI is called state 2. This phenomenon was discovered initially in 1969 as a phenomenon involving fluorescence changes upon specific light excitation (Murata 1969). The reversible phosphorylation of LHCII indicates the obvious activity of both a kinase and a phosphatase. A thylakoid membrane protein, later named STT7 in *C. reinhardtii*, was identified to participate in LHCII phosphorylation and to be required for state transition (Depège et al. 2003). STT7

possesses its active kinase domain in the stromal side of the chloroplast (Lemeille et al. 2009). The lumen side of the protein contains 2 cysteine thought to be involved in its regulation since mutation in one of them prevent kinase activity (Lemeille et al. 2009). These cysteine residues are thought to be part of the regulation system for STT7. The regulation mechanism, though speculative, might involve inactivation of the kinase by the thioredoxin system and 2 transmembrane intermediates (Rintamaki et al. 2000;Rochaix 2010). State transitions are mainly driven by the redox state of the PQ pool (Allen et al. 1981) but it was also demonstrated that cytochrome b6f played in important role for state transition. STT7 interacts with cytochrome b6f (Lemeille et al. 2009) and it was later shown that reduced plastoquinone (PQH_2) associated with the Qo site of the cytochrome b6f were what triggered the state transition (Wollman and Lemaire 1988) instead of just the PQH_2 pool alone. In that regard, the chlorophyll α molecule present in the cytochrome b6f might play a role in state transition activation (De Lavalette et al. 2008). In addition to the STT7 kinase, another thylakoid membrane kinase STN8 in plant (Stl1in *C. reinhardtii*) has been shown to participate in the phosphorylation of the PSII during state transition (Vainonen et al. 2005). This second protein is activated after phosphorylation by STT7 (Lemeille et al. 2010). Regarding phosphatases, 2 proteins have been shown to dephosphorylate some LHCII (Shapiguzov et al. 2010) or PSII subunits (Samol et al. 2012) in *A. thaliana*, suggesting that these proteins have an antagonist role compared the STN7 and STN8 (STT7/STL1 homologs) kinases. These proteins are part of the PP2C-type phosphatase family (Rochaix et al. 2012) and thought to dephosphorylate LHCII/PSII, allowing the reverse migration of LHCII toward PSII. Homologs of the same family are found in *C. reinhardtii* (Rochaix et al. 2012).

State transitions are an important aspect of light acclimation in *C. reinhardtii* where up to 80% of LHCII can be removed from PSII (Delosme et al. 1996). LHCII and PSII phosphorylation are processed in orderly fashion (Iwai et al. 2008). The major external LHCII are the first to be phosphorylated. These proteins bind together PSII complexes into mega-complexes, those being the first to be split. The phosphorylation of the P26 and P29 minor antennas and the D2 and CP43 PSII subunits is only being triggered later allowing the undocking of PSII antennas. It was long thought that LHCII once dissociated would migrate toward PSI where they would dock on the opposite side of the PSI LHCI belt. But in recent years, studies showed that most phosphorylated LHCII would not be transferred on PSI (Nagy et al. 2014). Actually, most LHCII would stay

associated with the PSII in a quenched state, where light energy would not be transferred anymore, or in free form once phosphorylated. About 15-20% of the total LHCII antenna would actually be transferred to PSI upon state transition. The author from this study also showed that the phosphorylation of LHCII and PSII also lead to structure changes on the stacked region of the thylakoids, which is thought to be mainly the result of PSII phosphorylation (Fristedt et al. 2009).

State transitions also participate in the redox equilibrium management between chloroplast and mitochondria. Both organelles are known for their numerous interactions and energetic exchanges (Hoefnagel et al. 1998). Studies showed that in ATP deprived condition, such as in mitochondrial mutants, reductive power could be transferred from mitochondria to the chloroplast and the resulting reduction of the plastoquinone pool by type II NDH would trigger transition to state 2 (Cardol et al. 2003). This transition to state 2 could help to balance the energetic deficit since state 2 is known to favor CEF (Alric 2010) (see above) which favors ATP production over NADPH. Studies in *dum22*, deficient in complex I and complex III, and *dum22*/*stt7-9* double mutants, deficient in complex I, complex III and state transition (Cardol et al. 2009) underlined to role of state transition for energetic acclimation since photoautotrophic growth was significantly reduced in *dum22/stt7-9* while *dum22* mutant alone was found to be almost locked in state 2.

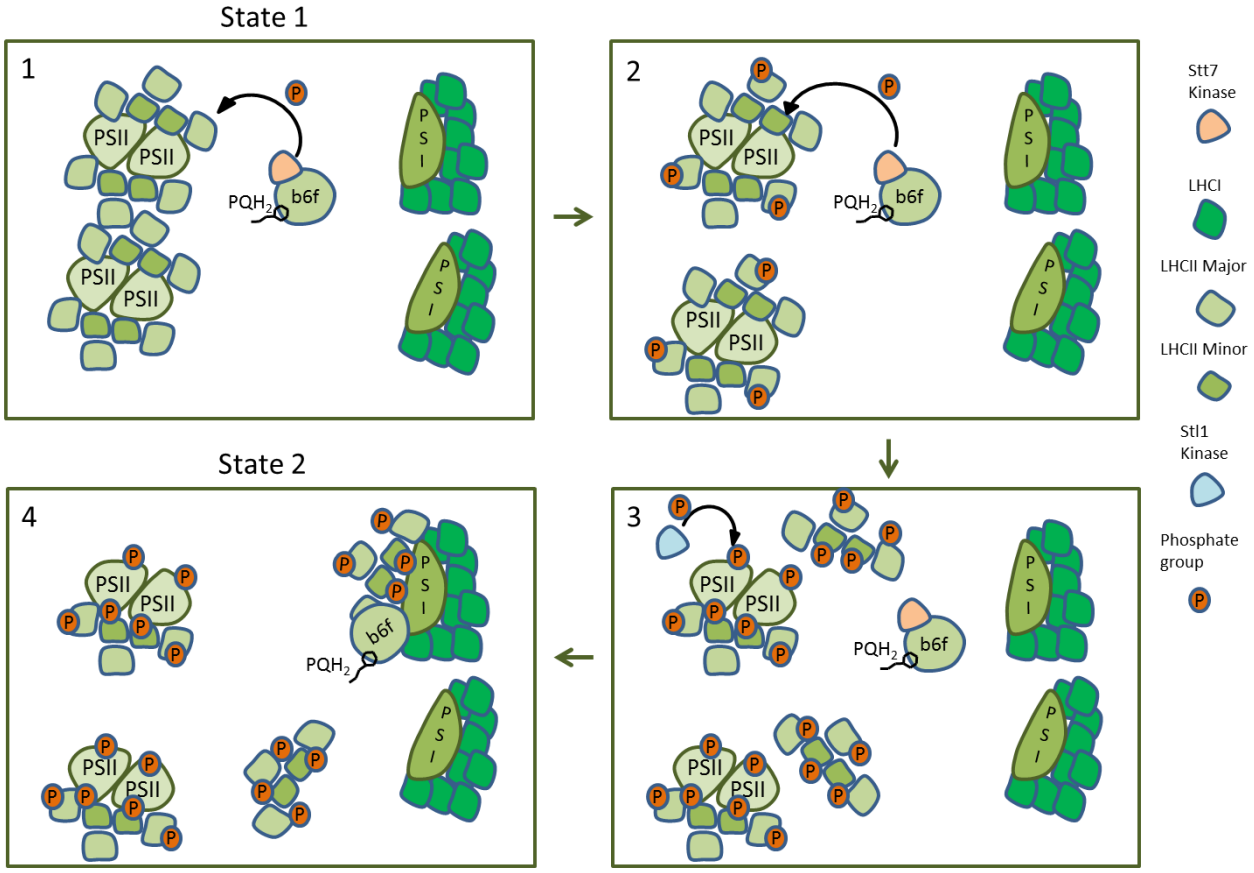

Figure 5: State transition mechanisms in *C. reinhardtii*. Top viewed. Frame 1: Sensing of PQH_2 at the Qo site of cytochrome b6f triggers phosphorylation of LHCII by the STT7 kinase. Major external LHCII antennas are the first to be phosphorylated, triggering the splitting of PSII megacomplexes. Frame 2: Minor LHCII antennas are phosphorylated, triggering the undocking of LHCII. Most LHCII will stay attached to PSII in a quenched state. Frame 3: STL1 kinase will phosphorylate the D2 and CP43 PSII proteins. Frame 4: Some of the phosphorylated LHCII will dock on the free side of PSI complexes favoring the formation of CEF supercomplexes.

1.4.8. Interactions Chloroplast-Mitochondria

Mitochondria and chloroplast are known to interact with each other (Hoefnagel et al. 1998) in order to fine tune their important energetic balance (Figure 6). In the chloroplast, too much reduced NADPH would prevent electrons to leave the PSI properly, leading to slow down photosynthesis and photosynthetic inhibition. NADPH can be exported from the chloroplast via different pathways such as the malate:OxaloacetateA shuttle or DHAP/3-PGA shuttle (Hoefnagel et al. 1998;Noguchi and Yoshida 2008). This reductive power can be sent to the mitochondria for extra ATP production thorugh the mitochondrial electron chain via the malate aspartate shuttle

(Scheibe 1987) or through classical glycolysis whose skeleton is provided by the chloroplast (Klein 1986). If not enough ATP can be produced in the chloroplast, such as in ATP synthase deficient strain, the later can be imported from mitochondria mainly through the DHAP/3-PGA shuttle working in reverse (Boschetti and Schmid 1998).

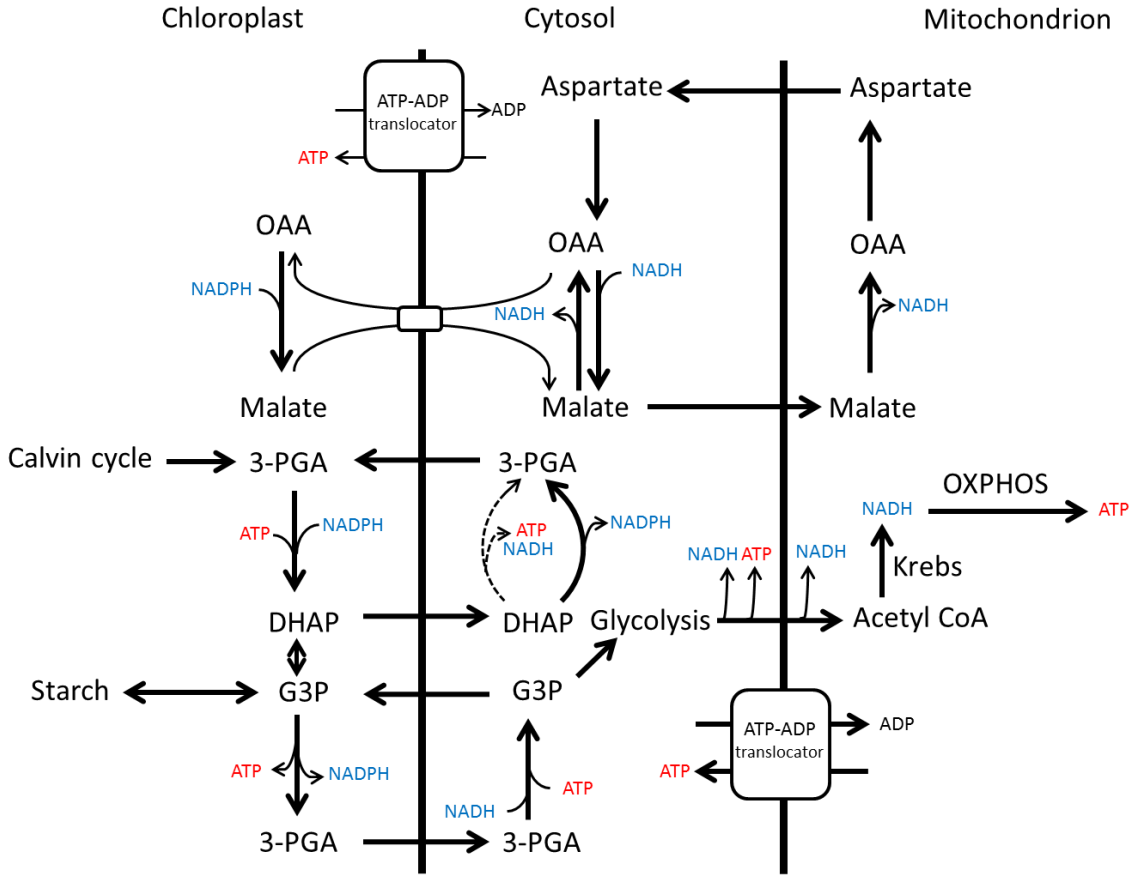

Figure 6: Schematic representation of the main pathways for NAD(P)H and ATP exchanges between organelles. Arrows indicate the main direction of the reactions. Dotted lines represent metabolic pathways significantly less used during normal physiological conditions. White square represents antiporters with corresponding molecules passing through. OAA: oxaloacetate; G3P: Glyceraldehyde 3-phosphate; DHAP: Dihydroxyacetone phosphate; 3-GPA: 3-Phosphoglyceric acid; OXPHOS: oxydative phosphorylation. Adapted from (Hoefnagel et al. 1998),(Noguchi and Yoshida 2008) and (Boschetti and Schmid 1998)

2. Objectives

Chlamydomonas reinhardtii started to be used as a model organism for complex I studies when the first screening method based on dark growth observations was established (Remacle et al. 2001). Though efficient in recovering null mutations, this method didn't allow for fast screening of the transformants and wasn't accurate enough to identify consistently partial deficiencies. These partial deficiences could be caused by mutations in proteins implicated in the assembly process of complex I, this topic being poorly documented in photosynthetic organisms. Chlorophyll fluorescence measurements, on the other hand, represent an accurate measurement method used in great abundance in photosynthetic studies. It is known that in *C. reinhardtii*, photosynthesis relies on mitochondria when its regulatory mechanisms are affected (Cardol et al. 2009). During this work, we tried to take advantages of the mitochondrial-photosynthetic interactions to identify conditions where weak mitochondrial deficiencies could be reflected on photosynthesis by coupling deficient photosynthetic mutants to mitochondrial mutations. We had thus two objectives in our work (i) to gain general knowledge on *Chlamydomonas* complex I (publication 1) and (ii) to develop an efficient screening method, based on chlorophyll fluorescence measurements, to identify and characterize partially deficient complex I mutants (publications 2 and 3).

RESULTS/PUBLICATIONS

Publication 1. **Inactivation of genes coding for mitochondrial Nd7 and Nd9 complex I subunits in *Chlamydomonas reinhardtii*. Impact of complex I loss on respiration and energetic metabolism**

Simon Massoz, Véronique Larosa, Charlotte Plancke, Marie Lapaille, Benjamin Bailleul, Dorothée Pirotte, Michèle Radoux, Pierre Leprince, Nadine Coosemans, René F. Matagne, Claire Remacle, Pierre Cardol (2014). Mitochondrion 19:365-374

This paper is the condensed work of a great number of people. It combines the analyses of RNAi-*NUO7* and RNAi-*NUO9* cell lines produced by P. Cardol several years ago, the analysis of the *amc14* mutant, an insertional mutant obtained during a previous mutagenesis (Massoz et al. 2015), and proteomic analysis done before my work in the lab, in addition to metabolic analysis that I performed to further investigate the impact of the loss of complex I.

Our initial goal was to finish the characterization of RNAi mutants isolated years ago and complete their characterization by analysing the *amc14* mutant, a mutant partially deficient for the NUO9 protein like one of the RNAi mutant previously isolated (RNAi-*NUO9* cell line). NUO7 and NUO9 are the only two proteins from the matrix arm of complex I that do not bear any iron-sulfur centers. Though they were never characterized in *Chlamydomonas,* mutants in these proteins have been studied in other organisms, offering a nice opportunity to investigate the similarities or differences of the role of these proteins in complex I. During this study, unexpected results led us to truly start to dig into *Chlamydomonas* complex I assembly during our future researches. Different modules (N and Q) of complex I showed different profile upon deletion of either NUO7 or NUO9, two subunits from the Q module of complex I. These results were the cause of our interest in complex I assembly (cf publications 3).

In addition, if the impact of complex I on photosynthesis had been the center of interest of previous studies (Cardol et al. 2003), metabolic studies had never been done on complex I mutants in *C. reinhardtii.* The metabolic analysis previously done on the *Δnd6* mutant was a great opportunity to further investigate the impact of loss of complex I on general metabolism. We measured different parameters (PSII antenna size, ROS content, chlorophyll $_{a+b}$ content, oxygen evolution in the light) in order to confirm whether these different pathways were altered or not. Our finding showed interesting results compared to previous proteomic studies in mutants less affected in their energy production such as RNAi-*AOX1* cell lines.

In this publication I have characterized the *amc14* insertion (Fig. 1C), the activity of various complexes in the *amc*14 mutant (Table 1), performed immunoblot analysis on the RNAi-

NUO7 and RNAi-*NUO9* mutants (Fig. 3D) and performed antenna size and ROS measurements on the RNAi-*NUO7* and RNAi-*NUO9* cell lines (Table 2.). I have also performed BN-PAGE analysis and participated to the redaction of the paper.

Inactivation of genes coding for mitochondrial Nd7 and Nd9 complex I subunits in *Chlamydomonas reinhardtii*. Impact of complex I loss on respiration and energetic metabolism (2014). Mitochondrion 19:365–374.

Simon Massoz [a], Véronique Larosa [a], Charlotte Plancke [a],Marie Lapaille [a], Benjamin Bailleul [a], Dorothée Pirotte [a], Michèle Radoux [a], Pierre Leprince [b], Nadine Coosemans [a], René F.Matagne [a], Claire Remacle [a], Pierre Cardol [a*]

[a] Genetics of Microorganisms, PhytoSYSTEMS, Department of Life Sciences, University of Liège, Belgium
[b] GIGA-Neuroscience, University of Liège, Belgium
* corresponding author : Corresponding author at: Laboratory of Genetics and physiology microalgae, PhytoSYSTEMS, Department of Life Sciences, University of Liège, B-4000, Liège, Belgium. Tel.: +32 43663840. E-mail address: pierre.cardol@ulg.ac.be (P. Cardol).

(1) Abstract (250 words)

In *Chlamydomonas*, unlike in flowering plants, genes coding for Nd7 (NAD7 NAD7/49 kDa) and Nd9 (NAD9/30 kDa) core subunits of mitochondrial respiratory-chain complex I are nucleus-encoded. Both genes possess all the features of mitochondrial respiratory-chain complex I are nucleus-encoded. Both genes possess all the features that facilitate their expression and proper import of the polypeptides in mitochondria. By inactivating their expression by RNA interference or insertional mutagenesis, we show that both subunits are required for complex I assembly and activity. Inactivation of complex I impairs the cell growth rate, reduces the respiratory rate, leads to lower intracellular ROS production and lower expression of ROS scavenging enzymes, and is associated to a diminished capacity to concentrate CO_2 without compromising photosynthetic capacity.

(2) Introduction

Rotenone-sensitive NADH:ubiquinone oxidoreductase (complex I, EC 1.6.5.3) is the largest enzyme complex of the mitochondrial respiratory chain. This membrane-bound enzymatic assembly of approximately 1000 kDa is composed of 45 subunits in the mammal *Bos taurus* (Carroll et al., 2006), 42 in the fungus *Yarrowia lipolytica* (Angerer et al., 2011), 49 in the land plant *Arabidopsis thaliana* (Peters et al., 2013) and 42 in the green alga *Chlamydomonas reinhardtii* (Cardol et al., 2004). At least 40 subunits are conserved in all eukaryotic lineages (Cardol, 2011). Fourteen of these subunits are homologous to the 14 constituents of the bacterial type-I dehydrogenase and are thus considered as the core of the mitochondrial complex I (Friedrich, 2001). In mammals and fungi, seven hydrophobic subunits (ND1, 2, 3, 4, 4L, 5, and 6) of these 14 components are encoded in the mitochondrial genome and constitute the core of the

membrane arm of the complex. Encoded in the nuclear genomes, the 7 remaining subunits (NDUFS7/PSST, NDUFS8/TYKY, NDUFV2/24 kD, NDUFS3/30 kD, NDUFS2/49 kD, NDUFV1/51 kD, NDUFS1/75 kD according to the human/bovine nomenclature) constitute the core of the matricial soluble arm which bears all the prosthetic groups (Fe–S clusters, FMN) that are required for electron transfer from NADH to ubiquinone (Sazanov and Hinchliffe, 2006). Several exceptions to this distribution between mitochondrion-encoded membrane constituents and nucleus encoded matricial subunits however exist in the green lineage: (i) the mt-DNA of most land plants code for 49 kD (NAD7) and 30 kD (NAD9) hydrophilic subunits; (ii) in the liverwort *Marchantia polymorpha*, a nad7 pseudogene is located in the mtDNA whereas a functional nad7 gene copy is found in the nuclear genome (Kobayashi et al., 1997); and (iii) the mitochondrial genomes of several chlorophycean unicellular green algae (including C. reinhardtii and *Scenedesmus obliquus*) code only for five complex I subunits (ND1, 2, 4, 5 and 6) (Bullerwell and Gray, 2004). Thanks to the sequencing of the nuclear genome of *C. reinhardtii* (Merchant et al., 2007), the *NUO3, NUO7, NUO9*, and *NUO11* algal nuclear genes have been identified as homologs of the ND3, ND7, ND9 and ND4L mitochondrial coding sequences from flowering plants (Cardol et al., 2005). To address the question of complex I assembly, *C. reinhardtii* has been demonstrated to constitute a particularly useful experimental model. Complex I deficient mutants survive in photo-autotrophic conditions (light + mineral medium) due to the operation of rotenone insensitive alternative NAD(P)H dehydrogenases (Lecler et al., 2012) and because their photosynthetic activity is barely affected (Cardol et al., 2003). Complex I deficient mutants are also viable in heterotrophic conditions (darkness + acetate as a carbon source). This provides an advantage to screen for complex I mutants, as they display robust growth in the light but slow growth under heterotrophic conditions (Remacle et al., 2008). Several mutations in four of the complex I subunits (ND1, 4, 5, and 6) encoded by the mitochondrial genome have been described so far in *Chlamydomona*s (Cardol et al., 2002, 2008; Larosa et al., 2012; Remacle et al., 2001, 2006). Several complex I deficient mutants (called amc for “assembly of mitochondrial complex I”) of nuclear origin have also been isolated by using a mutagenesis approach (Barbieri et al., 2011). In *C. reinhardtii*, RNA interference is an alternative powerful tool to knock-down the expression of specific nuclear genes (Schroda, 2006). The use of this technique allowed us to determine that ND3 and ND4L subunits are required for complex I activity and assembly in *Chlamydomonas* (Cardol et al., 2006). RNA interference also allowed

us to gain insight into the role of other respiratory chain enzymes, such as F1FO ATP synthase (Lapaille et al., 2010), rotenone-insensitive alternative NAD(P)H dehydrogenase (Lecler et al., 2012) and cyanide insensitive alternative oxidase (AOX) (Mathy et al., 2010). In this work, we aimed to inactivate the expression of the *NUO7* and *NUO9* nuclear genes (encoding Nd7 and Nd9 subunits) by using the RNA interference or insertional mutagenesis approaches in C. reinhardtii. To identify putative alterations of the energetic metabolism in complex I mutants (as previously observed for *AOX* defective mutants of Chlamydomonas (Mathy et al., 2010) , a comparative study of the cellular soluble proteome has been undertaken on a mutant totally deprived of complex I (*dum17* defective in mitochondrion-encoded ND6 subunit).

(3) Results

1. *NUO7* and *NUO9* genes possess features of *Chlamydomonas* nuclear genes and their polypeptide products are adapted for import into mitochondria

The endosymbiotic event that gave rise to mitochondria was followed by a massive migration of genes from the endosymbiont to the nucleus (Gray et al., 1999). As well as the highly hydrophobic components of complex I, the hydrophilic NAD7 and NAD9 subunits from most flowering plants remain encoded in the mitochondrial genome. In contrast, these genes are missing from the mitochondrial genome of *C. reinhardtii*, as it is also the case in mammals and fungi. We previously identified the *NUO7* and *NUO9* nuclear genes of *C. reinhardtii* (encoding Nd7 and Nd9 subunits) as homologs of the sequences encoding flowering plant NAD7 and NAD9 subunits, respectively (Cardol et al., 2004). To be efficiently expressed, mitochondrial genes that have been transferred to the nucleus have to acquire several distinct traits typical of nuclear genes and absent in mitochondrial genes (González-Halphen et al., 2004). (i) Efficient promoter. Based on signals obtained on Northern blot experiments (as shown in Fig. 2), one can infer that both *NUO7* and *NUO9* genes have acquired efficient promoters. (ii) Changes in codon usage. The pattern of codon usage in *NUO7* and *NUO9* genes is typical of nuclear genes (Table S1). Moreover, the GC content of both genes is about 63% and fits well with that of the nuclear genome (64%)(Merchant et al., 2007). In contrast, the GC content is only 45% for mtDNA (GenBank U03843 accession number). (iii) Acquisition of polyadenylation signal. The polyadenylation signal of *C. reinhardtii* nuclear genes (TGTAA) (Silflow, 1998) is found at

the end of cDNA sequences (GenBank XM_001697555 and XM_001690600 accession numbers). (iv) Acquisition of introns. Intronic sequences with orthodox splicing sites (Silflow, 1998) were identified: eleven were found in the *NUO7* gene (Phytozome Cre09.g405850 accession number) and one in the *NUO9* gene (Phytozome Cre07.g327400 accession number). (v) Presence of a putative mitochondrial targeting sequence (MTS).Most nucleus-encoded mitochondrial proteins contain a targeting sequence that sorts the intracellular localization (Glaser et al., 1998).When the deduced full-length ND7 and ND9 sequences were compared to the polypeptidic sequences of flowering plants, N-terminal extensions of about 75 and 85 residues, respectively, were found (Fig. S1). A targeting prediction to mitochondria was also given by Predalgo program (Tardif et al., 2012), with a peptide signal of 57 and 71 amino acids which possess all characteristics of MTS: (a) their composition is similar to the composition described for MTS of higher plants (Glaser et al., 1998) (data not shown); (b) the N terminal residues (1 to 18) have the potential to form amphiphilic α helixes with one hydrophilic and positively charged face and one a polar face (Fig. 1D). This amphiphilicity seems to be essential for the function of MTS (Emanuelsson et al., 2000). (c) Putative cleavage sites (Glaser et al., 1998) are found after residue 70 (RS↓AT) for Nd7 and residue 73 (RX7RK↓TT) for Nd9, which is consistent with the length of their protein homologues encoded by mtDNA from plants. Moreover, the deduced molecular masses of mature Nd7 (45211 Da) and Nd9 (24462 Da) subunits are in good agreement with their identification in SDS gel by mass spectrometry as 43 and 25-kDa bands of complex I, respectively (Cardol et al., 2004).

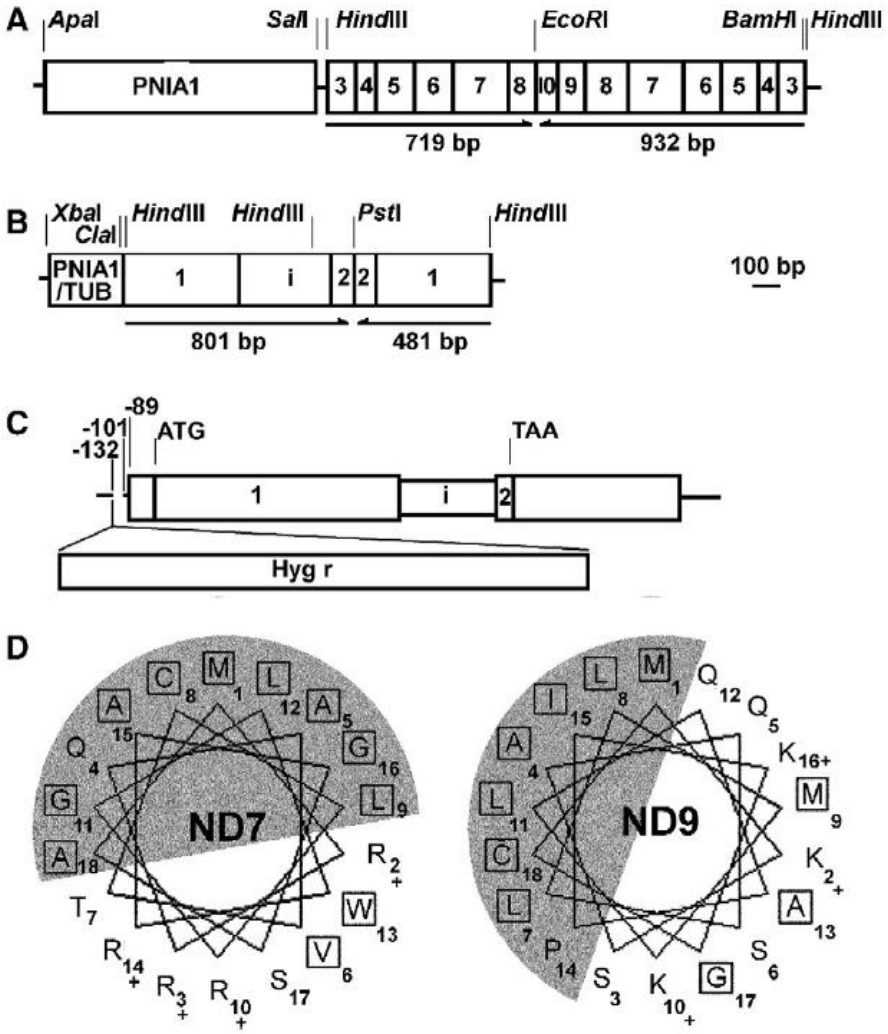

Fig. 1. (A–B), Schematic representation of double-strand (ds)RNAi constructs. XbaI/HindIII fragments of pND7-RNAi (A), and pND9-RNAi (B). PNIA1: promoter of the Chlamydomonas NIA1 gene encoding nitrate reductase. PNIA1/TUB1: 229-bp chimeric promoter. Numbers within rectangles correspond to the selected exons of the NUO7 and NUO9 genes (i = intron). For NUO9, we cloned an intron-containing gene fragment, directly linked to its cDNA antisense counterpart, downstream a chimeric promoter composed of 84-bp sequence of the NIA1 promoter fused to a minimal β-tubulin promoter. For NUO7,we cloned two complementary cDNAs fragments in opposite orientation downstream the complete NIA1 promoter. (C), Schematic representation of NUO9 gene with localization of the insertion inamc14.Numbers refer to bases relative to the initiation site of translation. (D), Position of the 18 N-terminal residues of ND7 and ND9 polypeptides along α helixes. Positively-charge residues are marked by a +. Non-polar residues are squared. Predicted apolar face of the amphiphilic helix is shaded.

2. RNAi mutants defective in *NUO7* or *NUO9* gene expression lack complex I activity

To suppress the expression of *NUO7* and *NUO9* genes (coding for Nd7 and Nd9 complex I subunits, respectively), a cell-wall less strain of *C. reinhardtii* auxotroph for arginine (strain 325.2) was co-transformed with the pASL plasmid (bearing the ARG7 gene), and the plasmid designed for RNA interference (pND7-RNAi or pND9-RNAi, Fig. 1). One hundred and twenty arg+ colonies of each transformation experiment were selected and tested by PCR for the presence of a pRNAi plasmid partial sequence in their genome, as described in Section below. Thirteen and seventeen co-transformants, called coND7 and coND9 clones, respectively, were obtained. To investigate complex I activity in the co transformants, high molecular-mass complexes from crude membrane fractions were separated by BN-PAGE. NADH dehydrogenase activity of the complex I matricial arm was then tested using NBT as an electron acceptor. Wild-type complex I activity was associated with a single band at 950 kDa, as previously found (Cardol et al., 2002, 2004). The staining level of each clone was determined and reported as a percentage of the wild-type staining. One coND7 clone (19) and two coND9 clones (54 and 115) showed a very low activity (~5%) after 2 h of incubation in the staining reaction mixture. To determine whether the complex I activity defect detected in coND7-19 mutant was correlated to a specific degradation of *NUO7* transcripts, the transcription levels of *NUO3*, *NUO7*, *NUO9*, *NUO11*, *NUO17* and *NUOP1* genes, coding for ND3, ND7, ND9, ND4L, ESSS/ NDUFB11 and B14.5b/NDUFC2 complex I subunits (bovine/human nomenclature), were investigated by Northern blot analyses (Fig. 2A).

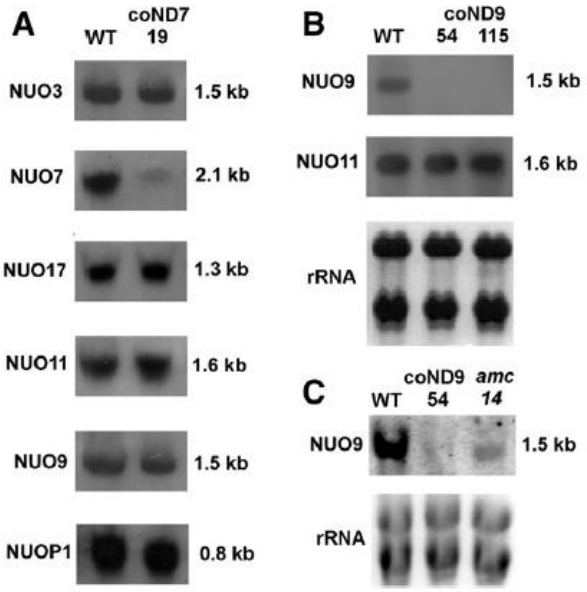

Fig. 2. Transcriptional analysis of several complex I genes in coND7 (A), coND9 (B), and *amc14* (C) mutant strains. Hybridization patterns were obtained with *NUO3, NUO7, NUO9, NUO11, NUO17*, and *NUOP1* probes on RNA blot (see Methods for details). An approximate size (in kb) is given for each transcript.

NUO7 transcripts were almost absent in coND7-19 whereas the levels of other transcripts were similar to the control strain. A similar analysis showed that *NUO9* transcript was undetectable in coND9-54 and coND9- 115 mutant strains, while other transcript amounts (e.g. *NUO11*) were equivalent to those detected in wild-type cells (Fig. 2B). Taken together, these results indicates that the complex I activity defect detected in the mutants is due to a specific loss of the *NUO7* or *NUO9* transcripts triggered by the RNA interference machinery. The frequency of transformants showing an altered complex I defect among those bearing the inactivation cassette was thus about 10%. This frequency is similar to the one reported in previous studies dedicated to the inactivation of other genes in other cellular processes by RNAi approach in Chlamydomonas (Schroda, 2006). Complex I-defective mutants show slow growth when cultivated under heterotrophic conditions (see Introduction). In the light, they also show a reduced growth compared to wild-type cells when fed with an exogenous organic carbon source (e.g. acetate) (Cardol et al., 2002; Remacle et al., 2001). In the light without acetate (phototrophic growth), the doubling time determined for wild-type cells (83 h ± 11 h) did not differ significantly from the values obtained for mutant cells, meaning that when the cell metabolism

relies mainly on photosynthesis (i.e. phototrophic growth), complex I activity plays a minor role in cell energetics.

Table 1
Respiratory rates (nmol $O_2 \cdot min^{-1} \cdot 10^{-7}$ cells) of wild-type and mutant cells were measured in the absence or in the presence of 100 μM rotenone.

	Control	Nd7	Nd9	Nd9	Nd9	ND6
	WT	co-19	co-54	co-115	*amc14*	*dum17*
Total respiration	41 ± 3	26 ± 2	28 ± 4	nd	26 ± 3	20 ± 4
Rotenone-sensitive respiration	26 ± 3	2 ± 1	2 ± 2	nd	11 ± 2	3 ± 3
NADH:DQ oxidoreductase[a]	108 ± 21	43 ± 6	50 ± 12	45 ± 8	78 ± 12	61 ± 13
Complex I activity[b]	53 ± 13	1.4 ± 0.8	2.1 ± 1.5	1.2 ± 1.1	27 ± 10	0
NADH:$Fe(CN)_6^{3-}$ oxidoreductase[c]	2312 ± 424	786 ± 222	401 ± 113	289 ± 57	1346 ± 189	389 ± 86
Complex IV activity[d]	237 ± 18	218 ± 4	263 ± 23	202 ± 24	262 ± 44	182 ± 51

Table 1. Specific enzyme activities were measured in crude membrane fractions. nd, not determined. Means ± SD from three to six experiments.

a NADH:duroquinone oxidoreductase (nmoles of NADH oxidized·min^{-1}·mg $protein^{-1}$).

b Rotenone-sensitive NADH:duroquinone oxidoreductase (nmoles of NADH oxidized·min^{-1}·mg $protein^{-1}$).

c NADH:ferricyanide oxidoreductase (nmoles of $K_3Fe(CN)_6^{3-}$ reduced·min−1·mg $protein^{-1}$).

d Cytochrome c oxidase (nmoles of cytochrome c oxidized·min^{-1}·mg $protein^{-1}$).

The difference between wild type and complex I mutants was however more pronounced when the mitochondrial metabolism was stimulated by acetate in the light (mixotrophic growth). For wildtype wall-less cells, the doubling time obtained (13 h ± 3 h) was in good agreement with previous reports (Baroli et al., 2004), while it was ~1.5 higher for mutants (19 h ± 3 h for coND7-19, 21 ± 3 h for coND9-54 and -115). Therefore, all experiments were conducted on cells grown in the presence of acetate in the light. Respiration of complex I mutant also lacks sensitivity to rotenone (Remacle et al., 2008), a potent inhibitor of ubiquinone reduction by complex I. Dark respiration rate of mutants grown in mixotrophic conditions was found to be ~40% inferior to the value obtained for wild-type cells (about 40 nmol O2·min−1 per 107 cells) and almost insensitive to rotenone (Table 1).

3. An insertion in the promoter region of *NUO9* gene partly impairs complex I activity in *amc14* mutant

A previous forward genetic screen allowed to isolate seven *amc* nuclear mutants (for assembly of mitochondrial complex I) displaying reduced or no complex I activity (Barbieri et al., 2011). To uncover additional AMC loci, we undertook another screen for nuclear mutants defective in complex I (see Section 2.3.2). Out of ~3000 insertional hygromycin resistant transformants, 5 showed features of complex I-defective mutants. One mutant strain (further

named amc14) showed a reduced growth in heterotrophic (darkness + acetate) and mixotrophic (light + acetate) conditions (Fig. S2A). Its rotenone-sensitive respiration was about 40% of the control wild-type strain. Moreover, in-gel staining of NADH dehydrogenase activities indicated that ~30–50% complex I activity was retained (Fig. S2B). Since the antibiotic resistance cosegregated with the *amc* phenotype (data not shown), we concluded that the AMC14 locus was tagged with the insertional marker. Using TAIL-PCR mapping, we found that the insertional marker was located in the promoter region of the *NUO9* gene, 132 bp upstream of the initiation codon (Fig. 1C and S2C). The size of the deletion that accompanied the insertion of the marker was at most 31 bp. Fig. 2C shows that the amount of *NUO9* transcript was greatly reduced in *amc14*. We can thus conclude that the insertion in the promoter region of *NUO9* gene impairs expression of the corresponding transcript.

4. Lack of complex I activity and assembly in the absence of Nd7 or Nd9 subunits

To confirm the defect in complex I activity due to impairment in *NUO7* or *NUO9* gene expression, enzyme activities were measured in crude membrane fractions and compared to values obtained for wild type (Table 1). In the RNAi mutants, the NADH:duroquinone oxidoreductase activity sensitive to rotenone (considered to represent the activity of complex I) was found to be null or almost null and the NADH: ferricyanide oxidoreductase which is mainly catalyzed (70–85%) by the matricial arm of complex I in Chlamydomonas (Cardol et al., 2002) was about 15–30% of wild-type activity. These results are similar to those obtained for mitochondrial *dum17* mutant defective in complex I ND6 subunit (Table 1). In the *amc14* mutant, the complex I and NADH:ferricyanide oxidoreductase activities were however up to 50–60% of the wild-type values. These results agree with the complex I defect observed by in-gel staining activities (Fig. S2B) and reduced amount of *NUO9* transcripts. In contrast, cytochrome c oxidase activity was determined as control and no significant difference could be observed between wild-type and mutant strains.

In order to gain further insights into the impact of the loss of Nd7 or Nd9 on membrane complex assembly, whole membrane fractions from RNAi complex I-null mutants and wild type were purified and subjected to BN-PAGE analyses. By staining the gel with Coomassie blue, respiratory-chain dimeric complex V (1600 kDa, Villavicencio-Queijeiro et al., 2009) and

complex I (950 kDa Cardol et al., 2004) were detected in wild-type extract (Fig. 3A). In contrast, no complex I was observed in the RNAi mutants while the amount of dimeric complex V was not altered.

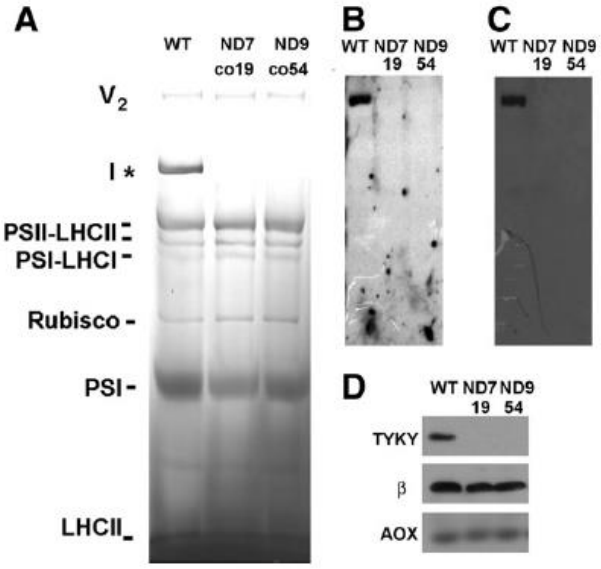

Fig. 3. Analysis of mitochondrial and chloroplastic native complexes in coND7 and coND9 mutants. 120 µg of crude membrane proteins were loaded on a BN-gel. After electrophoresis, the gel was submitted to NADH/NBT staining (*, NADH/NBT staining) and further stained with Coomassie blue (A) or blotted and probed with antisera against the whole complex I (B) or against PSST subunit (C). I and V2 correspond to respiratory-chain complexes I and V (dimeric state), respectively. Based on their electrophoretic mobility (Rexroth et al., 2004), PSI and PSII were identified. PSI, PSII, LHCI, LHCII correspond to photosynthetic complexes I, II, and to light harvesting complexes I and II. (D) 25 µg of crude membrane proteins were subjected to SDS-PAGE, blotted and probed with antisera against TYKY, ATP2 and AOX proteins.

These results were confirmed by comparing the amount of three proteins in membrane fraction by immunodetection on Western blot after SDS-PAGE: TYKY (complex I subunit encoded by *NUO8* gene), β subunit (complex V subunit encoded by *ATP2* gene) and AOX (respiratory-chain alternative oxidase) (Fig. 3D). In order to identify putative complex I subcomplexes, the protein complexes separated by BN-PAGE were also tested by immunodetection on Western blots with antisera against whole *N. crassa* complex I or against subunit PSST of *Y. lipolytica* (homologous of *C. reinhardtii* complex I subunit encoded by *NUO10* gene). In wild type, only the whole complex I is highlighted by both antibodies whereas no signal could be detected for mutants (Fig. 3B, C).

5. The loss of complex I leads to slight modifications of the energetic metabolism

We previously showed that among respiratory-deficient mutants, those affected solely for complex I activity were the less affected regarding their ATP content and photosynthetic electron transfer chain in the chloroplast (Cardol et al., 2003). In order to analyze the main consequences of suppression of complex I activity on the metabolic network of the cell, we carried out a comparative study on the cellular soluble proteome. This analysis was performed by using the mitochondrial *dum17* mutant which is fully defective in complex I and possesses a cell-wall (knock-out strain, mutated in the mitochondrial encoded nd6 gene (Cardol et al., 2002), instead of cell-wall less RNAi strains that are knock-down strains. To minimize variations between strains due to genetic drift, we compared two *dum17* mutant strains isolated 10 years ago (233 and 680 strains in our stock collection) with two wild-type strains (1′ and 2′ strains in our stock collection). A total of ~4800 protein spots were detected on the 2D gels (Fig. S3, pH range 3–11 non-linear). Based on a statistically significant Student's t-test (p b 0.05, n = 3) for higher than 1.3-fold increase or lower than 1.3- fold decrease in ratio of normalized spot abundance for 3 comparisons out of 4 (233/1′, 233/2′, 680/1′, 680/2′), 58 protein spots were accepted as being differentially expressed between wild-type and *dum17* mutant strains. Sixteen of them were identified along with 140 protein spots displaying no variation (Table 3 and Table S2). Only proteins related to energetic metabolism, which constituted the majority of identified spots, have been considered in the following analysis.

	WT	*dum17*	coND7-RNAi	coND9-RNAi
$Chlorophyll_{a+b}$	1 ± 0.04	0.95 ± 0.06	1.01 ± 0.03	0.98 ± 0.02
PSII antenna size	1 ± 0.12	1.14 ± 0.08	0.96 ± 0.08	0.92 ± 0.09
Pmax	1 ± 0.22	0.89 ± 0.12	0.85 ± 0.23	0.90 ± 0.21
H_2O_2	1 ± 0.07	0.65 ± 0.06	0.75 ± 0.31	0.88 ± 0.22

Table 2. Photosynthetic parameters and hydrogen peroxide production of complex I-deficientmutant cells relative to wild-type cells in mixotrophic conditions (light + acetate). Chlorophylla + b (23.8 ± 0.8 μg per 107 cells for wild-type cells). PSII antenna size was estimated as t1/2 (s) of chlorophyll fluorescence induction kinetics in the presence of DCMU at low light. Pmax, maximum rate of oxygen evolution in saturating light (61 ± 14 nmol $O2 \cdot min^{-1}$ per 10^7 cells in WT). Hydrogen peroxide production (DAB staining, arbitrary unit). Average of WT mt+/− cw+/− strains and complex I deficient mutants (233 and 680 dum17 strains; coND7 and coND9 strains) incubated in white light (50 μE m^{-2} s^{-1}). Mean value obtained for control cells were arbitrarily fixed to 1 (mean ± SD of N3 experiments).

Gene	Name	# spots (average ratios) (CI-/WT)	Protein ID
	Mitochondrial respiratory chain		
NUO9	Complex I Nd9 subunit	1 (−2.1*)	gi|159464845
NUOA9	Complex I 39 kDa subunit	1 (−1.9*)	gi|159489336
QCR1	Complex III 50 kD core 1 subunit	1 (−1.1)	gi|159477849
ATP1A	F_1F_0 ATP synthase alpha subunit	1 (1)	gi|159483185
ATP2	F_1F_0 ATP synthase beta subunit	2 (1,−1.1)	gi|159466892
ASA7	F_1F_0 ATP synthase Asa7 subunit	1 (1)	gi|159477303
	ROS scavenging		
FSD1	Chloroplastic superoxide dismutase [Fe]	1 (−1.5*)	gi|159464723
GSTS2	Glutathione S-transferase	1 (−1.7*)	gi|159482414
MSD1/SODA	Mitochondrial superoxide dismutase [Mn]	1 (−1.6*)	gi|159484019
	Krebs cycle, glycolysis, glyoxylate cycle		
AST1	Mitochondrial aspartate aminotransferase	1 (+2.0*)	gi|159473837
AST3	Chloroplastic aspartate aminotransferase	1 (+1.3*)	gi|159483981
PGK1	Phosphoglycerate kinase	1 (+1.1)	gi|159482940
ICL	Isocitrate lyase	5 (−1.1,−1.1,−1.1,1,+1.3)	gi|619932
MAS	Malate synthase	2 (−1.2,−1.1)	gi|159475042
ACH1	Aconitate hydratase	7(+1.1,+1.1,+1.1,+1.1,+1.3,1.4,+1.4*)	gi|159462944
ACS3	Acetyl CoA synthetase	1 (1)	gi|159488061
IDH3	NADP-dependent isocitrate dehydrogenase	1 (+1.1)	gi|159481269
GCSL	Dihydrolipoyl dehydrogenase	1 (+1.3)	gi|159474092
	Photosynthesis, Calvin cycle, carbon fixation		
CAH1	Periplasmic carbonic anhydrase alpha	3 (−2.4*,−2.8*,−6.7*)	gi|159468241
CA1	Mitochondrial carbonic anhydrase beta	2 (−1.2,−1.8)	gi|1323549
OEE1	Oxygen-evolving enhancer protein 1	3 (−1.1,−1.1,−1.1)	gi|74272687
OEE2	Oxygen-evolving enhancer protein 2	2 (−1.1,−1.9)	gi|159471964
LHCB M1	Light-harvesting complex II protein	1 (1)	gi|20269804
LHCB M2	Light harvesting complex II protein	2 (−1.2,−1.5*)	gi|4139216
LHCB M3	Light harvesting complex II protein	3 (−1.3,1,+1.2)	gi|159491492
LHCB5	Light harvesting complex II protein	1 (−1.5*)	gi|159475641
LHCB M10	Light harvesting complex II protein	4 (−1.1,−1.2,−1.2,−1.2)	gi|19423285
ATPA	ATP synthase CF1 alpha subunit	2 (+1.1,+1.2)	gi|1334356
ATPB	ATP synthase CF1 beta subunit	3 (+1.1,+1.1,+1.4)	gi|41179057
ATPC	ATP synthase CF1 gamma subunit	1 (−1.3)	gi|159476472
GAP1b	Glyceraldehyde-3-phosphate dehydrogenase	3 (1,−1.2,−1.3)	gi|159490469
PRK1	Phosphoribulokinase	1 (+1.3)	gi|159471788
RBCL	Rubisco large subunit	13 (−1.1,−1.1,1,1,1,1,+1.1,+1.1,+1.1,+1.2,+1.3,+1.3,+1.4)	gi|5360587
RBCS	Rubisco small subunit	1 (−3.7*)	gi|16975084
RCA1	Rubisco activase	2 (−1.1,1)	gi|159468147
SEBP1	Sedoheptulose-1; 7-bisphosphatase	2 (1,+1.3)	gi|159467635
TAL1	Transaldolase	1 (+1.1)	gi|159463680
TRK1	Transketolase	4 (−1.2,−1.3,−1.4,−1.5)	gi|159487741
STA6	ADP-glucose pyrophosphorylase small subunit	1 (+1.1)	gi|159467349
	Chlorophyll biosynthesis		
DXR1	1-Deoxy-D-xylulose 5-phosphate reductoisomerase	1 (+1.2)	gi|159471628
ChlH	Magnesium chelatase subunit I	2 (+1.1,+1.2)	gi|159466070
ChlP	Geranylgeranyl reductase	1 (1)	gi|159464036
POR	Light-dependent protochlorophyllide reductase	1 (−1.2)	gi|159462468
PPX1	Protoporphyrinogen oxidase	1 (+1.4)	gi|159472731

* t-test $p < 0.05$.

Table 3. Effects of complex I loss on soluble proteins involved energetic metabolism. Number of spots identified for each proteins are given with the average ratio (see Table S2 for details).

Apart from two complex I subunits that show a strong decrease in their expression, proteins belonging to respiratory chain complex III and ATP synthase did not show any modification, confirming that the lack of complex I has no impact on the major constituents of the respiratory chain (Cardol et al., 2002, 2008; Remacle et al., 2001). Several proteins involved in Krebs cycle, glyoxylate cycle or glycolysis were also identified and none varied, at the exception of one spot over seven corresponding to aconitate hydratase. In contrast, we observed an increase of the amount of two aspartate amino acid transferases (Ast1, Ast3) and we found a down-regulation of three major ROS scavenging enzymes, namely mitochondrial Mn superoxide

dismutase (Msd1, −1.7), chloroplastic Fe superoxide dismutase (Fsd1, −1.5) and cytosolic glutathione S-transferase (GstS2, −1.6). Since superoxide dismutases are scavengers of $O2^{-}$ into H2O2, we tested peroxide production. In *dum17* complex I-deficient cells, it was 35% inferior to the amount measured in wild type. Although not significant, a decrease was also observed in RNAi mutants (Table 2).

Regarding photosynthesis, two spots corresponding to components of PSII light-harvesting complex (Lhcbm2 and Lhcb5/CP26) showed a significant decrease (−1.5) but no differences were observed between wild type and complex I deficient mutants either for spots corresponding to other Lhc proteins (identified as Lhcbm1, 2, 3,10) or for PSII absorption cross section by fluorescence measurements (Table 2). A decrease in the amount of the carbonic anhydrase (alpha-type Cah1) located in the periplasm was observed and one spot corresponding to small subunit of Rubisco (RbcS) also showed a very strong decrease (−3.7) even when this was not paralleled with a reduced amount of the large subunit (RbcL) (13 identified spots) or with a difference in Rubisco amount on native gels (Fig. 3). To determine whether photosynthetic capacity could be modified in the complex I deficient mutants, polarographic measurements of oxygen exchange rates were performed. The maximum rates of oxygen evolution at saturating light intensity (N1000 μE·m−2·s−1) did not differ between wild type, *dum17* and RNAi mutants (Table 2). Supporting these results, numerous other chloroplastic proteins involved in photosystem II, light harvesting complex (including one additional spot corresponding to Lchbm2), pentose phosphate pathway or chlorophyll biosynthesis, have been identified and none did significantly vary between wild type and complex I mutant. The abundance of PSI and PSII complexes in association with Lhc complexes in wild-type and mutant cells has also been estimated on BN gels (Fig. 3A) and no difference could be observed. Additionally, spectrophotometric measurements of total chlorophyll (Chla + b) content in methanolic extract indicated that there is no significant difference between wild-type and mutants cells (Table 2).

(4) Discussion

Nd7 and Nd9 are two components of mitochondrial complex I in *C. reinhardtii* (Cardol et al., 2004). Belonging to the matricial arm of the complex, they are homologous to plant mitochondria-encoded NAD7 and NAD9, human nucleus-encoded 49 kD/NDUFS2 30

kD/NDUFS3 subunits and NuoD/C subunits of bacterial NDH-1 complex. In this work, we report the inactivation of the corresponding nuclear genes (*NUO7* and *NUO9*) in *Chlamydomonas*. Despite the fact that the two proteins are the only core subunits of the matricial arm that do not provide ligands for cofactors (FMN and Fe–S clusters) (Hinchliffe and Sazanov, 2005), their loss leads to the absence of complex I in *Chlamydomonas*, as also observed in all species investigated so far. In the fungus *N. crassa*, the disruption of the corresponding genes prevents the activity and assembly of the matricial arm while a membrane part of the complex is still present in mitochondrial membranes (Duarte et al., 1998; Schulte and Weiss, 1995). In *E. coli*, the nuoC gene encodes a fused version of the two subunits (Braun et al., 1998). Although no structurally intact complex is present in membranes of the nuoC-null mutant, a soluble 170 kD fragment corresponding to the NADH dehydrogenase module (NuoE/NDUFV2/24 kD, NuoF/NDUFV1/51 kD, NuoG/NDUFS1/75 kD) is still active (Erhardt et al., 2012). In tobacco (Nicotiana sylvestris), CMSI/ II mutants are impaired in the expression of mitochondrial nad7 gene (Lelandais et al., 1998; Pla et al., 1995). As a consequence, rotenone sensitive oxygen uptake is decreased and there is no complex I assembly (Gutierres et al., 1997; Pineau et al., 2005). The *Chlamydomonas amc14* mutant isolated in this work bears an insertion in the promoter region of *NUO9* gene, which consequently reduces gene expression and lowers in parallel complex I activity and assembly (data not shown), suggesting that the amount of fully assembled complex I is at least controlled by the amount of Nd9 subunit. In mutants deprived of ND1,3–6,or 4L membrane component, we reported the presence of a soluble ~200 kDa fragment showing NADH dehydrogenase activity which was attributed to the fraction of the matricial arm corresponding to the NADH dehydrogenase module (Cardol et al., 2002, 2006).

In human, the NADH dehydrogenase module (comprising notably NDUFV2/24 kD, NDUFV1/51 kD and NDUFS1/75 kD) is distinct from the hydrogenase module (comprising notably NDUFS3/Nd9, NDUFS2/ Nd7, NDUFS7/PSTT, NDUFS8/TYKY) and these two fractions (fractions FP and IP, respectively, e.g. Sazanov et al., 2000) are assembled separately (Antonicka et al., 2003; Vogel et al., 2007). In *NUO7* and *NUO9* knockdown *Chlamydomonas* mutants, while we found the soluble ~200 kD NADH dehydrogenase activity along with the 75 kD (NDUFS1) subunit detected in membrane extract (data not shown), subunits NDUFS7/PSTT and NDUFS8/TYKY of the hydrogenase module are absent. Interestingly it has been shown in human cell lines that two chaperones (NDUFAF3 and NDUFAF4) cooperate from early to late

stages of complex I assembly in association with at least NDUFS3/Nd9, NDUFS2/ Nd7, NDUFS8/TYKY (i.e. the hydrogenase module, Saada et al., 2009). Since most chaperones (including NDUFAF3 and NDUFAF4) and core subunits identified in human are conserved in *Chlamydomonas* (Cardol, 2011; Remacle et al., 2012), this strongly reinforces the idea that the assembly steps of complex I are conserved between human and *Chlamydomonas* (Cardol et al., 2008; Remacle et al., 2008). Complex I is acknowledged as a main contributor to superoxide production by mitochondria, where O2 reacts with reduced Flavin mononucleotide (Esterhazy et al., 2008; Kussmaul and Hirst, 2006). ROS (reactive oxygen species) are considered to be a major cause of cellular oxidative stress. In *Chlamydomonas* complex I mutant, concomitantly to a lower amount of mitochondrial Msd1, chloroplastic Fsd1 superoxide dismutase, and glutathione S-transferase Gst1, the H_2O_2 content was also lowered. Altogether, these observations suggest that in *Chlamydomonas*, the lower respiratory rate associated to complex I loss limits superoxide production and triggers the down regulation of ROS-scavenging enzymes. Another notable difference in protein expression between complex I deficient mutant and wild type is the strong down regulation of the periplasmic alpha carbonic anhydrase (Cah1). Carbonic anhydrase is the usual marker for *Chlamydomonas* cells grown under CO2-limiting conditions (Miura et al., 2004). Transcript abundance of CAH1 and activity of Cah1 were also considerably reduced by the addition of 10 mM acetate without compromising the photosynthetic capacity. This reduction could result from an increased internal CO2 concentration generated by high, acetate-stimulated respiratory rates (Fett and Coleman, 1994). The level of CAH1 transcript also decreased in cells subjected to ROS (oxygen peroxide, singlet oxygen, etc.), which led the authors to propose the existence of a cross talk between oxidative stress and regulation of the carbon-concentrating mechanism (Ledford et al., 2007). In this regard, the down regulation of Cah1 in complex I mutants also does not impair photosynthetic capacity and is not related to the lowering of ROS production observed in mutant cells. It might result from an increase of the internal CO2 related to a lower CO2 demand of cells (lower generation time) whatever is the rate of acetate assimilation.

In complex I-deficient mutants, only the respiratory complexes III and IV still contribute to the formation of the proton electrochemical potential and thus to the production of ATP (Cardol et al., 2003), which accounts for the “slow” growth phenotype of the mutants in the dark. Lower capacity of complex I-deficient mutant cells to reoxidize cellular NADH must limit the

rate of catabolic pathways (Krebs cycle, glycolysis and acetate assimilation). In photosynthetic organisms, reducing equivalents generated by photosynthetic electron transfer chain can in part be consumed by the mitochondrial respiratory chain, owing to metabolic exchanges between the two organelles (reviewed in Cardol et al., 2011; Noctor et al., 2007). This process can be mediated by the activity of the malate–aspartate shuttle (Noguchi and Yoshida, 2008), whose genes are present in *Chlamydomonas* (Merchant et al., 2007). Four enzymes participate in the malate shuttle: two membrane antiporters (glutamate/aspartate and malate/α-ketoglutarate) and soluble enzymes located at both sides of the mitochondrial and chloroplastic membranes (malate dehydrogenase, and aspartate aminotransferase). Aspartate aminotransferase (AAT), also called aspartate transaminase (AST), catalyzes the reversible conversion of aspartate and α-ketoglutarate to oxaloacetate and glutamate. Both the mitochondrial (Ast1) and chloroplastic (Ast3) AAT are upregulated in response to complex I deficiency supporting the idea that the import/export of reducing equivalents is critical for cell bioenergetics. In mixotrophic conditions, when compared to wild type, complex I mutants of *Chlamydomonas* are slightly more towards state II transition of the photosynthetic apparatus (Cardol et al., 2003), a condition in which plastoquinones are reduced by the activity of the NAD(P)H dehydrogenase Nda2 (Jans et al., 2008), LHCII are phosphorylated and associated to PSI (reviewed in Lemeille and Rochaix, 2010). In complex I deficient cells, we found that two protein spots corresponding to LHCII proteins Lhcb5/CP26 and Lhcbm2 were less abundant than in wild type but this was not paralleled with a change in other LHCII protein amounts, PSII-LHCII amount, or PSII absorption cross section. Both proteins play a critical role in state transition process and Lhcb5/CP26 is phosphorylated upon state transition (Ferrante et al., 2012; Takahashi et al., 2006). This might indicate that the decrease in Lhcb5 protein observed in complex I mutant is due to a slight difference in the ratio between non-phosphorylated/phosphorylated Lhcb5/CP26 protein.

The photosynthetic characterization of *Chlamydomonas* mitochondrial mutants has highlighted a significant role for the metabolic interactions between the chloroplast and the mitochondrion. Up to a 75% decrease of the photosynthesis efficiency was found in the case of dum19/25, a double mutant lacking the respiratory complexes I and IV activities whereas this parameter was barely affected in complex I mutants (Cardol et al. 2003). As a general conclusion, we can say that despite the halving of respiration rate and growth rate observed in mutant cells compared to wild type when cultivated in mixotrophic conditions, complex I mutants do not

show major modifications in the expression of metabolic pathways. As a direct comparison, in a mutant deprived of the alternative oxidase (AOX1) of the respiratory chain, although total respiration and growth were not impaired in mixotrophic conditions, a strong increase of intracellular ROS content was observed. By the same comparative proteomic approach, major modifications in the expression of proteins of primary metabolism were described in AOX1 mutant, namely a decrease of enzymes of the main catabolic pathways, an increase of enzymes involved in anabolic pathways and a strong up-regulation of the ROS scavenging system enzyme (Mathy et al., 2010). This suggests that the sensing of oxidative stress in the mitochondria would be a primary event that leads to the genetic control of the general metabolic pathways.

Supplementary data to this article can be found online at
http://dx.doi.org/10.1016/j.mito.2013.11.004.

(5) Material and methods

Strains and culture conditions

The *C. reinhardtii* strains used in this study are the wild-type 137c (ref. no 1′ mt+ and 2′ mt−) and their derivative dum17 mt− (ref nos 233 and 680, bearing a frameshift mutation in mitochondrial nd6 gene, Cardol et al., 2002), arg7–8 mt+ (ref. no 3A+), arg7–8 mt− (ref. no 4A−), cw15 mt+ (ref. nos 25 and 83) and cw15 arg7–8 mt+ (ref. no 325.2) lacking either cell-wall and/or argininosuccinate lyase. Cell cultures were grown in liquid or on agar media under continuous illumination (50 μE·m−2·s−1) at 25 °C. The routinely used medium was Tris minimal-phosphate (TMP) supplemented with 17 mM acetate (TAP) (Gorman and Levine, 1965). To measure the doubling time of strains, cell numbers were determined with a Z2 Coulter Counter analyzer (Beckman Coulter). Cells were harvested in mid-log phase of culture (corresponding to 2–5 × 106 cells/ml). Escherichia coli DH5α was used for cloning gene and cDNA sequences, and E. coli transformants were grown in L (Luria) medium in presence of ampicillin (50 μg/ml) or chloramphenicol (10 μg/ml) at 37 °C.

Construction of plasmids for dsRNA expression

A summary of DNA constructs for double strand RNA expression in *C. reinhardtii* is shown in Fig. 1. Oligonucleotides with restriction enzyme sites were purchased from Eurogentec (Liège, Belgium), T4 DNA ligase and endonucleases from Invitrogen, Taq polymerase from Promega. Two plasmids were used to express double strand RNA in. reinhardtii. The pNB1 plasmid (2895 bp) (Cardol et al., 2006) and the pPN10 plasmid (4420 bp) that was obtained by inserting a

1020-bp ApaI-SalI fragment of the pPN2 plasmid (Loppes and Radoux, 2001) containing the NIA1 full promoter into ApaI-SalI cohesive ends of the pBCKS + vector (Stratagene).

Construct of pND9-RNAi plasmid (4189 bp)

A 481-bp fragment of NUO9 cDNA (gb: AY351261)was amplified by PCR with ND9-3F (5′-ATCGATAAGCTTCAGGAGCCCACGATATACACCA CG-3′) and ND9-4R (5′-AAGCTTCTGCAGGCGTCTCCCAAGGGCTGTTG- 3′) primers containing ClaI-HindIII and HindIII-PstI restriction sites at their 5′ ends, respectively. The product was cloned into the pGEM-T easy vector and the excised HindIII fragment was inserted into the pNB1 plasmid. Constructs with inverse orientation (pND9-AS) were selected by a PCR analysis. The 801-pb corresponding gene fragment containing a 320-bp intron was amplified with the same primers, cloned into the pGEM-T easy vector (pND9-1) and the excised ClaI-NcoI Segment was then inserted into the ClaI-NcoI sites of pND9-AS to obtain the pND9-RNAi (Fig. 1B).

Construct of pND7-RNAi plasmid (6036 bp)

A 719-bp fragment of ND7 cDNA (gb: AY347483) was amplified by PCR with ND7-1F (5′-GGATCCAAGCTTGAACAACTTCACGCTGAACTTCGG-3′) and ND7-9R (5′-GAATTCTGAACTGCATCTTGCCGTACGC-3′) primers containing BamHI-HindIII and EcoRI restriction sites at their 5′ ends, respectively. The product was cloned into the pGEM-T easy vector (pND7-2) and the excised HindIII-EcoRI fragment was inserted into the pPN10 plasmid in sense orientation downstream the promoter (pND7-S). A 932-pb cDNA fragment amplified with ND7-1F primer and ND7-8R (5′-GAATTCCCTCGGTGTAGAGCTTGAAGTGG-3′) primer

bearing EcoRI restriction site at its 5′ end was cloned into the pGEM-T easy vector (pND7-1) and the excised BamHI-EcoRI fragment was inserted in inverse orientation into the pND7-S to obtain the pND7-RNAi plasmid (Fig. 1A).

Transformation of *C. reinhardtii* and selection clones

RNA interference

Transformation of the *Chlamydomonas* cw15 arg7–8 mt+ strain was carried out using the glass-bead method (Kindle, 1990) with 5 μg of pRNAi plasmid (linearized with ScaI for pND9-RNAi or SspI for pND9- RNAi) and 1 μg of pASL, linearized with BamHI. This pASL plasmid bears the *Chlamydomonas ARG7* gene that codes for the argininosuccinate lyase (Debuchy et al., 1989) and is used as a selectablemarker. Prototroph transformants were selected on TAP agar plates. The presence of sequences belonging to the right and to the left part of the RNAi plasmids in the transformants was checked by PCR with primers hybridizing int he *NUO7* or *NUO9* sequences and in the vector (universal primers 5′- GTAAAACGACGGCCAG-3′; 5′-CAGGAAACAGCTATGAC-3′). The stability of the phenotype observed for the transformants mentioned in this study was checked at least one year after their isolation.

Insertional mutagenesis

Amplification of hygromycin B resistance cassette (HygR, encoded by the APH7 gene) from the pHyg3 plasmid, electroporation of 3A+ or 4C cells with 100 ng of HygR cassette, and subsequent selection of hygromycine resistant transformants were carried out as described in Barbieri et al. (2011). The transmission pattern of the dark− and HygR loci in crosses was determined by random analysis of themeiotic products. Amplification of insertion-linked sequence by thermal asymmetric interlaced (TAIL)-PCR was conducted with degenerate primers as described in Dent et al. (2005) with APH7 (hygromycine) specific primers: Hygterm1 (5′-CCGCGAACTGCTCGCCTTCACCT-3′), Hygterm2 (5′-TTCGAGGAGACCCCGCTGGATC-3′), and Hygterm3 (5′-CGATCCGGAGGAACTGGCGCA-3′).

Protein analyses

Total protein extract or crude membrane fractions were isolated From cells disrupted by sonication (Remacle et al., 2001). Purified mitochondria were obtained according to Cardol et al. (2002). Proteins amounts were determined by the Bradford method (Bradford, 1976). NADH:ferricyanide oxidoreductase, complex I, complexes II + III and complex IV activities were measured according to Cardol et al. (2002) and Remacle et al. (2001). SDS–PAGE was conducted according to standard protocols. Blue native polyacrylamide gel electrophoresis (BNPAGE) analyses, and subsequent stainings of the gels by NADH/NBT (nitroblue tetrazolium) or Coomassie blue were performed as previously published (Cardol et al., 2004, 2006). SDS-gels and BN-gels were electroblotted according to standard protocols. The following antisera raised in rabbits were used: polyclonal antisera raised against whole pu purified complex I from *Neurospora crassa* (provided by H. Weiss and U. Schulte), Atp2 (β subunit of ATPase) from *Polytomella sp.* (provided by D. González-Halphen; used at a dilution 1:150,000), AOX of C. *reinhardtii* (obtained from S. Merchant; used at a dilution 1:50,000) or monoclonal antisera raised against PSST (1:2000) and TYKY (1:2000) subunits from *Y. lipolytica* (provided by V. Zickermann and U. Brandt). Detection was performed using the BM Chemiluminescence Western blot kit (Roche) with anti-rabbit POD-conjugated antibodies. 2D-DIGE electrophoresis and protein identification were conducted as previously described (Mathy et al., 2010). Briefly, preparation of each protein extract (25 µg) and labeling with CyDye (GE Healthcare) were conducted in triplicate. 3–11 NL IPG Drystrips (GE Healthcare) were used and images of 2D gels were analyzed with the DeCyder 6.5 software (GE Healthcare). For protein identification, preparative gels were loaded with 750 µg protein and spots of interest were picked using an Ettan Dalt Spot Picker (GE Healthcare). Proteins were subsequently digested in-gel and the resulting peptides mixtures were analyzed in MS and in LIFT MS/MS modes (Ultraflex II MALDI TOF/TOF, Bruker Daltonic, Laboratory of Mass Spectrometry, GIGA, University of Liège, Belgium). Protein identification was carried out using the Mascot search engine. Mass error was fixed at 70 ppm and peptidemodificationswere assessed as cysteine carbamidomethylation (fixedmodification) andmethionine oxidation (as a variable modification).

RNA analyses

Total RNA was extracted as previously described (Loppes and Radoux, 2001). For RNA blot analyses, RNA (15 µg) was separated on 0.8% agarose/formaldehyde gels and transferred onto Hybond N+- membrane (Amersham Pharmacia Biotech). Dig-labeled PCR products of cDNA fragments were used as gene probes and detected with anti- DIG-AP-conjugates and CDP-Star as substrate (Roche). Probes for detection of *NUO3, NUO7, NUO9, NUO11, NUO17,* and *NUOP1* were obtained as previously described (Cardol et al., 2006)

In vivo analysis of photosynthesis and respiration

Respiratory and photosynthetic activities were measured as O2 exchanges rates using a Clark-type oxygen electrode at 25 °C (Hansatech Instrument, King's Lynn, England). Saturation of photosynthesis was achieved at ~1000 µmol photons at 640 nm·m−2·s−1. PSII antenna size was evaluated by measuring the rate of chlorophyll fluorescence induction (half-time, t1/2, s) from open (FO) to closed (Fm) PSII centers in the presence of 3 low light (b200 µmol photons at 630 nm·m−2·s−1) with a JTS-10 spectrofluorometer (Biologic, France). This parameter is quantitatively related to the absorption cross-section of PSII (Butler, 1978). Hydrogen peroxide levels were determined by staining with 3-3′ diaminobenzidine (DAB) (Sigma) as described previously (Mathy et al., 2010). Filters with cell deposits were incubated during 20 min at 50 µE·m−2·s−1.

In silico analyses

Frequency of codon utilization was compared with data available for *C. reinhardtii* nuclear genes (http://www.kazusa.or.jp/codon/). Peptide signal was predicted using the Predalgo program (https://giavapgenomes. ibpc.fr/cgi-bin/predalgodb.perl?page=main) (Tardif et al., 2012). Alpha-helix predictions were computed with the Deleage– Roux and Levitt scales with the Protscale program on the Expasy server(http://us.expasy.org/). Position of residues along alpha helixes (3.6 residues per turn) was determined with the Pepwheel program (http:// emboss.bioinformatics.nl/cgi-bin/emboss/pepwheel) (Ramachandran and Sasisekharan, 1968).

(6) Acknowledgments

We thank JH Schumacher, B. Horrion and S. Borenzstein for their technical help. This work was supported by a FP7-funded project (Sunbiopath, GA245070), University of Liège (SFRD-11/05), the Fonds National de la Recherche Scientifique (an Incentive Grant for Scientific Research MIS F.4520, FRFC 2.4597.11; FRFC 2.4567.11; CDR J.0138.13) and a FRSM grant (3.4559.11 to PL). VL is a Postdoctoral Researcher, PL and PC are Research Associate of F.R.S.-FNRS.

(7) References

Angerer, H., Zwicker, K., Wumaier, Z., Sokolova, L., Heide, H., Steger, M., Kaiser, S., Nubel,E., Brutschy, B., Radermacher,M., Brandt, U., Zickermann, V., 2011. A scaffold of accessory subunits links the peripheral arm and the distal proton pumping module of mitochondrial complex I. Biochem. J. 437, 279–288.

Antonicka, H., Ogilvie, I., Taivassalo, T., Anitori, R.P., Haller, R.G., Vissing, J., Kennaway, N.G., Shoubridge, E.A., 2003. Identification and characterization of a common set of complex I assembly intermediates in mitochondria frompatientswith complex I deficiency.J. Biol. Chem. 278, 43081–43088.

Barbieri,M.R., Larosa, V., Nouet, C., Subrahmanian, N., Remacle, C., Hamel, P.P., 2011. A forward genetic screen identifies mutants deficient for mitochondrial complex I assembly in Chlamydomonas reinhardtii. Genetics 188, 349–358.

Baroli, I., Gutman, B.L., Ledford, H.K., Shin, J.W., Chin, B.L., Havaux, M., Niyogi, K.K., 2004.
Photo-oxidative stress in a xanthophyll-deficient mutant of Chlamydomonas. J. Biol. Chem. 279, 6337–6344.

Bradford, M.M., 1976. A rapid and sensitive method for the quantitation of microgram quantities of protein utilizing the principle of protein-dye binding. Anal. Biochem. 72, 248–254.

Braun,M., Bungert, S., Friedrich, T., 1998. Characterization of the overproduced NADH dehydrogenase fragment of the NADH:ubiquinone oxidoreductase (complex I) from Escherichia coli. Biochemistry 37, 1861–1867.

Bullerwell, C.E., Gray, M.W., 2004. Evolution of the mitochondrial genome: protist connections to animals, fungi and plants. Curr. Opin. Microbiol. 7, 528–534.

Butler,W.L., 1978. Energy distribution in the photochemical apparatus of photosynthesis. Annu. Rev. Plant Physiol. Plant Mol. Biol. 29, 345–378.

Cardol, P., 2011. Mitochondrial NADH:ubiquinone oxidoreductase (complex I) in eukaryotes: a highly conserved subunit composition highlighted by mining of protein databases. Biochim. Biophys. Acta 1807, 1390–1397.

Cardol, P., Boutaffala, L., Memmi, S., Devreese, B., Matagne, R.F., Remacle, C., 2008. In Chlamydomonas, the loss of ND5 subunit prevents the assembly of whole mitochondrial complex I and leads to the formation of a low abundant 700 kDa subcomplex. Biochim. Biophys. Acta 1777, 388–396.

Cardol, P., Forti, G., Finazzi, G., 2011. Regulation of electron transport in microalgae. Biochim. Biophys. Acta 1807, 912–918.

Cardol, P., Gloire, G., Havaux,M., Remacle, C.,Matagne, R., Franck, F., 2003. Photosynthesis and state transitions inmitochondrial mutants of Chlamydomonas reinhardtii affected in respiration. Plant Physiol. 133, 2010–2020.

Cardol, P., González-Halphen, D., Matagne, R.F., Remacle, C., 2005. Update on the mitochondrial OXPHOS proteome of the green alga Chlamydomonas reinhardtii. In: végétale, S.F.d.B. (Ed.), 7th International Congress on Plant Mitochondrial Biology (ICPM), Obernai, France, p. P18.

Cardol, P., Lapaille, M., Minet, P., Franck, F., Matagne, R.F., Remacle, C., 2006. ND3 and ND4L subunits of mitochondrial complex I, both nucleus encoded in Chlamydomonas reinhardtii, are required for activity and assembly of the enzyme. Eukaryot. Cell 5, 1460–1467.

Cardol, P., Matagne, R.F., Remacle, C., 2002. Impact of mutations affecting ND mitochondriaencoded subunits on the activity and assembly of complex I in Chlamydomonas. Implication for the structural organization of the enzyme. J. Mol. Biol. 319, 1211–1221.

Cardol, P., Vanrobaeys, F., Devreese, B., Van Beeumen, J., Matagne, R., Remacle, C., 2004. Higher plant-like subunit composition of the mitochondrial complex I from Chlamydomonas reinhardtii: 31 conserved components among eukaryotes. Biochim. Biophys. Acta 1658, 212–224.

Carroll, J., Fearnley, I.M., Skehel, J.M., Shannon, R.J., Hirst, J.,Walker, J.E., 2006. Bovine

complex I is a complex of forty-five different subunits. J. Biol. Chem. 281, 32724–32727.

Debuchy, R., Purton, S., Rochaix, J.D., 1989. The argininosuccinate lyase gene of Chlamydomonas reinhardtii: an important tool for nuclear transformation and for correlating the genetic and molecular maps of the ARG7 locus. EMBO J. 8, 2803–2809.

Dent, R.M., Haglund, C.M., Chin, B.L., Kobayashi, M.C., Niyogi, K.K., 2005. Functional genomics of eukaryotic photosynthesis using insertional mutagenesis of Chlamydomonas reinhardtii. Plant Physiol. 137, 545–556.

Duarte, M., Mota, N., Pinto, L., Videira, A., 1998. Inactivation of the gene coding for the 30.4-kDa subunit of respiratory chain NADH dehydrogenase: is the enzyme essential for Neurospora? Mol. Gen. Genet. 257, 368–375.

Emanuelsson, O., Nielsen, H., Brunak, S., von Heijne, G., 2000. Predicting subcellular localization of proteins based on their N-terminal amino acid sequence. J. Mol. Biol. 300, 1005–1016.

Erhardt, H., Steimle, S., Muders, V., Pohl, T., Walter, J., Friedrich, T., 2012. Disruption of individual nuo-genes leads to the formation of partially assembled NADH:ubiquinone oxidoreductase (complex I) in Escherichia coli. Biochim. Biophys. Acta 1817, 863–871.

Esterhazy, D., King,M.S., Yakovlev, G., Hirst, J., 2008. Production of reactive oxygen species by complex I (NADH:ubiquinone oxidoreductase) from Escherichia coli and comparison to the enzyme from mitochondria. Biochemistry 47, 3964–3971.

Ferrante, P., Ballottari,M., Bonente, G., Giuliano, G., Bassi, R., 2012. LHCBM1 and LHCBM2/ 7 polypeptides, components ofmajor LHCII complex, have distinct functional roles in photosynthetic antenna system of Chlamydomonas reinhardtii. J. Biol. Chem. 287, 16276–16288.

Fett, J.P., Coleman, J.R., 1994. Regulation of periplasmic carbonic anhydrase expression in Chlamydomonas reinhardtii by acetate and pH. Plant Physiol. 106, 103–108.

Friedrich, T., 2001. Complex I: a chimaera of a redox and conformation-driven proton pump? J. Bioenerg. Biomembr. 33, 169–177.

Glaser, E., Sjoling, S., Tanudji, M., Whelan, J., 1998. Mitochondrial protein import in plants. Plant Mol. Biol. 331–338.

González-Halphen, D., Funes, S., Perez-Martinez, X., Reyes-Prieto, A., Claros, M.G., Davidson, E., King, M.P., 2004. Genetic correction of mitochondrial diseases: using the natural migration of mitochondrial genes to the nucleus in chlorophyte algae as a model

system. Ann. N. Y. Acad. Sci. 1019, 232–239.

Gorman, D.S., Levine, R.P., 1965. Cytochrome f and plastocyanin: their sequence in the photosynthetic electron transport chain of Chlamydomonas reinhardtii. Proc. Natl. Acad. Sci. U. S. A. 54, 1665–1669.

Gray,M.W., Burger, G., Lang, B.F., 1999. Mitochondrial evolution. Science 283, 1476–1481.

Gutierres, S., Sabar,M., Lelandais, C., Chetrit, P., Diolez, P., Degand, H., Boutry, M., Vedel, F., de Kouchkovsky, Y., De Paepe, R., 1997. Lack of mitochondrial and nuclear-encoded subunits of complex I and alteration of the respiratory chain in Nicotiana sylvestris mitochondrial deletion mutants. Proc. Natl. Acad. Sci. U. S. A. 94, 3436–3441.

Hinchliffe, P., Sazanov, L.A., 2005. Organization of iron–sulfur clusters in respiratory complex I. Science 309, 771–774.

Jans, F., Mignolet, E., Houyoux, P.A., Cardol, P., Ghysels, B., Cuine, S., Cournac, L., Peltier, G., Remacle, C., Franck, F., 2008. A type II NAD(P)H dehydrogenase mediates lightindependent
plastoquinone reduction in the chloroplast of Chlamydomonas. Proc. Natl. Acad. Sci. U. S. A. 105 (51), 20546–20551.

Kindle, K.L., 1990. High frequency nuclear transformation of Chlamydomonas reinhardtii. Proc. Natl. Acad. Sci. U. S. A. 87, 1228–1232.

Kobayashi, Y., Knoop, V., Fukuzawa, H., Brennicke, A., Ohyama, K., 1997. Interorganellar gene transfer in bryophytes: the functional nad7 gene is nuclear encoded in Marchantia polymorpha. Mol. Gen. Genet. 256, 589–592.

Kussmaul, L., Hirst, J., 2006. The mechanism of superoxide production by NADH:ubiquinone oxidoreductase (complex I) from bovine heart mitochondria. Proc. Natl. Acad. Sci. U. S. A. 103, 7607–7612.

Lapaille, M., Thiry, M., Perez, E., Gonzalez-Halphen, D., Remacle, C., Cardol, P., 2010. Loss of mitochondrial ATP synthase subunit beta (Atp2) alters mitochondrial and chloroplastic function and morphology in Chlamydomonas. Biochim. Biophys. Acta 1797, 1533–1539.

Larosa, V., Coosemans, N., Motte, P., Bonnefoy, N., Remacle, C., 2012. Reconstruction of a humanmitochondrial complex Imutation in the unicellular green alga Chlamydomonas.
lant J. 70, 759–768.

Lecler, R., Vigeolas, H., Emonds-Alt, B., Cardol, P., Remacle, C., 2012. Characterization of an

internal type-II NADH dehydrogenase from Chlamydomonas reinhardtii mitochondria. Curr. Genet. 58, 205–216.

Ledford, H.K., Chin, B.L., Niyogi, K.K., 2007. Acclimation to singlet oxygen stress in Chlamydomonas reinhardtii. Eukaryot. Cell 6, 919–930.

Lelandais, C., Albert, B., Gutierres, S., De Paepe, R., Godelle, B., Vedel, F., Chetrit, P., 1998. Organization and expression of the mitochondrial genome in the Nicotiana sylvestris CMSII mutant. Genetics 150, 873–882.

Lemeille, S., Rochaix, J.D., 2010. State transitions at the crossroad of thylakoid signaling pathways. Photosynth. Res. 106 (1–2), 33–46.

Loppes, R., Radoux, M., 2001. Identification of short promoter regions involved in the transcriptional expression of the nitrate reductase gene in Chlamydomonas reinhardtii. Plant Mol. Biol. 45, 215–227.

Mathy, G., Cardol, P., Dinant, M., Blomme, A., Gerin, S., Cloes, M., Ghysels, B., DePauw, E., Leprince, P., Remacle, C., Sluse-Goffart, C., Franck, F.,Matagne, R.F., Sluse, F.E., 2010. Proteomic and functional characterization of a Chlamydomonas reinhardtii mutant lacking the mitochondrial alternative oxidase 1. J. Proteome Res. 9, 2825–2838.

Merchant, S.S., Prochnik, S.E., Vallon, O., Harris, E.H., Karpowicz, S.J., Witman, G.B., Terry, A., Salamov, A., Fritz-Laylin, L.K., Marechal-Drouard, L., Marshall, W.F., Qu, L.H., Nelson, D.R., Sanderfoot, A.A., Spalding, M.H., Kapitonov, V.V., Ren, Q., Ferris, P., Lindquist, E., Shapiro, H., Lucas, S.M., Grimwood, J., Schmutz, J., Cardol, P., Cerutti, H., Chanfreau, G., Chen, C.L., Cognat, V., Croft, M.T., Dent, R., Dutcher, S., Fernandez,E., Fukuzawa, H., Gonzalez-Ballester, D., Gonzalez-Halphen, D., Hallmann, A., Hanikenne, M., Hippler, M., Inwood, W., Jabbari, K., Kalanon, M., Kuras, R., Lefebvre, P.A., Lemaire, S.D., Lobanov, A.V., Lohr, M., Manuell, A., Meier, I., Mets, L., Mittag, M., Mittelmeier, T., Moroney, J.V., Moseley, J., Napoli, C., Nedelcu, A.M., Niyogi, K., Novoselov, S.V., Paulsen, I.T., Pazour, G., Purton, S., Ral, J.P., Riano-Pachon, D.M., Riekhof, W., Rymarquis, L., Schroda, M., Stern, D., Umen, J., Willows, R., Wilson, N., Zimmer, S.L., Allmer, J., Balk, J., Bisova, K., Chen, C.J., Elias, M., Gendler, K., Hauser, C.,Lamb, M.R., Ledford, H., Long, J.C., Minagawa, J., Page, M.D., Pan, J., Pootakham, W., Roje, S., Rose, A., Stahlberg, E., Terauchi, A.M., Yang, P., Ball, S., Bowler, C., Dieckmann, C.L., Gladyshev, V.N., Green, P., Jorgensen, R., Mayfield, S., Mueller- Roeber, B., Rajamani, S., Sayre, R.T., Brokstein, P.,

Dubchak, I., Goodstein, D., Hornick, L., Huang, Y.W., Jhaveri, J., Luo, Y., Martinez, D., Ngau, W.C., Otillar, B., Poliakov, A., Porter, A., Szajkowski, L., Werner, G., Zhou, K., Grigoriev, I.V., Rokhsar, D.S., Grossman, A.R., 2007. The Chlamydomonas genome reveals the evolution of key animal and plant functions. Science 318, 245–250.

Miura, K., Yamano, T., Yoshioka, S., Kohinata, T., Inoue, Y., Taniguchi, F., Asamizu, E., Nakamura, Y., Tabata, S., Yamato, K.T., Ohyama, K., Fukuzawa, H., 2004. Expression profiling-based identification of CO2-responsive genes regulated by CCM1 controlling a carbon-concentrating mechanism in Chlamydomonas reinhardtii. Plant Physiol. 135, 1595–1607.

Noctor, G., De Paepe, R., Foyer, C.H., 2007. Mitochondrial redox biology and homeostasis in plants. Trends Plant Sci. 12, 125–134.

Noguchi, K., Yoshida, K., 2008. Interaction between photosynthesis and respiration in illuminated leaves. Mitochondrion 8, 87–99.

Peters, K., Belt, K., Braun, H.P., 2013. 3D gel map of Arabidopsis complex I. Front. Plant Sci. 4, 153.

Pineau, B., Mathieu, C., Gerard-Hirne, C., De Paepe, R., Chetrit, P., 2005. Targeting the NAD7 subunit to mitochondria restores a functional complex I and a wild type phenotype in the Nicotiana sylvestris CMS II mutant lacking nad7. J. Biol. Chem. 280, 25994–26001.

Pla, M., Mathieu, C., De Paepe, R., Chetrit, P., Vedel, F., 1995. Deletion of the last two exons of themitochondrial nad7 gene results in lack of the NAD7 polypeptide in a Nicotiana sylvestris CMS mutant. Mol. Gen. Genet. 248, 79–88.

Ramachandran, G.N., Sasisekharan, V., 1968. Conformation of polypeptides and proteins. Adv. Protein Chem. 23, 283–438.

Remacle, C., Barbieri, M.R., Cardol, P., Hamel, P.P., 2008. Eukaryotic complex I: functional diversity and experimental systems to unravel the assembly process.Mol. Genet. Genomics 280, 93–110.

Remacle, C., Baurain, D., Cardol, P., Matagne, R.F., 2001. Mutants of Chlamydomonas reinhardtii deficient in mitochondrial complex I. Characterization of two mutations affecting the nd1 coding sequence. Genetics 158, 1051–1060.

Remacle, C., Cardol, P., Coosemans, N., Gaisne, M., Bonnefoy, N., 2006. High-efficiency biolistic transformation of Chlamydomonas mitochondria can be used to insert mutations in complex I genes. Proc. Natl. Acad. Sci. U. S. A. 103, 4771–4776.

Remacle, C., Hamel, P., Larosa, V., Subrahmanian, N., Cardol, P., 2012. Chapter 11. Complexes I in the green lineage. In: Sazanov, L.A. (Ed.), A Structural Perspective on Respiratory Complex I. Springer, New York.

Rexroth, S., Meyer Zu Tittingdorf, J.M., Schwassmann, H.J., Krause, F., Seelert, H., Dencher, N.A., 2004. Dimeric H+-ATP synthase in the chloroplast of Chlamydomonas reinhardtii. Biochim. Biophys. Acta 1658, 202–211.

Saada, A., Vogel, R.O., Hoefs, S.J., van den Brand, M.A., Wessels, H.J., Willems, P.H., Venselaar, H., Shaag, A., Barghuti, F., Reish, O., Shohat, M., Huynen, M.A., Smeitink, J.A., van den Heuvel, L.P., Nijtmans, L.G., 2009. Mutations in NDUFAF3 (C3ORF60), encoding an NDUFAF4 (C6ORF66)-interacting complex I assembly protein, cause fatal neonatal mitochondrial disease. Am. J. Hum. Genet. 84, 718–727.

Sazanov, L.A., Hinchliffe, P., 2006. Structure of the hydrophilic domain of respiratory complex I from Thermus thermophilus. Science 311, 1430–1436.

Sazanov, L.A., Peak-Chew, S.Y., Fearnley, I.M., Walker, J.E., 2000. Resolution of the membrane domain of bovine complex I into subcomplexes: implications for the structural organization of the enzyme. Biochemistry 39, 7229–7235.

Schroda, M., 2006. RNA silencing in Chlamydomonas: mechanisms and tools. Curr. Genet. 49, 69–84.

Schulte, U.,Weiss, H., 1995. Generation and characterization of NADH: ubiquinone oxidoreductasemutants in Neurospora crassa. Methods Enzymol. 260, 3–14.

Silflow, C.D., 1998. Organization of the nuclear genome. In: Rochaix, J.D., Goldschmidt-**Clermont, M., Merchant, S**. (Eds.), The Molecular Biology of Choloroplasts and Mitochondria in Chlamydomonas. Kluwer Academic Publishers, pp. 25–40.

Takahashi, H., Iwai, M., Takahashi, Y., Minagawa, J., 2006. Identification of the mobile light-harvesting complex II polypeptides for state transitions in Chlamydomonas reinhardtii. Proc. Natl. Acad. Sci. U. S. A. 103, 477–482Tardif, M., Atteia, A., Specht, M., Cogne, G., **Rolland, N., Brugiere, S., Hippler, M., Ferro, M., Bruley, C., Peltier, G., Vallon, O., Cournac,** L., 2012. PredAlgo: a new subcellular localization prediction tool dedicated to green algae. Mol. Biol. Evol. 29, 3625–3639.

Villavicencio-Queijeiro, A., Vazquez-Acevedo, M., Cano-Estrada, A., Zarco-Zavala, M., Tuena de Gomez, M., Mignaco, J.A., Freire, M.M., Scofano, H.M., Foguel, D., Cardol, P.,

Remacle, C., Gonzalez-Halphen, D., 2009. The fully-active and structurally-stable form of the mitochondrial ATP synthase of Polytomella sp. is dimeric. J. Bioenerg. Biomembr. 41, 1–13.
Vogel, R.O., Smeitink, J.A., Nijtmans, L.G., 2007. Humanmitochondrial complex I assembly: a dynamic and versatile process. Biochim. Biophys. Acta 1767, 1215–1227

Publication 2. **Isolation of *Chlamydomonas reinhardtii* mutants with altered mitochondrial respiration by chlorophyll fluorescence measurement**

Simon Massoz, Véronique Larosa, Bastien Horrion, René F. Matagne, Claire Remacle, Pierre Cardol* (2015), J Biotechnol 215:27-34

For a long time, the idea to be able to screen mitochondrial mutants using photosynthetic measurements has been one of the objectives of P. Cardol. Indeed previous studies on a state transition *stt7* deficient strain showed that photosynthetic parameters would fall down when the *stt7* mutant was associated with a *dum22* (*complex* I$^-$/*complex* III$^-$) mutation (Cardol et al. 2009). It was thus possible to observe photosynthetic deficiencies related to mitochondrial deficiencies in this very affected respiratory-deficient mutant. But whether photosynthetic deficiencies could be used for less impacted mutants remained to be demonstrated. This question was more specifically important regarding complex I mutations. Indeed, if complex III/IV deficient strains are easy to isolate based on the complete absence of growth in heterotrophic conditions (dark + acetate), complex I mutations remain on the "hard to get" side of the identification spectrum, due to only partial lack of growth.

A random insertional mutagenesis experiment was performed on a *stt7* recipient strain and on a WT recipient strain for comparison purposes. Thirty transformants from these experiments were selected for their respiratory and/or photosynthetic deficiencies. We then analysed the two mutagenesis in order to observe i) if photosynthetic parameters were correlated to respiratory deficiencies, and more specifically complex I deficiencies in *stt7* conditions ii) whether or not the *stt7* recipient strain would allow us to retrieve complex I mutants. Respiratory measurements allowed us to quickly find some candidate complex I mutants both in the *stt7* and WT backgrounds, some of which were confirmed to indeed possess decreased complex I activity (*amc14, amc15,* S19). Unfortunately, no impact on photosynthesis could be measured on the two mutants coupled with *stt7* mutation (S19, *amc15*), even though one was completely deficient for complex I activity (S19).

Regarding more affected mutations, one mutant affected in both *stt7* and the isocitrate lyase (*icl*) showed reduced photosynthetic efficiency and respiration. Such mutant is unable to grow in the dark, which is the equivalent to complex III/IV mutants. To go further in the analyses,

as we possessed some *complex III*/*stt7* double mutants previously obtained by crosses, we analysed them regarding their photosynthetic parameters and we showed that they also displayed reduced Fv/F_M and ϕPSII. The ϕPSII phenotype could eventually serve to screen complex III/IV mutants in a faster timescale than heterotrophic growth. While this attempt didn't work regarding the isolation of complex I mutants, this served as a proof of concept that the idea to use photosynthetic measurements to screen mitochondrial mutants is possible. Alongside that, a few mutants of interest could be retrieved and are presented on this paper awaiting further characterization.

In this work I have performed the drop test analysis on the *stt7* deficient series (Fig. 2), the analysis of the F_V/F_M parameters evolution (Fig. 3A), the fluorescence and respiratory analysis of the *stt7* series beside S02 and S21 (Table 1, Fig. 4), the TAIL-PCR analysis of all analysed mutants beside S21 (Table 1). I have analysed the respiration and ferricyanide reduction rate of various mutants (Fig 5A). I have done the BN-PAGE experiments for the different strains in order to verify their complex I activity (Fig 5B) and I have analysed the *dum11* and *dum11/stt7* double mutants regarding their respiration/photosynthesis activities (Fig. 5C).

Isolation of *Chlamydomonas reinhardtii* mutants with altered mitochondrial respiration by chlorophyll fluorescence measurement

Simon Massoz[1], Véronique Larosa[1], Bastien Horrion, René F. Matagne, Claire Remacle, Pierre Cardol[*] (2015) J Biotechnol 215:27-34.
Genetics and Physiology of Microalgae, PhytoSYSTEMS, Department of Life Sciences, University of Liège, B-4000 Liège, Belgium
[1]These authors contributed equally to the work
* Corresponding authour : Laboratory of Genetics and physiology microalgae, PhytoSYSTEMS,
Department of Life Sciences, University of Liège, B-4000, Liège, Belgium. Tel.: +32 43663840. E-mail address: pierre.cardol@ulg.ac.be (P. Cardol).

(1) Abstract (250 words)

The unicellular green alga *Chlamydomonas reinhardtii* is a model organism for studying energetic metabolism. Most mitochondrial respiratory-deficient mutants characterized to date have been isolated on the basis of their reduced ability to grow in heterotrophic conditions. Mitochondrial deficiencies are usually partly compensated by adjustment of photosynthetic activity and more particularly by transition to state 2. In this work, we explored the opportunity to select mutants impaired in respiration and/or altered in dark metabolism by measuring maximum photosynthetic efficiency by chlorophyll fluorescence analyses (F_V/F_M). Out of about 2900 hygromycin-resistant insertional mutants generated from wild type or from a mutant strain deficient in state transitions (*stt7*-9 strain), 22 were found to grow slowly in heterotrophic conditions and 8 of them also showed a lower F_V/F_M value. Several disrupted coding sequences were identified, including genes coding for three different subunits of respiratory-chain complex I (NUO9, NUOA9, NUOP4) or for isocitrate lyase (ICL1). Overall, the comparison of respiratory mutants obtained in wild-type or stt7 genetic backgrounds indicated that the F_V/F_M value can be used to isolate mutants severely impaired in dark metabolism

(2) Introduction

The energetic metabolism of photosynthetic eukaryotes mainly relies on cellular respiration and photosynthesis which occur in the mitochondrion and in the chloroplast, respectively. In both processes, electron transfers occur through various cofactors (haems, FeS clusters,...) covalently bound to multiproteic enzyme complexes embedded in membranes of the organelles. These electron transfers are coupled to the generation of a transmembrane electrochemical proton gradient whose energy is consumed by ATP synthases to synthesize ATP from ADP and

inorganic phosphate (Mitchell, 1961). Historically, respiratory and photosynthetic mutants of the model green alga *Chlamydomonas reinhardtii* have been isolated by quite different approaches. Mutants deficient in complexes I, III and/or IV of the respiratory chain were isolated by means of phenotypical screens based on their null (dk- phenotype) or slow growth (dk+/−phenotype) in heterotrophic conditions(darkness and acetate as an exogenous carbon source) and/or their inability to reduce triphenyl tetrazolium chloride in vivo (Barbieriet al., 2011; Cardol et al., 2002; Lown et al., 2001; Matagne et al.,1989; Dorthu et al., 1992; Remacle et al., 2001; Rich et al., 2001;Salinas et al., 2014). Conversely, mutants deficient in photosynthesis were isolated on the basis of their acetate requirement for growth, their light-sensitivity or by using chlorophyll fluorescence measurements (e.g. Dent et al., 2005; Gumpel et al., 1995; Johnson et al., 2007; Lown et al., 2001). Several screens based on peculiar chlorophyll fluorescence profiles have also been developed and applied to identify Chlamydomonas mutants impaired in specific processes linked to photosynthesis such as non-photochemical quenching (Niyogi et al., 1997), chlororespiration (Houille-Verneset al., 2011), cyclic electron flow around PSI (PSI-CEF) (Tolleter et al.,2011), or hydrogenase activity (Godaux et al., 2013). Mutants defective in the process of state transitions (ST) (Fleischmann et al., 1999) have also been isolated by that approach. ST represent a short term photosynthetic acclimation process that consists in the reversible association of photosystem II (PSII) light-harvesting protein complex (LHCII) with either PSII (in state 1) or PSI (in state 2) (Lemeille and Rochaix, 2010). Occurrence of state 2 relies on the reduction of the plastoquinone (PQ) pool, which triggers the phosphorylation of LHCII by a membrane-bound protein kinase named STT7 in *Chlamydomonas* (Lemeille and Rochaix, 2010). At the origin, ST were ascribed as a mechanism that enables an equal distribution of energy excitation between PS1 and PS2 (Murata, 1969). Later, it was established that intracellular demand for ATP controls also the redox state of the PQ pool (Gans and Rebeille, 1990) and ST (Bultéet al., 1990). More recently, the study of mitochondrial mutants defective in the activity of various proton-translocating respiratory complexes has shown that more the respiration is reduced, more important is the reorganization of the photosynthetic apparatus towards state 2 (Cardol et al., 2003). The increase of PSI antenna size upon state 2 is usually documented as a conditions that favours PSI-cyclic electron flow (CEF) (Alric, 2014, 2010) and thus ATP synthesis over NADP+ reduction in the chloroplast. The physiological significance of ST in Chlamydomonas reinhardtii was further highlighted by studying mutants

defective for ST and/or mitochondrial respiration. Concomitant impairment of ST and respiratory complexes I+III decreases the overall yield of photosynthesis, ultimately leading to a reduced fitness in phototrophic and mixotrophic conditions (Cardol et al., 2009). Both ST and PQ reduction can be followed by chlorophyll fluorescence emission measurements at room temperature (Wollman and Delepelaire, 1984). High throughput analysis of chlorophyll fluorescence by imaging system on algal cell colonies is also available (Houille-Vernes et al., 2011; Johnson et al., 2009).

In this work, we have used *Chlamydomonas* insertional mutants generated from wild-type or ST-deficient strains to evaluate the potential of chlorophyll fluorescence screening for the isolation of new mutants altered in the respiratory activity and more largely in the energetic metabolism.

(3) Results

In order to determine whether chlorophyll fluorescence screen could be applied to identify respiration-deficient mutants after transformation of *Chlamydomonas* cells, we generated insertional mutants and applied primary screens to select mutants impaired in their ability to grow heterotrophically (darkness + acetate) and/or presenting a reduced maximum PSII quantum yield in the dark (F_V/F_M). Transformation experiments were conducted on two wild-type strains (W series) and on a ST-deficient mutant strain (*stt7-9* mutation: S series). We expected indeed that concomitant impairment of ST and respiratory deficiency decreases the overall yield of photosynthesis (Cardol et al., 2009). On a total of about 2900 insertional mutants selected for their resistance to hygromycin (HygR) in phototrophic conditions (low light of 50 µmol photons. $m^{-2}s^{-1}$), twenty-two grew very slowly (dk+/−) or did not grow (dk−) in heterotrophic conditions (Fig. 1 for three mutants of each series (W13, W17, W19 from wild type, and S16, S18, and S19 from stt7-9).

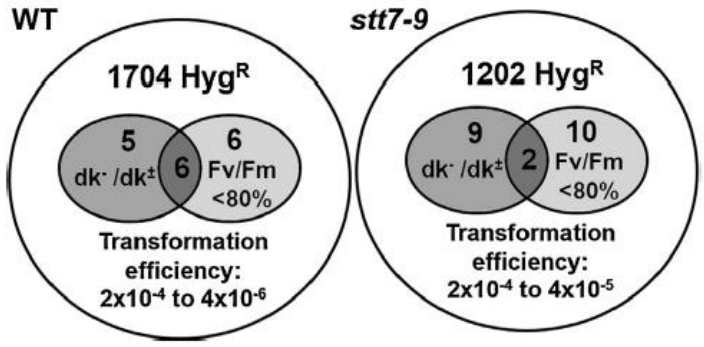

Fig. 1. Summary of transformation experiments and numbers of transformants presenting an altered dark growth, a reduced maximum PSII quantum yield (F_V/F_M), or both alterations.

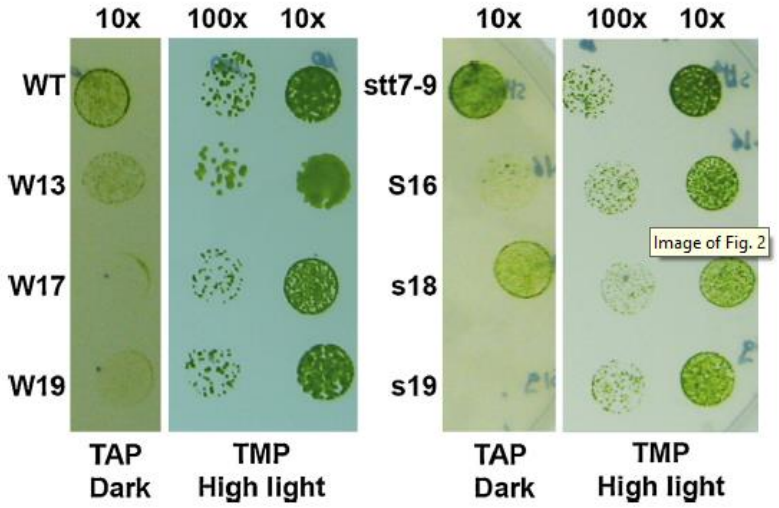

Fig. 2. Growth phenotype of wild-type, *stt7-9* and six mutant strains. Cells were cultivated in heterotrophic (dark, 20 mM acetate: TAP medium) or phototrophic (200 µmol photons. $m^{-2}s^{-1}$, no acetate: TMP medium) conditions. 30 µl of cell suspensions were spotted at two different cell densities (dilution 10X, 4.10^5cells per ml;100X, 4.10^4cells per ml).

In parallel, the population of insertional mutants was subjected to a fluorescence screen based on F_V/F_M parameter. Classically, the F_V/F_M parameter is measured after a prolonged acclimation (several hours) of the cells to the dark in order to release the redox pressure by PSII on PQ pool in the light. However, the mitochondrial mutants altered in respiratory activity have a reduced capacity for ATP synthesis in the dark, which leads to an enhancement of glycolysis, an increase of the reduced NADPH pool in the chloroplast and a partial reduction of PQ pool (Cardol et al., 2003). Thus, in order to determine the more appropriate conditions to apply the fluorescence screen, we first measured F_V/F_M during progressive acclimation from light to dark

of wild type and several previously-characterized mitochondrial mutant strains (*dum17*, deprived of complex I; *dum11*, deprived of complex III and *dum22* deprived of complexes I+III). The recipient strains had a mean F_V/F_M value of 0.66 (Fig. 3A), a value that is lower than the one found with dark-adapted cells in liquid medium (e.g ~0.75; Finazzi, 2001)(see also Table 1). While clear differences between wild type and complex III mutants (*dum11* or *dum22*) could be observed at the beginning of the dark acclimation process, it became difficult to distinguish the three strains after more than 2-3 hours of incubation in the dark (Fig. 3A).

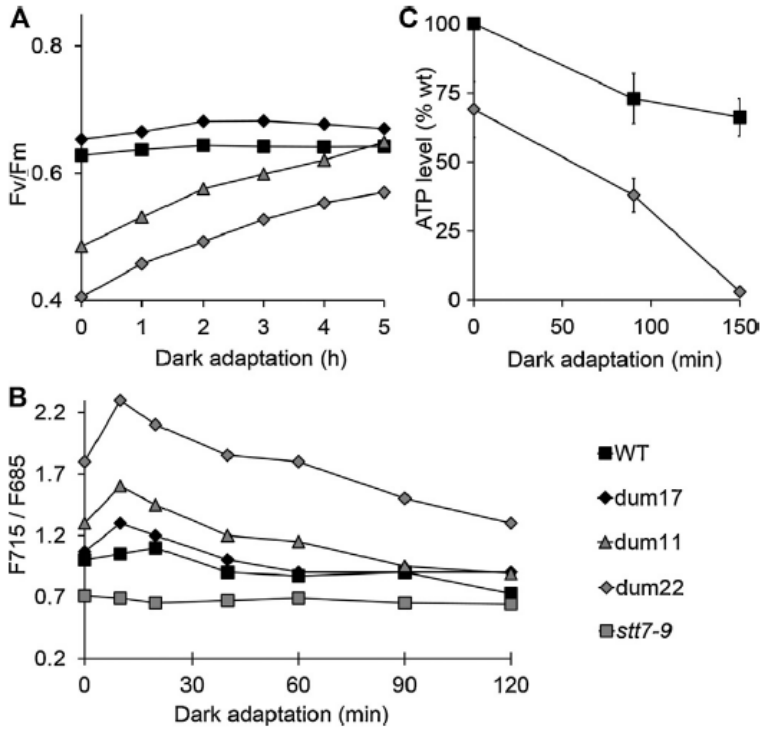

Fig. 3. Photosynthetic parameters of light-grown wild-type and mitochondrial mutant cells during dark acclimation. (A) F_v/F_M chlorophyll fluorescence parameter. (B) 77K Fluorescence F715/F685 ratio. (C) ATP level expressed in percent of the value determined for light-adapted wild-type cells. Mean values (n = 3) ± standard errors.

The compromised ability of mitochondrial mutants to accumulate starch and lipids in the light (Lecler et al.,2011) could limit the glycolytic activity during incubation in the dark and could thus explain the progressive release of the redox pressure on PQ pool from NADPH (i.e., the increase of F_V/F_M parameter). To test this hypothesis, we monitored state transition (ST), which are governed by the redox state of the PQ pool (Lemeille and Rochaix, 2010), by recording chlorophyll fluorescence spectra at 77K during dark adaptation. Excitation in the chlorophyll Soret band (440 nm) produces PSII and PSI fluorescence bands at 685 and 715 nm, respectively. In *stt7-9* mutant cells, deficient for ST, the F715/F685 ratio remained constant over

time (~0.6–0.7), the PSII fluorescence emission peak at 685 nm being larger than the PSI-band at 715 nm, because cells are locked in state 1 (Fig. 3B). In wild-type cells frozen to 77 K under the white light intensity used for growth (t = 0), the two bands had similar amplitudes while, as previously described (Cardol et al., 2003), a high relative amplitude of the PSI band, indicative of state 2, was found in mutant cells. Upon the first 20 minutes of dark incubation, state 2 was even slightly more pronounced in the mutant strains. However, a general trend towards state 1 occurred upon long-term dark-adaptation. Incidentally, in the most affected mutants (*dum22*), this shift back towards state 1 in the dark was also correlated to a depletion of ATP (Fig. 3C),which probably prevents LHCII phosphorylation by the STT7 kinase, irrespectively of the redox status of the PQ pool.

Based on the evolution of F_V/F_M parameter of mitochondrial mutants upon dark acclimation (Fig. 3A), the chlorophyll fluorescence screen was thus conducted using the F_V/F_M parameter of light-grown HygR transformants after adaptation to the dark for only 15 min. Twenty-four of the 2906 transformants (~0.8% irrespective of the recipient strain) had a F_V/F_M value lower than 80% of the controls (Fig. 1). Among them, only 8 corresponded to transformants with reduced or null growth in the dark on acetate-supplemented agar medium (dk+/−or dk−phenotype) (Fig. 1).

The 22 transformants displaying altered growth in the dark were then subjected to secondary screens to identify mutants impaired in respiration and/or in photosynthesis. F_V/F_M values were first con-firmed for cells in liquid medium (Table 1). Total respiratory rate in the dark was evaluated for each mutant strain (R in Table 1).Light saturation curves of the PSII apparent transport electron rate (rETRPSII) were also established (Fig. 4A). The initial slope of the light curve (α') is proportional to the quantum yield of linear photosynthetic electron flow from molecular oxygen to NADP+. This parameter was derived for all the mutants (P in Table 1) and plot-ted as a function of the rate of dark respiration for each mutant (Fig. 4B). Values presented in Fig. 4B referred to wild-type values normalized to 1. From this analysis, 10 of the 22 transformants (called R set in the following) showed a decreased respiration value comprised between 0.5 and 0.75. Among them, only one (S21) was also significantly affected in the photosynthetic efficiency (α'< 0.8).Other mutants of the R set behave like complex I-less mitochondrial mutants, i.e. showing a reduced respiratory rate associated to a weakly-affected photosynthesis. When cultivated in higher light in the absence of acetate (phototrophic growth), most R mutants grew like wild type (Table 1).

Mutant	Phenotype					5′ Flanking sequence		3′ Flanking sequence	
	F_V/F_M	P[c]	R[d]	TAP DK[e]	TMP HL[f]	Phytozome localization[g]	Candidate protein	Phytozome localization[g]	Candidate protein
S01	0.72 ± 0.01	0.80 ± 0.02	0.50 ± 0.03	–	+	cre08.g372100 (3'U:2072161)	HSP70A, cytosolic heat shock protein (XP_001701326)	cre08.g372100 (3'U:2072232)	HSP70A, cytosolic heat shock protein (XP_001701326)
S12	0.69 ± 0.05	0.90 ± 0.07	0.57 ± 0.29	+/–	+	x		x	
S13	0.70 ± 0.03	0.98	0.99	–	+	x		x	
S15	0.73 ± 0.04	0.69 ± 0.05	0.84 ± 0.17	+/–	+	n.i.		n.i.	
S16	0.73 ± 0.04	0.90 ± 0.07	0.60 ± 0.02	+/–	+	cre17.g704900 (5'U:1196736)	unknown protein (XP_001691571)	x	
S18	0.73 ± 0.06	0.94 ± 0.08	0.96 ± 0.03	+/–	+	cre13.g573550 (Term:648563)	unknown protein (XP_001693501)	x	
S19	0.73 ± 0.03	1.00 ± 0.04	0.65 ± 0.03	–	+	cre10.g441650 (CS:3098805)	unknown protein (XP_001690528)	cre10.g434450 (CS:2280874)	NUOA9, complex I subunit (XP_001702653)
S20	0.73 ± 0.02	0.90 ± 0.03	0.60 ± 0.02	+/–	+/–	n.i.		cre08.g378550 (3'U:3112737)	NUOP4, complex I subunit (XP_001694363)
S21	0.48 ± 0.06	0.75 ± 0.08	0.55	–	+/–	cre06.g282800 (prom:3949970)	ICL1, isocitrate lyase (XP_001695331)	x	
S23	0.74 ± 0.01	1.12 ± 0.09	1.17 ± 0.21	+/–	+	n.i.		n.i.	
S30	0.73 ± 0.01	0.96 ± 0.02	0.70 ± 0.02	+/–	+/–	x		x	
W03[a]	0.64 ± 0.01	0.77 ± 0.01	0.92 ± 0.16	+/–	+	x		x	
W05[a]	0.70 ± 0.07	1.02 ± 0.09	0.65 ± 0.08	+/–	+	x		cre07.g327400 (Prom:1928596)	NUO9, complex I subunit (XP_001690652)
W08[b]	0.72±	1.00 ± 0.04	0.79 ± 0.28	+/–	+	x		x	
W12[b]	0.55 ± 0.13	0.45 ± 0.19	1.06 ± 0.42	+/–	+	cre13.g590500 (Prom:4019067)	FAD6, Plastid W6 Fatty acid desaturase (XP_001693068)	cre13.g590450 (CS:4012957)	unknown protein (XP_001699069)
W13[a]	0.64 ± 0.10	0.87 ± 0.14	0.51 ± 0.21	+/–	+	x		x	
W17[a]	0.70 ± 0.04	0.94 ± 0.06	0.56 ± 0.03	+/–	+	cre03.g201300 (5'U:6199496)	copper monooxygenase (XP_001693220)	cre03.g201300 (CS:6199794)	copper monoxygenase (XP_001693220)
W19[b]	0.48 ± 0.07	0.52 ± 0.10	1.17 ± 0.15	+/–	+	n.i.		n.i.	
W21[b]	0.50 ± 0.06	0.29 ± 0.09	1.11 ± 0.37	+/–	+	n.i.		n.i.	
W25[a]	0.65 ± 0.01	0.25 ± 0.29	0.93 ± 0.25	+/–	–	cre12.g493950 (CS:1355209)	PSPS13, plastid small ribosomal S13/S18 (XP_001700563)	intergenic region	
W31[a]	0.46 ± 0.21	0.50 ± 0.06	0.79 ± 0.37	+/–	+	cre12.g538750 (5'U:6420156)	LSM1, ribonucleoprotein (XP_001692854)	cre12.g538750 (5'U:6420151)	LSM1, ribonu-cleoprotein (XP_001692854)
W32[a]	0.73 ± 0.02	1.00 ± 0.03	1.04 ± 0.18	+/–	+	x		x	

Table 1 Growth characteristics, respiration rate, photosynthetic efficiency and molecular characterization of the 22 mutants presenting altered growth in the dark.

a Transformants derived from Jex4 wild-type strain

b transformants derived from 1'wild-type strain.

c PSII Photosynthetic efficiency (P) and

d dark respiration rate (R) were normalized on control values (see text for details). Means and standard errors ($n \geq 2$).

e Growth on solid medium: 20 µl cell suspensions were plated on acetate-containing medium (TAP) in the dark and acetate-free medium (TMP) in high light (200 µmol photons. m^{-2}. s^{-1}), and incubated for 5 days under dark conditions, and 3 days under light conditions.

f +/−: reduced growth; - no growth.

g Genomic localization of the flanking sequence based on locus names and genomic position from http://phytozome.jgi.doe.gov/; CS, coding sequence; 5'U, 5'UTR; 3'U, 3'UTR; Prom, promotor region; Term, terminator region; x, multiple TAIL-PCR products were amplified or no TAIL-PCR product was obtained; n.i., a unique TAIL-PCR product has been obtained but the flanking genomic region was not identified.

This observation is illustrated for mutants S16, S18, S19, W13, and W17 in Fig. 2. This indicates that these mutants might be solely affected for mitochondrion-related dark metabolism. Seven mutants (called P set in the following) were altered in photosynthesis (α'< 0.8) while respiration was not diminished (> 0.75) (Fig. 4B). They however did not show typical acetate-requirement and light sensitivity of mutants impaired in photosynthetic electron transfer for they also grew like wildtype on minimal medium and in higher light (e.g. W19 in Fig. 2, Table 1). These 7 P transformants along with S21 transformant corresponded to the 8 HygR transformants showing a low F_V/F_M value (Table 1). Incidentally, we found that most of the 22 transformants distributed along a linear relationship between F_V/F_M and α' (Fig. 4C). Finally, 5 transformants (called N set in the following) were affected neither in respiration nor photosynthesis. In the cases of mutants from P and N sets, the apparent absence of a respiratory deficiency raises the question of the cause of the reduced heterotrophic growth.

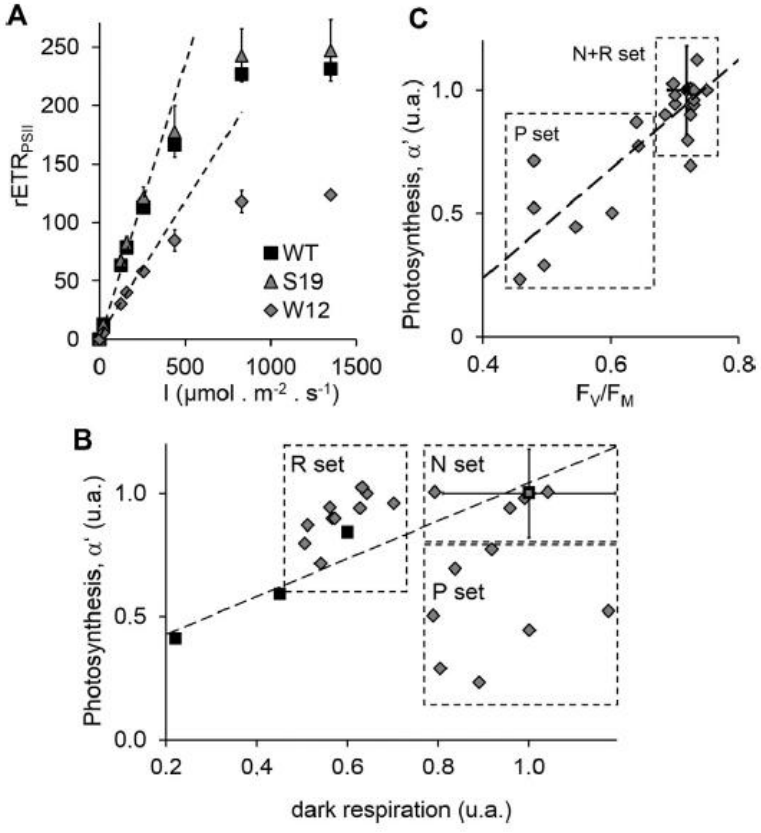

Fig. 4. Photosynthesis and respiration in HygR dk+/−or HygR dk−transformants.(A) Photosystem II apparent electron transfer rate (rETRPSII, µmols $e^{-}m^{-2}s^{-1}$) as a function of the light intensity (I, µmol photons at 520 nm. $m^{-2}s^{-1}$) in wild type(diamonds) and two HygR transformants (S19, squares; W12, triangles). Mean and standard deviations of two independent experiments. Measurements were determined in cells grown in liquid cultures under

mixotrophic conditions. (B) Relationship between dark respiratory rate and photosynthetic efficiency (α' parameter) in 22 transformants. All values are normalized on control values (see text for details and Table 1 for individual values). R set: HygR transformants with R < 0.75; Pset: HygR transformants with α'< 0.8 and R > 0.75; N set, HygR transformants with R > 0.75 and P > 0.8. Dark squares, values for wild type and previously characterized mitochondrial mutants (dum22, dum11, dum17) are in agreement with values previously published (Cardol et al., 2003). Dashed lines: linear regression. Standard errors bars are shown for wild type only (see other values in Table 1). (C) Relation-ship between maximum PSII quantum yield (F_V/F_M) and photosynthetic efficiency (α') in 22 HygR dk+/− transformants.

In the same plot, the three categories of mitochondrial mutants (complex I, complex III and complexes I+III mutants) are also shown. According to our previous results (Cardol et al., 2003), mitochondrial mutants and wild type distributed along a linear relationship. Interestingly, several mutants distributed along this linear relationship. The comparison of data sets also suggests that the more affected mitochondrial mutants (dark respiration below 0.5 like in complex III or complex I + III mutants) or non-photosynthetic mutants (α'< 0.2) were probably lost during the preservation of the HygR transformant collection in 96-well plates for several weeks (see supplemental Fig. 1).In order to identify the molecular lesion putatively responsible for the phenotype of our 22 mutants, flanking DNA was tentatively amplified using thermal asymmetric interlaced (TAIL)-PCR (Dent et al., 2005). At least one single DNA fragment (from either 3_or5_side) was amplified in 15 mutants. Most bands amplified using this technique are below 1000 bp, as observed in a previous report (Dent et al., 2005). Overall, it was possible to obtain at least one flanking DNA sequence for 11 mutants (Table 1). For transformants affected in respiration (R set), insertions were found in genes coding for heat shock protein (HSP70A), isocitrate lyase (ICL), 3 subunits of mitochondrial complex I (NUO9, NUOA9, NUOP4), a putative copper monooxygenase, and an unknown protein. For transformants impaired in photosynthesis, we found insertions in genes coding for plastid ribosomal subunit S13 (PSPS13), plastid ώ6 fatty acid desaturase (FAD6), and ribonucleoprotein (LSM1).

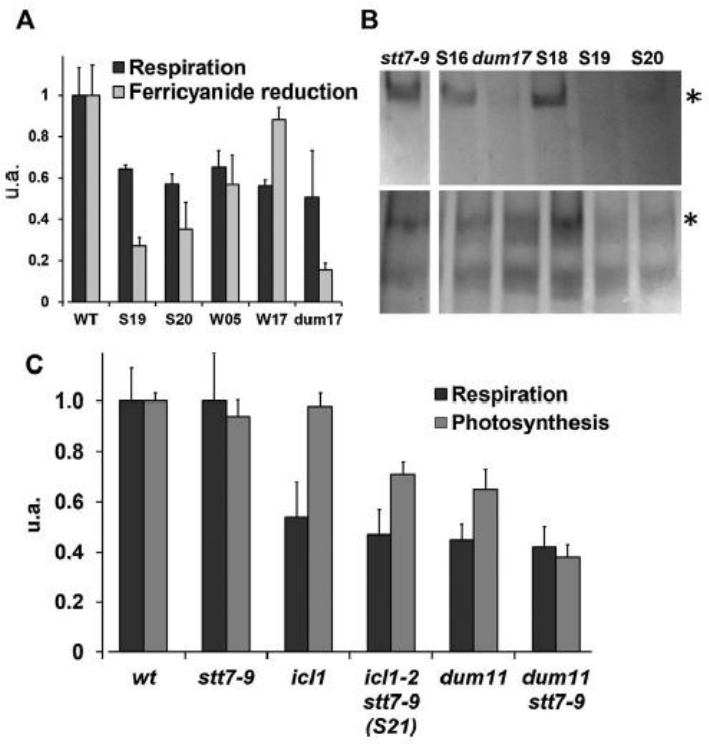

Fig. 5. Complex I activity of S19 (*nuoa9 stt7-9*) and S20 (*nuop4 stt7-9*) transformant strains. (A) Dark respiratory rates and specific activities of NADH:ferricyanide oxidoreductase (nmol of $K_3Fe(CN)_6$reduced min^{-1}mg $protein^{-1}$). (B) Analysis of mitochondrial and chloroplastic native complexes. 120 µg of crude membrane proteins solubilized by Triton X-100 (2% w/v, top) or n-dodecyl-B D-maltoside (2% w/v, bottom) were loaded on a BN-gel. After electrophoresis, the gel was submitted to NADH/NBT staining (*, NADH/NBT staining, ~950 kDa). (C) Dark respiratory rate and photosynthetic efficiency of wild type, S21 transformant, *stt7-9, icl1*-, *dum11*, and *dum11stt7-9* mutant strains. Values presented as means ± standard errors (n = 2–5) were normalized on wild-type values.

We next compared the photosynthetic performances of respiratory-deficient transformants in wild-type and STT7-deficient genetic backgrounds. Since our lab has a long interest in complex I-deficient mutants (Barbieri et al., 2011; Remacle et al.,2001), we focused our attention on two strains isolated from the STT7-deficient mutant strain for which gene candidates coded for complex I subunit (NUOA9 in S19, NUOP4 in S20). We also included in our analyses S21 which contains a cassette in ICL1 gene (coding for isocitrate lyase, ICL1), in view to compare it with another mutant lacking the same enzyme (Plancke et al., 2014). We moreover generated the two *dum17 stt7-9* and *dum11 stt7-9* double mutants. This gave us the opportunity to directly

investigate photosynthetic performances of these five *stt7-9* respiratory-deficient strains in comparison to *single dum17, dum11* and *icl1*- mutants. S19 and S20 behave like complex I-deficient *dum17* strain: their respiration was about 60% of that of wild type (Fig. 5A) and they grew slowly in the dark (Table 1). In both strains, deficiency in complex I activity was further confirmed by measuring NADH:ferricyanide activity on membrane fractions (Fig. 5A) and by probing NADH dehydrogenase activity of complex I isolated on Blue-Native gel (Fig. 5B). Few other transformants strains were chosen as controls (W17, Fig. 5A; S16and S18, Fig. 5B) and did not show any defect in complex I activity. This indicates that insertion identified in NUOA9 and NUOP4 genes might be responsible for the observed respiratory-deficiency and reduced growth phenotype of the two mutants.

Regarding PSII efficiency, we did not observe any difference between wild type, *stt7-9, dum17* (complex I mutant), *nuoA9 stt7-9* (S19), *nuop4 stt7-9* (S20), and *dum17 stt7-9* mutants (Table 1, Fig. 3A). We next analysed the S21 mutant that contains an insertion in ICL1 gene and is also deficient for state transition (*icl1-2 stt7-9*). In the dark, it behaves exactly as the original icl1 strain previously isolated in our laboratory (Plancke et al., 2014). It does not grow in heterotrophic conditions and its oxygen consumption rate in the dark is halved compared to wild type (Table 1 and Fig. 5C). By contrast, while icl1 is not impaired in photosynthesis (Plancke et al., 2014), the *icl1-2 stt7-9* (S21) trans-formant showed a lower PSII efficiency (Fig. 5C) most probably in relation to the *stt7-9* mutation. Photosynthetic performance was also reduced in *dum11 stt7-9* double mutant in comparison with single *dum11* mutant (Fig. 5C).

(4) Discussion

In this work, we investigated the possibility to isolate mutants impaired in respiration or more generally in dark energetic metabolism by screening hygromycin-resistant insertional trans-formants for altered chlorophyll fluorescence profile. The F_V/F_M parameter is the most widely used parameter in photosynthesis research. F_V/F_M reflects the maximum quantum yield of PSII photochemistry (Kitajima and Butler, 1975), which usually only depends on the redox state of the PSII-bound plastoquinone QA (see Schansker et al., 2014 for a critical discussion). In respiratory-deficient mutants, the reduced capacity of mitochondrial ATP synthesis directly exerts a reductive pressure on the PQ pool (Bulté et al., 1990; Cardol et al., 2009, 2003). In the

dark, the PQ pool and QA are in thermodynamic equilibrium, so that F_V/F_M directly reflects the redox state of the PQ pool and its measurement might indicate deficiencies in respiration. F_V/F_M is a convenient parameter, simple and fast to measure from colonies grown on agar plates by using an appropriate fluorescence imaging system (Johnson et al., 2009). In the present experiments, by selecting transformants in the light to recover mutants impaired in heterotrophic growth, non-photosynthetic mutants (e.g. PSII- strain, supplemental Fig. 1) were counter selected since they are highly light sensitive (e.g. Spreitzer and Mets, 1981). Twenty-four of the 2906 transformants had however a F_V/F_M value reduced by at least 20%, among which 8 corresponded to mutants altered in their ability to grow in the dark. The F_V/F_M parameter is usually proportional to the quantum yield of CO2 fixation (reviewed in Schanskeret al., 2014). Here we also found a linear relationship between F_V/F_M parameter and the effective yield of PSII photochemistry (Fig. 4C), which suggests that these 8 mutants are impaired in photosynthesis to various degrees. Two of these mutants have inserts in plastid proteins (ribosomal subunit or fatty acid desaturase). The reason for their defect in heterotrophic growth remains to be elucidated. They might correspond to mutants impaired in chloroplastic biosynthetic pathways required for mitochondrial biogenesis (e.g. lipid biosynthesis or Fe-S cluster biosynthesis). At this stage, any identification of the mutated gene responsible of the observed phenotype is however preliminary and the present observations will serve as a guide for future characterization of the mutants. The link between genomic localization and bio-chemical deficiencies indeed remains to be demonstrated (either by gene complementation or by linkage analysis). Alternatively, some mutants would bear several HygR cassettes or fragments in their genome and the one identified in this study would not be responsible for the growth phenotype. In any case, this class of mutants altered in both F_V/F_M value and dark growth is original because they do not possess the typical traits of mutants impaired in photosynthesis (e.g. light-sensitivity, acetate-requirement; see introduction).In contrast, several mutants with a low F_V/F_M grew in the dark as the wild-type strain. They most probably correspond to leaky photosynthetic mutants such as mutants in which a fraction of PSII centers is photo inhibited (reviewed in Schansker et al., 2014). Besides the mutants impaired in F_V/F_M, we isolated 14 mutants only impaired in heterotrophic growth. In particular, 3 new mutants defective in complex I activity were found (W05, S19, andS20). The W05 mutant was already studied in details: it bears a deletion in the promoter region of the NUO9 gene coding for ND9 subunit of complex I (Massoz et al., 2014). This mutation leads to a

reduced amount of ND9 subunit and accordingly to a reduced complex I amount. The two other strains lack the eukaryote specific 39-kDa complex I subunit (coded by NUOA9 in Chlamydomonas), and the small NUOP4 complex I subunit (to date found only in Chlamydomonas) (Cardol, 2011; Cardol et al., 2004). Associated or not to the *stt7-9* mutation responsible for the lack of chloroplastic state transition, mutations leading to complex I deficiency (dk+/−phenotype) do not confer any photosynthetic phenotype, so that these mutants cannot be identified by measuring F_V/F_M parameter. This is in line with the facts that in complex I mutants (i) ATP level is similar to the one in found in wild type, both in the light and in the dark (Cardol et al., 2003), and, (ii) although a diminished capacity to concentrate CO2 has been observed in complex I mutants, their photosynthetic capacity is not compromised (Massoz et al., 2014). The fact that complex I deficient mutants cannot be screened by fluorescence measurements (F_V/F_M) neither in wild-type nor in *stt7-9* backgrounds (see above) is a major short coming of our approach. We do not exclude to investigate in a near future the potential of other photosynthetic mutants. It has been recently shown that PSI-dependent cyclic electron flow is redox-controlled and occurs independently of state transitions (Alric, 2014; Takahashi et al., 2013). Two pathways are described: one involves the NDA2 NADPH:plastoquinone oxidoreductase (Jans et al., 2008), and the other relies on a PGR5-PGRL1 complex with putative ferredoxin:plastoquinone oxidoreductase activity (Tolleter et al., 2011; Hertle et al., 2013; Johnson et al., 2014). PGRL1-dependent pathway is the main cyclic electron pathway (Tolleter et al., 2011) and a defect in this pathway is compensated by an increase in respiration (Dang et al., 2014). The use of *pgrl1* mutant strain, directly impaired in cyclic electron flow, might thus be a good alternative to STT7-deficient strain in order to accentuate the phenotype of less affected mitochondrial strains such as complex I mutants. In contrast, in the case of strongly affected respiratory mutants (i.e. dk−mutants such as *dum11* and *dum22* lacking the cytochrome epathway of mitochondrial respiration), the association to *stt7-9* leads to a severe photosynthetic phenotype, so that these mutants could have been directly selected based on F_V/F_M or ϕPSII measurements. We however did not isolate such mutants in this work, probably because they were lost during the growth steps of the transformants in liquid medium in 96-well plates (e.g. dum11complex III mutant, see Supplemental Fig. 1). Such mutants are however viable when they are grown on solid medium in the light (reviewed in Salinas et al., 2014). An improvement to our screening approach could therefore be to keep mutants on solid agar medium during the

whole mutagenesis/screening process. It has however to be noticed that the altered photosynthesis *of dum11 stt7-9 or dum22 stt7-9* double mutants is associated to a severe growth reduction both in phototrophic and mixotrophic conditions (Cardol et al., 2009) (see also Fig. 5). The use of *stt7-9* mutant already allowed us to isolate the *stt7-9 icl1-2* double mutant which displays a photosynthetic phenotype which is not present in the single mutant (Fig. 5C). The phenotypical traits of *stt7-9 icl1-2* double mutant reinforce the idea that there is a mitochondrial cooperation going on because photosynthesis is compromised in STT7-deficient strain when respiration is impaired (Cardol et al., 2009). The isolation of such a mutant confirms that *stt7-9* genetic background acts as an amplifier for severe respiratory deficiencies, thus opening perspectives to identify new mutant strains.

Supplementary data associated with this article can be found, in the online version, at http://dx.doi.org/10.1016/j.jbiotec.2015.05.009

(5) Methods

Media and strains

In this study, we used two wild-type strains: 1' in our stock collection was derived from the wild-type 137c and Jex4 was isolated at IBPC (Paris, France) for its higher performance in insertional mutagenesis (Houille-Vernes et al., 2011). Mutant strains were also used: STT7-deficient *stt7-9* mutant strain (Cardol et al., 2009), complex I-deficient *dum17* strain (Cardol et al., 2002), complex III deficient *dum11* strain (Dorthu et al., 1992), and ICL1-deficient strain (Plancke et al., 2014). Cells were routinely cultivated on TAP medium at 50 μmol photons. $m^{-2}s^{-1}$.

Genetic crosses and isolation of dum (17 or 11) stt7-9 isolates.

The double mutants *dum17 stt7-9* and *dum11 stt7-9* were obtained by crossing a *stt7-9* mt+ strain with the *dum17* and *dum11* mt−strains, respectively. Zygotes were produced and matured during 3 days on nitrogen-free medium. Zygote germination was induced by transferring about 50 zygotes on fresh TAP medium at moderate light. Meiotic clones were then analysed to obtain strains bearing the double mutation. State transitions were monitored by following change in the maximal fluorescence yield (FM) after a saturating light pulse of light (200 ms, ~8000 μmol

photons. m−2s−1) on a JTS-10 spectrofluorometer (Biologic, France). In wild type, state1 was induced in the light (50 µmol photons. $m^{-2}s^{-1}$, ∼12 min) in the presence of DCMU (30 µM) while state 2 was achieved after 20 min of incubation in the dark in the presence of mitochondrial respiratory-chain inhibitors (cyanide potassium, 1 mM and salicyl hydroxamic acid, 1 mM). Meiotic products bearing the *dum17* or *dum11* mitochondrial mutation were identified based on their altered growth in heterotrophic conditions.

Transformation

Insertional mutagenesis of wild-type and *stt7-9* mutant strains was performed as described in (Barbieri et al., 2011). The strains were electroporated in presence of 1 µg of PCR product conferring the resistance to hygromycin B. The pHyg3 plasmid is derived from the pUC BM20 (Boehringer. Mannheim) and includes the APHVII gene (aminoglycoside phosphotransferase) from *Streptomyces hygroscopicus* leading to the hygromycin B antibiotic resistance under the control of the β2 tubulin promoter from *Chlamydomonas reinhardtii* .The APHVII gene also includes 3'UTRand the first intron from RBCS2 from *Chlamydomonas* (Bertholdet al., 2002). Transformants were selected in the light (50 µmol photons. $m^{-2}s^{-1}$) on TAP agar medium supplemented with 25 µg . μl^{-1} of hygromycin B. Transformants were then transferred to 96-well plates, grown and maintained in the light (50 µmol photons.m−2s−1) in liquid TAP medium under moderate shaking for several weeks. They were transferred back onto solid TAP agar medium prior to fluorescence analysis..

DNA extraction techniques and identification of flanking DNA

Extraction was performed according to (Newman et al., 1990). DNA concentration was measured using Synergy micro plate reader (Biotek). The identification of the flanking sequences was performed using the TAIL-PCR method (Dent et al., 2005). Flanking DNA was isolated from the side of the APHVII gene in both 5' and 3' using the APH7R3 (AGAATTCCTGGTCGTTC-CGCAG), APH7R4 (TAGGAATCATCCGAATCAATACG) and APH7R5 (CGGTCGAGAAGTAACAGGG) as specific primers for the 5_reac-tion and the Hygterm1(CGCGAACTGCTCGCCTTCACCT),Hygterm2(TCGAGGAGACCCCGCTGGATC) and Hygterm3 (CGATCCGGAG-GAACTGGCGCA) specific primers for the 3' reaction. The AD1, AD2, RMD227 and RMD228 aspecific primers were used as second set of primers for the TAIL-PCR reaction.

Biophysical analyses

Total respiration was measured using a Clark oxygen elec-trode (Hansatech instrument, King's Lynn, England) at 22C° in the dark. By convenience, the respiration was expressed on a 750 nm turbidity basis. Typical values for wild-type cell suspension atA750= 1 are ~9.5 10^6 cells per ml, 20.1 ± 1.7 µg chlorophyll per ml and 22.5 ± 4.8 nmol O2min−1per ml. The ratio between A750 nm and A664 nm was similar in all strains. In vivo fluorescence measurements at room temperature on cell liquid suspensions were performed using a JTS-10 spectrophotometer (Biologic, France)as described in (Godaux et al., 2013). Two parameters were calculated: the maximal quantum yield of PSII photochemistry[F_V/F_M= (F_M− F_O)/F_M] and the PSII quantum yield at a given light intensity [ϕPSII= (F_M'− F_S)/F_M'] (Genty et al., 1989; Kitajima and Butler, 1975). rETRPSII (photosystem II electron transport rate) at agiven light intensity was obtained by multiplying ϕPSII by the photon flux of actinic light. Since this value does not take into account the proportion of absorbed light, it represents an apparent value. Green LEDs peaking at 520 nm were used as actinic light source. Compared to red or white light sources, green light is less absorbed and gives rise to a higher ϕPSII values which account for high values of rETRPSII. The photosynthetic parameter α' was obtained by measuring the initial slope of the rETRPSII curve (Fig. 4A). Fluorescence emission spectra at 77 K were recorded using a LS50B spectrofluorometer (PerkinElmer) as previously described (Cardol et al., 2003). The fluorescence screening on solid medium was performed using a fluorescence camera (Beambio, paradigm camera speedzen) (Johnson et al., 2009).

Biochemical analyses

Crude membrane fractions were isolated by sonication (Remacle et al., 2001). Protein amounts were determined using the Brad-ford method (Bradford, 1976). NADH:ferricyanide activities were measured as described (Cardol et al., 2002). Blue-native polyacrylamide gel electrophoresis and the subsequent staining of the gel by NADH/NBT (nitroblue tetrazolium) was done as previously published (Cardol et al., 2006). ATP was extracted according to Gansand Rebeille (1990). ATP cellular level was determined using the Enliten luciferase/luciferin kit (Promega, Madison, WI).

(6) Acknowledgements

Borenzstein, B. Kameni, J.-H. Schumacher, and Michèle Radoux are warmly acknowledged

for their technical help. PC and CR acknowledged financial support from the Belgian Fondsde la Recherche Scientifique F.R.S.-F.N.R.S. (F.R.F.C. 2.4597.11, CDRJ.0032.15 and Incentive Grant for Scientific Research F.4520) and University of Liège (SFRD-11/05). CR acknowledged financial sup-port from the F.R.S.-F.N.R.S (F.R.F.C. 2.4567.11 and CDR J.0138.13).SM is supported by the Belgian FRIA F.R.S.-FNRS. VL and PC arePostdoctoral Researcher and Research Associate from F.R.S.-FNRS, respectively.

(7) References

Alric, J., 2010. Cyclic electron flow around photosystem I in unicellular green algae. Photosynth. Res. 106 (1–2), 47–56.

Alric, J., 2014. Redox and ATP control of photosynthetic cyclic electron flow in *Chlamydomonas reinhardtii*: (II) involvement of the PGR 5-PGRL1 pathway under anaerobic conditions. Biochim et Biophys Acta, http://dx.doi.org/10.1016/j.bbabio.2014.01.024, S0005-2728(14)00034-6.

Barbieri, M.R., Larosa, V., Nouet, C., Subrahmanian, N., Remacle, C., Hamel, P.P., 2011. A forward genetic screen identifies mutants deficient for mitochondrial complex I assembly in *Chlamydomonas reinhardtii*. Genetics 188, 349-358.

Berthold, P., Schmitt, R., Mages, W., 2002. An engineered Streptomyces hygroscopicus aph7 gene mediates dominant resistance against hygromycin B in *Chlamydomonas reinhardtii*. Protist 153, 401–412, http://dx.doi.org/10.1078/14344610260450136

Bradford, M.M., 1976. A rapid and sensitive method for the quantitation of microgram quantities of protein utilizing the principle of protein-dye binding. Anal. Biochem. 72, 248–254.

Bulté, L., Gans, P., Rebeillé, F., Wollman, F.A., 1990. ATP control on state transitions in vivo in *Chlamydomonas reinhardtii*. Biochim. Biophys. Acta 1020, 72–80.

Cardol, P., 2011. Mitochondrial NADH: ubiquinone oxidoreductase (complex I) in eukaryotes: a highly conserved subunit composition highlighted by mining of protein databases. Biochim Biophys Acta – Bioenerg. 1807, 1390–1397.

Cardol, P., Alric, J., Girard-Bascou, J., Franck, F., Wollman, F.-A., Finazzi, G., 2009.Impaired respiration discloses the physiological significance of state transitions in

Chlamydomonas. Proc. Nat. Acad. Sci. U. S. A. 106, 15979–15984.

Cardol, P., Gloire, G., Havaux, M., Remacle, C., Matagne, R., Franck, F., 2003. Photosynthesis and state transitions in mitochondrial mutants of *Chlamydomonas reinhardtii* affected in respiration. Plant Physiol. 133,2010–2020.

Cardol, P., Lapaille, M., Minet, M., Franck, F., Matagne, R.F., Remacle, C., 2006. ND3 and ND4L subunits of mitochondrial complex I both nucleus encoded in *Chlamydomonas reinhardtii* are required for activity and assembly of the enzyme. Eukaryot Cell 5, 1460–1467, http://dx.doi.org/10.1128/EC.00118-06,5/9/1460 [pii].

Cardol, P., Matagne, R.F., Remacle, C., 2002. Impact of mutations affecting ND mitochondria-encoded subunits on the activity and assembly of complex I in *Chlamydomonas*. Implication for the structural organization of the enzyme. J.Mol. Biol. 319, 1211–1221.

Cardol, P., Vanrobaeys, F., Devreese, B., Van Beeumen, J., Matagne, R.F., Remacle, C.,2004. Higher plant-like subunit composition of mitochondrial complex I from *Chlamydomonas reinhardtii*: 31 Conserved components among eukaryotes. Biochim. Biophys. Acta – Bioenerg 1658, 212–224.

Dang, K.-V., Plet, J., Tolleter, D., Jokel, M., Cuiné, S., Carrier, P., Auroy, P., Richaud, P.,Johnson, X., Alric, J., Allahverdiyeva, Y., Peltier, G., 2014. combined increases in mitochondrial cooperation and oxygen photoreduction compensate for deficiency in cyclic electron flow in *Chlamydomonas reinhardtii*. Plant Cell 26, 1–16, http://dx.doi.org/10.1105/tpc.114.126375

Dent, R.M., Haglund, C.M., Chin, B.L., Kobayashi, M.C., Niyogi, K.K., 2005. Functional genomics of eukaryotic photosynthesis using insertional mutagenesis of *Chlamydomonas reinhardtii*. Plant Physiol. 137, 545–556.

Dorthu, M.P., Remy, S., Michel-Wolwertz, M.R., Colleaux, L., Breyer, D., Beckers,M.C., Englebert, S., Duyckaerts, C., Sluse, F.E., Matagne, R.F., 1992. Biochemical genetic and molecular characterization of new respiratory deficient mutants in *Chlamydomonas reinhardtii*. Plant Mol. Biol. 18, 759–772

.**Finazzi, G**., 2001. Photoinhibition of *Chlamydomonas reinhardtii* in State 1 and State2: damages to the photosynthetic apparatus under linear and cyclic electron flow. J. Biol. Chem. 276, 22251–22257.

Fleischmann, M.M., Ravanel, S., Delosme, R., Olive, J., Zito, F., Wollman, F.A.,Rochaix,

J.D., 1999. Isolation and characterization of photoautotrophic mutantsof *Chlamydomonas reinhardtii* deficient in state transition. J. Biol. Chem. 274, 30987–30994.

Gans, P., Rebeille, F., 1990. Control in the dark of the plastoquinone redox state by mitochondrial activity in *Chlamydomonas reinhardtii*. Biochim. Biophys. Acta1015, 150–155.

Genty, B., Briantais, J.-M., Baker, A., 1989. The relationship between quantum yield of photosynthetic electron transport and quenching of chlorophyll fluorescence. Biochim. Biophys. Acta 990, 87–92

.Godaux, D., Emonds-Alt, B., Berne, N., Ghysels, B., Alric, J., Remacle, C., Cardol, P.,2013. A novel screening method for hydrogenase-deficient mutants inChlamydomonas reinhardtii based on in vivo chlorophyll fluorescence andphotosystem II quantum yield. Int. J. Hydrogen Energy 38, 1826–1836.

Gumpel, N.J., Ralley, L., Girard-Bascou, J., Wollman, F.A., Nugent, J.H.A., Purton, S., 1995. Nuclear mutants of *Chlamydomonas reinhardtii* defective in the biogenesis of the cytochrome b6f complex. Plant Mol. Biol. 29, 921–932, http://dx.doi.org/10.1007/B F000 14966

Houille-Vernes, L., Rappaport, F., Wollman, F.A., Alric, J., Johnson, X., 2011. Plastid terminal oxidase 2 (PTOX2) is the major oxidase involved in chlororespiration in Chlamydomonas. Proc. Nat. Acad. Sci. U. S. A. 108, 20820–20825, http://dx.doi.org/10.1073/pnas.1110518109 [pii] 1110518109.

Jans, F., Mignolet, E., Houyoux, P.A., Cardol, P., Ghysels, B., Cuine, S., Cournac, L.,Peltier, G., Remacle, C., Franck, F., 2008. A type II NAD(P)H dehydrogenase mediates light-independent plastoquinone reduction in the chloroplast of *Chlamydomonas*. Proc. Nat. Acad. Sci. U. S. A. 105, 20546–20551.

Johnson, X., Kuras, R., Wollman, F.A., Vallon, O., 2007. Gene hunting by complementation of pooled Chlamydomonas mutants. In: Allen, J. (Ed.), 14th International Congress of Photosynthesis. Springer, Glasgow UK, pp.1093–1097.

Johnson, X., Vandystadt, G., Bujaldon, S., Wollman, F.A., Dubois, R., Roussel, P., Alric,J., Beal, D., 2009. A new setup for in vivo fluorescence imaging of photosynthetic activity. Photosynthesis Res 102, 85–93, http://dx.doi.org/10.1007/s11120-009-9487-2

Kitajima, M., Butler, W.L., 1975. Quenching of chlorophyll fluorescence and primary photochemistry in chloroplasts by dibromothymoquinone. Biochim.Biophys. Acta 376, 105–115.

Lecler, R., Godaux, D., Vigeolas, H., Hiligsmann, S., Thonart, P., Franck, F., Cardol,

P.,Remacle, C., 2011. Functional analysis of hydrogen photoproduction in respiratory-deficient mutants of *Chlamydomonas reinhardtii*. Int. J. Hydrogen Energy 36, 9562–9570.

Lemeille, S., Rochaix, J.D., 2010. State transitions at the crossroad of thylakoid signaling pathways. Photosynth. Res. 106 (1–2), 33–46.

Lown, F.J., Watson, A.T., Purton, S., 2001. *Chlamydomonas* nuclear mutants that fail to assemble respiratory or photosynthetic electron transfer complexes. Biochem. Soc. Trans. 29, 452–455.

Massoz, S., Larosa, V., Plancke, C., Lapaille, M., Bailleul, B., Pirotte, D., Radoux, M.,Leprince, P., Coosemans, N., Matagne, R.F., Remacle, C., Cardol, P., 2014. Inactivation of genes coding for mitochondrial Nd7 and Nd9 complex I subunits in *Chlamydomonas reinhardtii* impact of complex I loss on respiration and energetic metabolism. Mitochondrion 19, 365–374, http://dx.doi.org/10.1016/j.mito.2013.11.004, Pt B.

Matagne, R.F., Michel-Wolwertz, M.R., Munaut, C., Duyckaerts, C., Sluse, F., 1989.Induction and characterization of mitochondrial DNA mutants in *Chlamydomonas reinhardtii*. J. Cell. Biol. 108, 1221–1226.

Mitchell, P., 1961. Coupling of phosphorylation to electron and hydrogen transfer by a chemi-osmotic type of mechanism. Nature 191, 144–148.

Murata, N., 1969. Control of excitation energy transfer in photosynthesis light-induced change of chlorophyll a fluorescence in *porphyra yezoensis*. Biochim. Biophys. Acta 172, 242–251.

Newman, S.M., Boynton, J.E., Gillham, N.W., Randolph-Anderson, B.L., Johnson,A.M., Harris, E.H., 1990. Transformation of chloroplast ribosomal RNA genes in *Chlamydomonas*: molecular and genetic characterization of integration events. Genetics 126, 875–888.

Niyogi, K.K., Bjorkman, O., Grossman, A.R., 1997. *Chlamydomonas* xanthophyll cycle mutants identified by video imaging of chlorophyll fluorescence quenching. Plant Cell 9, 1369–1380.

Plancke, C., Vigeolas, H., Hohner, R., Roberty, S., Emonds-Alt, B., Larosa, V.,Willamme, R., Duby, F., Onga Dhali, D., Thonart, P., Hiligsmann, S., Franck, F.,Eppe, G., Cardol, P., Hippler, M., Remacle, C., 2014. Lack of isocitrate lyase in *Chlamydomonas* leads to changes in carbon metabolism and in the response to oxidative stress under mixotrophic growth. Plant J. 77, 404–417, http://dx.doi.org/10.1111/tpj.12392

Remacle, C., Baurain, D., Cardol, P., Matagne, R.F., 2001. Mutants of *Chlamydomonas*

reinhardtii deficient in mitochondrial complex i characterization of two mutations affecting the nd1 coding sequence. Genetics 158, 1051–1060.

Rich, P.R., Mischis, L.A., Purton, S., Wiskich, J.T., 2001. The sites of interaction oftriphenyltetrazolium chloride with mitochondrial respiratory chains. FEMSMicrobiol. Lett. 202, 181–187.

Salinas, T., Larosa, V., Cardol, P., Marechal-Drouard, L., Remacle, C., 2014. Respiratory-deficient mutants of the unicellular green *alga Chlamydomonas*: are view. Biochimie 100, 207–218, http://dx.doi.org/10.1016/j.biochi.2013.10.006, S0300-9084(13)00355-6 [pii].

Schansker, G., Tóth, S.Z., Holzwarth, A.R., Garab, G., 2014. Chlorophyll a fluorescence: Beyond the limits of the QA model. Photosynth. Res., http://dx.doi.org/10.1007/s11120-013-98065

Spreitzer, R.J., Mets, L., 1981. Photosynthesis-deficient Mutants of *Chlamydomonas reinhardii* with associated light-sensitive phenotypes. Plant Physiol. 67,565–569, http://dx.doi.org/10.1104/pp.67.3.565

Takahashi, H., Clowez, S., Wollman, F.A., Vallon, O., Rappaport, F., 2013. Cyclic electron flow is redox-controlled but independent of state transition. Nature Commun. 4, 1954, http://dx.doi.org/10.1038/.

Tolleter, D., Ghysels, B., Alric, J., Petroutsos, D., Tolstygina, I., Krawietz, D., Happe, T.,Auroy, P., Adriano, J.M., Beyly, A., Cuiné, S., Plet, J., Reiter, I.M., Genty, B.,Cournac, L., Hippler, M., Peltier, G., 2011. Control of hydrogen photo-production by the proton gradient generated by cyclic electron flow in *Chlamydomonas reinhardtii*. Plant Cell 23, 2619–2630, http://dx.doi.org/10.1105/tpc.111.086876

Wollman, F.A., Delepelaire, P., 1984. Correlation between changes in light energy distribution and changes in thylakoid membrane polypeptide phosphorylation in *Chlamydomonas reinhardtii*. J. Cell. Biol. 98, 1–7.

Publication 3. **In vivo chlorophyll fluorescence screening allows the isolation of a *Chlamydomonas* mutant defective for NUOAF3, an assembly factor involved in early stage mitochondrial complex I assembly**

S. Massoz, M. Hanikenne, B. Bailleul, N. Coosemans, M. Radoux, P. Cardol, V. Larosa, C. Remacle. To be submitted.

This paper directly follows the *stt7* publication, as it was our second attempt at developing a fluorescence screening for complex I mutants. For this attempt, we decided to use the newly isolated *pgrl1* mutant, deficient in cyclic electron transfer in the chloroplast, as a recipient strain. In order to avoid bad surprises (such as the screening method not working on complex I mutants, see *stt7* publication), we first produced and analysed a *pgrl1/Δnd4* mutant and searched for adequate photosynthetic parameters. It was quickly found that photosynthetic parameters (ϕPSII) could be used to differentiate the *pgrl1/Δnd4* mutant from its parental strains.

As the differences between the *pgrl1/Δnd4* mutant and the parental strains were important, we started another mutagenesis and screened for ϕPSII. We could quickly obtain (~150th transformant) a complex I mutant confirming the validity of the approach. Two other mutants were later found. While only one of them was a clean mutant (tagged mutation of a lonely resistance cassette), we were lucky enough to find the whole spectrum of differently affected mutants, with one of the strain barely affected and another highly deficient in mitochondrial activities. These strains can serve as markers for the likely limits of what can be obtained in our screening. The *nuoaf3* mutant was identified as such after much effort, since the TAIL-PCR and all other tested molecular approaches proved inefficient in unveiling the insertion site. For this, we had to turn ourselves toward NGS techniques, with the help of Marc Hanikenne from my thesis committee. His precious help allowed us to identify the mutation in the *NUOAF3* gene.

NUOAF3 is a protein involved in complex I assembly of the Q module, only characterized in humans and some extent in *C. elegans*. This thus represented a great opportunity to investigate assembly in *C. reinhardtii* and compare it to humans. The defect in Q module brought by *NUOAF3* deficiency was similar to that observed in our RNAi-*NUO9* and RNAi-*NUO7* cell lines. This was a chance to confirm and further investigate the different impact of the

loss of the Q module on the N module and complex I assembly, this analysis being this time the central part of our work.

In this publication, I have done all the work except the isolation of the *pgrl1/Δnd4* mutant, the RT-PCR analysis (Fig. 6C) and the bioinformatics analysis of the sequencing results. I made the figures and participated to the redaction of the paper.

In vivo chlorophyll fluorescence screening allows the isolation of a *Chlamydomonas* mutant defective for NUOAF3, an assembly factor involved in early stage mitochondrial complex I assembly

S. Massoz[a,c], M. Hanikenne[b,c], B. Bailleul[a,d], N. Coosemans[a,c], M. Radoux[a,c], P. Cardol[a,c], V. Larosa[a,e*], C. Remacle[a,c*]

[a] InBioS - Genetics and Physiology of Microalgae, University of Liege, Belgium

[b] InBioS - Functional Genomics and Plant Molecular Imaging, University of Liège, Belgium

[c] PhytoSYSTEMS, University of Liège, Belgium

[d] present address : Institut de Biologie Physico-Chimique (IBPC), UMR 7141, Centre National de la Recherche Scientifique (CNRS), Université Pierre et Marie Curie, 13 Rue Pierre et Marie Curie, F-75005 Paris, France

[e] present address : Department of Biology, University of Padova

corresponding author : C. Remacle

co-corresponding author : V. Larosa

(1) Summary (250 words)

The green microalga *Chlamydomonas reinhardtii* is a model of choice for isolating complex I mutants but the current qualitative screening method, based on reduced growth in heterotrophic condition, is not suited for high throughput screening. As mitochondrial activity can compensate for deficiencies in photosynthesis, and vice versa, we reasoned that in the genetic background of a photosynthetic mutant requiring the mitochondrial cooperation, we could use photosynthetic parameters to identify respiratory mutants. To this aim, we associated the *pgrl1* mutation leading to defect in the formation of the electrochemical proton gradient in the chloroplast with a complex I mutation and showed that *complex I/pgrl1* double mutant displayed reduced photosystem II yield fluorescence (ΦPSII), whereas the single mutant *pgrl1* was unaltered. This allowed for an easy identification of complex I mutants following mutagenesis of a *pgrl1* strain. Out of ~3000 hygromycin-resistant insertional mutants generated in a *pgrl1* recipient strain, 46 had decreased ΦPSII and three were complex I mutants. One of the mutants was tagged and whole genome sequencing identified the resistance cassette in *NUOAF3*. NUOAF3 is a complex I assembly factor homologous to human NDUFAF3 and required in early stages of complex I assembly. Our study shows that the loss of NUOAF3 is responsible for loss of assembly of an early module of complex I (Q module), which leads to partial defect of complex I assembly/activity. Overall, we describe here a novel screening method which is fast and particularly suited for identification of *Chlamydomonas* complex I mutants.

(2) Significance statement (up to 2 sentences of no more than 75 words total)

Photosystem II yield fluorescence is a parameter that can be used to isolate complex I mutants in a *pgrl1* background in *Chlamydomonas*.

A small-scale pilot insertional library allowed the isolation of a mutant affected in *NUOAF3* coding for an early stage assembly factor.

(3) Introduction

Mitochondrial oxidative phosphorylation (OXPHOS) is responsible for a large and constant ATP production in the cell. It is composed of five multiprotein complexes: four oxidoreductases and an ATP synthase (Mitchell 1961). The ubiquinone:NADH oxidoreductase (complex I) is the main entry point of electrons in the respiratory chain. It catalyzes NADH oxidation and couples ubiquinone reduction to proton pumping from the matrix side to the intermembrane space of mitochondria. It is the most intricate of the five complexes with a size of ~1000 kDa in bovine heart (Vinothkumar et al. 2014) and about 950 kDa in the green microalga *Chlamydomonas reinhardtii* (Cardol et al. 2004). Comprising ~45 subunits in mammals (Vinothkumar et al. 2014) and up to 47 subunits in *C. reinhardtii* (Cardol 2011; Subrahmanian et al. 2016), it has an L shaped structure in all organisms investigated so far (Vinothkumar et al. 2014), with one matrix arm and one membrane arm. Fourteen of its subunits are considered to be the core of complex I, since all of them are present in the simplest form of the complex I, the type-I NADH dehydrogenase of some bacteria (Letts and Sazanov 2015). The seven core subunits ND1, ND2, ND3, ND4, ND4L, ND5, and ND6 compose the membrane arm of the complex, also called P module, responsible for proton translocation. These subunits are generally encoded in the mitochondrial genome, though the ND3 (NUO3) and ND4L (NUO11) subunits are encoded in the nuclear genome of *C. reinhardtii* (Cardol et al. 2006). The second set of core subunits consists of the NUO10/NDUFS7/PSST, NUO8/NDUFS8/TYKY, NUO9/NDUFS3/30 kDa, NUO7/NDUFS2/49 kDa subunits composing the Q module of complex I and the third set consists of NUO5/NDUFV2/24 kDa, NUO6/NDUFV1/51 kDa, NUOS1/NDUFS1/75 kDa subunits composing the N module of complex I (according to the *Chlamydomonas*/human/bovine nomenclature). These last two sets of subunits compose the matrix arm of complex I, bearing the prosthetic groups (8 Fe–S clusters, 1 FMN) responsible for electron transport from NADH to ubiquinone. In eukaryotes, the remaining subunits are called accessory subunits. Though not present in the bacterial type-I NADH dehydrogenase, studies showed that impairments in several of these subunits lead to complete or important defect in complex I activity and/or assembly (Stroud et al. 2013; Hoefs et al. 2011; Kmita et al. 2015; Rak and Rustin 2014; Szklarczyk et al. 2011). Complex I structure was determined in the bacterium *Thermus thermophilus* (Berrisford et al. 2016), the fungus *Yarrowia lipolytica* (Zickermann et al. 2015) and in beef (Vinothkumar et al. 2014), allowing a better understanding of the mechanisms of the complex I protons pumping

machinery (Hummer and Wikström 2016). Even though the subunit composition of complex I is well known in many organisms, the understanding of assembly processes is still at an early phase. Only 14 assembly factors have been discovered so far in humans (Sánchez-Caballero et al. 2016b) and analysis of their role points towards a modular assembly process (Sánchez-Caballero et al. 2016b). Our knowledge of complex I assembly in photosynthetic organisms is even more limited. On the 14 assembly factors described in humans, 11 have putative homologs in *Arabidopsis* (Subrahaminian et al. 2014) but only one homolog has been functionally analyzed: INDL (homolog of human NUBPL) in *A. thaliana*. The role of INDL is more complex in plants as the factor has been suggested to participate to both the assembly of Fe-S clusters like in humans (Sheftel et al. 2009) but also in mitochondrial translation (Wydro et al. 2013). In addition, an assembly factor which is not conserved in humans has also been described: L-galactono-1,4-lactone dehydrogenase (GLDH), catalyzing the last step of ascorbate biosynthesis, has been shown to be necessary for the assembly of membrane arm of complex I in *A. thaliana* (Schimmeyer et al. 2016).

To examine complex I assembly, *C. reinhardtii* constitutes an interesting model organism. Indeed respiratory-deficient mutants can be obtained and easily survive in phototrophic (light + mineral medium) and mixotrophic conditions (light + acetate) due to the action of type-II NADH dehydrogenase in the mitochondria (Lecler et al. 2012). They are barely affected in photosynthesis (Cardol et al. 2003). In heterotrophic conditions (acetate + dark), complex I mutants show a partial growth deficiency phenotype (review in Salinas et al. 2014). This phenotype allowed previous screening of complex I mutants (Remacle et al. 2001; Barbieri et al. 2011). However, this method is not adapted for high throughput screening since it is fastidious as growth analysis cannot be directly made on the transformation plates and requires subsequent transfer of the colonies to additional petri dishes where growth in the dark can be analyzed only after 10-15 days. In addition, the “slow growth in the dark ” criterium is quite subjective. With the objective of discovering proteins involved in complex I biogenesis, a high throughput and quantitative method is thus required in order to isolate complex I mutants that could conserve a residual activity and potentially represent interesting assembly intermediates.

Mitochondrion and chloroplast interact to preserve their respective energetic equilibrium (Hoefnagel et al. 1998). Mutants deficient in photosynthesis usually show a dependency toward mitochondrial activity for proper photosynthesis efficiency. Notably, tight interplays between

state transitions, a major regulation process of photosynthesis, and respiratory activity have been well demonstrated, using inhibitors of mitochondrial respiration or by analyzing single and double mutants, defective for mitochondrial respiration and/or state transitions (Cardol et al. 2009). A *Chlamydomonas* mutant inactivated in *pgrl1* (PGRL1: proton gradient related 1) has been recently isolated. The lack of *pgrl1* is correlated with a reduced light induced electrochemical proton gradient, which is attributed to a reduced cyclic electron flow and leads to a reduced chloroplastic ATP production (Tolleter et al. 2011, Dang et al. 2014). Interestingly, this mutant displays an increased mitochondrial activity and altered photosynthesis in the presence of mitochondrial inhibitors (Dang et al. 2014). This indicates that mitochondrial activity compensates for the lack of *pgrl1* and opens the possibility to use photosynthesis as a fast and non-invasive probe of mitochondrial activity.

Previously, we explored the possibility to screen for mutants impaired in respiration by measuring photosynthetic efficiency from fluorescence analysis (F_V/F_M, photosynthetic efficiency) using a state-transition deficient (*stt7*) strain as recipient for insertional mutagenesis. Overall, the comparison of respiratory mutants obtained in wild-type or *stt7* genetic backgrounds indicated that fluorescence could be used to isolate mutants severely impaired in dark metabolism but not to isolate complex I deficient mutants (Massoz et al. 2015).

In order to perform complex I screening, a more affected photosynthetic mutant is required. The *pgrl1* mutant cited above seems interesting since the lack of *pgrl1* causes an increased dependence towards mitochondrial activity. We report here our results concerning the use of the *pgrl1* mutant as recipient strain for insertional mutagenesis. We demonstrate that complex I assembly deficient mutants can be recovered using a screening method based on fluorescence measurements in a *pgrl1* background in the green alga *C. reinhardtii*.

(4) Results

1. Selection and characterization of a recipient *pgrl1*/Δ*nd4* strain for insertional mutagenesis

In order to investigate if the *pgrl1* mutation could be used as a genetic background to isolate complex I-deficient mutants on the basis of a fluorescence phenotype, we crossed *Δnd4* mt^- with *pgrl1* mt^+ to create a *pgrl1*/Δ*nd4* double mutant. The *Δnd4* mutation is a 69 bp deletion affecting the very beginning of ND4 and leading to partially assembled complex I (Remacle et al. 2006). The *pgrl1* mutant has been obtained by insertional mutagenesis using a paromomycin

resistance cassette (Tolletter et al. 2011). One *pgrl1/*Δ*nd4* meiotic product was selected and the photosynthetic parameters were assessed to uncover to best conditions in which the *pgrl1* background would allow us to separate the double mutant from its parents, the *Δnd4* and *pgrl1* mutant strains.

We first tested variations of the F_V/F_M (PSII quantum yield in the dark) and ϕPSII (PSII quantum yield in light adapted cells) parameters in the *pgrl1/*Δ*nd4* double mutant as they are quick and easy to measure by imaging methods directly on agar plates and would represent ideal parameters to base a screening protocol on. The four strains (*Δnd4*, *pgrl1*, *pgrl1/*Δ*nd4*, and WT) were first tested for Fv/Fm parameter over 50 minutes of dark acclimation period (Fig. 1a). At the very start, before any real acclimation, the *pgrl1/*Δ*nd4* strain demonstrated very affected F_V/F_M, but these differences faded quickly in less than ten minutes. Nevertheless, such results indicated that photosynthetic measurements in the light could be used to discriminate the *pgrl1/*Δ*nd4* mutant from its parental strains. We thus established a light saturation curve of the relative electron transport rate through PSII ($rETR_{PSII}$) (Fig. 1b). In this experiment, the *pgrl1/*Δ*nd4* double mutant exhibited a decreased $rETR_{PSII}$ compared to WT, single *pgrl1* or *Δnd4* strains. This shows that in such conditions, only the coupled *pgrl1* and *Δnd4* mutations lead to a specific photosynthetic defect. The $rETR_{PSII}$ values depend on the ϕPSII parameter which can be obtained more quickly than the whole light saturation curve from a single fluorescence measurement. We thus next performed ϕPSII fluorescence measurements on the *pgrl1/*Δ*nd4* double mutant and the parental strains (Fig. 1c-d). The *pgrl1/*Δ*nd4* double mutant shows a 42% ϕPSII decrease at 240 $\mu E.m^{-2}.s^{-1}$ with a ϕPSII value of 0.34 ± 0.012, compared to the average 0.58 ± 0.014 for the three other tested strains (Fig. 1c). This difference is easily detected by the camera when the fluorescence of the colonies is converted into false colors (Fig. 1d). Altogether, these results show that fluorescence screening of complex I mutant is possible using ϕPSII measurements in a *pgrl1* background.

2. Insertional mutagenesis using *pgrl1* as recipient strain for transformation allows recovery of complex I mutants

We then proceeded to a random insertional mutagenesis on *pgrl1* strain using the hygromycin cassette as selection marker. 3059 insertional transformants were generated and selected for hygromycin resistance (Hyg^R) after 2-3 weeks growth (Fig. 2a). Transformants were transferred and sorted on TAP medium plates and then subjected to a primary screen based on

their ϕPSII on agar plate at 240 $\mu E.m^{-2}.s^{-1}$. As the ϕPSII value for WT was 0.59±0.05 (Fig. 1c), transformants with a ϕPSII significantly lower than the WT value were selected as candidate respiratory-deficient mutants (ϕPSII < 0.5). In order to avoid pleiotropic phenotype, we decided that the lowest selected ϕPSII value would be 0.2 since the *pgrl1/*Δ*nd4* mutant exhibits a ϕPSII value of 0.34 ± 0.012 (Fig. 1c). We could obtain 46 transformants that showed ϕPSII values between 0.2 and 0.5 (Fig. 2a). These candidate respiratory-deficient mutants were then submitted to a secondary screen based on their NADH:$Fe(CN)_6^{3-}$ oxidoreductase activity (NADH:FeCN activity) on crude membrane fractions. The NADH dehydrogenase activity of the hydrophilic domain of complex I is the main contributor to NADH:FeCN activity in *Chlamydomonas* crude membrane extracts (Remacle et al. 2001). Indeed, only 15% of this activity remains in the *pgrl1/*Δ*nd4* mutant which can be attributed to type II NADH dehydrogenases from chloroplast and mitochondrial origin (Terashima et al. 2010; Lecler et al. 2012) .Three transformants, respectively named M1, M2, and M3, were found to have lower NADH:FeCN activity compared to the *pgrl1* recipient strain and higher than the activity of the *pgrl1/*Δ*nd4* mutant (Table 1). Complex I mutants in *C. reinhardtii* typically show an increased complex II+III activity (Remacle et al. 2001, Cardol et al. 2008). This could also be observed for the M1 and M3 transformants, while the M2 did not show any significant increase in this activity. Complex IV activity used as reference was shown to be unchanged in the M1 and M3 strains, but decreased by about 55% in the M2 strain. These results suggest that while the M1 and M3 strains are *bona fide* partially affected complex I mutants, the M2 strain seems to be affected partially for its whole respiratory chain.

To assess the cosegregation between hygromycin resistance and complex I mutations, crosses were made between the WT+ ($4A^+$) (mt^+ hygromycin and paromomycin sensitive strain) and the three double *pgrl1/complex I* (*pgrl1/CI*) mutants (mt^- hygromycin resistant and paromomycin resistant) (Table 2). Unfortunately crosses between WT and M2 did not produce any meiotic progeny. 450 and 200 descendants were analyzed from the crosses with the M1 and M3 strains respectively. The M1 meiotic products showed a 50/50 hygromycin resistance segregation suggesting the insertion of a functional cassette in a single locus. The M3 mutant showed higher Hyg^R percentage segregation (63%) suggesting that more than one insertion could be present in its genome.

To confirm or deny the cosegregation between hygromycin cassette and complex I

phenotype, we selected the *pgrl1* descendants from the previous crosses M1 mt^- x WT+ and M3 mt- x WT+ thanks to their specific paromomycin (Pm^R) resistance. We then screened the Pm^R descendants for hygromycin resistance. In such conditions, if the respiratory defect segregates with the hygromycin cassette, all Hyg^R descendants, being *pgrl1/CI*, will exhibit the previously characterized fluorescence phenotype. If it is not the case, we will be able to retrieve some Hyg^R clones *pgrl1/CI*$^+$ that will not display any fluorescence phenotype. The 45 Hyg^R/Pm^R meiotic products obtained from M1 x WT cross showed perfect cosegregation between hygromycin resistance and altered ΦPSII (Fig. 3a, Table 2), confirming that the single insertion defined previously is indeed responsible for complex I phenotype. The M3 progeny displayed some Hyg^R clones without any altered fluorescence. In addition, some Hyg^S/Pm^R clones were found to possess decreased fluorescence phenotype, linked to reduced complex I activity. This allowed us to conclude that the complex I defect was not linked to a functional hygromycin cassette in the M3 transformant.

To insure the lack of impact of the *pgrl1* mutation on complex I phenotype, one Hyg^R Pm^S descendant (M1') from the M1 mt- x WT+ cross and one Hyg^S Pm^S descendant (M3') from the M3 mt- x WT+ cross were isolated and their complex I activity was measured using NADH:FeCN activity. Meiotic products deprived from the *pgrl1* mutation displayed the exact same complex I deficiency as in the presence of *pgrl1*, while the photosynthetic deficiency was lost upon removal of *pgrl1* (Fig. 3b).

The growth phenotype of the double mutants was then assessed under mixotrophic, phototrophic and heterotrophic conditions as illustrated for the M1 and M3 strains (Fig. 2b). M1 showed a reduced growth in both mixotrophic and phototrophic conditions, underlining the defect in photosynthesis. M1 also showed a partial growth decrease in heterotrophic conditions, which is typical for complex I mutants (Salinas et al. 2014). The M3 strain did not show any detectable growth phenotype, even in heterotrophic conditions, probably because the complex I defect was not impactful enough to alter growth. To confirm complex I phenotype, crude membrane extracts of each strain were submitted to Blue-Native PolyAcrylamide Gel Electrophoresis (BN-PAGE) where complex I could be detected by in-gel activity, using the NADH/NBT staining method (Fig. 4a). The dimeric ATP synthase at 1600 kDa (Lapaille et al. 2010) is shown as loading control. The M1 strain showed a severe decrease in complex I activity compared to the single *pgrl1* strain. This decrease was parallel to a decrease in complex I amount (Coomassie Blue

staining), correlating the lack of activity to a lack of complex I assembly. The M3 strain did not show any major differences compared to *pgrl1*. The M2 showed a severe decrease in complex I activity and presence, and this lack of complex I was accompanied by a decrease in the ATP synthase amount.

NADH:FeCN activity was plotted against photosynthetic activity (ϕPSII) (Fig. 5). The ϕPSII and NADH:FeCN activity plot showed a good correlation between the two parameters except for the M2 strain. The M2 mutant is not part of this correlation because the photosynthetic defect is much stronger than if only caused by complex I defect since this strain is affected in several respiratory complexes (complex I, complex IV, ATP synthase).

In order to identify the molecular lesion putatively responsible for the phenotype of the only tagged mutant (M1), genomic DNA flanking the cassette was tentatively amplified using thermal asymmetric interlaced (TAIL)-PCR (Dent et al. 2005). PCR product could be amplified for the M1 mutant but two consecutives hygromycin cassettes were detected, preventing the flanking region to be identified.

3. Molecular characterization of the M1 mutation

Genetic analyses showed that the hygromycin cassette located in the M1 strain was responsible for complex I defect but as mentioned above, TAIL-PCR failed and the flanking sequences could not be identified despite several attempts. In order to identify the mutation in the M1 mutant, we decided to take advantage of the combination of bulked segregant analysis (Michelmore et al. 1991;Giovannoni et al. 1991) and the NGS (next generation sequencing) technology. This method requires the sequencing of a pool of mutated individuals obtained by crosses with a WT reference and the identification of the causative region by deep sequencing. All the mutant individuals conserve the mutated locus while genomic environment is fluctuating as a result of crossing-overs during meiosis. This method has been successfully applied to various organisms including recently macroalgae (Billoud et al. 2015). We thus first created a pool of 50 Hyg^R descendants by crossing the M1 mt^- strain with WT+. These Hyg^R meiotic products were sequenced as a single pool sample based on the fact that all Hyg^R individuals bear the mutated locus responsible for complex I defect while genomic environment may vary due to random insertion of non-functional hygromycin cassette or DNA carrier.

Genome *de novo* assembly of 296.6 Mio quality-filtered Illumina 75bp paired-end reads (~178x coverage) for the mutant pool yielded 15364 scaffolds with N50=33720. Fragments of the

hygromycin cassette were identified on only two scaffolds (121 and 2306), both mapping adjacently on chromosome 12 of the reference *Chlamydomonas* genome assembly v5.0 available on Phytozome. The hygromycin cassette fragments were located at the extremity of both scaffolds, defining the insertion site in the genome of the M1 strain (supplemental data S1). This insertion was located inside the second exon of the Cre12.g496800 gene at position 393 from ATG (Fig. 6a). The inserted DNA was actually made of at least two consecutive cassettes. The first one, most likely functional, is almost complete with the 3' terminal region in reverse orientation and the second one, in opposite direction, is lacking the promoter region up to the first intron. The 3' ends of the two cassettes were not properly matching, leading to the conclusion that additional DNA is likely present in between. PCR amplifications were then performed. The amplification product using primers located in exon 1(AF-F) and exon 3 (AF-R) gave a fragment of the expected size (707 bp) in the reference *pgrl1* strain while no product was found in M1 probably because the fragment size is too long. In contrast, an amplification product of the expected size (490 bp) was found in M1 using AF-F and a primer specific of the cassette (R4), while no product was found in WT (Fig. 6b), which indicates that the M1 strain indeed possesses a cassette at the position indicated by NGS. RT-PCR confirmed the absence of expression of Cre12.g496800 in the M1 mutant (Fig. 6c).

To further ascertain our genome sequence analysis, the Illumina reads obtained for the mutant pool were mapped on the *Chlamydomonas* reference genome (v5.0 on Phytozome) together with 75bp paired-end reads obtained for the WT parental strain from the cross ($4A^+$, 80.2 Mio quality-filtered reads, ~48x coverage) and the recipient strain for transformation *pgrl1* (67.2 Mio quality-filtered reads, ~40x coverage) (Supplemental data S2). Each chromosome was then scanned to identify mutations (e.g. deletions or genomic reorganization) that would be specific to the pool of mutants and absent in the parents. A pattern specific to the pooled genome was detected in the region flanking the second exon of the Cre12.g496800 gene on chromosome 12, as visualized using the IGV genome browser (Supplemental data S2). For many reads, the paired reads are mapped on another chromosome, harbouring the RBCS2 gene used as promoter to express the hygromycin resistance gene in the mutagenic cassette, further establishing the presence of the hygromycin cassette in the Cre12.g496800 gene. This region was the only one that showed this specific pattern in the Hyg^R pool, and among the three sequenced strains, thus demonstrating again that this unique region was causative of default of assembly in complex I.

The Cre12.g496800 gene product, annotated in Phytozome v5.5 of the *Chlamydomonas* genome as “nuclear protein E3-3”, blasted with "1 alpha subcomplex assembly factor 3” of various organisms. “1 alpha subcomplex assembly factor 3” is an assembly factor of complex I also known as NDUFAF3 and functionally characterized in *H. sapiens* and *C. elegans* (Saada et al. 2009; van den Ecker et al. 2012). Fig. 7 shows the alignment of *Chlamydomonas* Cre12.g496800 gene product with NDUFAF3 (*H. sapiens*), NUAF3 (*C. elegans*) and assembly factors 3 from various organisms. This shows unambiguously that the Cre12.g496800 gene product is homologous to NDUFAF3. In good agreement with the nomenclature of previously annotated assembly factor (NUOAF1) of *Chlamydomonas*, we propose this protein to be named NUOAF3.

NDUFAF3 is found associated with an early Q module NUO10/NDUFS7/PSST, NUO8/NDUFS8/TYKY, NUO9/NDUFS3/30 kDa, NUO7/NDUFS2/49 kDa during assembly in humans (*Chlamydomonas*/human/bovine nomenclature) (Sánchez-Caballero et al. 2016b). We thus decided to check the impact of the loss of NUOAF3 on NUO7 and NUO8 subunits of the Q module by Western blotting (Fig. 6d). This analysis showed a decreased amount of these proteins. In contrast, the NUOS1 subunit of the N module (bovine 75 kDa subunit) did not seem to be affected by the NUOAF3 mutation. NUOS1 is part of a ± 200 kDa subcomplex that can be detected on BN-PAGE from isolated mitochondria in *C. reinhardtii* (Cardol et al. 2002) using NADH/NBT staining because this module retains NADH dehydrogenase activity. BN-PAGE on isolated mitochondria were thus performed and stained with NADH/NBT. The staining reveals the 200 kDa subcomplex to be present in equal amount in the *pgrl1* and *nuoaf3* strains (M1) (Fig. 5a). These results are in good agreement with the unaltered presence of NUOS1 in Western blot, since this protein is part of this subcomplex.

(5) Discussion

We here investigated the possibility to isolate respiratory complex I deficient mutants, in a *pgrl1* background, based on their altered chlorophyll fluorescence profile. The *pgrl1* mutant, deficient in photosynthetic cyclic electron flow (CEF), is able to grow normally in most conditions but has been shown to be unable to adapt its photosynthesis to compensate for a sudden inhibition of mitochondrial function upon addition of myxothiazol (complex III inhibitor) (Dang et al. 2014), meaning that chloroplastic activity is strictly dependent on mitochondrial

activity in this mutant. In this work, we showed that a complex I mutation can be associated with the *pgrl1* mutation leading to a decreased PSII efficiency and that such phenotype can be used to screen for complex I mutants. The decreased in PSII efficiency probably involves complex mechanisms relying on the interdependency between mitochondria and chloroplasts. A tentative explanation is proposed below. In *pgrl1/CI*- mutants, the entering flux of electrons from NADH in the respiratory chain is restricted to type-II NADH dehydrogenases (Lecler et al. 2012), which limits the rate of respiration coupled to ATP synthesis (Remacle et al. 2001). In addition to the lack of ATP from mitochondria, mutated cells cannot increase their chloroplastic ATP production due to the *pgrl1* mutation which causes altered CEF. This would lead to an excess of NADH in the mitochondria and a decreased ATP overall in the cell. The excess of NADH, unable to be consumed by the mitochondria, would be exported in the chloroplast where it could reduce the plastoquinone pool (Cardol et al. 2003). In addition, The ATP/NADPH equilibrium of 1.5 needed for Calvin cycle to work properly (Allen et al. 2002) would be disturbed and slowed by such an increased NADPH/ATP ratio, leading to an accumulation of NAPDH until Photosystem I acceptor (NADP) would be lacking, slowing down the whole photosynthesis. All of these disruptions would logically impact photosynthesis and thus reflect on ΦPSII measurements.

The ΦPSII parameter was chosen because it can be measured easily on colonies grown on agar plates by using an appropriate fluorescence imaging system (Johnson et al. 2009) while displaying sufficient differences between WT and double mutants. During our screening, we could isolate three complex I deficient strains out of the 3059 screened transformants. These three complex I mutants represent 0.13% of the total amount of transformants. This number is in good agreement and if not better than previous mutagenesis to obtain complex I mutants (Barbieri et al. 2011). Indeed, one complex I mutant is isolated out of 1000 in the present work compared to one out of 5000 transformants screened in the previous analysis.

Both the M3 mutant showing a complex genotype and the M3' mutant which is only defective for complex I activity showed a 25% decrease of NADH:FeCN activity. This decrease is not important enough to show any growth phenotype under heterotrophic conditions and could not be detected in BN-PAGE. But the M3 mutant could be easily detected using fluorescence measurements since the complex I deficiency is associated with the *pgrl1* mutation in this strain. These data suggest that our method is indeed able to detect leaky mutations where growth phenotype cannot be observed (Fig. 2c) and that the fluorescence screening protocol is more

sensitive than the previously heterotrophic growth dependent screening protocol. For such weakly affected mutants, the use of fluorescence to analyze segregation after crosses is compulsory.

The M2 mutant showed a decrease in respiratory complexes I, III, IV and V. Such respiratory phenotype is most likely close to the limit of what such "dual-mutation screening system" can produce. It is interesting to note that such mutant falls in the range of selected ΦPSII of interest, while already being a pleiotropic phenotype. This suggests that, as shown in Fig. 2b, the selection of transformants of interest should be limited to those whose ΦPSII is significantly lower than WT but higher than 0.2. Unfortunately, we could not go further in the analyses of neither the M2 mutant nor the M3 because the most affected mutant (M2) could not be crossed and the M3 mutant is not tagged.

The M1 strain showed a 70% decrease of assembly and activity of complex I compared to WT. As the mutation is tagged with the hygromycin cassette, we sequenced the whole genome a pool of meiotic products to identify the mutation. As the number of meiotic products in the sequenced pool was sufficient, all the differences between the individuals were equalized except for the insertion, which is responsible for complex I phenotype. Combining classical segregation analyses (Fig. 3a, Table 2) with this genomic approach thus unambiguously established that the complex I phenotype is caused by a single insertion located in the *NUOAF3* (Cre12.g496800) gene. NUOAF3 is homologous to NDUFAF3, which is proposed to act as an early stage assembly factor in human, involved in the stability of the Q module and/or the binding of the Q and P modules (Sánchez-Caballero et al. 2016). The assembly of the core subunits involves an early Q subcomplex of the matrix arm including NUO10/NUO8/NUO7/NUO9, assembling itself with the membrane associated ND1 subunit. This subcomplex would then assemble with a membrane ND3 (NUO3)/ND6/ND2/ND4L (NUO11) subcomplex, called the Pp module for 'proton translocating proximal module'. Later, the ND5/ND4 membrane proteins representing the Pd module for 'proton translocating distal module' would complete the assembly of the membrane arm. A hydrophilic NUO5/NUO6/NUOS1/ subcomplex (N module) would finalize the assembly of the matrix arm. Our results showed that similarly to humans, *Chlamydomonas* NUOAF3 would be required for the proper assembly of the Q module since its absence leads to the strong reduction of proteins such as NUO7 and NUO8 belonging to that module. This decrease in proteins from the Q module was shown to be directly caused by the loss of NUOAF3. Indeed

RNA blot was performed on *NUO8* and showed that the steady-state level of the transcript was not affected (Supplemental data S3). The decreased amount of NUO8 observed by Western blotting is thus likely due to the degradation of this subunit because of the Q module inability to assemble/stabilize itself. As NUO7 and NUO8 subunits are in reduced amounts but still detected, this suggests that *nuoaf3* mutants can still partially assemble the Q module and thus produce small amount of fully active complex I as shown by BN-PAGE, as it is also the case in humans (Saada et al. 2009). In contrast, the amount of the NUOS1 subunit belonging to the N module is not affected. The N module forms a free subcomplex before to be assemble with the others and is the last one to be assembled in humans (Sánchez-Caballero et al. 2016b). We could detect the N module in the *Chlamydomonas nuoaf3* mutant using NADH/NBT staining on BN-PAGE. The N module is also detected in other mutants affected in the Q module (RNAi-*NUO7* and RNAi-*NUO9* cell lines, Massoz et al. 2014), and in mutants affected in the P module (*nd4* and *nd5* mutants, Cardol et al. 2002; Cardol et al. 2008). These results suggest that the N module is also the last one to be assembled in *Chlamydomonas* like in humans. However, differences are probably present between the two organisms since NDUFAF3 has been showed to work in concert with another assembly factor named NDUFAF4 in humans while homologues to NDUFAF4 could not be found in the *Chlamydomonas* genome (Subrahmanian et al. 2016).

When looking at the pattern of coexpression of *NUOAF3* (Cre12.g496800) on Phytozome (https://phytozome.jgi.doe.gov), eight genes encoding complex I proteins were found with correlated expression > 0.85 (supplemental Table 1), belonging to the Q, the N or the P modules.

Overall, we here described a novel screening method for weakly affected respiratory mutants, specifically useful to get complex I mutants, where the *pgrl1* mutation acts as a revealing filter. This allowed identifying an assembly factor involved in complex I biogenesis and should greatly facilitate the discovery of the remaining assembly elements involved in complex I biogenesis.

(6) Material and methods

Strains

All strains are derived from the 137C strain from *Chlamydomonas* collection. The 4A mt+ strain (WT+) (Dent et al. 2005) was used as reference strain in all experiments. The *pgrl1* mutant (strain 1116 in our stock collection) was produced by crossing the original *pgrl1* paromomycin

resistant mutant (Tolleter et al. 2011, gift from Dr G. Peltier, CEA Cadarache) with the WT strain from our collection (collection number: 1'). A complex I *Δnd4* deficient mutant (strain 686) (Remacle et al. 2006) was crossed with *pgrl1* mutant (strain 1116) to produce the a *pgrl1/*Δ*nd4* double mutant (strain collection number 1128). Cells were cultivated on TAP medium at 50 $\mu E.M^{-2}.s^{-1}$. Double mutants were maintained at 30 $\mu E.m^{-2}.s^{-1}$.

Crosses

Zygotes were produced and matured during three days on nitrogen-free medium. Zygote germination was induced by transferring about 50 zygotes on fresh TAP medium at moderate light. Paromomycin and hygromycin resistance of meiotic products was assessed on TAP agar medium added with 25 $\mu g.\mu l^{-1}$ of hygromycine or 10 $\mu g.\mu l^{-1}$ of paromomycin. Fluorescence phenotype was assessed as described below.

Transformation

Cells were cultivated in a 12 hours dark – 12 hours light (50 $\mu E.m^{-2}.s^{-1}$) cycle three days prior to transformation and harvested at the start of the light cycle in order to avoid aggregates. Insertional mutagenesis on the *pgrl1* strain (1116) was performed as described in (Barbieri et al. 2011) using twice the amount of cells per transformation. Cells were electroporated in presence of 0.5 µg of 1.7 kb PCR product conferring resistance to hygromycin B (*APHVII* gene) and 1 µl of herring sperm (concentration: 10 $mg.ml^{-1}$). The *APHVII* gene includes the coding region for aminoglycoside phosphotransferase from *Streptomyces hygroscopicus* leading to the hygromycin B antibiotic resistance under the control of *C. reinhardtii* β2 tubulin promoter and 3' UTR of *RBCS2*. The *APHVII* gene also includes the first intron from *Chlamydomonas RBCS2* (Berthold et al. 2002). Transformants were selected in the light (40 $\mu E.\ m^{-2}s^{-1}$) on TAP agar medium supplemented with hygromycin B for a 2 to 3 weeks incubation period. Transformants were then transferred onto solid TAP agar medium prior to fluorescence analysis.

Molecular analyses

Total DNA was extracted using the procedure of (Newman et al. 1990). PCR amplifications were performed according standard protocols using Taq polymerase (Promega). Amplification of insertion-linked sequence by thermal asymmetric interlaced (TAIL)-PCR was performed as described previously (Dent et al. 2005) using AD1, AD2 (Liu et al. 1995), RMD227 and RMD228 (Dent et al. 2005) as non-specific primers. For *APHVII*, the specific primers for primary, secondary and tertiary reactions were respectively APH7-R3 (5'-

AGAATTCCTGGTCGTTC-CGCAG-3'), APH7-R4 (5'-TAGGAATCATCCGAATCAATACG-3'), and APH7-R5 (5'-CGGTCGAGAAGTAACAGGG-3') at the 5' and HygTerm1 (5'-CGCGAACTGCTCGCCTTCACCT-3'), HygTerm2 (5'-TCGAGGAGACCCCGCTGGATC-3'), and HygTerm3 (5'-CGATCCGGAG-GAACTGGCGCA-3') at the 3' end of the coding sequence of the cassette PCR products were sequenced by Beckman Coulter Genomics and aligned to the *Chlamydomonas* genome sequence database (v5.5 on Phytozome v11.0). RT-PCR analyses were performed according to standard protocols. AF-F (5'-TGCCGGGCTCTGTGTTGGTGTCG-3') and AF-R (5'-TGCGCGTCTGGCAGGTTCTCG-3') were used to produce and amplifiy NUOAF3 cDNA. P1Tub (5'-AACACCTTCTTCTCGGAGAC-3') and P2Tub (5'-GAGCTGAGCATGAAGTGGAT-3') were used to produce and amplify α tubulin cDNA.

Biophysical analyses

In vivo fluorescence measurements at room temperature on solid medium was performed using a fluorescence camera (Beambio, paradigm camera speedzen) (Johnson et al. 2009). Two parameters were calculated: the maximal quantum yield of PSII photochemistry [$F_V/F_M = (F_M - F_O)/F_M$] and the PSII quantum yield at a given light intensity [$\Phi PSII = (F_M' - F_S)/F_M'$] (Genty et al. 1989;Kitajima and Butler 1975). $rETR_{PSII}$ (photosystem II relative electron transport rate) at a given light intensity was obtained by multiplying ΦPSII by the photon flux of actinic light. Since this value does not take into account the proportion of absorbed light (depending on the PSII absorption cross-section), it represents a relative value. Green LEDs peaking at 532 nm were used as actinic light source. Compared to red or white light sources, green light is less absorbed and gives rise to a higher ΦPSII value for the same photon flux, which accounts for high values of $rETR_{PSII}$.

Growth analysis

Drop tests were performed on solid medium starting with cultures at Abs_{750}= 0.02 and Abs_{750}=0.05 cells densities for mixotrophic/phototrophic and heterotrophic conditions respectively. Plates were observed after 4 days in the light or 9 days in the dark. Growth analysis in liquid cultures was performed on 24 hours dark pre-incubated cultures. Growth analysis was then started on Abs_{750}=0.05 standardized cultures. Abs_{750} measurements were performed at 10 a.m. and 16 p.m. for three days and doubling time was determined.

Biochemical analyses

Crude membrane fractions were recovered by sonication (Remacle et al. 2001). Protein

amounts were determined using the Bradford assay method (Bradford 1976). NADH:ferricyanide activity, complex II+III and complex IV activities were measured as described (Remacle et al. 2001;Cardol et al. 2002). Blue-Native PolyAcrylamide Gel Electrophoresis (BN-PAGE) and the subsequent staining of the gel by NADH/NBT (nitroblue tetrazolium) or coomassie blue was done as previously published (Cardol et al. 2002). Western blots were performed using standard protocols. Antibodies against NUO8 (Genescript Piscataway, NJ), NUO7 (Genescript Piscataway, NJ) and NUOS1 (Genescript Piscataway, NJ) were used at 1/5000 dilution. Antibodies against AOX (gift from Dr S. Merchant, UCLA) we used at 1/25000 dilution.

Sequencing

The pool of hygromycin resistant (Hyg^R) meiotic products was obtained by crossing WT+ with the M1 mt- mutant. DNA of 50 Hyg^R meiotic products was individually extracted as described in (Blaby et al. 2013). DNA concentrations were then measured as previously described and DNAs pooled together in equal amount for sequencing. Genomic DNA library preparation (TruSeq DNA PCR-Free) and Illumina Sequencing (PE 2x75 on a NextSeq500 machine) were performed at the GIGA-R Sequencing platform (University of Liège) following manufacturer's protocol (Illumina Inc, San Diego CA, USA). Read quality was assessed using FastQC (v0.10.1) and quality trimming and removal of adapters was conducted using Trimmomatic (v0.32, (Bolger et al. 2014)) with the following parameters: trim bases with quality score lower than Q20 in 5' and 3' of reads; remove any reads with Q<20 in any sliding window of 10 bases; crop 3 bases in 3' of all reads, discard reads shorter than 72 bases and retain paired reads only. Overall quality filtering discarded between 13 and 18% of the raw reads. De novo assembly of the Hyg^R pool was obtained using Velvet (v1.2.10, (Zerbino and Birney 2008), with the following parameters: -clean yes -exp_cov 30 -cov_cutoff 0.316, to yield 20892 contigs (N50 = 25517 bp). The contigs were further scaffolded using all quality-filtered reads with SSPACE (v3.0, Boetzer et al. 2011), to yield 15364 scaffolds. For reference guided assembly, the Chlamydomonas reference genome v5.0 and corresponding gff annotation file were downloaded from the Phytozome FTP server on Sept 24, 2015. The reference genome was used to map quality-filtered reads of the Hyg^R pool, 4A+ and pgrl1 strains using bwa-mem algorithm (v0.7.12-r1039, Li and Durbin 2010) with default parameters. The resulting bam files were visualized and analyzed using IGV (Robinson et al. 2011).

Acknowledgements

Simon Massoz is recipient of F.R.I.A. (Fond de Recherche Industrielle et Agricole). M.H. and P.C. are Research Associates of the FNRS. Funding was provided by the ‘‘Fonds de la Recherche Scientifique–FNRS’’ (PDR-T.0206.13) (MH), (FRFC 2.4597, CDR J.0032, CDR J.0079 and Incentive Grant for Scientific Research F.4520) (PC), the University of Liège (SFRD-12/03) (MH), the European Research Council (H2020-EU BEAL project 682580) (PC).

Bibliography

Allen JF, Abrahams JP, Leslie AG, et al (2002) Photosynthesis of ATP—Electrons, Proton Pumps, Rotors, and Poise. Cell 110:273–276. doi: 10.1016/S0092-8674(02)00870-X

Barbieri R, Larosa V, Nouet C, et al (2011) A forward genetic screen identifies mutants deficient for mitochondrial complex I assembly in Chlamydomonas reinhardtii. Genetics 188:349–358. doi: 10.1534/genetics.111.128827

Berrisford JM, Baradaran R, Sazanov LA (2016) Structure of bacterial respiratory complex I. BBA - Bioenerg. doi: 10.1016/j.bbabio.2016.01.012

Berthold P, Schmitt R, Mages W (2002) Gene Mediates Dominant Resistance against Hygromycin B in Chlamydomonas reinhardtii. Protist 153:401–412.

Billoud B, Jouanno É, Nehr Z, et al (2015) Localization of causal locus in the genome of the brown macroalga Ectocarpus : NGS-based mapping and positional cloning approaches to which extent can current forward genetic approaches be profitable to macroalgal localisation of a mutant locus. 6:1–12. doi: 10.3389/fpls.2015.00068

Blaby IK, Glaesener AG, Mettler T, et al (2013) Systems-level analysis of nitrogen starvation-induced modifications of carbon metabolism in a Chlamydomonas reinhardtii starchless mutant. Plant Cell 25:4305–23. doi: 10.1105/tpc.113.117580

Boetzer M, Henkel C V., Jansen HJ, et al (2011) Scaffolding pre-assembled contigs using SSPACE. Bioinformatics 27:578–579. doi: 10.1093/bioinformatics/btq683

Bolger AM, Lohse M, Usadel B (2014) Trimmomatic: A flexible trimmer for Illumina sequence

data. Bioinformatics 30:2114–2120. doi: 10.1093/bioinformatics/btu170

Bradford MM (1976) A rapid and sensitive method for the quantitation of microgram quantities of protein utilizing the principle of protein-dye binding. Anal Biochem 72:248–254. doi: 10.1016/0003-2697(76)90527-3

Cardol P (2011) Mitochondrial NADH:Ubiquinone oxidoreductase (complex I) in eukaryotes: A highly conserved subunit composition highlighted by mining of protein databases. Biochim Biophys Acta - Bioenerg 1807:1390–1397. doi: 10.1016/j.bbabio.2011.06.015

Cardol P, Alric J, Girard-bascou J, Franck F (2009) Impaired respiration discloses the physiological significance of state transitions in Chlamydomonas. Proc Natl Acad Sci U S A 106:15979–15984.

Cardol P, Boutaffala L, Memmi S, et al (2008) In Chlamydomonas, the loss of ND5 subunit prevents the assembly of whole mitochondrial complex I and leads to the formation of a low abundant 700 kDa subcomplex. Biochim Biophys Acta - Bioenerg 1777:388–396. doi: 10.1016/j.bbabio.2008.01.001

Cardol P, Gloire G, Havaux M, et al (2003) Photosynthesis and State Transitions in Mitochondrial Mutants of Chlamydomonas reinhardtii Affected in Respiration. Plant Physiol 133:2010–2020. doi: 10.1104/pp.103.028076.transition

Cardol P, Lapaille M, Minet P, et al (2006) ND3 and ND4L subunits of mitochondrial complex I, both nucleus encoded in Chlamydomonas reinhardtii, are required for activity and assembly of the enzyme. Eukaryot Cell 5:1460–1467. doi: 10.1128/EC.00118-06

Cardol P, Matagne RF, Remacle C (2002) Impact of mutations affecting ND mitochondria-encoded subunits on the activity and assembly of complex I in chlamydomonas. Implication for the structural organization of the enzyme. J Mol Biol 319:1211–1221. doi: 10.1016/S0022-2836(02)00407-2

Cardol P, Vanrobaeys F, Devreese B, et al (2004) Higher plant-like subunit composition of mitochondrial complex I from Chlamydomonas reinhardtii: 31 Conserved components among eukaryotes. Biochim Biophys Acta - Bioenerg 1658:212–224. doi: 10.1016/j.bbabio.2004.06.001

Dang K, Plet J, Tolleter D, et al (2014) Combined increases in mitochondrial cooperation and oxygen photoreduction compensate for deficiency in cyclic electron flow in Chlamydomonas reinhardtii. Plant Cell 26:3036–3050. doi: 10.1105/tpc.114.126375

Dent RM, Haglund CM, Chin BL, et al (2005) Functional genomics of eukaryotic photosynthesis using insertional mutagenesis of Chlamydomonas reinhardtii 1. 137:545–556. doi: 10.1104/pp.104.055244.1

Genty B, Briantais J, Baker NR (1989) electron transport and quenching of chlorophyll fluorescence. Biochim Biophys Acta 990:87–92. doi: 10.1016/S0304-4165(89)80016-9

Giovannoni JJ, Wing R a, Ganal MW, Tanksley SD (1991) Isolation of molecular markers from specific chromosomal intervals using DNA pools from existing mapping populations. Nucleic Acids Res 19:6553–6558.

Hoefnagel MHN, Atkin OK, Wiskich JT (1998) Interdependence between chloroplasts and mitochondria in the light and the dark. Biochim Biophys Acta - Bioenerg 1366:235–255. doi: 10.1016/S0005-2728(98)00126-1

Hoefs SJG, van Spronsen FJ, Lenssen EWH, et al (2011) NDUFA10 mutations cause complex I deficiency in a patient with Leigh disease. Eur J Hum Genet 19:270–4. doi: 10.1038/ejhg.2010.204

Hummer G, Wikström M (2016) Molecular simulation and modeling of complex I. Biochim Biophys Acta - Bioenerg 1857: 915-921. doi: 10.1016/j.bbabio.2016.01.005

Johnson X, Vandystadt G, Bujaldon S, et al (2009) A new setup for in vivo fluorescence imaging of photosynthetic activity. Photosynthesis Res 102: 85–93. doi: 10.1007/s11120-009-9487-2

Kitajima M, Butler WL (1975) Quenching of chlorophyll fluorescence and primary photochemistry in chloroplasts by dibromothymoquinone. Biochim Biophys Acta 376:105–115.

Kmita K, Wirth C, Warnau J, et al (2015) Accessory NUMM (NDUFS6) subunit harbors a Zn-binding site and is essential for biogenesis of mitochondrial complex I. Proc Natl Acad Sci 112: 5685-5690. doi: 10.1073/pnas.1424353112

Lapaille M, Escobar-Ramirez A, Degand H, et al (2010) Atypical subunit composition of the chlorophycean mitochondrial F 1FO-ATP synthase and role of asa7 protein in stability and oligomycin resistance of the enzyme. Mol Biol Evol 27:1630–1644. doi: 10.1093/molbev/msq049

Lecler R, Cardol P, Remacle C, Barbare E (2012) Characterization of an internal type-II NADH dehydrogenase from Chlamydomonas reinhardtii mitochondria. Curr Genet 58:205–216. doi: 10.1007/s00294-012-0378-2

Letts JA, Sazanov LA (2015) Gaining mass: The structure of respiratory complex I-from bacterial towards mitochondrial versions. Curr Opin Struct Biol 33:135–145. doi: 10.1016/j.sbi.2015.08.008

Li H, Durbin R (2010) Fast and accurate long-read alignment with Burrows-Wheeler transform. Bioinformatics 26:589–595. doi: 10.1093/bioinformatics/btp698

Liu YG, Mitsukawa N, Oosumi T, Whittier RF (1995) Efficient isolation and mapping of Arabidopsis thaliana T-DNA insert junctions by thermal asymmetric interlaced PCR. Plant J 8:457–63.

Massoz S, Larosa V, Horrion B, et al (2015) Isolation of Chlamydomonas reinhardtii mutants with altered mitochondrial respiration by chlorophyll fluorescence measurement. J Biotechnol 215:27-34. doi: 10.1016/j.jbiotec.2015.05.009

Massoz S, Larosa V, Plancke C, et al (2014) Inactivation of genes coding for mitochondrial Nd7 and Nd9 complex I subunits in Chlamydomonas reinhardtii. Impact of complex I loss on respiration and energetic metabolism. Mitochondrion 19:365–374. doi: 10.1016/j.mito.2013.11.004

Merchant SS, Prochnik SE, Vallon O, et al (2007) The Chlamydomonas genome reveals the evolution of key animal and plant functions. Science (80-) 318:245–252.

Michelmore RW, Paran I, Kesseli R V (1991) Identification of markers linked to disease-resistance genes by bulked segregant analysis - a rapid method to detect markers in specific genomic regions by using segregating populations. Proc Natl Acad Sci U S A 88:9828–9832. doi: 10.1073/pnas.88.21.9828

Mitchell P (1961) Coupling of phosphorylation to electron and hydrogen transfer by chemi-osmotic type of mechanism. Nature 191:144–148.

Newman SM, Boynton JE, Gillham NW, et al (1990) Transformation of chloroplast ribosomal RNA genes in Chlamydomonas: Molecular and genetic characterization of integration events. Genetics 126:875–888.

Rak M, Rustin P (2014) Supernumerary subunits NDUFA3, NDUFA5 and NDUFA12 are required for the formation of the extramembrane arm of human mitochondrial complex I. FEBS Lett 588:1832–1838. doi: 10.1016/j.febslet.2014.03.046

Remacle C, Baurain D, Cardol P, Matagne F (2001) Mutants of Chlamydomonas reinhardtii deficient in mitochondrial complex I : characterization of two mutations affecting the nd1

coding sequence. Genetics 158:1051–1060.

Remacle C, Cardol P, Coosemans N, et al (2006) High-efficiency biolistic transformation of Chlamydomonas mitochondria can be used to insert mutations in complex I genes. Proc Natl Acad Sci U S A 103:4771–6. doi: 10.1073/pnas.0509501103

Robinson JT, Thorvaldsdóttir, Helga Winckler W, Guttman M, et al (2011) Integrative Genomics Viewer. Nat Biotechnol 29:24–26. doi: 10.1038/nbt.1754.Integrative

Saada A, Vogel RO, Hoefs SJ, et al (2009) Mutations in NDUFAF3 (C3ORF60), Encoding an NDUFAF4 (C6ORF66)-Interacting Complex I Assembly Protein, Cause Fatal Neonatal Mitochondrial Disease. Am J Hum Genet 84:718–727. doi: 10.1016/j.ajhg.2009.04.020

Salinas T, Larosa V, Cardol P, et al (2014) Respiratory deficient mutants of the unicellular green alga Chlamydomonas : A review. Biochimie 100:207–218. doi: 10.1016/j.biochi.2013.10.006

Sánchez-Caballero L, Guerrero-Castillo S, Nijtmans L (2016) Unraveling the complexity of mitochondrial complex I assembly; a dynamic process. Biochim Biophys Acta - Bioenerg 1857:980-990. doi: 10.1016/j.bbabio.2016.03.031

Schimmeyer J, Bock R, Meyer EH (2016) l-Galactono-1,4-lactone dehydrogenase is an assembly factor of the membrane arm of mitochondrial complex I in Arabidopsis. Plant Mol Biol 90:117–126. doi: 10.1007/s11103-015-0400-4

Sheftel AD, Stehling O, Pierik AJ, et al (2009) Human ind1, an iron-sulfur cluster assembly factor for respiratory complex I. Mol Cell Biol 29:6059–6073. doi: 10.1128/MCB.00817-09

Stroud D a., Formosa LE, Wijeyeratne XW, et al (2013) Gene knockout using transcription activator-like effector nucleases (TALENs) reveals that human ndufa9 protein is essential for stabilizing the junction between membrane and matrix arms of complex I. J Biol Chem 288:1685–1690. doi: 10.1074/jbc.C112.436766

Subrahmanian N, Remacle C, Hamel PP (2016) Plant mitochondrial complex I composition and assembly: a review. BBA - Bioenerg 1857:1001-1014. doi: 10.1016/j.bbabio.2016.01.009

Szklarczyk R, Wanschers BFJ, Nabuurs SB, et al (2011) NDUFB7 and NDUFA8 are located at the intermembrane surface of complex I. FEBS Lett 585:737–743. doi: 10.1016/j.febslet.2011.01.046

Terashima M, Specht M, Naumann B, Hippler M (2010) Characterizing the anaerobic response of Chlamydomonas reinhardtii by quantitative proteomics. Mol Cell Proteomics 9:1514–1532.

doi: 10.1074/mcp.M900421-MCP200

Tolleter D, Reiter IM, Genty B, et al (2011) Control of hydrogen photoproduction by the proton gradient generated by cyclic electron flow in Chlamydomonas reinhardtii. Plant Cell 23:2619–2630. doi: 10.1105/tpc.111.086876

van den Ecker D, van den Brand MA, Ariaans G, et al (2012) Identification and functional analysis of mitochondrial complex I assembly factor homologues in C. elegans. Mitochondrion 12:399–405. doi: 10.1016/j.mito.2012.01.003

Vinothkumar KR, Zhu J, Hirst J (2014) Architecture of mammalian respiratory complex I. Nature 515:80–84. doi: 10.1038/nature13686.

Wydro MM, Sharma P, Foster JM, et al (2013) The evolutionarily conserved iron-sulfur protein INDH is required for complex I assembly and mitochondrial translation in Arabidopsis [corrected]. Plant Cell 25:4014–27. doi: 10.1105/tpc.113.117283

Zerbino DR, Birney E (2008) Velvet: Algorithms for de novo short read assembly using de Bruijn graphs. Genome Res 18:821–829. doi: 10.1101/gr.074492.107

Zickermann V, Wirth C, Nasiri H, et al (2015) Mechanistic insight from the crystal structure of mitochondrial complex I. 5:4–10.

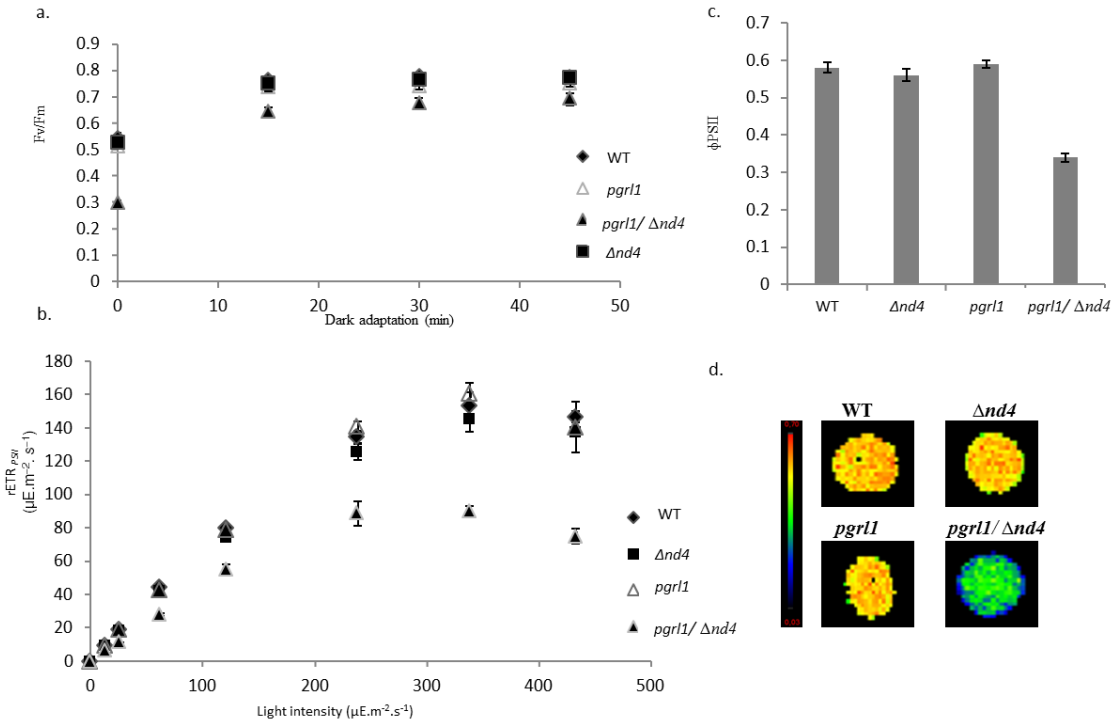

Figure 1. Photosynthetic parameters of light-grown wild-type (black diamond), *Δnd4* (black square), *pgrl1* mutant (empty triangle) and *pgrl1*/Δ*nd4* double mutant (black triangle). Fluorescence measurements were performed on agar plates using a fluorescence camera (Beambio, paradigm camera speedzen). (a) Evolution of the Fv/Fm parameter during dark adaptation. (b) Photosystem II apparent electron transfer rate ($rETR_{PSII}$, $\mu E.m^{-2}.s^{-1}$) as a function of the light intensity. Strains were adapted three minutes at every light intensity. (c) ΦPSII parameter value after 3 minutes acclimation at 240 $\mu E.m^{-2}.s^{-1}$. (d) ΦPSII parameter fluorescence images in false color. ΦPSII scale from 0.7 (red) to 0.03 (blue). ΦPSII were measured after 3 minutes light acclimation at 240 $\mu E.m^{-2}.s^{-1}$.

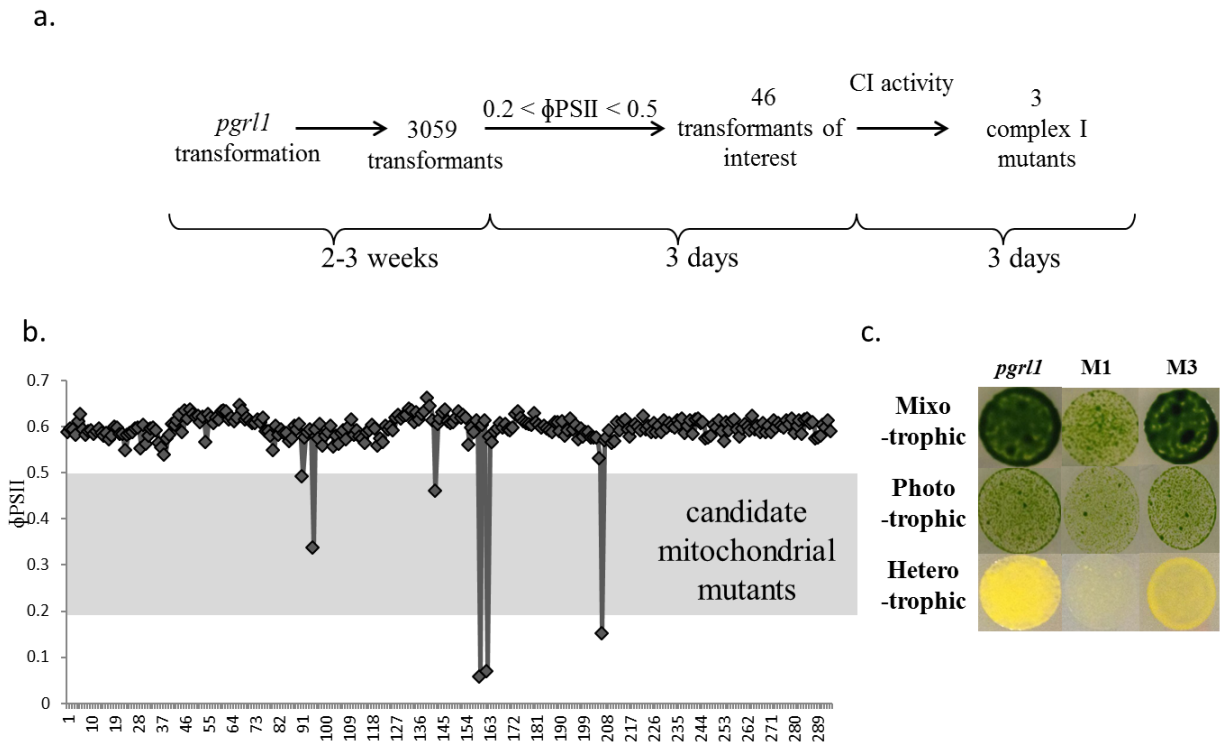

Figure 2. Transformation results. (a) Timeframe of the screening strategy. Time needed for each step represented in accolade (bottom) (b) ΦPSII parameters for 300 transformants on *pgrl1* background. Candidate mitochondrial mutants are selected on the basis of a ΦPSII between 0.2 and 0.5. (c) Growth phenotype of the *pgrl1* strain, the M1 and the M3 mutants. Cells cultivated in mixotrophic conditions (TAP medium; 40 µE.m^{-2}.s^{-1}) and phototrophic conditions (TMP medium; 40 µE.m^{-2}.s^{-1}) were grown for three days. Cells cultivated in heterotrophic conditions (TAP medium) were grown for nine days. 30 µl of a 4.10^5 cells per ml culture were used as starting point for all conditions.

strains	ΦPSII	complex I activity	complexes II+III activity	complex IV activity
pgrl1	0.58±0.014	3256±81	83±2	593±18
pgrl1/Δnd4	0.34±0.012	487±50	122±2.3	681±17
M1	0.38±0.011	1107±95	115±1.7	575±10
M2	0.26±0.01	810±190	70±10	264±4
M3	0.47±0.014	2236±32	102±1	700±45

Table 1. Photosynthetic parameters and mitochondrial complexes activities. Complex I activity in nmoles of $K_3Fe(CN)_6^{3-}$ reduced.min^{-1}.mg protein^{-1}; complexes II+III activity in nmoles of cytochrome *c* reduced.min^{-1}.mg protein^{-1}; complex IV activity in nmoles of cytochrome *c* oxidized.min^{-1}.mg protein^{-1}. Photosynthetic ΦPSII parameters were obtained for a light intensity of 240 µE.m^{-2}.s^{-1}.

strains	number of meiotic products	Hyg^R	Pm^R/Hyg^R	ΦPSII phenotype among Pm^R/Hyg^R
M1	450	50%	10%	100%
M3	200	63%	24%	46%

Table 2. Segregation analysis from the crosses between the M1 mt- and M3 mt- transformants and WT+ strain. ΦPSII phenotype was measured at 240 $\mu E.m^{-2}.s^{-1}$.

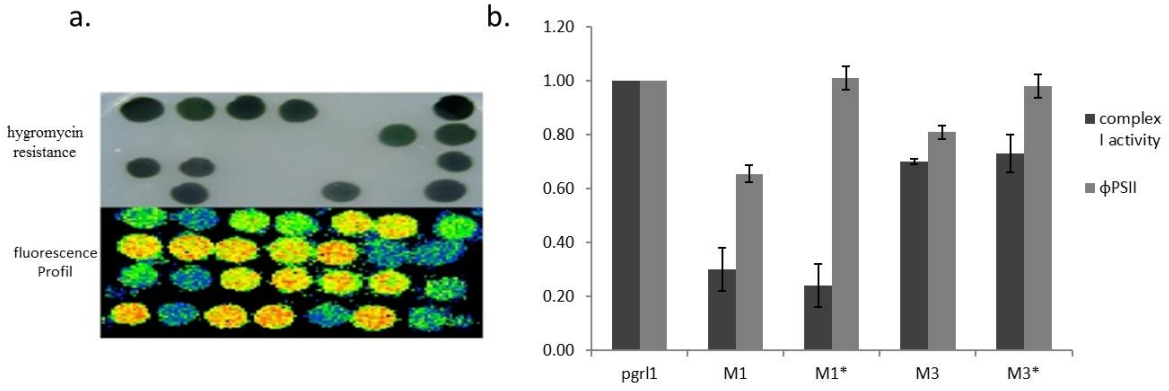

Figure 3. Cosegregation analysis. (a) Cosegregation between Hyg^R descendants (top) and the fluorescence phenotype of altered ΦPSII measured at 240 $\mu E.m^{-2}.s^{-1}$ (bottom). Cells were cultivated for three days under moderate light conditions (50 $\mu E.m^{-2}.s^{-1}$). Yellow: WT type photosynthetic parameters, Blue: reduced photosynthetic parameters. (b) Black: complex I activity (NADH:Ferricyanide oxidoreductase activity, nmoles of $K_3Fe(CN)_6^{3-}$ reduced.min^{-1}.mg $protein^{-1}$) and ΦPSII (dark grey) in a *pgrl1* strain, the M1 mutant, a M1* mutant (M1 mutant without *pgrl1* mutation), the M3 mutants and a M3* mutant (M3 mutant without *pgrl1* mutation). Activities and ΦPSII were normalized on *pgrl1* recipient strain values.

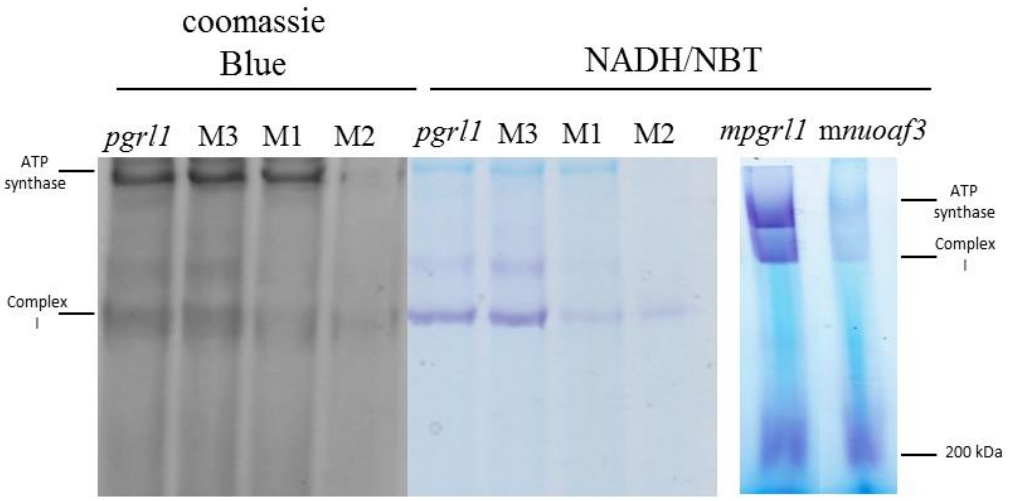

Figure 4. Analysis of complex I activity and assembly. 100 µg of crude membrane proteins solubilized by Triton X-100 (2%) were loaded on a BN-PAGE. After electrophoresis, the gel was submitted to NADH/NBT staining or coomassie blue staining (left). (right) 100 µg of mitochondria enriched protein extracts were solubilized by n-dodecyl maltoside (1%) and loaded on BN-PAGE for the *pgrl1 (mpgrl1)* and M1 (m*nuoaf3*) strains.

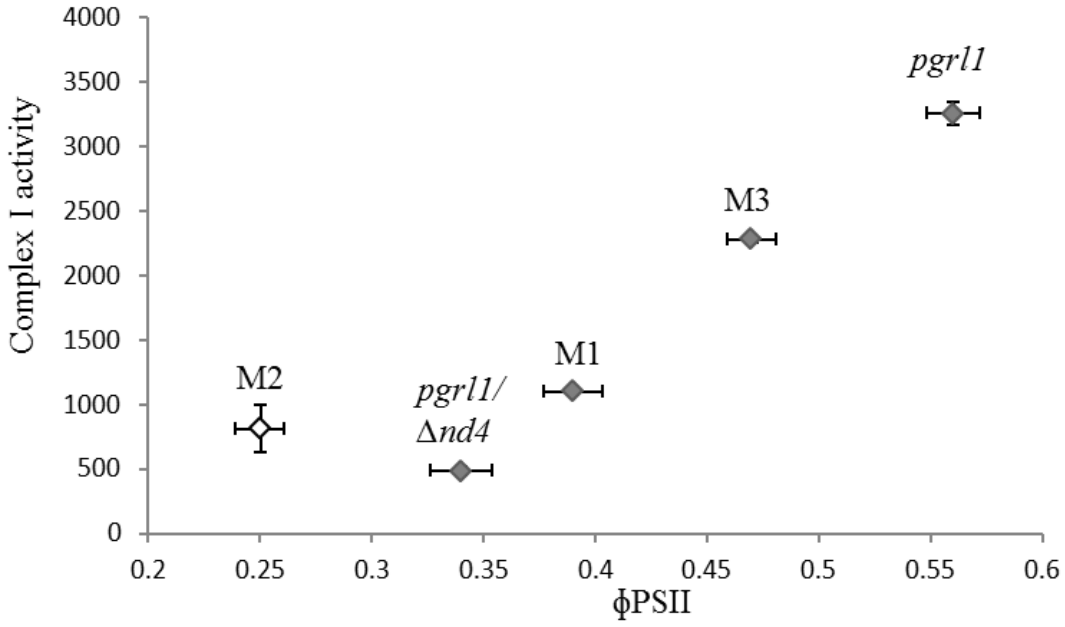

Figure 5. Relationship between ΦPSII parameter and NADH:ferricyanide oxidoreductase activity (nmoles of $K_3Fe(CN)_6^{3-}$ reduced·min^{-1}·mg $protein^{-1}$).

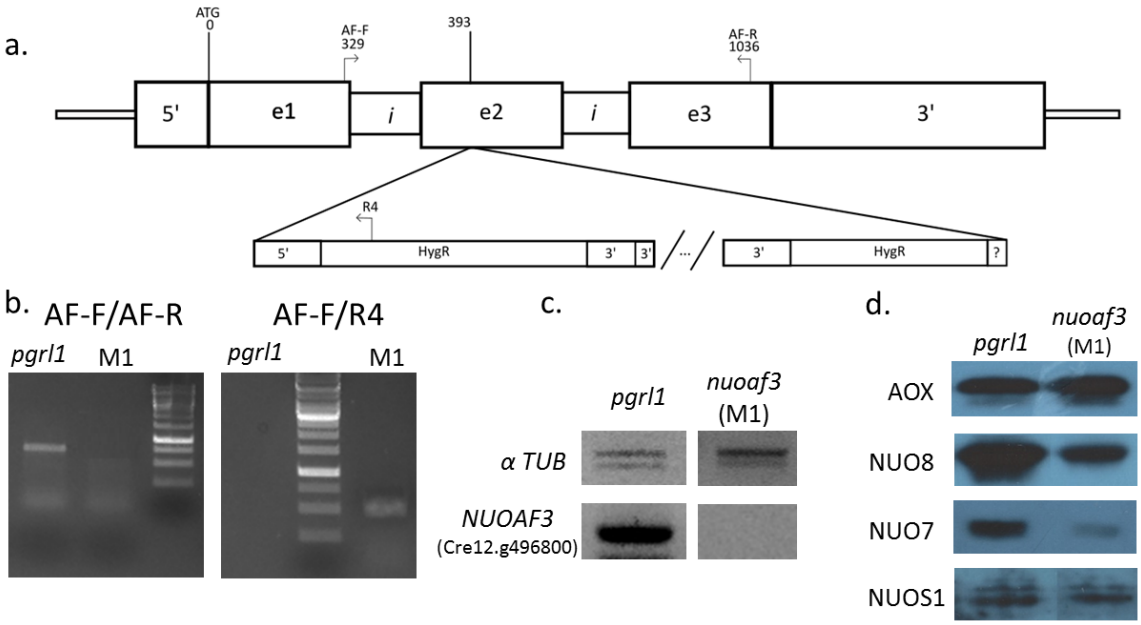

Figure 6. Molecular characterization of the insertion in the M1 mutant (*nuoaf3*). (a) Schematic representation of the Hyg^R cassettes insertion in the *nuoaf3* (M1) mutant. Numbers refer to bases relative to the initiation site of translation. (b) PCR confirmation of the insertion based on primers as described in (a). Fermentas 1kb was used as DNA ladder (c) RT-PCR analysis using primers binding α tubulin (size:662bp) and *NUOAF3* (size:330 bp) cDNAs. α tubulin is used as control (d) Western blot analysis on total proteins extracts using antisera against NUO8, NUO7, NUOS1 (lower band) and AOX.

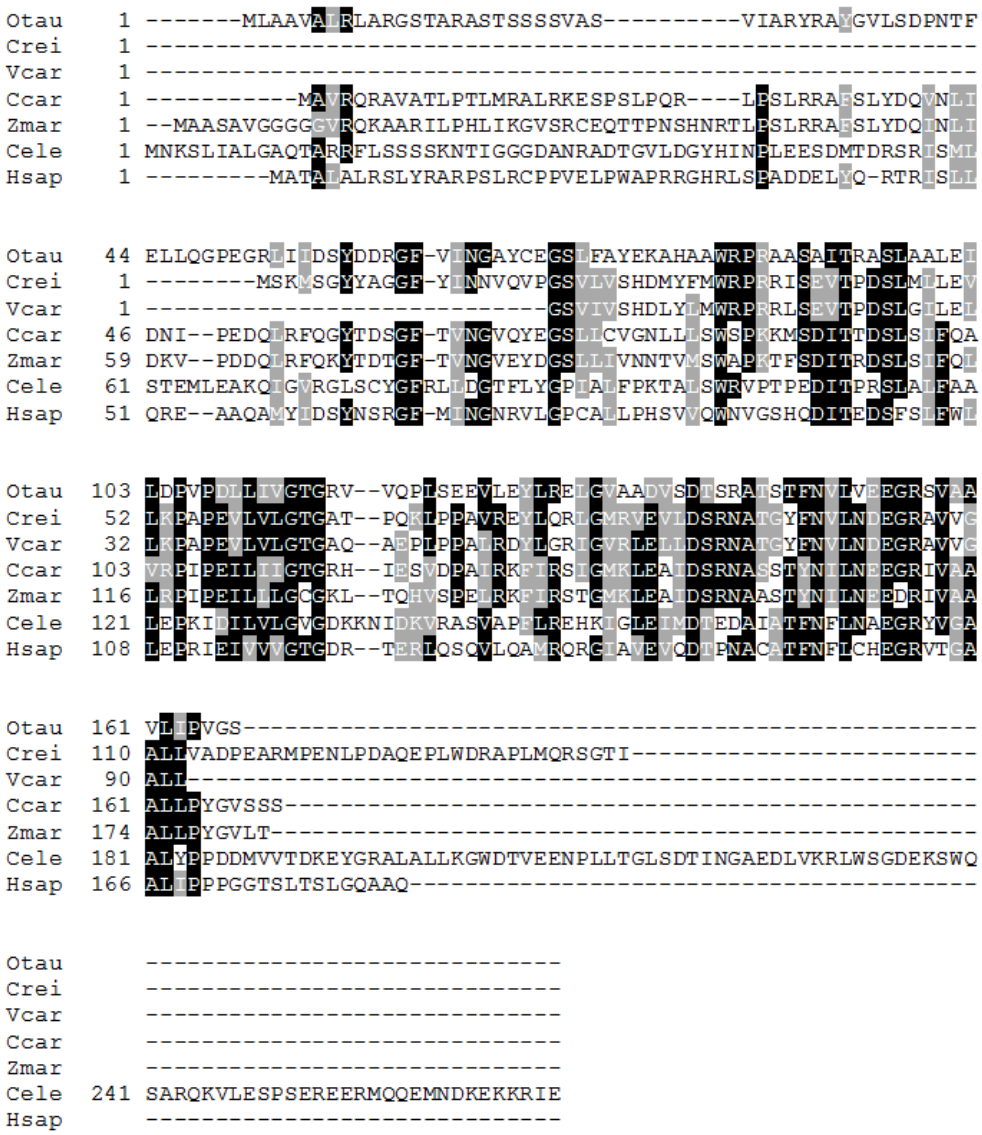

Figure 7. Sequences alignment for 1 alpha subcomplex assembly factor 3 of different organisms. Otau: *Ostreococcus tauri*, Crei: *Chlamydomonas reinhardtii* (NUOAF3), Hsap: *Homo sapiens* (NDUFAF3), Zmar: *Zostera marina*, Cele: *Caenorhabditis elegans*, Ccar: *Cynara cardunculus*, Vcar : *Volvox carteri* (partial).

Supplemental Data

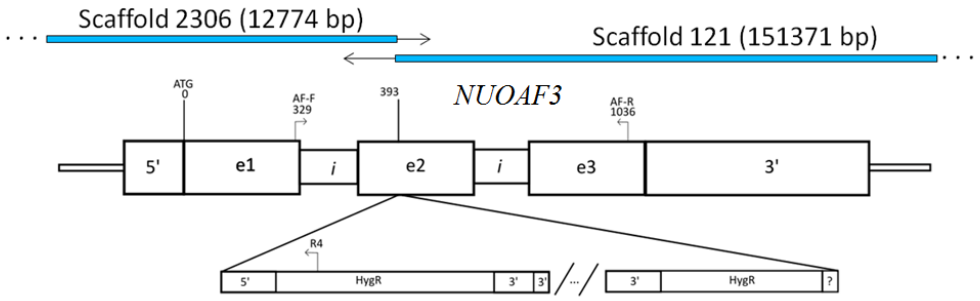

Supplemental data S1: Location and matching of the 2 scaffolds containing the hygromycin cassette sequences. Blue: Scaffold that could be aligned on the reference genome. Thin black: sequence of the scaffold that could be aligned on hygromycin cassette. Arrows give the orientation.

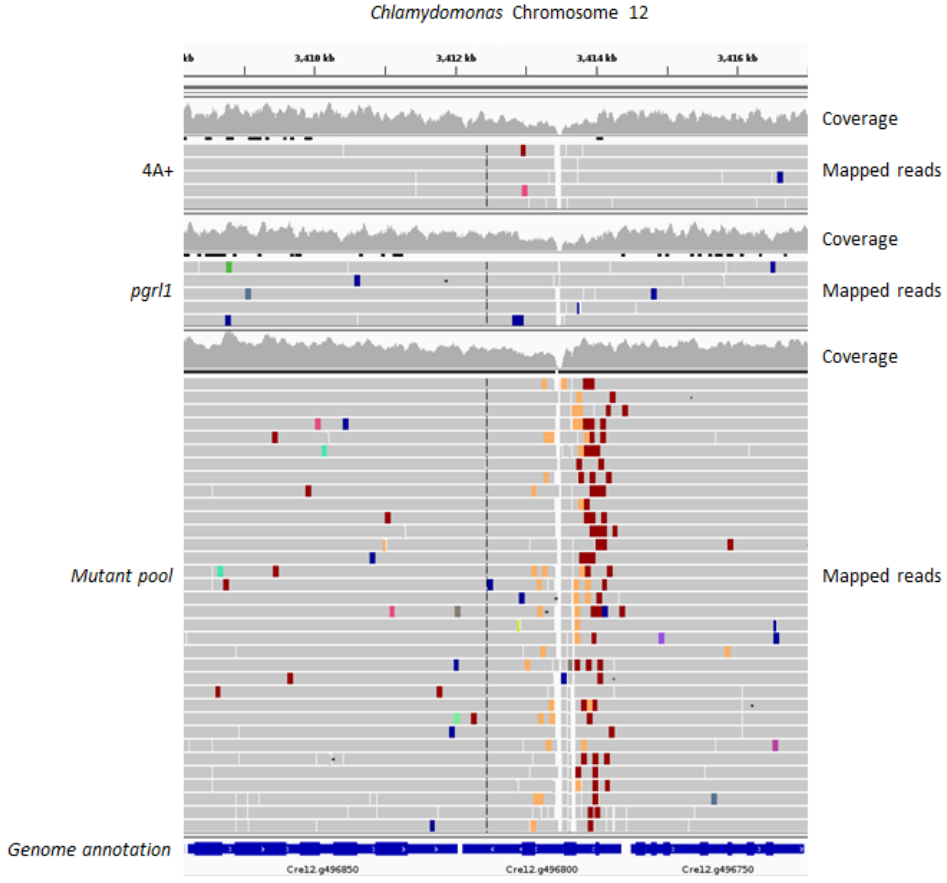

Supplemental data S2: Screenshot of read mapping for 4A+ (WT), *pgrl1* and mutant pool (M1) on the chromosome 12 of the *Chlamydomonas* v5.5 genome visualized in the IGV genome browser. Reads highlighted in orange and dark red in the mutant pool delineate the hygromycin cassette insertion site.

Supplemental Table 1

complex I genes coexpressed with *NUOAF3*	Co-expression coefficient
Cre13.g584700 - NDUFAF7 homolog	0.9
Cre09.g405850 - NUO7 - Q module	0.895
Cre12.g555150 - NUOB10 - P module	0.891
Cre08.g378550 - NUOP4 - ?	0.89
Cre12.g535950 - NUOS1 - N module	0.881
Cre05.g240800 - NUO17 - P module	0.868
Cre10.g422600 - NUO6 - N module	0.858
Cre03.g204650 - NUOB4 - P module	0.85

Supplemental Table 1: Co-expression genes pattern for *NUOAF3* for a co-expression coefficient above 0.85. Only genes identified as complex I component or assembly factor are displayed. Data retrieved from phytozome (http://phytozome.jgi.doe.gov/).

Supplemental data S3

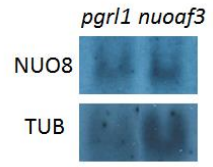

Supplemental data S3: RNA blot using probes against *NUO8* and alpha tubulin for the *pgrl1* and *nuoaf3* mutant. 15µg of total RNA were loaded.

SUPPLEMENTAL RESULTS

4. Supplemental results to publication 3

Molecular characterization of M1, M2 and M3 mutants

In order to identify the molecular lesion putatively responsible for the phenotype of the 3 double mutants (M1, M2 and M3), flanking DNA was tentatively amplified using thermal asymmetric interlaced (TAIL)-PCR (Dent et al. 2005) (Supplemental data S1). PCR products could be amplified for each strain, but the flanking sequences could only be identified for two strains, M2 and M3. Insertions in a pheophorin and in an ABC transporter could be identified in the M2 strain, giving out at least 2 insertions in its genome. Pherophorins are part of a membrane protein family and some of them are involved in the mating process. This insertion might explain why the M2 strain could not be crossed. A single insertion was detected in the M3 strain in a Serine/Threonine Kinase using primers located at the 3' end of the hygromycin cassette. This insertion was shown not to segregate with Hyg^R by PCR analysis (supplemental data S2). In addition, mutants possessing complex I deficiency without Hyg^R and without an insertion in the kinase gene could be identified, showing that the kinase gene loss wasn't responsible for the complex I deficiency observed initially.

Strains	5' flanking sequence		3' flanking sequence	
	Phytozome localisation	Candidate protein	Phytozome localisation	Candidate protein
M1	n.a	n.a	u.	u.
M2	Cre12.g546800 (Prom:8641501)	Pheophorin (XP_001693968)	Cre17.g717050 (I:2605844)	ABC transporter (XP_001690733)
M3	n.a	n.a	Cre01.g046052 (3U:6478012)	Serine/Threonine kinase (XP_001689730)

Supplemental data S1: Genomic localization of the flanking sequence obtained by TAIL PCR based on locus names and genomic position from http://phytozome.jgi.doe.gov/; I, Intron; 3U, 3'UTR; Prom, promoter region; n.a, no data available; u, TAIL-PCR fragment could be obtained but the flanking region could not be identified.

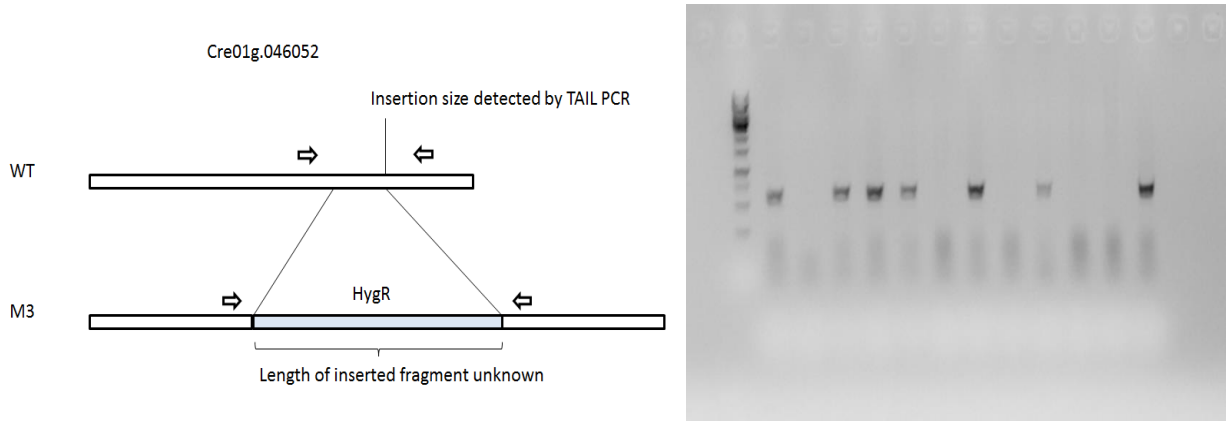

Supplemental data S2: **Left**: scheme of the protocols used for the identification of the insertion in the Cre01g.046052 gene. Primers (arrows) for a region before and after the detected insertion site were designed and PCR amplification was perfomed. If the gene is WT, normal PCR amplification can be performed. If a cassette is inserted, the fragment will be too long for normal PCR amplification and thus cannot be amplified. **Right**: Identification of the presence of absence of the insertion in the Cre01g.046052 (kinase) in various Hyg^R/Pm^R displaying a fluorescence phenotype (and thus, complex I deficient). The different clones were produced by crossing the M3 mt- mutant with 4A+ WT strain. Presence of a amplification product means a WT version of the kinase gene, absence of the product means the presence of a Hyg^R cassette inside the kinase gene.

CONCLUSIONS

5. Conclusion

Isolation of complex I mutants in *C. reinhardtii* is a fruitful way to understand more about complex I function and assembly. Complex I mutants survive under mixotrophic (acetate + light) conditions, while displaying reduced growth under heterotrophic (acetate + dark) conditions (Salinas et al. 2014). The slow growth in the dark has been used to screen complex I mutants during the last 15 years (Remacle et al. 2001; Cardol et al. 2002; Barbieri et al. 2011). Nevertheless, this screening method presents several flaws (i) a long incubation time before the dark growth phenotype can be analyzed (ii) extra effort due to the necessity to transfer potential mutants from solid to liquid culture in order to analyze their growth phenotype using drop tests (iii) relative imprecision of the method because complex I mutants still sustain growth in the dark, leading to the detection of mainly null or very affected complex I mutants.

Structural subunits of complex I are for the most part well known in the main reference organisms (fungi, mammals and land plants) including *C. reinhardtii*, though the exact role of most supernumerary subunits remains to be elucidated. But complex I assembly factors remain for the major part unidentified. Mutations in these assembly factors and probably in some supernumerary subunits are likely to cause only partial complex I deficiencies, which cannot be easily detected using the dark growth screening method previously used. Hence developing a novel screening method to improve the detection of complex I mutants, especially in regard to random mutagenesis experiments, would be one of the first requirements if one wants to discover such mutants.

Idea behind the fluorescence screening

Photosynthetic fluorescence measurements, more specifically PSII chlorophyll fluorescence measurements, are an interesting tool to quickly determinate photosynthesis efficiency. PSII fluorescence is linked to the redox status of the PQ available for PSII electron transfer. If electrons can be transferred from Q_A to Q_B properly, then no fluorescence is emitted; if no oxidized plastoquinones are available for electron transport, the excited electrons in PSII will relax their energy as fluorescence. PSII fluorescence measurements thus reflect the ability for electron transfer from PSII to the rest of the electron transport chain and thus give the

photosynthesis efficiency. Mitochondria and chloroplast energetic and redox components are linked together. NADH can be exported from the chloroplast to be consumed inside the mitochondria to produce ATP. The later can then be exported outside the mitochondria. It is known that mitochondrial defects affect photosynthesis, and vice versa, notably by contributing to reduce the PQ pool in the chloroplast (Cardol et al. 2003). This has been shown to lead to adaptations of the photosynthetic apparatus, notably an increased in state transition toward state 2. Such shift decreases the reduction rate of PQ by PSII, but also favors the formation of the CEF supercomplexes, leading to an increased ATP production that could help compensate the diminished ATP production in mitochondria (Minagawa and Tokutsu 2015). In addition, photosynthesis deprived from its regulatory mechanisms showed great dependency on increased mitochondria activity (Dang et al. 2014). From this, has come the idea to use photosynthesis, whose defect might reflect mitochondrial dysfunctions given the right conditions, to screen for complex I mutations. Chlorophyll fluorescence would represent an ideal parameter to use for screening since specific numerical data can be extracted, the opposite of the subjectivity of discriminating the presence or absence of dark growth phenotype such as previously performed.

Modular assembly of complex I

During this work, four types of complex I mutants were studied. The *amc14* partially deficient for NUO9, RNAi-*NUO9* and RNAi-*NUO7* cell lines, and *nuoaf3*, a mutant deficient for the NUOAF3 (NDUFAF3 homolog) assembly factor. All these proteins are involved in the constitution (Subrahmanian et al. 2016) or assembly (Saada et al. 2009) of the Q module of complex I. The Q module of complex I is the first to be assembled during biogenesis (Sánchez-Caballero et al. 2016). As a result, removal of NUO9 or NUO7 leads to a complete deficiency of complex I assembly. Analysis on the *amc14* mutant showed that the amount of NUO9 limits the amount of complex I that can be assembled. *nuoaf3* could still assemble a slight amount of complex I, consistent with the identical phenotype that was observed for with the loss of NUOAF3 homolog in humans (Saada et al. 2009). While the Q module is lacking, some subcomplexes are produced independently during complex I assembly. The N module is one example. It is a 200 kDa subcomplex, that can be depleted without affecting the rest of complex I

assembly in humans (in NDUFV1 mutant ;Ogilvie et al. 2005) and can be found alone in some assembly deficiency mutants in human cell lines (Guarani et al. 2014). It is proposed to be one of the last subcomplexes to be added during assembly. In all our four mutants, we searched for the presence of the N module either by immunoblotting or in BN-PAGE analysis, taking advantage of its "NADH-NBT activity" staining properties in gel. In all four mutants, the N module could be found, indicating that, similarly to humans, this module could assemble itself on its own. It is interesting to note that the N module could be found in unaffected amount in partially deficient complex I (*amc14* and *nuoaf3*) mutants. This might be a hint to a greater stability on this specific subcomplexe (unlike, for example, ND1 containing subcomplex whose stability relies on being assembled to the rest of complex I (Zurita Rendón and Shoubridge 2012). A stable, protected from degradation, N module would be expected if, like in humans, it was one of the last part of complex I to be assembled, while probably being produced at the same time as other subcomplexes. It would be interesting to look for the presence of a P_P or (P_P +P_d) subcomplex in these mutants, but no detection protocols do exist currently in *Chlamydomonas*.

Our results regarding the *nuoaf3* mutant show that this assembly factor is important but not essential for complex I assembly, since the mutant can still assemble some fraction of complex I. This most likely means that other assembly factors probably participate in similar function during assembly. Depending on which role is predominant for NUOAF3, stabilization of Q module or interaction with ND1 containing subcomplex (Sánchez-Caballero et al. 2016) TIMMDC1 might be a good candidate that might suffice on its own to assemble the Q module with ND1 when NUOAF3 isn't functional (Guarani et al. 2014).

Final words

The main organisms to study eukaryotic complex I are fungi (*Yarrowia lypolytica* and *Neurospora crassa*) and mammals, where well defined experiments to study complex I are established. In current regards to the improvements for the screening of complex I mutants in *C. reinhardtii* described in this work, I believe we have now made enough progress for *Chlamydomonas* to be set on equal footing as a model organism for complex I assembly study in plants and to some extends, as a general model organism since our screening method allows for detection of minor deficiencies such as those found in assembly factors. However biochemistry

of complex I is difficult to handle in *Chlamydomonas* and will need improvements to truly compete with other models organisms, specifically in subcomplexes detection. One could imagine to flag a complex I subunit with an His-tag that could make the isolation of purified complex I and subcomplexes bearing this subunit easier as it has been made in *Y. lipolytica* (Kerscher et al. 2002). Subsequent proteomics could allow defining subunit composition of these (sub)complexes. This is technically possible by transforming a mutant inactivated in a nuclear subunit (I.e. NUOB10, Barbieri et al. 2011) or a mitochondrial mutant (such as one affected in nd4, *Δnd4* mutant used in this study) with a wild type copy of the gene bearing a His-tag and isolating His-tag transformants with restored complex I activity. The detection of subcomplexes on BN-PAGE is also a challenge. However using appropriate antibodies already existing such as those against the NUO7, NUO9, NUOS1 subunitd, we could detect some of the subcomplexes by immunodetection directly on BN-PAGE. Development of novel antibodies against membrane arm related subunits, such as carbonic anhydrase subunits, could also help to track the P module sub-assembly process. All of this would allow for accurate complex I assembly and subcomplexes studies in *Chlamydomonas reinhardtii* for the future.

BIBLIOGRAPHY

5. Bibliography

Allegretti M, Klusch N, Mills DJ, et al (2015) Horizontal membrane-intrinsic α-helices in the stator a-subunit of an F-type ATP synthase. Nature 521:237–40. doi: 10.1038/nature14185

Allen JF, Abrahams JP, Leslie AG, et al (2002) Photosynthesis of ATP—Electrons, Proton Pumps, Rotors, and Poise. Cell 110:273–276. doi: 10.1016/S0092-8674(02)00870-X

Allen JF, Bennett J, Steinback KE, Arntzen CJ (1981) Chloroplast protein phosphorylation couples plastoquinone redox state to distribution of excitation energy between photosystems. Nature 291:25–29. doi: 10.1038/291025a0

Allen JWA, Jackson AP, Rigden DJ, et al (2008) Order within a mosaic distribution of mitochondrial c-type cytochrome biogenesis systems? FEBS J 275:2385–2402. doi: 10.1111/j.1742-4658.2008.06380.x

Alric J (2015) The plastoquinone pool, poised for cyclic electron flow? Front Plant Sci 6:1–4. doi: 10.3389/fpls.2015.00540

Alric J (2010) Cyclic electron flow around photosystem I in unicellular green algae. Photosynth Res 47–56. doi: 10.1007/s11120-010-9566-4

Amunts A, Toporik H, Borovikova A, Nelson N (2010) Structure determination and improved model of plant photosystem I. J Biol Chem 285:3478–3486. doi: 10.1074/jbc.M109.072645

Arselin G, Vaillier J, Salin B, et al (2004) The modulation in subunits e and g amounts of yeast ATP synthase modifies mitochondrial cristae morphology. J Biol Chem 279:40392–40399. doi: 10.1074/jbc.M404316200

Asada K (2000) The water-water cycle as alternative photon and electron sinks. Philos Trans R Soc Lond B Biol Sci 355:1419–1431. doi: 10.1098/rstb.2000.0703

Atteia A, Adrait A, Brugire S, et al (2009) A proteomic survey of chlamydomonas reinhardtii mitochondria sheds new light on the metabolic plasticity of the organelle and on the nature of the α-proteobacterial mitochondrial ancestor. Mol Biol Evol 26:1533–1548. doi: 10.1093/molbev/msp068

Baniulis D, Yamashita E, Zhang H, et al (2008) Structure-function of the cytochrome b6f complex. Photochem Photobiol 84:1349–1358. doi: 10.1111/j.1751-1097.2008.00444.x

Baradaran R, Berrisford JM, Minhas GS, Sazanov L a (2013) Crystal structure of the entire respiratory complex I. Nature 494:443–8. doi: 10.1038/nature11871

Barbieri R, Larosa V, Nouet C, et al (2011) A forward genetic screen identifies mutants deficient for mitochondrial complex I assembly in Chlamydomonas reinhardtii. Genetics 188:349–358. doi: 10.1534/genetics.111.128827

Barrientos A, Gouget K, Horn D, et al (2009) Suppression mechanisms of COX assembly defects in yeast and human: Insights into the COX assembly process. Biochim Biophys Acta - Mol Cell Res 1793:97–107. doi: 10.1016/j.bbamcr.2008.05.003

Barros MH, Carlson CG, Glerum DM, Tzagoloff A (2001) Involvement of mitochondrial ferredoxin and Cox15p in hydroxylation of heme O. FEBS Lett 492:133–138. doi: 10.1016/S0014-5793(01)02249-9

Bernard DG, Gabilly ST, Dujardin G, et al (2003) Overlapping Specificities of the Mitochondrial Cytochrome c and c 1 Heme Lyases. J Biol Chem 278:49732–49742. doi: 10.1074/jbc.M308881200

Berrisford JM, Baradaran R, Sazanov LA (2016) Structure of bacterial respiratory complex I. Biochim Biophys Acta 1857:892–901. doi: 10.1016/j.bbabio.2016.01.012

Berthold P, Schmitt R, Mages W (2002) Gene Mediates Dominant Resistance against Hygromycin B in Chlamydomonas reinhardtii. Protist 153:401–412.

Billoud B, Jouanno É, Nehr Z, et al (2015) Localization of causal locus in the genome of the brown macroalga Ectocarpus : NGS-based mapping and positional cloning approaches TO WHICH EXTENT CAN CURRENT FORWARD GENETIC APPROACHES BE PROFITABLE TO MACROALGAL LOCALISATION OF A MUTANT LOCUS. 6:1–12. doi: 10.3389/fpls.2015.00068

Blaby IK, Blaby-Haas C, Tourasse N, et al (2014) The Chlamydomonas genome project: a decade on Ian. Trends Plant Sci 10:54–56. doi: 10.1038/nmeth.2250.

Blaby IK, Glaesener AG, Mettler T, et al (2013) Systems-level analysis of nitrogen starvation-induced modifications of carbon metabolism in a Chlamydomonas reinhardtii starchless mutant. Plant Cell 25:4305–23. doi: 10.1105/tpc.113.117580

Boetzer M, Henkel C V., Jansen HJ, et al (2011) Scaffolding pre-assembled contigs using SSPACE. Bioinformatics 27:578–579. doi: 10.1093/bioinformatics/btq683

Bolger AM, Lohse M, Usadel B (2014) Trimmomatic: A flexible trimmer for Illumina sequence data. Bioinformatics 30:2114–2120. doi: 10.1093/bioinformatics/btu170

Boschetti A, Schmid K (1998) Energy supply for ATP-synthase deficient chloroplasts of

Chlamydomonas reinhardii. Plant Cell Physiol 39:160. doi: 10.1093/oxfordjournals.pcp.a029353

Bradford MM (1976) A rapid and sensitive method for the quantitation of microgram quantities of protein utilizing the principle of protein-dye binding. Anal Biochem 72:248–254. doi: 10.1016/0003-2697(76)90527-3

Brand AM Van Den, Jonckheere A, Wanschers BFJ, et al (2014) A mutation in the human CBP4 ortholog UQCC3 impairs complex III assembly , activity and cytochrome b stability. Hum Mol Genet 23:6356–6365. doi: 10.1093/hmg/ddu357

Brandt U (2011) A two-state stabilization-change mechanism for proton-pumping complex i. Biochim Biophys Acta - Bioenerg 1807:1364–1369. doi: 10.1016/j.bbabio.2011.04.006

Brasseur G, Tron P, Dujardin G, Slonimski P (1997) The nuclear ABCl gene is essential for the correct conformation and functioning of the cytochrome bc, complex and the neighbouring complexes I1 and IV in the mitochondrial respiratory chain. Eur J Biochem 246:103–111.

Bricker DK, Taylor EB, Schell JC, et al (2012) A mitochondrial pyruvate carrier required for pyruvate uptake in yeast, Drosophila, and humans. Science 337:96–100. doi: 10.1126/science.1218099

Bych K, Kerscher S, Netz DJ a, et al (2008) The iron-sulphur protein Ind1 is required for effective complex I assembly. EMBO J 27:1736–1746. doi: 10.1038/emboj.2008.98

Cano-Estrada A, V??zquez-Acevedo M, Villavicencio-Queijeiro A, et al (2010) Subunit-subunit interactions and overall topology of the dimeric mitochondrial ATP synthase of Polytomella sp. Biochim Biophys Acta - Bioenerg 1797:1439–1448. doi: 10.1016/j.bbabio.2010.02.024

Cardol P (2011) Mitochondrial NADH:Ubiquinone oxidoreductase (complex I) in eukaryotes: A highly conserved subunit composition highlighted by mining of protein databases. Biochim Biophys Acta - Bioenerg 1807:1390–1397. doi: 10.1016/j.bbabio.2011.06.015

Cardol P, Alric J, Girard-bascou J, Franck F (2009) Impaired respiration discloses the physiological significance of state transitions in Chlamydomonas. Proc Natl Acad Sci U S A 106:15979–15984.

Cardol P, Boutaffala L, Memmi S, et al (2008) In Chlamydomonas, the loss of ND5 subunit prevents the assembly of whole mitochondrial complex I and leads to the formation of a low abundant 700 kDa subcomplex. Biochim Biophys Acta - Bioenerg 1777:388–396. doi: 10.1016/j.bbabio.2008.01.001

Cardol P, Gloire G, Havaux M, et al (2003) Photosynthesis and State Transitions in Mitochondrial Mutants of Chlamydomonas reinhardtii Affected in Respiration. Plant Physiol 133:2010–2020. doi: 10.1104/pp.103.028076.transition

Cardol P, González-Halphen D, Reyes-Prieto A, et al (2005) The mitochondrial oxidative phosphorylation proteome of Chlamydomonas reinhardtii deduced from the Genome Sequencing Project. Plant Physiol 137:447–459. doi: 10.1104/pp.104.054148

Cardol P, Lapaille M, Minet P, et al (2006) ND3 and ND4L subunits of mitochondrial complex I, both nucleus encoded in Chlamydomonas reinhardtii, are required for activity and assembly of the enzyme. Eukaryot Cell 5:1460–1467. doi: 10.1128/EC.00118-06

Cardol P, Matagne RF, Remacle C (2002) Impact of mutations affecting ND mitochondria-encoded subunits on the activity and assembly of complex I in chlamydomonas. Implication for the structural organization of the enzyme. J Mol Biol 319:1211–1221. doi: 10.1016/S0022-2836(02)00407-2

Cardol P, Vanrobaeys F, Devreese B, et al (2004) Higher plant-like subunit composition of mitochondrial complex I from Chlamydomonas reinhardtii: 31 Conserved components among eukaryotes. Biochim Biophys Acta - Bioenerg 1658:212–224. doi: 10.1016/j.bbabio.2004.06.001

Carilla-Latorre S, Gallardo ME, Annesley SJ, et al (2010) MidA is a putative methyltransferase that is required for mitochondrial complex I function. J Cell Sci 123:1674–1683. doi: 10.1242/jcs.066076

Chaux F, Peltier G, Johnson X (2015) A security network in PSI photoprotection: regulation of photosynthetic control, NPQ and O2 photoreduction by cyclic electron flow. Front Plant Sci 6:1–7. doi: 10.3389/fpls.2015.00875

Cheng VWT, Piragasam RS, Rothery RA, et al (2015) Redox State of Flavin Adenine Dinucleotide Drives Substrate Binding and Product Release in Escherichia coli Succinate Dehydrogenase. Biochemistry 54:1043–1052. doi: 10.1021/bi501350j.Redox

Cohen RO, Shen G, Golbeck JH, et al (2004) Evidence for Asymmetric Electron Transfer in Cyanobacterial Photosystem I: Analysis of a Methionine-to-Leucine Mutation of the Ligand to the Primary Electron Acceptor A0. Biochemistry 43:4741–4754. doi: 10.1021/bi035633f

Colin M, Dorthu MP, Duby F, et al (1995) Mutations affecting the mitochondrial genes encoding the cytochrome oxidase subunit I and apocytochrome b of Chlamydomonas reinhardtii. Mol

Gen Genet 249:179–184. doi: 10.1007/bf00290364

Colina-Tenorio L, Miranda-Astudillo H, Cano-Estrada A, et al (2015) Subunit Asa1 spans all the peripheral stalk of the mitochondrial ATP synthase of the chlorophycean alga polytomella sp. Biochim Biophys Acta - Bioenerg 1857:359–369. doi: 10.1016/j.bbabio.2015.11.012

Conte A, Papa B, Ferramosca A, Zara V (2015) Biochimica et Biophysica Acta The dimerization of the yeast cytochrome bc 1 complex is an early event and is independent of Rip1. BBA - Mol Cell Res 1853:987–995. doi: 10.1016/j.bbamcr.2015.02.006

Dalcorso G, Pesaresi P, Masiero S, et al (2008) A Complex Containing PGRL1 and PGR5 Is Involved in the Switch between Linear and Cyclic Electron Flow in Arabidopsis. Cell 132:273–285. doi: 10.1016/j.cell.2007.12.028

Dang K, Plet J, Tolleter D, et al (2014) Combined Increases in Mitochondrial Cooperation and Oxygen Photoreduction Compensate for Deficiency in Cyclic Electron Flow in Chlamydomonas reinhardtii. Plant Cell 26:3036–3050. doi: 10.1105/tpc.114.126375

De Lavalette ADL, Finazzi G, Zito F (2008) b6f-associated chlorophyll: Structural and dynamic contribution to the different cytochrome functions. Biochemistry 47:5259–5265. doi: 10.1021/bi800179b

Dekker JP, Boekema EJ (2005) Supramolecular organization of thylakoid membrane proteins in green plants. Biochim Biophys Acta 1706:12–39. doi: 10.1016/j.bbabio.2004.09.009

Delosme R, Olive J, Wollman FA (1996) Changes in light energy distribution upon state transitions: An in vivo photoacoustic study of the wild type and photosynthesis mutants from Chlamydomonas reinhardtii. Biochim Biophys Acta - Bioenerg 1273:150–158. doi: 10.1016/0005-2728(95)00143-3

Dent RM, Haglund CM, Chin BL, et al (2005) Functional Genomics of Eukaryotic Photosynthesis Using Insertional Mutagenesis of Chlamydomonas reinhardtii 1. Plant Physiol 137:545–556. doi: 10.1104/pp.104.055244.1

Depège N, Bellafiore S, Rochaix J-D (2003) Role of chloroplast protein kinase Stt7 in LHCII phosphorylation and state transition in Chlamydomonas. Science 299:1572–1575. doi: 10.1126/science.1081397

Desplats C, Mus F, Cuiné S, et al (2009) Characterization of Nda2, a plastoquinone-reducing type II NAD (P) H dehydrogenase in chlamydomonas chloroplasts. J Biol Chem 284:4148–4157. doi: 10.1074/jbc.M804546200

Dibrov E, Fu S, Lemire BD (1999) The Saccharomyces cerevisiae TCM62 gene encodes a chaperone necessary for the assembly of the mitochondrial succinate dehydrogenase (complex II). J Biol Chem 273:32042–32048. doi: 10.1074/jbc.273.48.32042

Dickson VK, Silvester J a, Fearnley IM, et al (2006) On the structure of the stator of the mitochondrial ATP synthase. EMBO J 25:2911–8. doi: 10.1038/sj.emboj.7601177

Dinant M, Baurain D, Coosemans N, et al (2001) Characterization of two genes encoding the mitochondrial alternative oxidase in Chlamydomonas reinhardtii. Curr Genet 39:101–108. doi: 10.1007/s002940000183

Do TQ, Hsu AY, Jonassen T, et al (2001) A Defect in Coenzyme Q Biosynthesis is Responsible for the Respiratory Deficiency in Saccharomyces cerevisiae abc1 Mutants. J Biol Chem 276:18161–18168. doi: 10.1074/jbc.M100952200

Dorthu MP, Remy S, Michel-Wolwertz MR, et al (1992) Biochemical, genetic and molecular characterization of new respiratory-deficient mutants in Chlamydomonas reinhardtii. Plant Mol Biol 18:759–772.

Drapier D, Rimbault B, Vallon O, et al (2007) Intertwined translational regulations set uneven stoichiometry of chloroplast ATP synthase subunits. Embo J 26:3581–3591. doi: 7601802 [pii]\r10.1038/sj.emboj.7601802

Duarte M, Mota N, Pinto L, Videira A (1998) Inactivation of the gene coding for the 30.4-kDa subunit of respiratory chain NADH dehydrogenase: Is the enzyme essential for Neurospora? Mol Gen Genet 257:368–375. doi: 10.1007/s004380050659

Dudkina N V., Heinemeyer J, Keegstra W, et al (2005) Structure of dimeric ATP synthase from mitochondria: An angular association of monomers induces the strong curvature of the inner membrane. FEBS Lett 579:5769–5772. doi: 10.1016/j.febslet.2005.09.065

Dudkina N V., Oostergetel GT, Lewejohann D, et al (2010) Row-like organization of ATP synthase in intact mitochondria determined by cryo-electron tomography. Biochim Biophys Acta - Bioenerg 1797:272–277. doi: 10.1016/j.bbabio.2009.11.004

Dudkina N V., Sunderhaus S, Braun HP, Boekema EJ (2006) Characterization of dimeric ATP synthase and cristae membrane ultrastructure from Saccharomyces and Polytomella mitochondria. FEBS Lett 580:3427–3432. doi: 10.1016/j.febslet.2006.04.097

Dumont ME, Ernst JF, Hampsey DM, Sherman F (1987) Identification and sequence of the gene encoding cytochrome c heme lyase in the yeast Saccharomyces cerevisiae. EMBO J 6:235–

241.

Dunning CJR, McKenzie M, Sugiana C, et al (2007) Human CIA30 is involved in the early assembly of mitochondrial complex I and mutations in its gene cause disease. Embo J 26:3227–3237. doi: 10.1038/sj.emboj.7601748

Efremov RG, Baradaran R, Sazanov L a (2010) The architecture of respiratory complex I. Nature 465:441–445. doi: 10.1038/nature09066

Efremov RG, Sazanov LA (2011) Structure of the membrane domain of respiratory complex I. supplementary information. Nature 476:414–20. doi: 10.1038/nature10330

Eletsky A, Jeong M, Kim H, et al (2012) Solution NMR Structure of Yeast Succinate Dehydrogenase Flavinylation Factor Sdh5 Reveals a Putative Sdh1 Binding Site. Biochemistry 51:8475–8477. doi: 10.1038/nature13314.A

Elurbe DM, Huynen MA (2016) The origin of the supernumerary subunits and assembly factors of complex I: A treasure trove of pathway evolution. Biochim Biophys Acta - Bioenerg. doi: 10.1016/j.bbabio.2016.03.027

Fairclough W V., Forsyth A, Evans MCW, et al (2003) Bidirectional electron transfer in photosystem I: Electron transfer on the PsaA side is not essential for phototrophic growth in Chlamydomonas. Biochim Biophys Acta - Bioenerg 1606:43–55. doi: 10.1016/S0005-2728(03)00083-5

Fassone E, Duncan AJ, Taanman JW, et al (2010) FOXRED1, encoding an FAD-dependent oxidoreductase complex-I-specific molecular chaperone, is mutated in infantile-onset mitochondrial encephalopathy. Hum Mol Genet 19:4837–4847. doi: 10.1093/hmg/ddq414

Figueroa-Martinez F, Nedelcu AM, Smith DR, Reyes-Prieto A (2015) When the lights go out: The evolutionary fate of free-living colorless green algae. New Phytol 206:972–982. doi: 10.1111/nph.13279

Formosa LE, Mimaki M, Frazier AE, et al (2015) Characterization of mitochondrial FOXRED1 in the assembly of respiratory chain complex I. Hum Mol Genet 24:2952–2965. doi: 10.1093/hmg/ddv058

Francis BR, Thorsness PE (2011) Hsp90 and mitochondrial proteases Yme1 and Yta10/12 participate in ATP synthase assembly in Saccharomyces cerevisiae. Mitochondrion 11:587–600. doi: 10.1016/j.mito.2011.03.008

Franzén LG, Falk G (1992) Nucleotide sequence of cDNA clones encoding the β subunit of

mitochondrial ATP synthase from the green alga Chlamydomonas reinhardtii: The precursor protein encoded by the cDNA contains both an N-terminal presequence and a C-terminal extension. Plant Mol Biol 19:771–780. doi: 10.1007/BF00027073

Friedrich T, Weiss H (1997) Modular evolution of the respiratory NADH:ubiquinone oxidoreductase and the origin of its modules. J Theor Biol 187:529–40. doi: 10.1006/jtbi.1996.0387

Fristedt R, Willig A, Granath P, et al (2009) Phosphorylation of Photosystem II Controls Functional Macroscopic Folding of Photosynthetic Membranes in Arabidopsis. Plant Cell 21:3950–3964. doi: 10.1105/tpc.109.069435

Fromm S, Braun H, Peterhansel C (2016) Mitochondrial gamma carbonic anhydrases are required for complex I assembly and plant reproductive development. new Phytol 211:194–207. doi: 10.1111/nph.13886

Funes S, Davidson E, Gonzalo Claros M, et al (2002) The typically mitochondrial DNA-encoded ATP6 subunit of the F1F0-ATPase is encoded by a nuclear gene in Chlamydomonas reinhardtii. J Biol Chem 277:6051–6058. doi: 10.1074/jbc.M109993200

Garone C, Donati MA, Sacchini M, et al (2013) Mitochondrial encephalomyopathy due to a novel mutation in ACAD9. JAMA Neurol 70:1177–1179. doi: 10.1001/jamaneurol.2013.3197

Genty B, Briantais J, Baker NR (1989) Electron transport and quenching of chlorophyll fluorescence. Biochim Biophys Acta 990:87–92. doi: 10.1016/S0304-4165(89)80016-9

Ghezzi D, Arzuffi P, Zordan M, et al (2011) Mutations in TTC19 cause mitochondrial complex III deficiency and neurological impairment in humans and flies. Nat Genet 43:259–63. doi: 10.1038/ng.761

Giordano M, Beardall J, Raven JA (2005) CO2 concentrating mechanisms in algae: mechanisms, environmental modulation and evolution. Annu Rev Plant Biol 56:99–131. doi: 10.1146/annurev.arplant.56.032604.144052

Giovannoni JJ, Wing R a, Ganal MW, Tanksley SD (1991) Isolation of molecular markers from specific chromosomal intervals using DNA pools from existing mapping populations. Nucleic Acids Res 19:6553–6558.

Glaser E, Dessi P (1999) Integration of the mitochondrial-processing peptidase into the cytochrome bc1 complex in plants. J Bioenerg Biomembr 31:259–274. doi:

10.1023/A:1005475930477

Gledhill JR, Walker JE (2005) Inhibition sites in F1-ATPase from bovine heart mitochondria. Biochem J 386:591–598. doi: 10.1042/BJ20041513

Godaux D, Bailleul B, Berne N, Cardol P (2015) Induction of Photosynthetic Carbon Fixation in Anoxia Relies on Hydrogenase Activity and Proton-Gradient Regulation-Like1-Mediated Cyclic Electron Flow in Chlamydomonas reinhardtii 1. Plant Physiol 168:648–658. doi: 10.1104/pp.15.00105

Godaux D, Emonds-Alt B, Berne N, et al (2013) A novel screening method for hydrogenase-deficient mutants in Chlamydomonas reinhardtii based on in vivo chlorophyll fluorescence and photosystem II quantum yield. Int J Hydrogen Energy 38:1826–1836. doi: 10.1016/j.ijhydene.2012.11.081

Goodenough U, Blaby I, Casero D, et al (2014) The path to triacylglyceride obesity in the sta6 strain of Chlamydomonas reinhardtii. Eukaryot Cell 13:591–613. doi: 10.1128/EC.00013-14

Gruschke S, Kehrein K, R??mpler K, et al (2011) Cbp3-Cbp6 interacts with the yeast mitochondrial ribosomal tunnel exit and promotes cytochrome b synthesis and assembly. J Cell Biol 193:1101–1114. doi: 10.1083/jcb.201103132

Gruschke S, Römpler K, Hildenbeutel M, et al (2012) The Cbp3–Cbp6 complex coordinates cytochrome. J Cell Biol 199:137–150. doi: 10.1083/jcb.201206040

Guarani V, Paulo J, Zhai B, et al (2014) TIMMDC1/C3orf1 Functions as a Membrane-Embedded Mitochondrial Complex I Assembly Factor through Association with the MCIA Complex. Mol Cell Biol 34:847–861. doi: 10.1128/MCB.01551-13

Haltia T, Finel M, Harms N, et al (1989) Deletion of the gene for subunit III leads to defective assembly of bacterial cytochrome oxidase. EMBO J 8:594–596.

Hamaji T, Smith DR, Noguchi H, et al (2013) Mitochondrial and Plastid Genomes of the Colonial Green Alga Gonium pectorale Give Insights into the Origins of Organelle DNA Architecture within the Volvocales. PLoS One. doi: 10.1371/journal.pone.0057177

Hankamer B, Barber J, Boekema EJ (1997) structure and membran organization of photosystem II in green plants. Plant Mol Biol 48:641–671.

Hao H, Khalimonchuk O, Schraders M, et al (2009) SDH5, a Gene Required for Flavination of Succinate Dehydrogenase Is Mutated in Paraganglioma. Science (80-) 325:1139–1142.

Hasan SS, Proctor EA, Yamashita E, et al (2014) Traffic within the cytochrome b6f lipoprotein

complex: Gating of the quinone portal. Biophys J 107:1620–1628. doi: 10.1016/j.bpj.2014.08.003

Heide H, Bleier L, Steger M, et al (2012) Complexome profiling identifies TMEM126B as a component of the mitochondrial complex i assembly complex. Cell Metab 16:538–549. doi: 10.1016/j.cmet.2012.08.009

Helfenbein KG, Ellis TP, Dieckmann CL, Tzagoloff A (2003) ATP22, a nuclear gene required for expression of the F0 sector of mitochondrial ATPase in Saccharomyces cerevisiae. J Biol Chem 278:19751–19756. doi: 10.1074/jbc.M301679200

Hertle AP, Blunder T, Wunder T, et al (2013) Article PGRL1 Is the Elusive Ferredoxin-Plastoquinone Reductase in Photosynthetic Cyclic Electron Flow. MOLCEL 49:511–523. doi: 10.1016/j.molcel.2012.11.030

Hirst J, Carroll J, Fearnley IM, et al (2003) The nuclear encoded subunits of complex I from bovine heart mitochondria. Biochim Biophys Acta - Bioenerg 1604:135–150. doi: 10.1016/S0005-2728(03)00059-8

Hoefnagel MHN, Atkin OK, Wiskich JT (1998) Interdependence between chloroplasts and mitochondria in the light and the dark. Biochim Biophys Acta - Bioenerg 1366:235–255. doi: 10.1016/S0005-2728(98)00126-1

Hoefs SJG, van Spronsen FJ, Lenssen EWH, et al (2011) NDUFA10 mutations cause complex I deficiency in a patient with Leigh disease. Eur J Hum Genet 19:270–4. doi: 10.1038/ejhg.2010.204

Hofhaus G, Attardi G (1993) Lack of assembly of mitochondrial DNA-encoded subunits of respiratory NADH dehydrogenase and loss of enzyme activity in a human cell mutant lacking the mitochondrial ND4 gene product. EMBO J 12:3043–3048.

Hosler JP (2004) The influence of subunit III of cytochrome c oxidase on the D pathway, the proton exit pathway and mechanism-based inactivation in subunit I. Biochim Biophys Acta - Bioenerg 1655:332–339. doi: 10.1016/j.bbabio.2003.06.009

Hummer G, Wikström M (2016) Biochimica et Biophysica Acta Molecular simulation and modeling of complex I. BBA - Bioenerg 1857:915–21. doi: 10.1016/j.bbabio.2016.01.005

Iwai M, Takahashi Y, Minagawa J (2008) Molecular remodeling of photosystem II during state transitions in Chlamydomonas reinhardtii. Plant Cell 20:2177–2189. doi: 10.1105/tpc.108.059352

Iwai M, Takizawa K, Tokutsu R, et al (2010) Isolation of the elusive supercomplex that drives cyclic electron flow in photosynthesis. Nature 464:1210–1213. doi: 10.1038/nature08885

Jans F, Mignolet E, Houyoux P-A, et al (2008) A type II NAD(P)H dehydrogenase mediates light-independent plastoquinone reduction in the chloroplast of Chlamydomonas. Proc Natl Acad Sci U S A 105:20546–51. doi: 10.1073/pnas.0806896105

Jansson S (1999) A guide to the Lhc genes and their relatives in Arabidopsis. Trends Plant Sci 4:236–240. doi: 10.1016/S1360-1385(99)01419-3

Jia L, K D, A. stuart R (2007) Oxa1 Directly Interacts with Atp9 and Mediates Its Assembly into the Mitochondrial F1Fo-ATP Synthase Complex. Mol Biol Cell 18:986–994. doi: 10.1091/mbc.E06

Jiang W, Brueggeman AJ, Horken KM, et al (2014) Successful transient expression of Cas9 and single guide RNA genes in Chlamydomonas reinhardtii. Eukaryot Cell 13:1465–1469. doi: 10.1128/EC.00213-14

Jinkerson RE, Jonikas MC (2015) Molecular techniques to interrogate and edit the Chlamydomonas nuclear genome. Plant J 82:393–412. doi: 10.1111/tpj.12801

Johnson X, Steinbeck J, Dent RM, et al (2014) Proton Gradient Regulation 5-Mediated Cyclic Electron Flow under ATP- or Redox-Limited Conditions : A Study of D ATPase pgr5 and D rbcL pgr5 Mutants in the Green Alga. Plant Physiol 165:438–452. doi: 10.1104/pp.113.233593

Johnson X, Vandystadt G, Bujaldon S, et al (2009) A new setup for in vivo fluorescence imaging of photosynthetic activity. Photosynth Res 102:85–93. doi: 10.1007/s11120-009-9487-2

Joza N, Oudit GY, Brown D, et al (2005) Muscle-Specific Loss of Apoptosis-Inducing Factor Leads to Mitochondrial Dysfunction , Skeletal Muscle Atrophy , and Dilated Cardiomyopathy Muscle-Specific Loss of Apoptosis-Inducing Factor Leads to Mitochondrial Dysfunction , Skeletal Muscle Atrophy , an. Mol Cell Biol 25:10261–10272. doi: 10.1128/MCB.25.23.10261

Kaila VR, Verkhovsky MI, Wikström M (2010) Proton-coupled electron transfer in cytochrome oxidase. Chem Rev 110:7062–7081. doi: 10.1021/cr1002003

Karpova O V., Newton KJ (1999) A partially assembled complex I in NAD4-deficient mitochondria of maize. Plant J 17:511–521. doi: 10.1046/j.1365-313X.1999.00401.x

Kerscher S, Kashani-poor N, Zwicker K, et al (2001) Exploring the Catalytic Core of Complex I

by Yarrowia lipolytica Yeast Genetics 1.

Kitajima M, Butler WL (1975) QUENCHING OF CHLOROPHYLL FLUORESCENCE AND PRIMARY PHOTOCHEMISTRY IN CHLOROPLASTS BY DIBROMOTHYMOQUINONE. Biochim Biophys Acta 376:105–115.

Klein U (1986) Compartmentation of glycolysis and of the oxidative pentose-phosphate pathway in Chlamydomonas reinhardii. Planta 167:81–86. doi: 10.1007/BF00446372

Klodmann J, Braun H-P (2011) Proteomic approach to characterize mitochondrial complex I from plants. Phytochemistry 72:1071–1080. doi: 10.1016/j.phytochem.2010.11.012

Klodmann J, Sunderhaus S, Nimtz M, et al (2010) Internal architecture of mitochondrial complex I from Arabidopsis thaliana. Plant Cell 22:797–810. doi: 10.1105/tpc.109.073726

Kmita K, Wirth C, Warnau J, et al (2015) Accessory NUMM (NDUFS6) subunit harbors a Zn-binding site and is essential for biogenesis of mitochondrial complex I. Proc Natl Acad Sci 112:5685–5690. doi: 10.1073/pnas.1424353112

KOK B, FORBUSH B, McGLOIN M (1970) Cooperation of Charges in Photosynthetic O 2 Evolution–I. a Linear Four Step Mechanism. Photochem Photobiol 11:457–475. doi: 10.1111/j.1751-1097.1970.tb06017.x

Kotlyar AB, Sled VD, Burbaev DS, et al (1990) Coupling site I and the rotenone-sensitive ubisemiquinone in tightly coupled submitochondrial particles. FEBS Lett 264:17–20. doi: 10.1016/0014-5793(90)80753-6

Kuffner R, Rohr A, Schmiede A, et al (1998) Involvement of two novel chaperones in the assembly of mitochondrial NADH : ubiquinone oxidoreductase (complex I). J Mol Biol 283:409–417. doi: 10.1006/jmbi.1998.2114

Kunze M, Hartig A (2013) Permeability of the peroxisomal membrane: Lessons from the glyoxylate cycle. Front Physiol 4 AUG:1–12. doi: 10.3389/fphys.2013.00204

Lapaille M, Escobar-Ram??rez A, Degand H, et al (2010) Atypical subunit composition of the chlorophycean mitochondrial F 1FO-ATP synthase and role of asa7 protein in stability and oligomycin resistance of the enzyme. Mol Biol Evol 27:1630–1644. doi: 10.1093/molbev/msq049

Lauersen K, Willamme R, Coosemans N, et al (2016) Peroxisomal microbodies are at the crossroads of acetate assimilation in the green microalga Chlamydomonas reinhardtii. Algal Res 16:266–274.

Lecler R, Cardol P, Remacle C, Barbare E (2012) Characterization of an internal type-II NADH dehydrogenase from Chlamydomonas reinhardtii mitochondria. Curr Genet 58:205–216. doi: 10.1007/s00294-012-0378-2

Lefebvre-Legendre L, Vaillier J, Benabdelhak H, et al (2001) Identification of a nuclear gene (FMC1) required for the assembly/stability of yeast mitochondrial F(1)-ATPase in heat stress conditions. J Biol Chem 276:6789–6796. doi: 10.1074/jbc.M009557200

Lemeille S, Turkina M V, Vener A V, Rochaix J-D (2010) Stt7-dependent phosphorylation during state transitions in the green alga Chlamydomonas reinhardtii. Mol Cell Proteomics 9:1281–1295. doi: 10.1074/mcp.M000020-MCP201

Lemeille S, Willig A, Depège-Fargeix N, et al (2009) Analysis of the chloroplast protein kinase Stt7 during state transitions. PLoS Biol 7:0664–0675. doi: 10.1371/journal.pbio.1000045-S.pdf

Letts JA, Sazanov LA (2015) Gaining mass: The structure of respiratory complex I-from bacterial towards mitochondrial versions. Curr Opin Struct Biol 33:135–145. doi: 10.1016/j.sbi.2015.08.008

Li H, Durbin R (2010) Fast and accurate long-read alignment with Burrows-Wheeler transform. Bioinformatics 26:589–595. doi: 10.1093/bioinformatics/btp698

Li X, Zhang R, Patena W, et al (2016) An Indexed , Mapped Mutant Library Enables Reverse Genetics Studies of Biological Processes in Chlamydomonas reinhardtii. Plant Cell 28:367–87. doi: 10.1105/tpc.16.00465

Lis R Van, Atteia A, Mendoza-hernández G, González-halphen D (2003) Identification of Novel Mitochondrial Protein Components of Chlamydomonas reinhardtii . A Proteomic Approach 1. Plant Physiol 132:318–330. doi: 10.1104/pp.102.018325.proteins

Liu YG, Mitsukawa N, Oosumi T, Whittier RF (1995) Efficient isolation and mapping of Arabidopsis thaliana T-DNA insert junctions by thermal asymmetric interlaced PCR. Plant J 8:457–63.

Lown FJ, Watson a T, Purton S (2001) Chlamydomonas nuclear mutants that fail to assemble respiratory or photosynthetic electron transfer complexes. Biochem Soc Trans 29:452–5. doi: 10.1042/BST0290452

Lucker B, Kramer DM (2013) Regulation of cyclic electron flow in Chlamydomonas reinhardtii under fluctuating carbon availability. Photosynth Res 117:449–459. doi: 10.1007/s11120-

013-9932-0

Massoz S, Larosa V, Horrion B, et al (2015) Isolation of Chlamydomonas reinhardtii mutants with altered mitochondrial respiration by chlorophyll fluorescence measurement. J Biotechnol 215:27–34. doi: 10.1016/j.jbiotec.2015.05.009

Massoz S, Larosa V, Plancke C, et al (2014) Inactivation of genes coding for mitochondrial Nd7 and Nd9 complex I subunits in Chlamydomonas reinhardtii. Impact of complex I loss on respiration and energetic metabolism. Mitochondrion 19:365–374. doi: 10.1016/j.mito.2013.11.004

Mathiesen C, Hägerhäll C (2002) Transmembrane topology of the NuoL, M and N subunits of NADH:quinone oxidoreductase and their homologues among membrane-bound hydrogenases and bona fide antiporters. Biochim Biophys Acta - Bioenerg 1556:121–132. doi: 10.1016/S0005-2728(02)00343-2

Mathieu L, Marsy S, Saint-Georges Y, et al (2011) A transcriptome screen in yeast identifies a novel assembly factor for the mitochondrial complex III. Mitochondrion 11:391–396. doi: 10.1016/j.mito.2010.12.002

Mathy G, Cardol P, Dinant M, et al (2010) Proteomic and functional characterization of a chlamydomonas reinhardtii mutant lacking the mitochondrial alternative oxidase. J Proteome Res 9:2825–2838. doi: 10.1021/pr900866e

Maul JE, Lilly JW, Cui L, et al (2002) The Chlamydomonas reinhardtii plastid chromosome: islands of genes in a sea of repeats. Plant Cell 14:2659–79. doi: 10.1105/tpc.006155.present

Mavridou DAI, Ferguson SJ, Stevens JM (2013) Cytochrome c assembly. IUBMB Life 65:209–216. doi: 10.1002/iub.1123

Mccarty RE, Evron Y, Johnson EA (2000) THE CHLOROPLAST ATP SYNTHASE: A Rotary Enzyme. Plant Mol Biol 51:83–109.

McCommis KS, Finck BN (2015) Mitochondrial pyruvate transport: a historical perspective and future research directions. Biochem J 466:229–262. doi: 10.1007/978-1-4614-5915-6

McKenzie M, Tucker EJ, Compton AG, et al (2011) Mutations in the gene encoding C8orf38 block complex i assembly by inhibiting production of the mitochondria-encoded subunit ND1. J Mol Biol 414:413–426. doi: 10.1016/j.jmb.2011.10.012

Merchant SS, Prochnik SE, Vallon O, et al (2007) The Chlamydomonas Genome Reveals the Evolution of Key Animal and Plant Functions. Science (80-) 318:245–252.

Meyer Zu Tittingdorf JMW, Rexroth S, Schäfer E, et al (2004) The stoichiometry of the chloroplast ATP synthase oligomer III in Chlamydomonas reinhardtii is not affected by the metabolic state. Biochim Biophys Acta - Bioenerg 1659:92–99. doi: 10.1016/j.bbabio.2004.08.008

Michelmore RW, Paran I, Kesseli R V (1991) Identification of Markers Linked To Disease-Resistance Genes By Bulked Segregant Analysis - a Rapid Method To Detect Markers in Specific Genomic Regions By Using Segregating Populations. Proc Natl Acad Sci U S A 88:9828–9832. doi: 10.1073/pnas.88.21.9828

Milani G, Jarmurszkiewicz W, Sluse-go CM, et al (2001) Respiratory chain network in mitochondria of Candida parapsilosis : ADP / O appraisal of the multiple electron pathways. FEBS Lett 508:231–235.

Mimaki M, Wang X, McKenzie M, et al (2012) Understanding mitochondrial complex I assembly in health and disease. Biochim Biophys Acta - Bioenerg 1817:851–862. doi: 10.1016/j.bbabio.2011.08.010

Minagawa J (2011) State transitions-the molecular remodeling of photosynthetic supercomplexes that controls energy flow in the chloroplast. Biochim Biophys Acta - Bioenerg 1807:897–905. doi: 10.1016/j.bbabio.2010.11.005

Minagawa J, Tokutsu R (2015) Dynamic regulation of photosynthesis in Chlamydomonas reinhardtii. Plant J 82:413–428. doi: 10.1111/tpj.12805

Miranda-Astudillo H, Cano-Estrada A, V??zquez-Acevedo M, et al (2014) Interactions of subunits Asa2, Asa4 and Asa7 in the peripheral stalk of the mitochondrial ATP synthase of the chlorophycean alga Polytomella sp. Biochim Biophys Acta - Bioenerg 1837:1–13. doi: 10.1016/j.bbabio.2013.08.001

Mitchell P (1961) Coupling of phosphorylation to electron and hydrogen transfer by chemi-osmotic type of mechanism. Nature 191:144–148.

Molen TA, Rosso D, Piercy S, Maxwell DP (2006) Characterization of the alternative oxidase of Chlamydomonas reinhardtii in response to oxidative stress and a shift in nitrogen source. Physiol Plant 127:74–86. doi: 10.1111/j.1399-3054.2006.00643.x

Møller IM, Rasmusson AG, Fredlund KM (1993) NAD(P)H-ubiquinone oxidoreductases in plant mitochondria. J Bioenerg Biomembr 25:377–384. doi: 10.1007/BF00762463

Munekage Y, Hojo M, Meurer J, et al (2002) PGR5 is involved in cyclic electron flow around

photosystem I and is essential for photoprotection in Arabidopsis. Cell 110:361–371. doi: 10.1016/S0092-8674(02)00867-X

Murata N (1969) Control of excitation transfer in photosynthesis I. Light-induced change of chlorophyll a fluoresence in Porphyridium cruentum. Biochim Biophys Acta - Bioenerg 172:242–251. doi: 10.1016/0005-2728(69)90067-X

Nagy G, Ünnep R, Zsiros O, et al (2014) Chloroplast remodeling during state transitions in Chlamydomonas reinhardtii as revealed by noninvasive techniques in vivo. Proc Natl Acad Sci U S A 111:5042–7. doi: 10.1073/pnas.1322494111

Newman SM, Boynton JE, Gillham NW, et al (1990) Transformation of chloroplast ribosomal RNA genes in Chlamydomonas: Molecular and genetic characterization of integration events. Genetics 126:875–888.

Nield J, Kruse O, Ruprecht J, et al (2000) Photosystem II complexes allows for comparison of their OEC organisation.

Noguchi K, Yoshida K (2008) Interaction between photosynthesis and respiration in illuminated leaves. Mitochondrion 8:87–99. doi: 10.1016/j.mito.2007.09.003

Nurani G, Franzén LG (1996) Isolation and characterization of the mitochondrial ATP synthase from *Chlamydomonas reinhardtii*. cDNA sequence and deduced protein sequence of the alpha subunit. Plant Mol Biol 31:1105–16.

Ogilvie I, Kennaway NG, Shoubridge EA (2005) A molecular chaperone for mitochondrial complex I assembly is mutated in a progressive encephalopathy. J Clin Invest 115:2784–2792. doi: 10.1172/JCI26020

Ohnishi T (1998) Iron-sulfur clusters/semiquinones in Complex I. Biochim Biophys Acta - Bioenerg 1364:186–206. doi: 10.1016/S0005-2728(98)00027-9

Oster G, Wang H (2003) Rotary protein motors. Trends Cell Biol 13:114–121. doi: 10.1016/S0962-8924(03)00004-7

Oyedotun KS, Sit CS, Lemire BD (2007) The Saccharomyces cerevisiae succinate dehydrogenase does not require heme for ubiquinone reduction. Biochim Biophys Acta - Bioenerg 1767:1436–1445. doi: 10.1016/j.bbabio.2007.09.008

Paumard P, Vaillier J, Coulary B, et al (2002) The ATP synthase is involved in generating mitochondrial cristae morphology. EMBO J 21:221–230. doi: 10.1093/emboj/21.3.221

Paupe V, Prudent J, Dassa EP, et al (2015) CCDC90A (MCUR1) is a cytochrome c oxidase

assembly factor and not a regulator of the mitochondrial calcium uniporter. Cell Metab 21:109–116. doi: 10.1016/j.cmet.2014.12.004

Peltier G, Tolleter D, Billon E (2010) Auxiliary electron transport pathways in chloroplasts of microalgae. Photosynth Res 106:19–31. doi: 10.1007/s11120-010-9575-3

Pereira B, Videira A, Duarte M (2013) Novel insights into the role of Neurospora crassa NDUFAF2, an evolutionarily conserved mitochondrial complex I assembly factor. Mol Cell Biol 33:2623–34. doi: 10.1128/MCB.01476-12

Perez-Martinez X, Antaramian A, V??zquez-Acevedo M, et al (2001) Subunit II of Cytochrome c Oxidase in Chlamydomonad Algae Is a Heterodimer Encoded by Two Independent Nuclear Genes. J Biol Chem 276:11302–11309. doi: 10.1074/jbc.M010244200

Perez-Martinez X, Funes S, Tolkunova E, et al (2002) Structure of nuclear-localized cox3 genes in Chlamydomonas reinhardtii and in its colorless close relative Polytomella sp. Curr Genet 40:399–404. doi: 10.1007/s00294-002-0270-6

Petroutsos D, Terauchi AM, Busch A, et al (2009) PGRL1 Participates in Iron-induced Remodeling of the Photosynthetic Apparatus and in Energy Metabolism in. J Biol Chem 284:32770–32781. doi: 10.1074/jbc.M109.050468

Phillips JD, Graham LA, Trumpower BL (1993) Subunit 9 of the Saccharomyces cerevisiae cytochrome bc1 complex is required for insertion of EPR-detectable iron-sulfur cluster into the Rieske iron-sulfur protein. J Biol Chem 268:11727–11736.

Plancke C, Vigeolas H, Höhner R, et al (2014) Lack of isocitrate lyase in Chlamydomonas leads to changes in carbon metabolism and in the response to oxidative stress under mixotrophic growth. Plant J 77:404–417. doi: 10.1111/tpj.12392

Prakash SK, Cormier TA, Mccall AE, et al (2002) Loss of holocytochrome c -type synthetase causes the male lethality of X-linked dominant micro- phthalmia with linear skin defects (MLS) syndrome. Hum Mol Genet 11:3237–3248.

Rak M, Gokova S, Tzagoloff A (2011) Modular assembly of yeast mitochondrial ATP synthase. EMBO J 30:920–930. doi: 10.1038/emboj.2010.364

Rak M, Rustin P (2014) Supernumerary subunits NDUFA3, NDUFA5 and NDUFA12 are required for the formation of the extramembrane arm of human mitochondrial complex I. FEBS Lett 588:1832–1838. doi: 10.1016/j.febslet.2014.03.046

Remacle C, Baurain D, Cardol P, Matagne F (2001) Mutants of Chlamydomonas reinhardtii

Deficient in Mitochondrial Complex I : Characterization of Two Mutations Affecting the nd1 Coding Sequence. Genetics 158:1051–1060.

Remacle C, Cardol P, Coosemans N, et al (2006) High-efficiency biolistic transformation of Chlamydomonas mitochondria can be used to insert mutations in complex I genes. Proc Natl Acad Sci U S A 103:4771–6. doi: 10.1073/pnas.0509501103

Remacle C, Coosemans N, Jans F, et al (2010) Knock-down of the COX3 and COX17 gene expression of cytochrome c oxidase in the unicellular green alga Chlamydomonas reinhardtii. Plant Mol Biol 74:223–233. doi: 10.1007/s11103-010-9668-6

Rhein VF, Carroll J, Ding S, et al (2013) NDUFAF7 methylates arginine 85 in the NDUFS2 subunit of human complex i. J Biol Chem 288:33016–33026. doi: 10.1074/jbc.M113.518803

Rintamaki E, Martinsuo P, Pursiheimo S, Aro EM (2000) Cooperative regulation of light-harvesting complex II phosphorylation via the plastoquinol and ferredoxin-thioredoxin system in chloroplasts. Proc Natl Acad Sci U S A 97:11644–11649. doi: 10.1073/pnas.180054297

Roach T, Na CS, Krieger-Liszkay A (2015) High light-induced hydrogen peroxide production in Chlamydomonas reinhardtii is increased by high CO2 availability. Plant J 81:759–766. doi: 10.1111/tpj.12768

Robinson JT, Thorvaldsdóttir, Helga Winckler W, Guttman M, et al (2011) Integrative Genomics Viewer. nat biotechnol 29:24–26. doi: 10.1038/nbt.1754.Integrative

Rochaix JD (2002) Chlamydomonas, a model system for studying the assembly and dynamics of photosynthetic complexes. FEBS Lett 529:34–38. doi: 10.1016/S0014-5793(02)03181-2

Rochaix JD, Lemeille S, Shapiguzov a, et al (2012) Protein kinases and phosphatases involved in the acclimation of the photosynthetic apparatus to a changing light environment. Philos Trans R Soc B-Biological Sci 367:3466–3474. doi: 10.1098/rstb.2012.0064

Rochaix SLJ (2010) State transitions at the crossroad of thylakoid signalling pathways. Photosynth Res 33–46. doi: 10.1007/s11120-010-9538-8

Rodriguez-Salinas E, Riveros-Rosas H, Li Z, et al (2012) Lineage-specific fragmentation and nuclear relocation of the mitochondrial cox2 gene in chlorophycean green algae (Chlorophyta). Mol Phylogenet Evol 64:166–176. doi: 10.1016/j.ympev.2012.03.014

Rouault TA (2015) Mammalian iron-sulphur proteins: novel insights into biogenesis and function. Nat Rev Mol Cell Biol 16:45–55. doi: 10.1038/nrm3909

Rühle T, Leister D (2015) Assembly of F1F0-ATP synthases. Biochim Biophys Acta 1847:849–860. doi: 10.1016/j.bbabio.2015.02.005

Rutter J, Winge DR, Schiffman JD (2010) Succinate dehydrogenase - Assembly, regulation and role in human disease. Mitochondrion 10:393–401. doi: 10.1016/j.mito.2010.03.001

Saada A, Vogel RO, Hoefs SJ, et al (2009) Mutations in NDUFAF3 (C3ORF60), Encoding an NDUFAF4 (C6ORF66)-Interacting Complex I Assembly Protein, Cause Fatal Neonatal Mitochondrial Disease. Am J Hum Genet 84:718–727. doi: 10.1016/j.ajhg.2009.04.020

Sager R, Palade GE (1957) Structure and development of the chloroplast in Chlamydomonas: I. The Normal Green Cell. J Cell Biol 3:463–488.

Salinas T, Larosa V, Cardol P, et al (2014) Biochimie Respiratory deficient mutants of the unicellular green alga Chlamydomonas : A review. Biochimie 100:207–218. doi: 10.1016/j.biochi.2013.10.006

Samol I, Shapiguzov a, Ingelsson B, et al (2012) Identification of a Photosystem II Phosphatase Involved in Light Acclimation in Arabidopsis. Plant Cell 24:2596–2609. doi: 10.1105/tpc.112.095703

Sánchez-Caballero L, Guerrero-Castillo S, Nijtmans L (2016a) Unraveling the complexity of mitochondrial complex I assembly; a dynamic process. Biochim Biophys Acta - Bioenerg 1857:880–890. doi: 10.1016/j.bbabio.2016.03.031

Sánchez-Caballero L, Guerrero-Castillo S, Nijtmans L (2016b) Unraveling the complexity of mitochondrial complex I assembly; a dynamic process. Biochim Biophys Acta - Bioenerg. doi: 10.1016/j.bbabio.2016.03.031

Sazanov LA (2015) REVIEWS A giant molecular proton pump : structure and mechanism of respiratory complex I. Nat Publ Gr 16:375–388. doi: 10.1038/nrm3997

Sazanov LA, Hinchliffe P (2006) Structure of the Hydrophilic Domain. Science (80-) 311:1430–1437.

Scheibe R (1987) Minireview NADP + -malate dehydrogenase in C3-plants : Regulation and role of a light-activated enzyme. Physiol Plant 71:393–400.

Schiff M, Haberberger B, Xia C, et al (2014) Complex I assembly function and fatty acid oxidation enzyme activity of ACAD9 both contribute to disease severity in ACAD9 deficiency. Hum Mol Genet 24:3238–3247. doi: 10.1093/hmg/ddv074

Schimmeyer J, Bock R, Meyer EH (2016) l-Galactono-1,4-lactone dehydrogenase is an assembly

factor of the membrane arm of mitochondrial complex I in Arabidopsis. Plant Mol Biol 90:117–126. doi: 10.1007/s11103-015-0400-4

Schlehe JS, Journel MSM, Taylor KP, et al (2013) The mitochondrial disease associated protein Ndufaf2 is dispensable for Complex-1 assembly but critical for the regulation of oxidative stress. Neurobiol Dis 58:57–67. doi: 10.1016/j.nbd.2013.05.007

Schulte U, Weiss H (1995) NGeneration NADH : Ubiquinone and Characterization of Oxidoreductase Mutants Neurospora crassa. method Enzymol 260:3–13.

Shao N, Beck CF, Lemaire SD, Krieger-Liszkay A (2008) Photosynthetic electron flow affects H2O2 signaling by inactivation of catalase in Chlamydomonas reinhardtii. Planta 228:1055–1066. doi: 10.1007/s00425-008-0807-0

Shapiguzov A, Ingelsson B, Samol I, et al (2010) The PPH1 phosphatase is specifically involved in LHCII dephosphorylation and state transitions in Arabidopsis. Proc Natl Acad Sci 107:4782–4787. doi: 10.1073/pnas.0913810107

Sharma V, Belevich G, Gamiz-Hernandez AP, et al (2015) Redox-induced activation of the proton pump in the respiratory complex I. Proc Natl Acad Sci U S A 112:11571–6. doi: 10.1073/pnas.1503761112

Sheftel AD, Stehling O, Pierik AJ, et al (2009) Human ind1, an iron-sulfur cluster assembly factor for respiratory complex I. Mol Cell Biol 29:6059–6073. doi: 10.1128/MCB.00817-09

Shiba T, Kido Y, Sakamoto K, et al (2013) Structure of the trypanosome cyanide-insensitive alternative oxidase. Proc Natl Acad Sci 110:4580–4585. doi: 10.1073/pnas.1218386110

Siedow JN, Umbach AL, Moore AL (1995) The active site of the cyanide-resistant oxidase from plant mitochondria contains a binuclear iron center. FEBS Lett 362:10–14. doi: 10.1016/0014-5793(95)00196-G

Sizova I, Fuhrmann M, Hegemann P (2001) A Streptomyces rimosus aphVIII gene coding for a new type phosphotransferase provides stable antibiotic resistance to Chlamydomonas reinhardtii. Gene 277:221–229. doi: 10.1016/S0378-1119(01)00616-3

Sizova I, Greiner A, Awasthi M, et al (2013) Nuclear gene targeting in Chlamydomonas using engineered zinc-finger nucleases. Plant J 73:873–882. doi: 10.1111/tpj.12066

Smith DR, Hua J, Lee RW (2010) Evolution of linear mitochondrial DNA in three known lineages of Polytomella. Curr Genet 56:427–438. doi: 10.1007/s00294-010-0311-5

Smith DR, Lee RW (2009) The mitochondrial and plastid genomes of Volvox carteri: bloated

molecules rich in repetitive DNA. BMC Genomics 10:132. doi: 10.1186/1471-2164-10-132

Smith PM, Fox JL, Winge DR (2012) Biogenesis of the cytochrome bc 1 complex and role of assembly factors. Biochim Biophys Acta - Bioenerg 1817:276–286. doi: 10.1016/j.bbabio.2011.11.009

Soto IC, Fontanesi F, Liu J, Barrientos A (2012) Biogenesis and assembly of eukaryotic cytochrome c oxidase catalytic core. Biochim Biophys Acta 1817:883–897. doi: 10.1016/j.bbabio.2011.09.005

Stauber EJ, Fink A, Markert C, et al (2003) Proteomics of Chlamydomonas reinhardtii Light-Harvesting Proteins. Eukaryot Cell 2:978–994. doi: 10.1128/EC.2.5.978

Stevens DR, Rochaix JD, Purton S (1996) The bacterial phleomycin resistance gene ble as a dominant selectable marker in Chlamydomonas. Mol Gen Genet 251:23–30. doi: 10.1007/s004380050135

Strand DD, Livingston AK, Satoh-Cruz M, et al (2015) Activation of cyclic electron flow by hydrogen peroxide in vivo. Proc Natl Acad Sci 112:201418223. doi: 10.1073/pnas.1418223112

Strotmann H, Shavit N, Leu S (1998) assembly and function of the chloroplast ATP synthase. Mol Biol chloroplasts mitochondria Chlamydomonas 477–499.

Stroud D a., Formosa LE, Wijeyeratne XW, et al (2013) Gene knockout using transcription activator-like effector nucleases (TALENs) reveals that human ndufa9 protein is essential for stabilizing the junction between membrane and matrix arms of complex i. J Biol Chem 288:1685–1690. doi: 10.1074/jbc.C112.436766

Subrahmanian N, Remacle C, Hamel PP (2016) Plant mitochondrial Complex I composition and assembly: a review. BBA - Bioenerg 1857:1001–1014. doi: 10.1016/j.bbabio.2016.01.009

Suga M, Qin X, Kuang T, Shen JR (2016) Structure and energy transfer pathways of the plant photosystem I-LHCI supercomplex. Curr Opin Struct Biol 39:46–53. doi: 10.1016/j.sbi.2016.04.004

Sugiana C, Pagliarini DJ, McKenzie M, et al (2008) Mutation of C20orf7 Disrupts Complex I Assembly and Causes Lethal Neonatal Mitochondrial Disease. Am J Hum Genet 83:468–478. doi: 10.1016/j.ajhg.2008.09.009

Sunderhaus S, Dudkina N V., Jansch L, et al (2006) Carbonic anhydrase subunits form a matrix-exposed domain attached to the membrane arm of mitochondrial complex I in plants. J Biol

Chem 281:6482–6488. doi: 10.1074/jbc.M511542200

Suorsa M, Sirpio S, Aro E (2009) Towards Characterization of the Chloroplast NAD (P) H Dehydrogenase Complex. Mol Plant. doi: 10.1093/mp/ssp052

Susin S a, Lorenzo HK, Zamzami N, et al (1999) Molecular characterization of mitochondrial apoptosis-inducing factor. Nature 397:441–446. doi: 10.1038/17135

Svensson-Ek M, Abramson J, Larsson G, et al (2002) The X-ray crystal structures of wild-type and EQ(I-286) mutant cytochrome c oxidases from Rhodobacter sphaeroides. J Mol Biol 321:329–339. doi: 10.1016/S0022-2836(02)00619-8

Szklarczyk R, Wanschers BFJ, Nabuurs SB, et al (2011) NDUFB7 and NDUFA8 are located at the intermembrane surface of complex i. FEBS Lett 585:737–743. doi: 10.1016/j.febslet.2011.01.046

Takahashi H, Clowez S, Wollman F-A, et al (2013) Cyclic electron flow is redox-controlled but independent of state transition. Nat Commun 4:1954. doi: 10.1038/ncomms2954

Terashima M, Petroutsos D, Hüdig M, et al (2012) Calcium-dependent regulation of cyclic photosynthetic electron transfer by a CAS , ANR1 , and PGRL1 complex. PNAS 109:17717–17722. doi: 10.1073/pnas.1207118109

Terashima M, Specht M, Naumann B, Hippler M (2010) Characterizing the anaerobic response of Chlamydomonas reinhardtii by quantitative proteomics. Mol Cell Proteomics 9:1514–1532. doi: 10.1074/mcp.M900421-MCP200

Tikhonov AN (2014) The cytochrome b6f complex at the crossroad of photosynthetic electron transport pathways. Plant Physiol Biochem 81:163–183. doi: 10.1016/j.plaphy.2013.12.011

Tokutsu R, Kato N, Bui KH, et al (2012) Revisiting the supramolecular organization of photosystem II in Chlamydomonas reinhardtii. J Biol Chem 287:31574–31581. doi: 10.1074/jbc.M111.331991

Tolleter D, Reiter IM, Genty B, et al (2011) Control of Hydrogen Photoproduction by the Proton Gradient Generated by Cyclic Electron Flow in Chlamydomonas reinhardtii. Plant Cell 23:2619–2630. doi: 10.1105/tpc.111.086876

Trumpower B (1990a) The protonmotive Q cycle. J Biol Chem 265:11409–11412. doi: 10.3109/10409239409086800

Trumpower BL (1990b) Cytochrome bc1 complexes of microorganisms. Microbiol Rev 54:101–129.

Tucker EJ, Wanschers BFJ, Szklarczyk R, et al (2013) Mutations in the UQCC1-Interacting Protein , UQCC2 , Cause Human Complex III Deficiency Associated with Perturbed Cytochrome b Protein Expression. Genetics. doi: 10.1371/journal.pgen.1004034

Tzagoloff A, Jang J, Glerum M, Wu M (1996) FLX1 Codes for a Carrier Protein Involved in Maintaining a Proper Balance of Flavin Nucleotides in Yeast Mitochondria. J Biol Chem 271:7392–7397.

Umena Y, Kawakami K, Shen J-R, Kamiya N (2011) Crystal structure of oxygen-evolving photosystem II at a resolution of 1.9 Å. Nature 473:55–60. doi: 10.1038/nature09913

Un N, Yu, Ywe D, Cox J, et al (2014) The LYR factors SDHAF1 and SDHAF3 mediate maturation of the iron-sulfur subunit of succinate dehydrogenase. Cell Metab 253–266. doi: 10.1021/jf104742n.Biological

Vahrenholz C, Riemen G, Pratje E, et al (1993) Mitochondrial DNA of Chlamydomonas reinhardtii: the structure of the ends of the linear 15.8-kb genome suggests mechanisms for DNA replication. Curr Genet 24:241–247. doi: 10.1007/BF00351798

Vainonen JP, Hansson M, Vener A V. (2005) STN8 protein kinase in Arabidopsis thaliana is specific in phosphorylation of photosystem II core proteins. J Biol Chem 280:33679–33686. doi: 10.1074/jbc.M505729200

van den Ecker D, van den Brand MA, Ariaans G, et al (2012) Identification and functional analysis of mitochondrial complex I assembly factor homologues in C. elegans. Mitochondrion 12:399–405. doi: 10.1016/j.mito.2012.01.003

van Lis R, Atteia A, Mendoza-hernández G, González-halphen D (2003) Identification of Novel Mitochondrial Protein Components of Chlamydomonas reinhardtii . A Proteomic Approach 1. Plant Physiol 132:318–330. doi: 10.1104/pp.102.018325.proteins

van Lis R, Mendoza-Hernández G, Groth G, Atteia A (2007) New insights into the unique structure of the F0F1-ATP synthase from the chlamydomonad algae Polytomella sp. and Chlamydomonas reinhardtii. Plant Physiol 144:1190–9. doi: 10.1104/pp.106.094060

Van Vranken J, Na U, R.Wing D, Rutter J (2015) Protein-mediated assembly of succinate dehydrogenase and its cofactors. Crit Rev Biochem Mol Biol 50:168–180. doi: 10.1530/ERC-14-0411.Persistent

Vazquez-Acevedo M, Cardol P, Cano-Estrada A, et al (2006) The mitochondrial ATP synthase of chlorophycean algae contains eight subunits of unknown origin involved in the formation of

an atypical stator-stalk and in the dimerization of the complex. J Bioenerg Biomembr 38:271–282. doi: 10.1007/s10863-006-9046-x

Vázquez-Acevedo M, Vega-deLuna F, Sánchez-Vásquez L, et al (2016) Dissecting the peripheral stalk of the mitochondrial ATP synthase of chlorophycean algae. Biochim Biophys Acta - Bioenerg. doi: 10.1016/j.bbabio.2016.02.003

Vignais PM, Billoud B (2007) Occurrence , Classification , and Biological Function of Hydrogenases : An Overview. 4206–4272.

Villavicencio-Queijeiro A, Pardo JP, Gonz??lez-Halphen D (2015) Kinetic and hysteretic behavior of ATP hydrolysis of the highly stable dimeric ATP synthase of Polytomella sp. Arch Biochem Biophys 575:30–37. doi: 10.1016/j.abb.2015.03.018

Vinothkumar KR, Zhu J, Hirst J (2014) Architecture of mammalian respiratory complex I. Nature 515:80–84. doi: 10.1038/nature13686.

Vogel RO, Dieteren CEJ, Van Den Heuvel LPWJ, et al (2007a) Identification of mitochondrial complex I assembly intermediates by tracing tagged NDUFS3 demonstrates the entry point of mitochondrial subunits. J Biol Chem 282:7582–7590. doi: 10.1074/jbc.M609410200

Vogel RO, Janssen R, Ugalde C, et al (2005) Human mitochondrial complex I assembly is mediated by NDUFAF1. Febs J 272:5317–5326. doi: 10.1111/j.1742-4658.2005.04928.x

Vogel RO, Janssen RJRJ, Van Den Brand MAM, et al (2007b) Cytosolic signaling protein Ecsit also localizes to mitochondria where it interacts with chaperone NDUFAF1 and functions in complex I assembly. Genes Dev 21:615–624. doi: 10.1101/gad.408407

Wächter A, Bi Y, Dunn SD, et al (2011) Two rotary motors in F-ATP synthase are elastically coupled by a flexible rotor and a stiff stator stalk. Proc Natl Acad Sci U S A 108:3924–3929. doi: 10.1073/pnas.1011581108

Walker JE, Dickson VK (2006) The peripheral stalk of the mitochondrial ATP synthase. Biochim Biophys Acta - Bioenerg 1757:286–296. doi: 10.1016/j.bbabio.2006.01.001

Wang ZG, White PS, Ackerman SH (2001) Atp11p and Atp12p are Assembly Factors for the F1-ATPase in Human Mitochondria. J Biol Chem 276:30773–30778. doi: 10.1074/jbc.M104133200

Wenz T, Hielscher R, Hellwig P, et al (2009) Role of phospholipids in respiratory cytochrome bc1 complex catalysis and supercomplex formation. Biochim Biophys Acta - Bioenerg 1787:609–616. doi: 10.1016/j.bbabio.2009.02.012

Wikström M, Jasaitis A, Backgren C, et al (2000) The role of the D- and K-pathways of proton transfer in the function of the haem-copper oxidases. Biochim Biophys Acta - Bioenerg 1459:514–520. doi: 10.1016/S0005-2728(00)00191-2

Wlseman A, Gillham NW, Boynton JE (1977) Nuclear mutations affecting mitochondrial structure and function in Chlamydomonas. J Cell Biol 73:56–77.

Wollman FA, Lemaire C (1988) Studies on kinase-controlled state transitions in Photosystem II and b6f mutants from Chlamydomonas reinhardtii which lack quinone-binding proteins. BBA - Bioenerg 933:85–94. doi: 10.1016/0005-2728(88)90058-8

Wydro MM, Sharma P, Foster JM, et al (2013) The evolutionarily conserved iron-sulfur protein INDH is required for complex I assembly and mitochondrial translation in Arabidopsis [corrected]. Plant Cell 25:4014–27. doi: 10.1105/tpc.113.117283

Xia D, Esser L, Tang WK, et al (2013) Structural analysis of cytochrome bc1 complexes: Implications to the mechanism of function. Biochim Biophys Acta - Bioenerg 1827:1278–1294. doi: 10.1016/j.bbabio.2012.11.008

Yano J, Kern J, Yachandra vittal K, et al (2015) Light-Dependent Production of Dioxygen in Photosynthesis.

Yasuda R, Noji H, Kinosita K, Yoshida M (1998) F1-ATPase is a highly efficient molecular motor that rotates with discrete 120??steps. Cell 93:1117–1124. doi: 10.1016/S0092-8674(00)81456-7

Zalutskaya Z, Lapina T, Ermilova E (2015) The Chlamydomonas reinhardtii alternative oxidase 1 is regulated by heat stress. Plant Physiol Biochem 97:229–234. doi: 10.1016/j.plaphy.2015.10.014

Zara V, Conte L, Trumpower BL (2007) Identification and characterization of cytochrome bc1 subcomplexes in mitochondria from yeast with single and double deletions of genes encoding cytochrome bc1 subunits. FEBS J 274:4526–4539. doi: 10.1111/j.1742-4658.2007.05982.x

Zeng X, H. Barros M, SHulman T, Tzagoloff A (2008) ATP25, a New Nuclear Gene of Saccharomyces cerevisiae Required for Expression and Assembly of the Atp9p Subunit of Mitochondrial ATPase. Mol Biol Cell 19:308–317. doi: 10.1091/mbc.E07

Zerbino DR, Birney E (2008) Velvet: Algorithms for de novo short read assembly using de Bruijn graphs. Genome Res 18:821–829. doi: 10.1101/gr.074492.107

Zhang R, Patena W, Armbruster U, et al (2014) High-Throughput Genotyping of Green Algal Mutants Reveals Random Distribution of Mutagenic Insertion Sites and Endonucleolytic Cleavage of Transforming DNA. Plant Cell 26:1398–1409. doi: 10.1105/tpc.114.124099

Zhang Z, Huang L, Shulmeister VM, et al (1998) Electron transfer by domain movement in cytochrome bc1. Nature 392:677–684. doi: 10.1038/33612

Zhu J, Egawa T, Yeh S-R, et al (2007) Simultaneous reduction of iron-sulfur protein and cytochrome b(L) during ubiquinol oxidation in cytochrome bc(1) complex. Proc Natl Acad Sci U S A 104:4864–9. doi: 10.1073/pnas.0607812104

Zickermann V, Wirth C, Nasiri H, et al (2015) Mechanistic insight from the crystal structure of mitochondrial complex I. 5:4–10.

Zollner A, Rödel G, Haid A (1992) Molecular cloning and characterization of the Saccharomyces cerevisiae CYT2 gene encoding cytochrome-c1-heme lyase. Eur J Biochem 207:1093–1100.

Zurita Rendón O, Shoubridge E a. (2012) Early complex I assembly defects result in rapid turnover of the ND1 subunit. Hum Mol Genet 21:3815–3824. doi: 10.1093/hmg/dds209

Zurita Rendon O, Silva Neiva L, Sasarman F, Shoubridge EA (2014) The arginine methyltransferase NDUFAF7 is essential for complex I assembly and early vertebrate embryogenesis. Hum Mol Genet 23:5159–5170. doi: 10.1093/hmg/ddu239